THESIS FOR THE DEGREE OF DOCTOR OF PHILOSOPY

Removal of ultrafine particles by intermediate air filters in ventilation systems

Evaluation of performance and analysis of applications

Bingbing Shi

Building Services Engineering
Department of Energy and Environment
CHALMERS UNIVERSITY OF TECHNOLOGY
Göteborg, Sweden 2012

Removal of ultrafine particles by intermediate air filters in ventilation systems
Evaluation of performance and analysis of applications
Bingbing Shi

ISBN 978-91-7385-782-6
Doktorsavhandling vid Chalmers tekniska högskola
Ny Serie nr: 3463
ISSN 0346-718X

Technical report D2012:06
Building Services Engineering
Department of Energy and Environment
Chalmers University of Technology
SE-412 96 GÖTEBORG
Sweden
Telephone +46 31 772 1000

Printed by
Chalmers Reproservice
Göteborg 2012

Removal of ultrafine particles by intermediate air filters in ventilation systems

Evaluation of performance and analysis of applications

BINGBING SHI
Building Services Engineering
Chalmers University of Technology

Abstract

Epidemiological and toxicological studies demonstrate that ultrafine particles (UFPs) are strongly related with respiratory and cardiovascular diseases and syndromes. One common method to reduce human exposure to particulate air pollution is the use of intermediate class filters (M5-F9 class filters according to EN779:2012). However, the efficiency of such filters, with respect to UFPs, is not well explored. Furthermore, neither the European standard nor the US standard for classification of intermediate class filters comprises performance with respect to UFPs or particles of the most penetrating size (MPPS). This could turn out to be a major lack in classification standards since UFPs have been pointed out as a potential serious health hazard. To fill in the gap, the purpose of the thesis is to evaluate the performance of intermediate class filters available on the Swedish market, and to correlate the efficiency for UFPs (EF_{UFP}) and MPPS-size particles (EF_{MPPS}) with the EN779 classification efficiency for particles of the size 0.4μm ($EF_{0.4\mu m}$). The thesis also contains analyses of 1) air filtration for indoor particles of outdoor and indoor origin; 2) how to efficiently apply intermediate air filters in two-step air filtration systems and 3) ionizer assisted air filtration.

Size-resolved filtration efficiencies of 23 filter sheets and 8 full-scale filters were tested in laboratory experiments with four types of upstream aerosols. The relationships between EF_{UFPs}, EF_{MPPS} and $EF_{0.4\mu m}$ were investigated under different testing conditions. The results showed that the electrostatic force from charged filter fibers has big influence on the shape of the efficiency curves. Additionally, the electrical charge state of the upstream aerosol is critical for the testing of charged synthetic filters. Linear relationships were found between EF_{UFPs}, EF_{MPPS} and $EF_{0.4\mu m}$ within the observed efficiency range for both glass fiber and charged synthetic filters. In general, EF_{MPPS} was 10-20%-units lower than $EF_{0.4\mu m}$. The values of EF_{UFPs} were close to $EF_{0.4\mu m}$ for glass fiber filters, while EF_{UFPs} were lower than $EF_{0.4\mu m}$ for charged synthetic filters.

Theoretical analysis showed that filter operating hours and classes are critical to the cost of two-step filtration, i.e. a solution where a pre-filter protects the main filter. Under suitable operation, two-step filtration is not necessarily more expensive than single-step filtration. Another analysis investigated suitable filter class, filtration locations, and the ratio of supply to outdoor air flow rate, for efficient removal of particles coming from indoor and outdoor sources. The results can be used to recommend suitable air filters and ventilation rates/modes or to predict the existing system performances. Yet a separate study, based on measurements, shows that an F7 class filter assisted with an ionizer may reach an efficiency similar to that of a single F9 class filter.

Keywords: indoor air quality, ultrafine particles, air cleaning, filter standard, intermediate filter, measurements, modelling, lifetime cost, particle source, health effect

This Ph.D. project has been funded by FORMAS (The Swedish Research Council for Environment, Agricultural Sciences and Spatial Planning) Grant (242-2007-1583) through the project Ultrafine Particles in the Indoor Air: Measures to Substantially Reduce Human Exposure (project no. 47401-CTH) to Building Services Engineering of Chalmers University of Technology.

Foreword

Grateful acknowledgment is given to the all support from the division of Building Services Engineering, Chalmers University of Technology and the finical support from FORMAS. Additionally, the work could not have been done without the support of many individuals and organizations.

I would like to thank my supervisor, Associate Professor Lars Ekberg, who has provided me plenty of research opportunities and encouragement. I would like to thank Professor Per Fahlén, for giving me this opportunity to share his knowledge and special visions in the whole HVAC field. I would like to thank Associate Professor Sarka Langer, for her invaluable help and guidance in the aerosol tests. I would like to thank Professor Jan Olof Dalenbäck, for his inspiration and valuable advices on the manuscript.

Additionally, special thanks to all organizations supporting my research, SP, Vokes Air, Camfil, Dinair, Topas, Transjonic and Akademiska hus for providing me equipment, filters and a location for field measurements.

I also would like to thank all my colleagues at Building Services Engineering for their encouragement and sharing of knowledge. Special thanks to Håkan Larsson for his invaluable help and patience in the laboratory and equipment; to Tommy Sundström for his patient help and support in equipment software and computers, to Katarina Bergkvist for her important help on both administrative issues in Chalmers and daily life in Göteborg.

My love is reserved for my family and my boyfriend Yifeng, who have always been there for me.

Göteborg, November 2012

Bingbing Shi

To my loved ones

Contents

Page

Symbols, abbreviations and definitions

Symbols

Latin letters

ΔP	filter pressure drop	[Pa]
$\Delta P_{initial}$	filter initial pressure drop	[Pa]
$\overline{\Delta P}$	average pressure drop of a filter during the lifetime	[Pa]
C_c	Cunningham correction factor	[-]
C_{up}	particle number concentration in the upstream air	[#/cm^3]
C_{down}	particle number concentration in the downstream air	[#/cm^3]
D	particle diffusion coefficient	[-]
d	diameter	[μm]
R	interception parameter; $R = \frac{d_p}{d_f}$	[-]
E	single-fiber efficiency	[%]
E_Σ	total single-fiber efficiency	[%]
EF	overall filter efficiency	[%]
EF_{UFPs}	filter efficiency on ultrafine particles	[%]
EF_{MPPS}	filter efficiency on MPPS-sized particles	[%]
$EF_{0.4\mu m}$	filter efficiency on 0.4μm-sized particles	[%]
EF_0	size-resolved efficiency of the single filter	[%]
EF_1	size-resolved efficiency of the pre-filter	[%]
EF_2	size-resolved efficiency of the main filter	[%]
G	particle gravitational settling coefficient	[-]
g	acceleration of gravity	[m/s^2]
M_{tot}	overall particle deposition on a filter	[mg]
m_{out}	particle size-resolved mass concentration in outdoor air	[mg/(μm*m^3)]
m_{pre}	particle size-resolved mass concentration in the downstream air of the pre-filter	[mg/(μm*m^3)]
m_{f0}	particle size-resolved mass deposition on the single filter	[mg/(μm*m^3)]
m_{f1}	particle size-resolved mass deposition on the pre-filter	[mg/(μm*m^3)]
m_{f2}	particle size-resolved mass deposition on the main filter	[mg/(μm*m^3)]
P	overall filter penetration rate	[%]
q	electric charge on the particle	[e]
t	filter medium thickness	[m]
U_o	face velocity; $U_o = \frac{\dot{V}}{A}$	[m/s]
$\dot{V}$	volumetric flow rate	[m^3/s]
V	volume of the room	[m^3]
A	cross-sectional area of the filter;	[m^2]
k	Air exchange rate	[h^{-1}]
EF_{OA}	outdoor air filtration efficiency	[%]
EF_{IA}	indoor air filtration efficiency	[%]

Greek letters

α	packing density	[%]
μ	viscosity;	[Pa·s]
η	overall efficiency of the fan and motor	[-]
τ	relaxation time	[s]
ρ_p	density of particles	[kg/m^3]
ε_f	relative permittivity (dielectric constant) of the fiber	[-]
ζ_o	permittivity of a vacuum	[-]

Subscripts

p	particles	f	fiber
R	interception	I	impaction
D	diffusion	G	gravitational setting
q	electrostatic deposition	v	outdoor air
c	recirculation	d	particle deposition
inf	infiltration air	exf	exfiltration air
i,o	indoor particles of outdoor origin	i,s	indoor particles of indoor emission

Abbreviations

MPPS	Most Penetrating Particle Size
UFPs	Ultrafine Particles
PAHs	Polycyclic Aromatic Hydrocarbons
SOA	Secondary Organic Particle
VOC	Volatile Organic Compounds
SVOC	Semi Volatile Organic Compounds
MVOC	Microbial Volatile Organic Compounds
ETS	Environmental Tobacco Smoke
BC	Black Carbon
OC	Organic Carbon
I/O	Ratio of Indoor to Outdoor Particles Concentration
IDA	Indoor Air
ODA	Outdoor Air
AER	Air Exchange Rate
SMPS	Scanning Mobility Particle Sizer (SMPS) Spectrometer
DMA	Differential Mobility Analyzer
CPC	Condensation Particle Counter
APC	Aerodynamic Particle Counter
DEHS	Di-Ethyl-Hexyl-Sebacat (aerosol)
SEM	Scanning Electron Microscope
ULPA	Ultra-low Penetration Air (filter)
HEPA	High-efficiency Particulate Air (filter)
EPA	Efficient Particulate Air (filter)
MERV	Minimum Efficiency Reporting Value
GF	Glass Fiber Filter/filter Sheet
CS	Charged Synthetic Fiber Filter/filter Sheet
US	Uncharged Synthetic Fiber Filter/filter Sheet
$PM_{2.5}$	Fine Particles with Diameter less than 2.5μm
PM_{10}	Respirable Particles with Diameter less than 10μm

$PM_{2.5\text{-}10}$ Coarse Particles with Diameter between 2.5μm and 10μm

Definitions

Ku Kuwabara Hydrodynamic Number; $Ku = -\frac{\ln \alpha}{2} + \frac{3}{4} + \alpha - \frac{\alpha^2}{4}$

Stk Stokes Number; $Stk = \frac{\tau U_o}{d_f}$

Pe Peclet Number; $Pe = \frac{d_f U_o}{D}$

1 Introduction

Ultrafine particles (UFPs) are particulate matter with sizes less than 0.1 micrometer (100nm), which typically contribute to 80% of the number concentration and a large portion of surface area of particulate matter in atmospheric environments[102]. Epidemiological and toxicological studies have established that UFPs are associated with the respiratory and cardiovascular morbidity and mortality. Moreover, many studies demonstrated that UFPs are more closely associated with morbidity and mortality than other fractions of particles, especially on cardiovascular diseases. Considering that people spend over 85% of their time indoors, a substantial reduction of indoor ultrafine particles concentrations may obviously reduce ultrafine particle exposure to the population. Therefore, efficient air cleaning techniques on UFPs are critical to reduce indoor UFPs level.

1.1 Background

Among various air cleaning techniques, air filtration is the most common used air purification method. Reducing personal exposure to indoor UFPs greatly relies on efficient filters being available on the market. However, the broadly used intermediate filters in residential and commercial buildings can be expected to have a big efficiency difference for capturing UFPs. At present, two particle filter standards are widely used, i.e. EN779 (2012)[42] and ASHRAE 52.2 (2007)[5]. Neither of them comprises performance with respect to ultrafine particles (UFPs) or particles of the most penetrating size (MPPS) for classification of intermediate class filters (also denoted medium and fine filters). This could turn out to be a major lack in classification standards since UFPs have been pointed out as a potential serious health hazard. Thus, it is meaningful to investigate the filtration efficiency of various intermediate filters in the market regarding their ability to capture UFPs (EF_{UFPs}) and MPPS-sized particles (EF_{MPPS}), as well as the correlation between $EF_{UFPs,}$ EF_{MPPS} and the efficiency used for filter classification. In the European filter standard EN779, the classification efficiency is the filtration efficiency for 0.4 μm-sized particles ($EF_{0.4\mu m}$)[42].

Due to the energy crisis, energy use has become an important criterion in evaluation of air cleaning applications. The pressure drop of ventilation air filters is increased with filter classes and is enhanced by the dust load in the long-term operation. Operating suitable filter class within suitable lifetime is important to saving energy during the long-term operation. At present, two-step filtration is commonly interested by the possible low life-time pressure drop through flexible changing the pre-filter and main-filter. Another way of reducing energy use is to reduce the pressure drop of the filters – while maintaining sufficient filtration efficiencies. Ionizer assisted air filtration may be such a kind of technology. Many studies have shown that ionization before a filter could enhance the original filtration efficiency for removing airborne particles, aeroallergens and airborne microorganisms and has negligible pressure drop increase[3, 55, 85, 115, 138]. However, the reliability of the performance and the potential generation of by-products (e.g. ozone) are critical problems associated with this application.

Additionally, the particles from indoor and outdoor sources have different particle properties, different emission intervals and different association with occupants'

activities. It has been found that indoor particle sources (including cooking, cleaning and movement of people) may contribute to 57-80% of indoor coarse particles, and 8-37% of indoor 0.02-0.3μm particles in residential buildings in Boston[1]. Therefore, it is of interest to know how to efficiently capture indoor particles both from indoor emission and outdoor penetration. Based on indoor particles dynamics, the above objective could be investigated from ventilation/filtration system design aspects, such as filter location and class, recirculated air flow percentage and supply air flow rate.

1.2 Objective

The first study objective is to investigate the efficiency of intermediate air filters to capture UFPs and submicron particles and the critical testing methods. Besides general build-up of knowledge, the objective is to evaluate various expressions of the filtration efficiency. The efficiency for removal of UFPs and particles of MPPS-size are of special interest, since it may be motivated to include the consideration of these particle sizes in future filter standards. The second objective is to investigate various filtration aspects on a system level. Here, a model study is developed on how to choose filter class and ventilation mode to remove indoor particles of different origins according to indoor particle dynamical fate. Then, two solutions on how to economically and efficiently filtrate "small particles" are studied. One solution is to use two-step filters instead of single filters. Another is to enhance filter efficiency through ionizer assisted air filtration.

1.3 Perspective

The research is funded by FORMAS and shall be seen in the context of evaluating measures to substantially reduce indoor personal exposure to UFPs. The reason for focusing on intermediate class fiber filters is that this type of filtration is the most common air cleaning technology used for protection of general indoor environments and the people occupying buildings. Most probably, major filter manufacturers have comprehensively studied such filters with respect to UFP removal. However, publication of results appears to be rather scarce. The issue has also been addressed by researchers in the field of indoor air quality. This thesis contributes to the knowledge in the area, with two fields focus: 1) evaluation of filter performance, 2) design and operation of systems with respect to filter performance, energy efficiency and costs. The study is conducted in three parts.

- The first part is the literature study and is presented in Chapter 2. It is aimed to demonstrate the motivation to remove indoor UFPs, the control priority of particle sources as well as the application and problems of particle removal techniques at present.

- The second part is an air filtration study of intermediate air filters and presented in Chapter 3-6. It is composed by four sub-parts.
    - Single-fiber efficiency theory and a simulation study based on measurements of filter media properties. It focuses on the effect of filter electrostatic charge on the shape of the efficiency curves.
    - Size-resolved filtration efficiency of intermediate air filters to capture UFPs and submicron particles.

- Relationship study between EF_{UFPs}, EF_{MPPS} and $EF_{0.4\mu m}$ and the influence from air velocity and electrical charge of upstream aerosol.
- Filter testing methods and the influencing factors. The influence factors include upstream aerosols, neutralizers, air velocities and filter media. The electrical charge of upstream aerosol and filter fiber are in special attention.

– The third part focused on system aspects of intermediate air filtration. It includes three parts in Chapter 7-9:
  - Identification of suitable filter locations, filter classes and ventilation modes to remove indoor particles originating from outdoor penetration and from indoor emission, respectively. The study is based on a particle number balance model.
  - Single-step and two-step filtration solutions are compared with respect to minimized annual total cost given certain filtration efficiency requirements.
  - Investigation of the performance of ionizer assisted air filtration. The purpose is to identify a suitable air filter and to study the influence of ion concentration and possible by-products emission.

1.4 Methodology

Chapter 2 is developed through an interdisciplinary literature review in the fields of aerosol science, indoor air quality and air cleaning technology. According to the literature summary, the research objectives are identified.

The ventilation air filter study in Chapter 3-6 is mainly conducted in laboratory experiments and assisted with simulations based on the single-fiber efficiency theory.

The application studies in Chapter 7-8 are based on mathematic models with experimental data as support. The experiment results come from previous laboratory measurements and measurements presented in the literature.

The study of ionizer-assisted air filtration presented in Chapter 9 is conducted in three experiments in a small-scale filter test rig, a full-scale filter test rig and in the field.

1.5 Thesis outline

According to the above research objectives, the thesis is organized as follows.

Chapter 1 is the introduction part. It presents the study motivation, the methodology and the thesis outline.

Chapter 2 is a literature study in the fields of aerosol science, indoor air quality and air cleaning techniques. It provides the background information and motivation of the study.

Chapter 3 is the study of single-fiber efficiency theory, in which calculated efficiency values are compared with measured efficiency values.

Chapter 4 is the methodological chapter for the experimental study of full-scale filters and filter sheets. The results are utilized in Chapter 5-6.

Chapter 5 presents the measured size-resolved efficiency of intermediate filters as well as the influence of the testing methodology.

Chapter 6 presents the relationship between EF_{UFPs}, EF_{MPPS} and $EF_{0.4\mu m}$, as well as the influential factors.

Chapter 7 is the modelling study on the control strategy of indoor particles from indoor emission and outdoor penetration according to their respective indoor dynamical fate. In this modelling study, the effect of filter locations on indoor particle removal is initially investigated in quality and quantity.

Chapter 8 is the modelling study on the economical analysis and efficiency of single-step and two-step air filtration in urban and rural environments.

Chapter 9 presents the experimental study on ionizer-assisted air filtration in various settings. It is also the pre-study of the long-term performance of ionizer-assisted air filtration in demand controlled ventilation (DCV) systems.

Chapter 10 summarizes the main conclusions achieved from the whole work presented in the thesis and outlines ideas for future research work.

1.6 List of publications

Peer reviewed papers

- **Shi, Bingbing**; Ekberg, Lars. Field Evaluation of Ionizer-Assisted Air Filtration. *Clima 2013, manuscript. The abstract has been accepted.*
- **Shi, Bingbing**; Ekberg, Lars; Langer, Sarka. Filtration efficiency of intermediate class filters for UFP and MPPS-sized particles and the relation to 0.4μm-sized particles. *Aerosol science and Technology. Submitted.*
- **Shi, Bingbing**; Ekberg, Lars; Trüschel, Anders. et al. (2012) Influence of filter fiber material on removal of ultrafine and submicron particles using carbon fiber ionizer-assisted ventilation air filters. *ASHRAE Transactions, 2012, Volume 118 (Part 1),pp. 602-611.*
- **Shi, Bingbing**; Ekberg, Lars; Langer, Sarka. (2011) Removal of ultrafine particles and particles of the most penetrating size by new intermediate class filters. *Proceedings of the Indoor Air 2011 Conference, Austin, USA.*
- **Shi, Bingbing**; Ekberg, Lars; Afshari, Alireza; et al. (2010) The effectiveness of portable air cleaners against tobacco smoke in multizone residential environments. *Proceedings of the CLIMA 2010 Conference: 10th REHVA World Congress 'Sustainable Energy use in Buildings', r5-ts45-op02.*
- Afshari, Alireza; **Shi, Bingbing**; Bergsøe, Niels, et al. (2010) Quantification of ultrafine particles from second-hand tobacco smoke infiltration. *Proceedings of the CLIMA 2010 Conference: 10th REHVA World Congress 'Sustainable Energy use in Buildings', r5-ts69-op01.*
- **Shi, Bingbing**; Ekberg, Lars; Fahlén, Per. (2009) Ultrafine particles control strategy in printer rooms: model and experiment study on portable air cleaner and HVAC combination. *Proceeding of Healthy Buildings 2009, Syracuse, USA.*

- Ekberg, Lars; **Shi, Bingbing**. (2009) Removal of ultrafine particles by ventilation air filters. *Proceeding of Healthy Buildings 2009, Syracuse, USA.*

Non peer reviewed papers

- Ekberg, Lars; **Shi, Bingbing**. Kan ventilationsfilter fånga ultrafina partiklar inomhus. Husbyggaren - SBR - Svenska Byggingenjörers Riksförbund , 1 (2011) pp. 24-25.
- Ekberg, Lars; **Shi, Bingbing**. (2010) Removal of ultrafine particles by ventilation air filters. *SWESIAQ conference Nordic Indoor Air Update, Stockholm, Sweden.*
- Afshari, Alireza; Bergsøe, N.C.; **Shi, Bingbing**, et al. (2010). Naborøg og overførsel af partielforurening. *HVAC - Magasin for klima- og energiteknik, miljø, bygningsinstalltioner & -Netværk, 1 (2010) pp. 24-30.*

–

2 Literature review

UFPs have attracted broad attention in recent years due to their adverse health effects. Epidemiological and toxicological studies have shown that UFPs are probably more hazardous than particles in other fractions. Their special physical and chemical properties make them much easier to cause various health effects than particles in other size fractions. At the same time, UFPs have also become a hot topic in the related fields of aerosol sources, indoor air quality and air cleaning techniques. This chapter provide a state-of-art review of the current ultrafine particle literature. The aim is to present the motivation of the work as well as future studies.

2.1 UFPs and health effects

2.1.1 UFPs

Airborne particles are normally classified according to their aerodynamic diameter in specific size fractions, such as PM_{10} (respirable particles, d_p<10μm), $PM_{2.5\text{-}10}$ (coarse particles, 2.5 to 10μm), $PM_{2.5}$ (fine particles, d_p<2.5μm) and UFPs (ultrafine particles, d_p <0.1μm), see Figure 2.1.

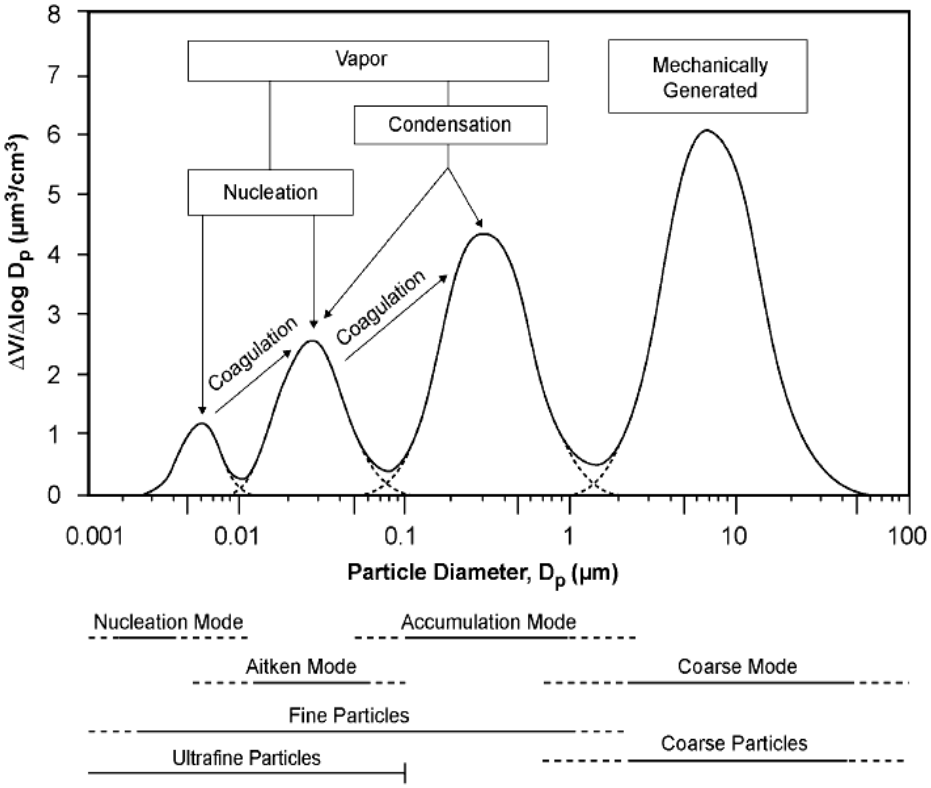

Figure 2.1 Volume size distribution that might be observed in traffic[146].

Particulate matter could be generated from various sources and distributed in different particle size modes, i.e. nucleation, Aitken mode, accumulation and coarse mode. UFPs are mainly derived from combustion and condensed phase species generated from the nucleation of gas phase species. They are initially formed in the nucleation mode, and then grow by coagulation into the Aitken and Accumulation modes.

UFPs exhibit special physical, chemical and biological characteristics compared to particles in other size fractions. For example, UFPs have an extremely large ratio of surface area to mass[16, 109], and a high deposition rate in the low respiratory tract[109]. Their relatively large surface area greatly enhances the capacity to carry a substantial amount of adsorbed or condensed toxic air pollutants into the lower respiratory tract[31]. Consequently, many studies indicate that UFPs have a much higher potential to cause health risks than larger particles [16, 29, 31, 33, 72, 111, 121, 126, 139]. Recently, toxicological and epidemiological studies have focused on health effects due to personal exposure on UFPs.

2.1.2 Epidemiological studies

Since the event of London great smog in December 1952, air pollution and its health effect have been attracting worldwide attention. In the London smog event, the number of fatalities would be approximately 12,000[11] rather than the 3,000-4,000 which were generally reported for the episode. Airborne particles were commonly accepted as one of the main causes. Hund et al.[66] presented that UFPs from coal and diesel combustion is one of several possible etiologic agents in the event. After the London smog event, many epidemiological studies started to investigate what and how air pollutants associate with mortality and morbidity. An critical study from Dockery et al.[35] established a clear association between fine particulate matter and the mortality in six U.S. cities. The initial epidemiological studies focused on the relationship between particle mass concentration (e.g.10 $\mu g/m^3$) and daily mortality. From then on, many studies identified an increased rate of mortality with increased mass concentration of fine particles[15, 123, 136]. Pope et. al. [123] found that each 10 $\mu g/m^3$ elevation in fine particulate air pollution was associated with approximately a 4%, 6%, and 8% increased risk of all-cause, cardiopulmonary, and lung cancer mortality respectively. However, many later epidemiological studies found that particle number concentration values can better estimate the health consequences induced by particle exposure compared to particle mass concentration values [26, 31, 61, 64]. On one hand, fine particles, especially UFPs, have small mass concentrations, but their number and surface concentrations are substantially higher compared to that of PM_{10}. On the other hand, small particles have higher deposition rate in the low respiratory tract than large particles. Thus, small particles can carry higher concentrations of toxic air pollutants into the lower respiratory tract[26, 31]. Up to now, some epidemiological studies and toxicological studies have presented associations between the exposure to UFPs and respiratory and cardiovascular diseases [17, 52, 130, 142, 160]. Gilmour et al.[52] discovered that, in rats exposed to fine and ultrafine carbon particles, there is a consistent inflammatory effect of UFPs, which is even stronger than for the same exposure to fine particles. Stölzel et al.[142] found an association between UFPs and cardio-respiratory mortality. Wichmann et al.[160] found a more delayed association for UFPs than for fine particles and the overall association was slightly stronger for respiratory diseases than for cardiovascular diseases.

2.1.3 Toxicological studies

Furthermore, toxicological studies have demonstrated that UFPs can translocate to extrapulmonary organs via the blood circulation[83, 110] and to the central nervous system via olfactory nervous[39, 109] as well as induce the formation of reactive oxygen species[158]. Some studies found that UFPs have substantially higher

toxicity per unit mass than larger particles [19, 62]. Li et al.[88] established that UFPs had stronger potential toward oxidative stress due to enhanced biologic potency than coarse and fine particles. Wilson et al.[161] demonstrated that the interaction of UFPs and metal components in the lung generated inflammation.

At present, epidemiological and toxicological studies are focused on distinguishing the health effect of UFPs from that of fine particles and health effects of UFPs on cardiovascular system. Toxicological studies found inhaled fine particles and UFPs are transported into the organisms through different routes. Being different to larger fine particles, UFPs escape phagocytosis by alveolar macrophages and translocate to extrapulmonary organs, leading to the production of oxygen radicals[131].

2.1.4 Potential mechanisms

Up to now, scientists have concluded that five mechanisms of airborne particles can result in adverse health effects: pulmonary effects; cardiovascular effects; blood effects; prenatal outcomes and neurotoxic effects. Figure 2.2 summarizes on what organs can be affected by airborne particles through the above five mechanisms[119].

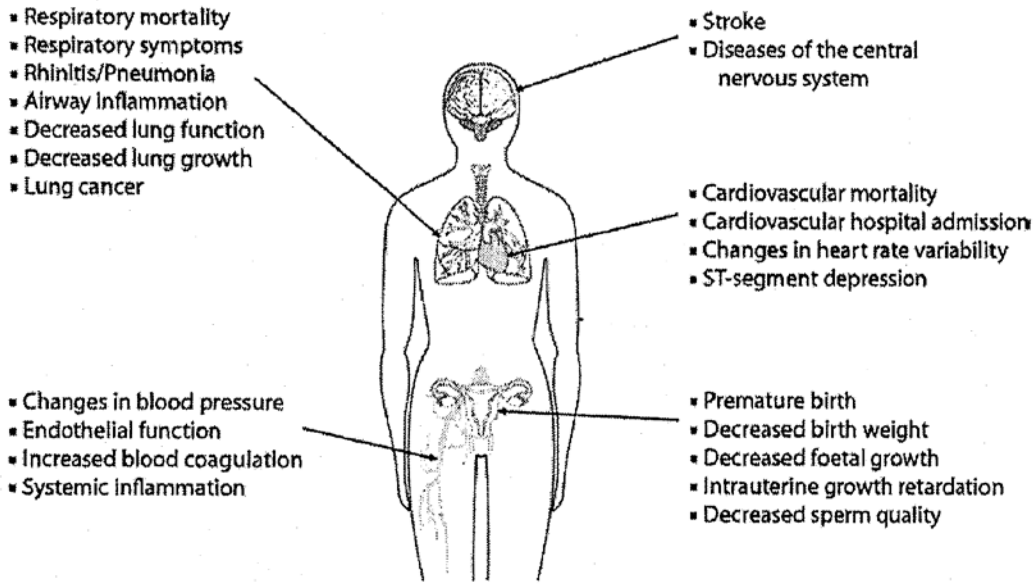

Figure 2.2 Organs of human body that can be affected by air pollution [119].

Particulate matter involves in all five mechanisms to induce the health effects. For lungs, the mechanism appears to be clear and should be oxidative stress/inflammation. Furthermore, many studies found that UFPs were more potent than fine and coarse particles to induce oxidative stress[88]. For the cardiovascular systems, there are three hypothesized mechanisms, see Figure 2.3. For blood, a general opinion is that the blood markers of inflammation are positively associated with airborne particles[122, 130, 137]. Pietropaoli et al.[122] discovered that the pulmonary diffusing capacity for carbon monoxide (CO) is reduced after inhalation of carbon UFPs for two hours in healthy subjects. However, the mechanism is difficult to be concluded due to the limited studies at present. For prenatal outcomes, Slama et al.[141] summarized three possible biological mechanisms although they are not clear enough due to insufficient studies. The study demonstrated that $PM_{2.5}$ and PM_{10} are positive in these three

mechanisms, and UFPs need to be studied in the future research. For neurotoxic effects, the main hypotheses include air pollution-induced inflammation and/or oxidative stress and a translocation of UFPs to the brain. It is already demonstrated that airborne particles can influence children's olfactory neurons[21]. Additionally, a critical paper from Peters et al.[120] reviewed the evidence for mechanisms involved in the translocation of particles from the lung to other organs, including the brain. The above five mechanisms are achieved or hypothesized from previous studies. More studies are needed to clarify and further prove these mechanisms.

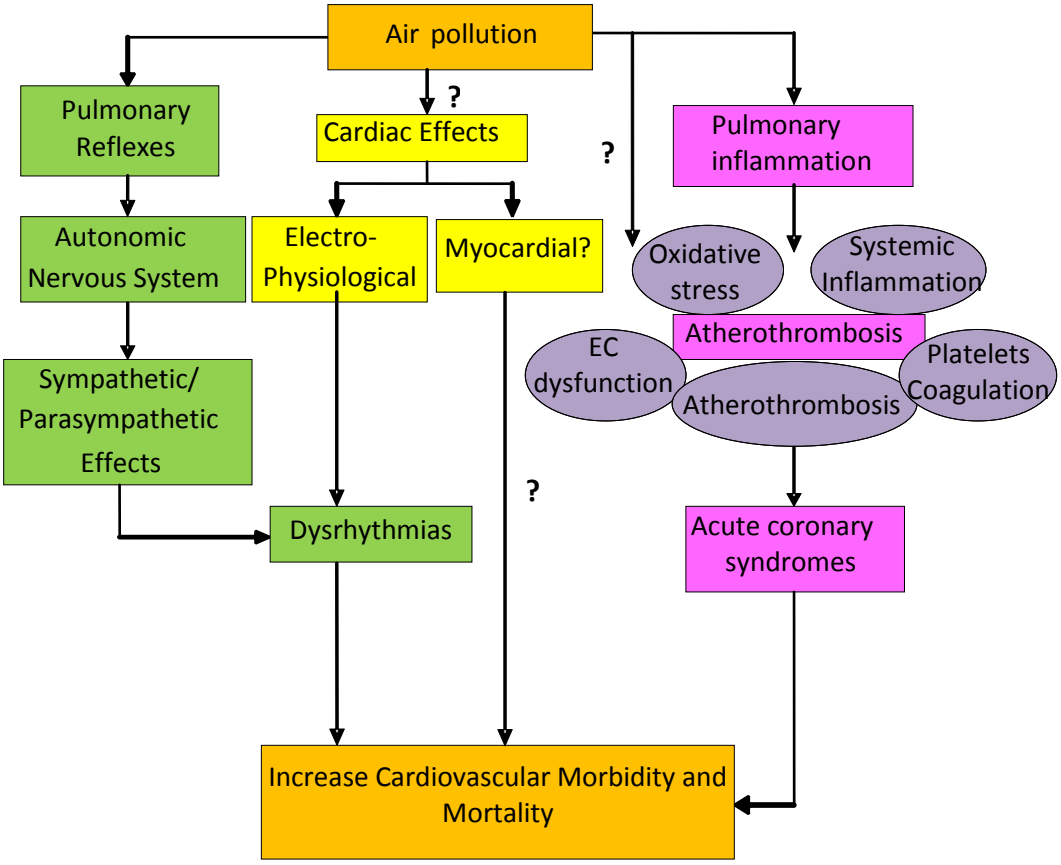

Figure 2.3 Possible mechanisms that link air pollution with increased cardiovascular morbidity and mortality[4]. The question symbol means that the indicated mechanisms are based on assumptions.

Figure 2.3 shows three main pathways linking ambient air pollution to cardiovascular health effects[131]. 1) particles deposited in the pulmonary tree can alter systematic autonomic balance leading to parasympathetic nervous system withdrawal and/or sympathetic nervous system (left side in the figure); 2) Circulating pro-oxidative and/or proinflammatory mediators released from the lungs may induce a systemic chain reaction (middle in the figure); 3) UFPs or soluble particle constituents may rapidly translocate from the pulmonary epithelium into the circulation and interact directly with the cardiovascular system (right side in the figure). Pathway 3 is limited to UFPs, while the other two pathways may well be possible for coarse PM fractions. In blood circulation, UFPs might also have direct effects on the heart and other organs.

2.1.5 Particle properties

The chemical composition and physical properties of particles are critical to their health effects. Table 2.1 presents the critical characteristics of different particle fractions.

Table 2.1 Characteristics of different particle fractions, adapted from Araujo and Nowell, 2009[4]. The number of "+" represents the relative amount.

Parameter	Coarse particle ($PM_{2.5-10}$)	Fine particles ($PM_{2.5}$)	Ultrafine particles (UFPs)
Number per μm^3	+	++	+++
Mass (μg) per μm^3	+++	++	+
Surface area	+	++	+++
Lung penetrability	+	++	+++
Bioavailability of active compounds	+	++	+++
Redox activity	+	++	+++
Relative content (% of total mass)			
Elemental carbon	+	++	+++
Organic carbon	+	++	+++
PAHs	+	+	+++
Metals	+++	++	+

In Table 2.1, UFPs have a higher order of magnitude than fine and coarse particles for all characteristics except mass concentration and metal content. The health effects of UFPs introduced in sections 2.1.1-2.1.3 could be explained from the physical properties of UFPs summarized in Table 2.1. For the chemical content, pro-oxidative polycyclic aromatic hydrocarbons (PAH) could promote oxidative stress[105]. The black carbon (BC) and organic carbon (OC) contribute the toxicity of the particles [34, 103] through oxidative stress. UFPs could also interact with metal components in lung and generate inflammation[161]. Therefore, it is reasonable to suspect that UFPs are the most toxic particles among different particle fractions.

2.2 UFPs exposure and the ratio of indoor to outdoor particle concentration

The study of personal exposure to airborne particles is motivated by epidemiological studies. The exposure to ambient particles has been in focus for many years because the health effects caused by ambient particles are established in many epidemiological studies [35, 75, 91, 123, 157]. Comparatively, there is not

enough literature that show whether the health effects from indoor aerosols are significant or not. Some literature has demonstrated that the health effects are not caused by exposure to indoor generated particles[162], while more literature has stated that the published research is not sufficient to conclude that indoor particle sources are irrelevant to health effect[27].

Since epidemiological studies have found statistical associations between ambient particle concentrations and mortality/morbidity, ambient concentrations are commonly used as an important estimator on personal particle exposure in epidemiology studies. However, personal exposure to particles is the sum of personal exposure to outdoor-generated particles and indoor-generated particles in various microenvironments where people spend time. Since people in the world spend about 85% of their time in indoor environments, investigating the relationship of indoor and outdoor particulate matter and the relative contributions of particles of indoor and outdoor origin are critical to effectively control personal exposure to particles of indoor and outdoor origin. The ratio of indoor to outdoor particle concentration (I/O) is an important parameter to identify the influence of outdoor particles on the indoor environment. Because epidemiological studies have focused on health effects associated with ambient particle levels, it is meaningful to research this ratio for various settings.

The I/O concentration ratios depend on building type and indoor personal activities. Matson [94] observed that the I/O ratios for office buildings were between 0.5 and 0.8 over working time in absence of indoor UFP sources, e.g. cigarette smoking. However, the I/O ratios in residential buildings were up to approximately 2.5 as an average for about 15 hours. The high I/O ratios in residential buildings were associated with cooking and candle burning. Several previous studies have concluded that outdoor particle sources, primarily local traffic, are major contributors to the indoor particles with the absence of strong indoor sources, while indoor sources can result in very high, short-term increases in indoor concentrations[81, 94, 96, 152, 166].

The I/O ratios of UFPs are greatly depending on particle size. Zhu et al.[166] observed that larger particles (70~100nm) had higher I/O ratios (0.6~0.9), while smaller particles with 10~20 nm in diameter had lower I/O ratios (0.1~0.4); both observations under infiltration conditions with air exchange rates (AER) of 0.3~1.1 h^{-1}. Additionally, Koponen et al.[81] established that the I/O ratio of nucleation mode particles was not strongly depending on the ventilation rate, while the opposite was observed for accumulation mode particles.

The I/O ratios can be adjusted by the ventilation mechanism. Zhu et al.[166] observed that for buildings with mechanical ventilation, the highest I/O ratios were found when windows are open; a case when the I/O ratios were very close to 1.0 across all particle sizes. However, much lower I/O ratios were observed with closed windows under mechanical ventilation conditions which were probably attributed to the filtration of particles in the supply air through the ventilation system. Increasing ventilation rates enhances I/O ratio of particles larger than 90 nm.

The I/O ratios are closely related with the class of air filters in ventilation systems. Hussein et al.(2004)[67] observed I/O ratios for UFPs in the range 20%~85% in an office building without strong indoor sources and a G3 class filter in the supply

air. Matson [94] observed I/O ratios about 45%-50% in a building equipped with F6 class of supply air filter at an air change rate around 1.5h^{-1}. Additionally, Koponen et al. [81] discovered that when operating an F7 class filter in the supply air, the I/O ratios of UFPs are only 5%~25%. In Figure 2.4, the I/O ratio curves are compared with the penetration curves of the filters used in the studies mentioned above. In the figure, the I/O ratio is lower than the penetration factor of the corresponding filter. The difference is expected to be the deposition rate of ultrafine particle during the transportation.

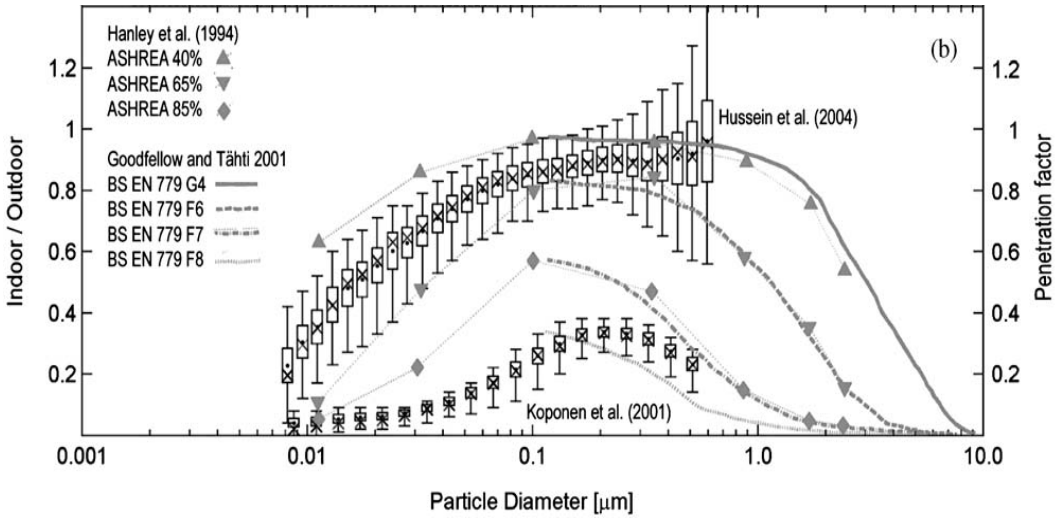

Figure 2.4 Indoor-to-outdoor concentration ratios presented as mean (dot), median (×), standard deviation (box), and 5% and 95% percentiles (bars)[68]. I/O values observed in office rooms served by mechanical ventilation systems: G3 class filter and air exchange rate of 3h^{-1} in Hussein et al. [67], and F7 class filter and air exchange rate of 3.75h^{-1} in Koponen et al.[81]. The results are compared to the ASHRAE class filter standards[58] and BS EN779 at the minimum efficiency[58].

The I/O ratios are additionally influenced by air penetration through the building envelope. Liu and Nazaroff (2001)[90], Thornburg et al. (2001)[144] and Hussein (2005)[68] studied the size-resolved penetration factor and models for estimation of this factor. As a common result, the maximum penetration factor was found for particles between 0.1 μm and 1.0 μm in diameter.

In summary, the I/O ratios decrease when the particle infiltration through the building envelope and the air-handling unit is reduced. Mounting a high efficiency filter in supply air and using room air cleaners or filtrated recirculated air can further reduce I/O ratios. However, if a strong particle source is present indoors, the I/O ratios would substantially increase and the relationship between indoor and outdoor particle concentration would be weak. Consequently, with the presence of strong indoor sources, outdoor particle concentration cannot be used as a reliable estimator in the prediction of indoor concentrations and personal exposure in epidemiological studies[152]. Furthermore, the chemical composition, size and physical characteristics are probably different for the indoor-generated particles and outdoor-generated particles due to the different properties of particle sources, see section 2.3. Therefore, it is supposed that distinguishing between personal exposure to particles of indoor origin and outdoor origin is indispensible to better assess human exposure to UFPs and to evaluate air cleaning strategies.

2.3 Outdoor and indoor main sources of UFPs

The special properties of UFPs include: small enough to penetrate into cell membranes; extremely large surface area per unit mass and the highest deposition efficiency in alveolar region of the lungs. Thus they are generally supposed to deliver large amounts of potentially toxic compounds to cell. Numerous previous literature studies have established that different particle emission sources give specific particle size distributions and chemical compositions, which are associated with different health effects. It is reasonable to apply different control priorities on different particle sources. This section presents the main sources of UFPs in indoor and outdoor environments and the properties of the generated particles.

2.3.1 Outdoor combustion

Particulate matter from combustion is generated from the direct combustion process and secondary combustion particles including sulfates and nitrates. Pope et al. (2002) established that long-term exposure to fine particles from combustion would increase the risk of cardiopulmonary and lung cancer mortality by approximately 6% and 8% respectively[123]. Many toxicological studies indicate that UFPs deposited in the lung can cause a greater inflammatory response than larger particles[40, 77, 108]. The main reason could be that UFPs not only have the highest deposition efficiency in the alveolar region of the lungs, but also have an extremely large surface area per unit mass which make them absorb much more contaminants in combustion flue gas than larger particles do. The contaminants in gas from the combustion include toxic metal (lead, cadmium arsenic, chromium and zinc), sulfur, PAHs, CO, NO_x and partially oxidized hydrocarbons[154]. Normally, the source could be distinguished as traffic exhaust and coal/biomass combustion.

2.3.1.1 Traffic exhaust

Traffic exhaust is one of two main outdoor sources of UFPs[50, 79], and the other is atmospheric reactions. Up to date, a large portion of epidemiological studies on airborne particles have focused on combustion particles from gasoline- and diesel-powered motor vehicles. The particles from such sources have the clearest close association with significant health effects[7, 30, 72], such as DNA damage. Many studies have presented significant high concentrations of UFPs near major freeways, and have implied increased exposure to harmful pollutants in the around areas [127, 165]. Most of particles emitted by engines are in the ultrafine particle size range[20, 60, 79], while most of particle mass is in the accumulation mode, 50nm<d_p<1000 nm[79]. Figure 2.5 shows the size-resolved number concentration of particles emitted from a heavy duty diesel engine[20]. The different curves represent particles emitted from different engines at different operating conditions. The mean particle diameter is in the range from 60 nm to 100 nm[59, 60].

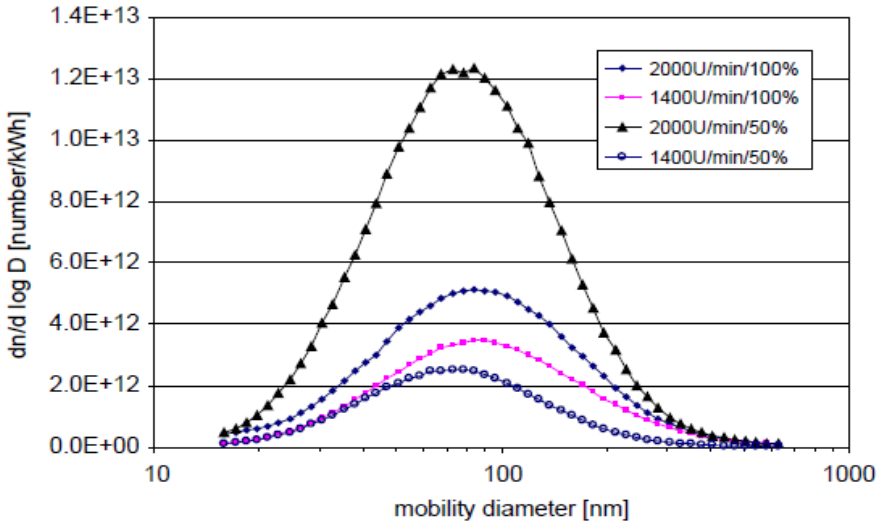

Figure 2.5 Size-resolved concentration of particles emitted from a heavy-duty diesel engine [20].

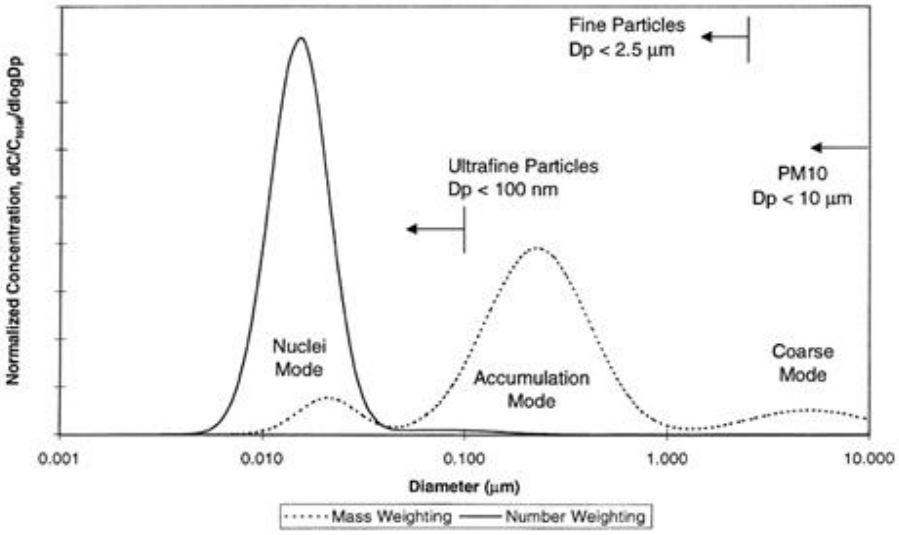

Figure 2.6 Typical size distribution of engine exhaust particles in mass and number weighting. The diagram is adopted from Kittelson,1998[79].

Figure 2.6 shows the idealized size distribution of engine exhaust particles in mass and number weighting[79]. Most of particle mass exists in the accumulation mode, especially in the diameter range 0.1-0.3µm. Particles in this mode are carbonaceous agglomerates and associated absorbed materials residue. However, most of the particle number is found in the nuclei mode, typically in 0.005-0.05µm diameter range. Particles in this mode are composed of volatile organic and sulfur compounds that form during exhaust dilution and cooling, some of them also contain solid carbon metal compounds. Additionally, the coarse mode contains 5-20% of the particle mass, but just a very few percent of the particle number. In summary, the particles from automobile exhaust distribute 1-20% of the mass and 90% of the number in nuclei mode. In addition, researchers have found that the UFP concentration around a highway or freeway was increased with traffic volume, while reduced with wind speed and relative humidity [25].

2.3.1.2 Coal and biomass combustion

Coal and biomass combustion is another strong UFPs source. Unlike traffic exhaust, the sources of such are normally located in suburb and rural areas in modern society. This means that the emission does not closely and directly affect the health of the population in urban, at least not as the emission of traffic exhaust does.

Combustions from coal and biomass also have particle size distributions that are different from that of traffic exhaust. Urciuolo et al.[145] indicated that the diameter of particles with peak concentration generated from biomass combustion of pine shells was 5 nm and 15 nm and from coal combustion was 4-5 nm. An example study is presented in Figure 2.7.

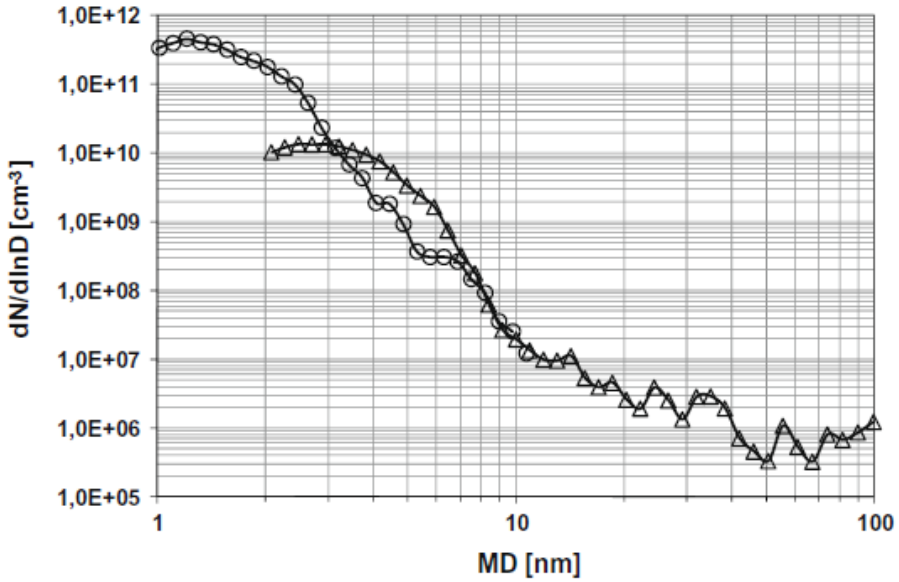

Figure 2.7 Particle size-resolved number concentration in the air flame feeding the Colombian coal[23]. MD: the equivalent diameter of a sphere of equal volume.

Figure 2.7 shows the size-resolved number concentration of particles generated during coal combustion[23]. The study indicated that the number concentration of particles of sizes between 1 nm and 3 nm are significantly high. However, when increasing particle diameter, particle size-resolved number concentrations are reduced by four orders of magnitude. In general, the diameter of most of fuel combustion particles is in the size range of UFPs. Additionally, the local flame temperatures and the oxygen concentration surrounding coal particles would affect the particle formation mechanisms[22].

2.3.2 Indoor main sources

2.3.2.1 Tobacco smoke

Epidemiological and toxicological studies have demonstrated that environmental tobacco smoke (ETS) has a close relationship with many adverse health effects including lung cancer, asthma onset and exacerbation and acute respiratory

illness[112]. Recent studies established that tobacco smoking also caused cancer in the organs of nasal cavities, paranasal sinuses, nasopharynx, liver, stomach, kidney and uterine cervix[133]. Moreover, non-smokers exposed to second-hand smoke are also at the risk of increased morbidity and mortality related with heart disease, asthma, infant death syndrome and other related diseases[133]. The study indicated that non-smokers exposed to secondhand tobacco smoke at the workplace have a 16-19% increase in lung cancer risk. To protect non-smokers from the exposure of second-hand tobacco smoke, many countries have implemented laws to ban indoor smoke in public buildings after 2000.

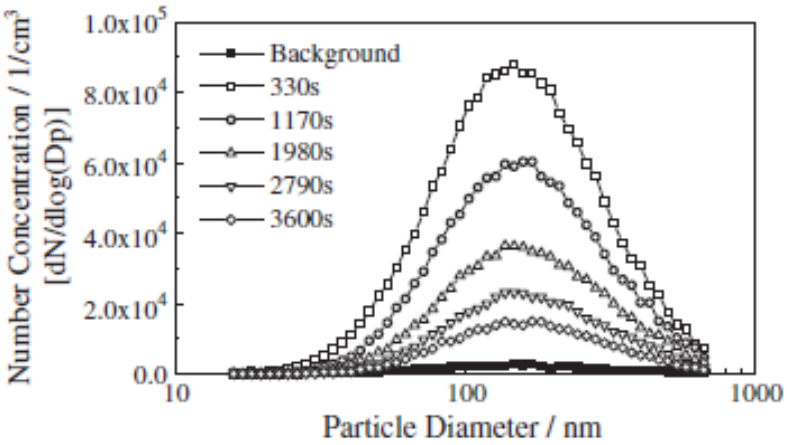

Figure 2.8 Size-resolved number concentration of ETS particles varied with time due to one low-tar cigarette[106].

Figure 2.8 shows that the size-resolved number concentration of ETS particles varied with time in a decay process[106] after the cigarette was extinguished. The presented ETS particles were emitted from a low-tar cigarette. The figure shows that the large number of ETS particles are in the size range of submicron and UFPs.

After the smoking restriction in public buildings, some studies have surveyed that children were still at risk of high exposure to second-hand tobacco smoke in their home[97, 135]. Additionally, in the investigation of 328 asthmatic children living in low-income census tracts of seven U.S. cities, the major indoor particle source was tobacco smoking[151]. The study indicated that poor ventilation was prevalent in the asthmatic children's homes. The poor ventilation was considered to aggravate the children's exposure to the second-hand smoke.

Considering that second-hand ETS could be continuously elevated in residential buildings after the smoke ban, efficient removal of ETS particles through ventilation systems or portable air cleaners is supposed to be an effectual solution to protect people, especially children, from second-hand smoke in residential buildings.

2.3.2.2 Combustion of cooking and candles

Besides tobacco smoke, a large amount of UFPs are also generated from gas stove cooking, especially frying[149, 150], through incomplete combustion of fuel, oil and food. Some epidemiologic studies established that gas stove cooking is associated with some health effects including respiratory diseases and lung cancer [76, 80, 98]. For example, cooking was a significant particle source in homes of 328 surveyed

asthmatic children[151]. Wallace et al.[150] established that cooking were capable to emit about 10^{14} particles over 15 min of the cooking period, furthermore more than 90% of them were UFPs. Figure 2.9 shows the mean source strength (particles/h) and the associated standard deviations for the measured 33 cooking episodes. Comparing the particles in morning and evening cooking over a whole year (600 h) to that in non-cooking period at the same time, the study indicated that cooking was able to generate more than 10 times of UFPs compared with the number which was observed during non-cooking periods.

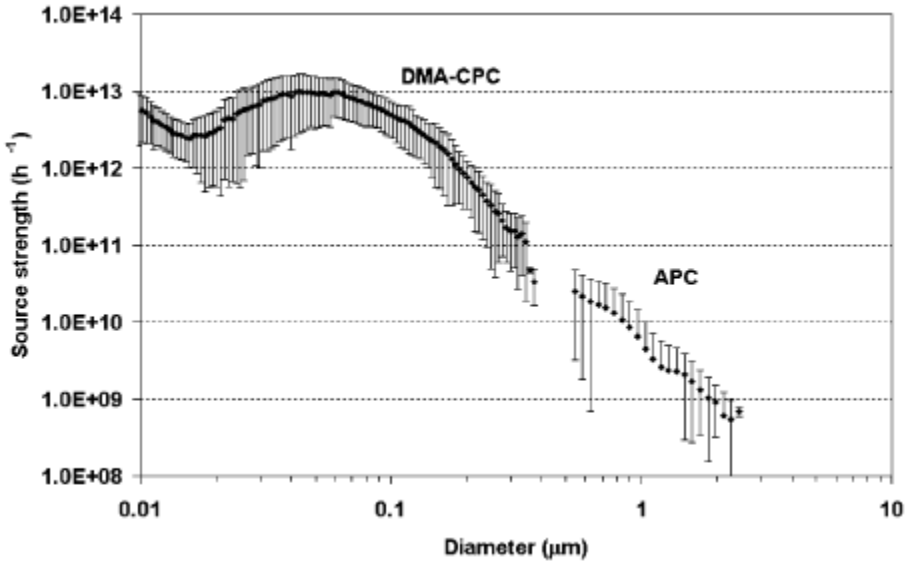

Figure 2.9 Mean source strength (particles/h) and associated standard deviations for 33 cooking episodes employing a differential mobility analyzer linked to a condensation particle counter (DMA-CPC) and an aerodynamic particle counter (APC)[150].

Candle burning is another significant source of UFPs. Incomplete combustion in the flame generates a large amount of soot particles. Soot particles from candles are dominating in size from 0.03 to 3 μm [2]. Thus, there might be a health hazard from candle burning[113, 155]. It is also related with the release of metal additives from the wick and colour pigments. Heavy metals such as zinc, tin and lead are added to the wick to improve mechanical stability in some certain types of candles. The added colouring pigments probably also contain heavy metals.

Pagels J. et al.[113] established the size-resolved particle number concentration for four candles, see Figure 2.10. The experiment was conducted in a chamber with a volume of 21.6m^3 and an air exchange rate of 0.5h^{-1}. Candle I was made up with white pure stearin wax, while Candle II was made up of a wax consisting of a combination of stearin and paraffin. In the figure, the particle size distributions are dominated by particles <1000 nm, especially in the UFPs size range. Additionally, Li and Hopke estimated that, for particle emissions from a steady burning single paraffin wax candle, the initial particle size distribution was around 30 nm in diameter and dominated by UFPs[89].

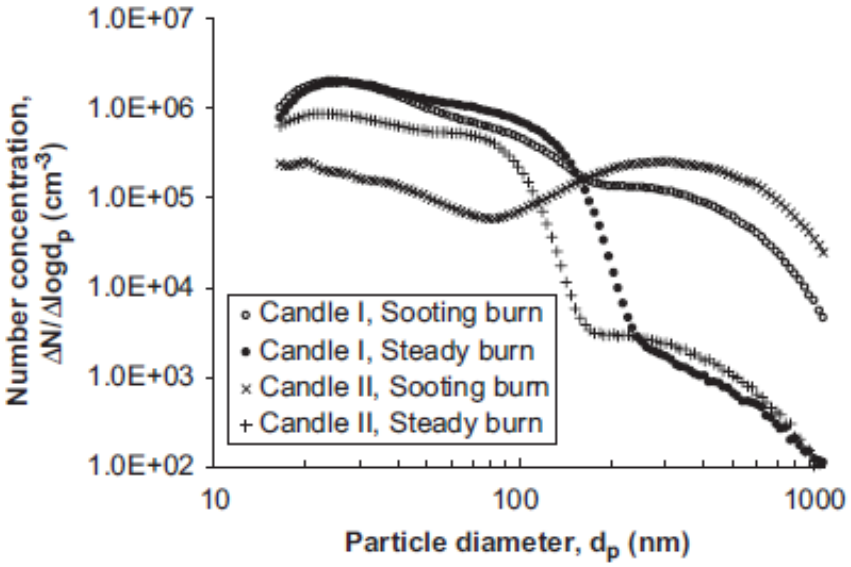

Figure 2.10 Size-resolved particle number concentration in a 21.6 m^3 chamber during steady and sooting burn of four candles. Air exchange rate was 0.5 h^{-1}[113].

2.3.2.3 Printers

In recent years, many researchers have found that laser printers and photocopiers are important indoor sources of particulate matter, ozone, volatile organic compounds (VOCs) and semi volatile organic compounds (SVOCs)[63, 134, 159]. As for the above sources, UFPs dominate the number concentrations of the generated particles. However, the emission rates of particle number are related with printer specific and influenced by toner coverage and cartridge age[63].

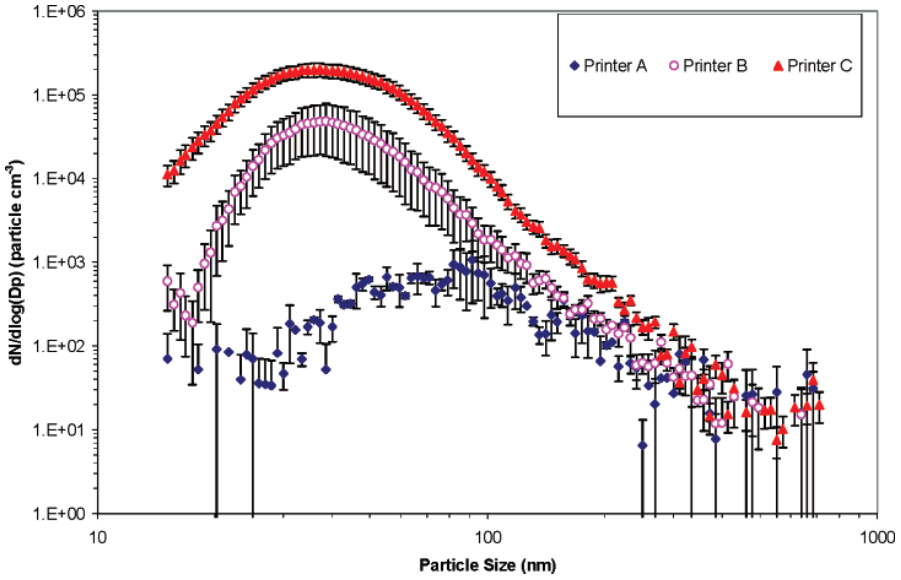

Figure 2.11 Average size-resolved number concentrations of particles generated by the three different printers[63]. Standard errors are presented as error bars.

Figure 2.11 shows the average size-resolved number concentrations and the associated standard errors of particles generated by the printer A-C [63]. The

particles emitted from the three printers have significantly different number concentrations and size distribution. UFPs dominate 76% of number concentration of total submicron particles generated by printer A, while for printer B and C, this value was about 98%-99%. Additionally, the emission rate of printer C is approximately two orders of magnitude higher than that of printer A and one order of magnitude high than that of printer B. Moreover, this study also indicated that the operation with new cartridge and large toner coverage emitted more particles than the operation with old cartridge and small toner coverage.

To understand and control particle generation during printing, some limited studies showed the possible mechanisms of UFPs formation in photocopying[86, 101]. Lee et al.[86] summarized three possible mechanisms: nucleation and condensation of low vapor pressure substances; oxidation of VOC; ion-induced nucleation. Corona devices are suspected to be a critical component in printer because their byproducts, ozone, NO_x, radicals and ions, are closely associated with the second and third mechanisms. As same as the first two mechanisms pointed out by Lee et al.[86], Morawska et al.[101] suspect that the particles are formed through: direct volatilization and nucleation of low vapor pressure substances (e.g. SVOC) from toners; secondary organic particle (SOA) formation through a chemical reaction between VOC and ozone. Additionally, the study established that particle emission rates are closely associated with fuser temperature fluctuation.

2.3.2.4 Cleaning products and air-fresheners

There is an increasing interest on indoor chemical reactions leading to SOA formation. Terpenes, such as pinene and limonene, are widespread used as an additive in detergents and air-fresheners for a pleasant fragrance. Many investigations have indicated that the chemical reaction between terpenes and ozone in the indoor environment generates a great amount of secondary organic aerosol which is dominated in the ultrafine particle size range[100, 132, 143]. At present, limited health effect studies have reported that SOA were not the agents causing adverse effects on mice when they are short-term exposed to a by-product mixture of terpenes and ozone[163]. However, the long-term health effect is still unclear now.

Indoor O_3 concentration is critical to SOA formation. Morawska et al.[100] reported that during cleaning activity utilizing detergents in a school, when indoor O_3 the concentration is less than 0.005ppm, UFPs number concentration only slightly increases. However, if the O_3 concentration is above this level, UFPs are formed at a substantial rate. Furthermore, Langer et al.[84] established that the peak concentration of the generated UFPs was logarithmically related to initial $[O_3]$*[limonene].

Figure 2.12 shows the evolution of particle concentration during the chemical reaction between ozone and limonene in a chamber. The generated SOA were initially dominated in UFPs size range (0.02-0.1 μm in test), and subsequently the particles grew in size. Morawska et al.[100] made a similar observatoin of SOA formation when using detergents for cleaning in a school. Additionally, air relative humidity can effectively influence the growth of SOA[147].

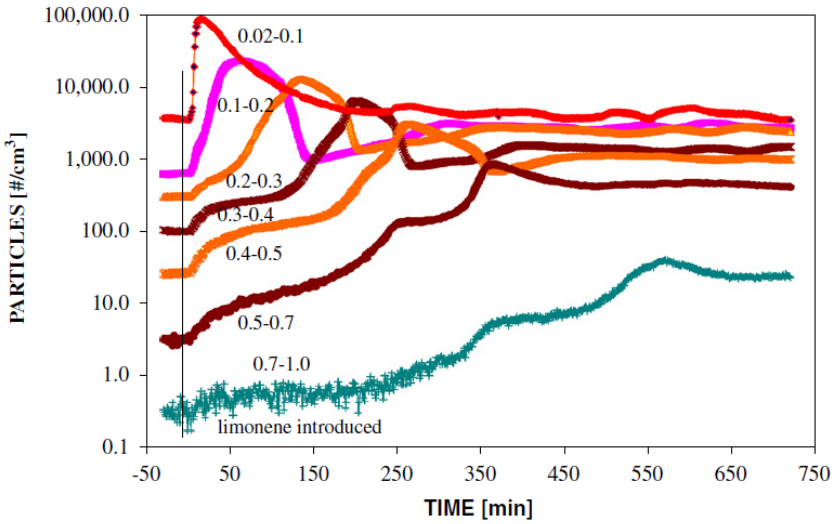

Figure 2.12 Evolution of particle concentration during the chemical reaction between ozone and limonene in a chamber[132]. Initial O_3: 163 ppb; Initial limonene: 155 ppb; Air exchange rate: 0.7 h^{-1}.

2.3.2.5 Industry workplace

UFPs are also generated during the work process in industries. Typically, UFPs are produced in workplaces involving hot processes such as smelting, welding, soldering and plasma spraying. Wake et al.[148] measured that UFP number concentrations were above 5.0×10^5 particles/cm^3 in the process of plasma spraying, galvanizing, welding, steel foundry, welding, plastic welding and hand soldering. Some studies also demonstrated that the number concentration of UFPs in the workplace were $>1.0\times10^5$ particles/cm^3 in a welding process[18], 2.0×10^4-2.8×10^5 particles/cm^3 in an iron foundry process[24], 7.0×10^4-2.8×10^5 particles/cm^3 in an automotive grey-iron foundry process[46]. Additionally, UFPs can also be generated during mechanical processes as such as grinding, cutting and polishing[167]. This study demonstrated that UFPs were generated by various substrates through vaporization or combustion of the substrate material.

2.4 Particle removal techniques

2.4.1 Air filtration

Among various air cleaning techniques, air filtration is the most widely used and developed method for air cleaning. Corresponding to the efficiency from low to high, air filters are classified to be coarse filters (G1-G4), medium filters (M5-M6), fine filters(F7-F9), Efficient Particulate Air (EPA) filter (E10-E12), high-efficiency particulate air (HEPA) filters (H13-H14) and ultra-low penetration air (ULPA) filters (U15-U17) in standards EN779:2012[42] and EN1822-1:2009[44]. In the previous standard EN779:2002[41], both medium filters (M5-M6) and fine filters (F7-F9) are grouped as fine filters or intermediate filters (F5-F9). To the previous standard EN1822-1:1998[43], the E10-E12 filter classes were denoted H10-H12, and were considered to belong to the HEPA filter category.

Among the above filters, the low packing density filters (e.g. coarse, intermediate filters) are commonly used in commercial and residential buildings. They have a wide range of collection efficiencies for ultrafine and submicron particles. HEPA

and ULPA filters are commonly used in indoor environments with special requirements, such as clean rooms in laboratories, factories and hospitals. Additionally, HEPA filters are also often used in portable air cleaners. The filtration efficiencies of HEPA and ULPA filter are substantially high, while the corresponding pressure drops are also high, which means that they are uneconomical to be used in commercial and residential buildings.

There are plenty of theoretical and experimental studies on the air filtration of fibrous filters. The total filtration efficiency is the sum of the particle collection efficiencies achieved by the mechanisms of interception, inertial impaction, diffusion, gravitational settling and electrostatic attraction. The particle collection efficiencies of these five mechanisms are determined by filter media properties, for example fiber diameter, packing density, media thickness, and working conditions, such as air flow velocity. The filtration theory and simulation study are further introduced in Chapter 3.

Filter application decision should be made under consideration of the indoor and outdoor particle concentration[45]. For example, to achieve a moderate indoor air quality, EN13779 recommends two-step filtration by F5 and F7 class filters or at least a single stage filtration by F7 class filter. Additionally, the air leakage in building envelopes and ventilation systems can greatly influence the real application performance of air filters. High air leakage in the building envelope can greatly reduce the performance of class F7 and higher class filters. A 10-mm gap causes a minimum efficiency reporting value (MERV) 15 filter (approximately filter class F9 in EN779) to perform as a MERV 8 filter (approximately filter class G4 in EN779) [153]. More literatures on filter applications are summarized in section 2.5.

A main problem of mechanical air filters is that the dirty filter may act as a pollution source (the clean outdoor air is drawn through the “dirty” filter). Oxidation of pollutants in the filter (e.g. chemical reaction with ozone) results in new pollutants, e.g. odorous ones. Regular replacement of air filters within a suitable time [45] and the application of activated carbon filters[9] are efficient solutions. The detail of the filter by-products and solutions are discussed in 2.6.

2.4.2 Ion generators

An ion generator, also called ionizer, is an electronic device that charges aerosol particles electrically. The work mechanisms are: firstly, airborne particles are charged when ions attach on them; then, the charged particles stick to each other and become big particles, finally, the particles attract to or deposit on the surrounding surfaces, e.g. ventilation duct and filter. The technique has the advantage of potentially high collection efficiency on fine particles and an almost zero pressure drop of the ionizer itself. Ionizers are sometimes used together with air filters in ventilation systems or in portable air cleaners. Many studies have investigated ionization for removal of airborne particles, aeroallergens and airborne microorganisms from indoor air in various settings [3, 55, 85, 114, 115, 138]. The studies found that air filters assisted with ionizers located upstream can enhance the collection efficiency of the filter, while not affect the pressure drop. The most commonly used technique is negative ions discharged by unipolar corona. Additionally, because ionizers may generate by-products, such as ozone and NO_x, low ozone generation is an important evaluation criterion on ionizers.

As a common interesting application at present, ionizer assisted air filtration becomes popularly used in the ventilation systems. However, the long-term performance of this application has been investigated to a little extent only. Also, studies of the suitable filters and ion concentrations are very limited. Thus, to evaluate the present application and support further development, it is in a high requirement to conduct studies on this topic.

2.4.3 Electrostatic precipitators

Electrostatic precipitator is another kind of electronic air purifier utilizing an ionizer. They charge particles in a similar way. Firstly, the particles are charged when they pass through an ionizing mechanism with air flow; then the charged particles pass a group of plates which have the opposite charges, e.g. positively charged plates corresponding to negatively charged particles. Finally, the charged particles stick to the plates by the electrostatic force and are then removed from the air stream. They are capable of efficiently removing fine particles from the air stream and having very low air flow resistance. In many cases, an electrostatic precipitator is used together with an ion generator in ventilation systems or portable air cleaners. The ion generator works as a pre-processor in front of electrostatic precipitator. Ozone is still a potential main by-product of electrostatic precipitators.

2.5 Filter applications and recommendations

Air filters could be a critical factor on indoor air quality. Considering that air filters are commonly used in the supply air of mechanical ventilation systems, they play an important role on the transport of air pollutants from outdoor to indoor or between multi-rooms. Jamriska et al.[74] indicated that the removal efficiency of a “medium” filter (filtration efficiency was 20% according to Australian standard AS1324.2 on Dust No.1) on submicron particles was only 34% in an office building. Furthermore, Fisk et al.[48] established that the indoor submicron particle concentration in a tightly sealed mechanically ventilated building was substantially reduced when replacing a normal filter with ASHRAE dust spot efficiency of 22% with a high efficiency filter with removal efficiency of 95% on particles of 0.3μm in diameter. Afterwards Fisk et al.[47] modelled the performance and costs of filters with different efficiencies. The model study showed that utilizing filters with ASHRAE Dust Spot Efficiency above 85% only modestly incrementally reduced the indoor fine particle concentration, while filters with an efficiency rating of 45% or lower could not efficiently filtrate these particles. Finally, they recommended filters with ASHRAE Dust Spot Efficiencies of 65~85% to effectively control indoor concentration of fine particles. The recommend filters correspond roughly to fine-filters of class F6 and F7 in European standard EN779:2002. The modelling assumed that the infiltration rate was 0.25/h in most cases, which is normal air leakage level of well sealed buildings. Furthermore, Matson and Ekberg[95] measured and modelled that supply air filters of classes F7-F8 may result in about 70% reduction of the indoor concentration of UFPs supplied to the building from outdoors.

The standard EN13779 recommends single-step or multi-step filtration depending on the different outdoor air (ODA) quality and the desired indoor air (IDA) quality, see Table 2.2. The indoor air quality in IDA 1-4 is from high to low. When outdoor air is dusty (ODA2) or seriously polluted by dust or gases (ODA3),

multi-step filtration and alternative filtration technologies (e.g. chemical filters and electrostatic filters) are recommended. For hygienic reasons, the filter in the first filtration step is suggested to be replaced after a maximum of one year, and filter in the second filtration step should be replaced after maximum of two years. Finally, EN13779 stresses that, to achieve moderate indoor air quality, F7 class filters is the minimum requirement when there is only one step of air filtration.

Table 2.2 Recommended minimum filter classes per filter section [45]

Outdoor Air Quality	**Indoor Air Quality**			
	IDA 1 (High)	**IDA 2 (Medium)**	**IDA 3 (Moderate)**	**IDA 4 (Low)**
ODA 1 (pure air)	F9	F8	F7	F5
ODA2 (dust)	F7+F9	F6+F8	F5+F7	F5+F6
ODA3 (very high concentration of dust or gases)	F7+GF+F9[a]	F7+GF+F9[a]	F5+F7	F5+F6
[a] GF= Gas filter (carbon filter) and or chemical filter.				

Besides the outdoor air quality, the air tightness of both the building envelopes and air handling units also greatly influence the removal performance of filters on outdoor origin particles, especially when using filter classes F7 or higher. Ward and Siegel[153] modelled that a 1-mm gap reduced the performance of a MERV15 filter to be that of a MERV 14 filter, while a 10-mm gap caused a MERV 15 filter to perform as a MERV 8 filter. Here, the MERV 8, 14 and 15 filters in ASHRAE standard 52.2 are roughly corresponding to class G4, F8 and F9 filters in European standard EN779.

In summary, the literature showed that under proper operation and low air leakage through building envelopes and air handling units, air filters of class F7 and higher classes are capable to effectively filtrate fine particles. When outdoor air is dirty, pre-filter as well as some alternative filtration techniques are recommended, such as chemical filters and electrostatic filters.

2.6 By-products of used filters

By-products of used filters have attracted wide attention in the HVAC field in recent years because they could be a strong source of sensory pollution in the ventilation system [9, 27, 116]. Many studies have demonstrated that the by-products of used filters were mainly from microbiology grown on the surface of used filters[117] and the chemical reactions between ozone and used filters[9]. They may induce a substantial economic loss[8] though the sick building syndrome[28] and reducing occupant productivity. Clausen et al.[118] stated that cleaning and renovating of the ventilation system was associated with the sick building syndrome in the occupants of an office building. The authors pointed out that removing the pollution source from the ventilation system can substantially improve the air quality in a building.

On one hand, microbial contamination is a common contamination on ventilation filters. The microbial activity increases with increasing air relative humidity, especially when the relative humidity is above 70%. However, this does not mean that keeping the relative humidity in the supply air below 70% can prevent the growth of microorganisms. Some studies showed that the real influential factor on the growth of the organisms was the water content of a material rather than the water in the air [49, 104, 117]. When filters are exposed directly to water, the microorganisms on filters can grow up quickly and become airborne. In turn, the airborne microorganisms can induce health risks [53, 54], for example microfungi can increase the risk of severe allergic reaction. Additionally, during the growth of microorganisms, dirty filters would emit microbial volatile organic compounds (MVOCs) with an unpleasant odor. MVOC is a sensory pollution and can cause eye and upper respiratory tract irritation[82].

On the other hand, some further studies concluded that it was unlikely that microorganisms were the main pollution being responsible for the deterioration of the air quality downstream of a used filter[27, 117]. Some researchers have demonstrated that the chemical reaction between ozone and the chemical composition on used filters should be the main reason. During such chemical reactions, used air filters remove a fraction of ozone from the air stream[69, 71] and at the same time, odors and volatile organic compounds were released from the ventilation filters[70]. Some studies have further shown that the products of this chemical reaction were sensory pollutants[10, 70, 71]. For example, Bekö et al.[10] established that an ozone-treated used filter sample gave an air quality of low acceptability compared to air-treated samples and nitrogen-treated samples in sensory panel tests.

How could we control the by-products of used filters in ventilation systems? Pasanen et al.[116] demonstrated that a pre-filter can effectively protect the fine filter from odor-causing particles. The results showed that the emissions from coarse pre-filters were similar to those from the higher efficiency filters without pre-filters. Furthermore, the emissions of the main filters were significantly lower if they were used together with pre-filter. In the paper, the test results of atmospheric samples showed that the odor emissions per mass unit particles were the highest in the coarse fraction (>10.0 μm) among the particle diameter range of <2.1 μm, 2.1~10.0 μm and >10.0 μm. Additionally, Clausen[27] pointed out that, to reduce the by-products generation, it was critical to remove the collected particles on the filter surface, or prevent ozone from coming in contact with the collected particles. The suggested engineer solutions were removing the particles from the filter surface in a short regular interval or using activated carbon filter to remove ozone.

Using a pre-filter in front of a main filter and replacing the pre-filter with a short interval may be a solution to control the by-products from the used filters. Furthermore, combined active carbon on the pre-filter can further reduce the generation of the by-products. The standard EN13779 recommends that a pre-filter should be used in front of the main filter when the outdoor air is dusty (ODA 2) and with very high concentration of dust or gases (ODA 3). However, single-step air filtration is used in many buildings at current, because it is often believed that a multi-step air filtration system unavoidably costs more than single-step air filtration do. Actually, this worry greatly has blocked the application of multi-step

filtration systems as suggested in EN13779 and should be checked by lifetime cost investigation.

2.7 Single-step and two-step air filtration

To achieve higher filtration efficiency, besides applying a "high" class air filter, another solution is to use a pre-filter together with an intermediate filter. The latter measure has attracted more and more attention in recent years.

It has been suggested that, under suitable operation, the two-step air filtration is probably more economical in the long time operation. Based on this idea, a seminar was organized in ASHRAE 2012 winter conference, Chicago. However, it is not rare that only a single filter is used in HVAC supply-air streams at present. There is a concern that fixing a pre-filter could increase the total cost for the second filter application. But two-step filtration is not inevitably obviously more expensive than that of single-step filtration. Pre-filters can block a large amount of coarse particles, which can greatly reduce the dust loading on the main filter. Thus, the main filter lifetime can be extended.

Compared to single-step high class filters, besides the same high filtration efficiency, two-step filtration has the advantage to limit the by-products emission from used filters. Pasanen et al. (1994) [116] investigated the odor emission during half-year filter operation with and without pre-filters. They found that the pre-filter can effectively protected the fine filter from odor-causing particles. The odor emissions from the coarse pre-filters were close to the emissions from the higher efficiency filter but without pre-filters. Moreover, the odor emissions of the main filters were significantly lower if they were used together with pre-filters. In a study of Bekö et al. [9], they observed that the downstream air of a combination of a pre-filter and an F7 filter was more acceptable than the air passing through a stand-alone F7 filter. And the authors supposed the monthly replacing this pre-filter was one of the reasons.

In the application, the economical cost is influenced by the filter class, surrounding ambient particle concentration, electricity prices and especially the filter lifetime. To keep the filtration economical, the influence of the above factors on the annual total cost needs to be studied. Additionally, since it is common that the pressure drop increases due to dust loading are substantially different between laboratory tests and field filter tests, it is important to conduct the study based on the pressure drop of the field filter tests.

2.8 Indoor particles of indoor/outdoor origin and indoor dynamic fate

Particles of indoor and outdoor origins are associated with various human activities, which are different regarding particle emission times, source strengths and size distributions. For example, traffic exhaust contributes substantially to fine and submicron particles in ambient air, especially during the rush hours. However, indoor particle emission is greatly depending on the occupants' activities. The result from Abt et al. (2000) [1] demonstrated that when air exchange rates were lower than 1 h^{-1}, indoor particle sources (including cooking, cleaning and movement of people) contributed to 57-80% of the indoor coarse particles, and to 8-37% of the indoor 0.02-0.3μm particles. Up to now, numerous

previous studies also have shown that particles from different indoor/outdoor emission sources have different particle size distribution and chemical compositions, and they could result in different health effects [4, 7, 30, 40, 79, 98, 103, 133, 150, 154, 165].

At present, some studies have investigated the contributions of indoor generated particles and outdoor particles penetrated to the indoor environments, while few of them discussed how to control indoor particles according their origins [1, 92, 128]. In addition, many researchers studied lots of advanced ventilation measures to control total indoor particles, however few of them investigated the efficiencies of these systems to remove indoor particles contributed by indoor sources and outdoor sources respectively [93, 107]. Therefore, it is valuable to combine the above two topics to fill the gap.

Indoor particles from indoor emission and outdoor infiltration have different air dynamic transmission routes. For all indoor particles, the common dynamical mechanisms include indoor deposition, recirculated air filtration, indoor particle exfiltration and exhaustion. The distinctive transmission route for outdoor origin particles are outdoor/supply air filtration and outdoor particle infiltration. Here, outdoor particle infiltration includes the penetration of outdoor particles through the building envelope and outdoor supply air. Therefore, the optimal filter locations, classes and ventilation modes would be different to remove indoor generated particles and outdoor infiltration particles. Therefore, it is important to develop the knowledge on how to operate air filtration and ventilation to best control indoor generated particles and outdoor infiltration particles simultaneously.

2.9 Discussion and summary

The toxicity of particles depends on particle physical and chemical properties generated by specific particle sources. Up to now, many epidemiological and toxicological studies show that the UFPs generated by combustion are probably the most hazardous particles compared to particles in other fractions and generated by other particle sources. These combustion sources mainly include diesel fuel, coal and gasoline as well as environmental tobacco smoke. Therefore, special attention should be granted to the particles generated from outdoor traffic and indoor cooking and smoking.

Air filtration is the commonest particle capturing technology at present. However, both the products in the market and filter standards lack description or requirement on the performance to filtrate UFPs. It is important to conduct a study to fill in this gap.

Specific control of indoor and outdoor origin UFPs in indoor environments is motivated by that the particles from indoor and outdoor sources have different particle properties, different emission intervals and different association with occupants' activities. Because indoor particles from indoor emission and from outdoor infiltration have different air dynamic transmission routes, it is reasonable to manage the air filtration at the most efficient filtration locations to filtrate the particles from the two source types.

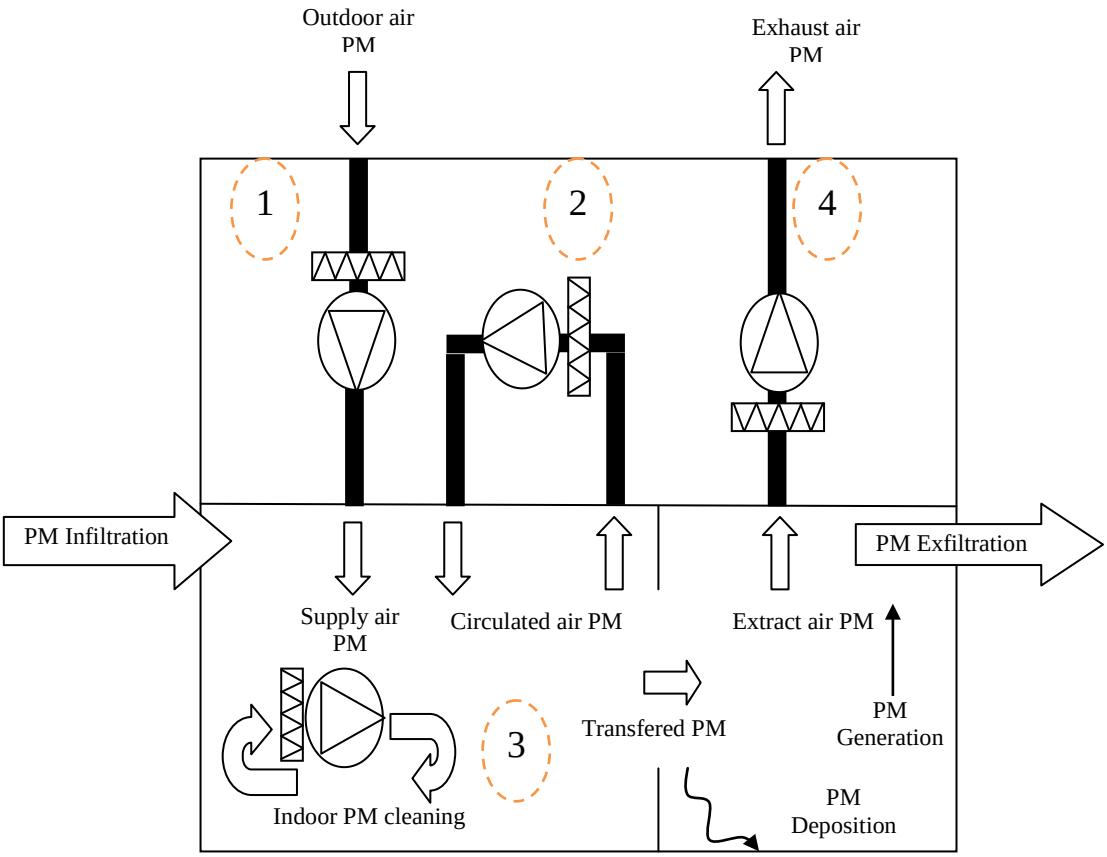

Figure 2.14 Schematic of particulate matter (PM) transportation in buildings

Figure 2.14 shows a schematic of particulate matter transportation in buildings. In the figure, we assume air filters are placed in locations 1-4. Filter #2 in the recirculated air works in principle as a room air cleaner, i.e. as Filter #3. In the figure, outdoor-generated and indoor-generated particles are filtrated by filters in different locations. Outdoor-generated particles are removed by filters in locations 1-4, while indoor particles are only removed by filter in locations 2-4.

According to the literature study, the following air filtration applications are valuable to be studied.

1. Specific selection of filters, filter locations and ventilation modes to remove indoor particles of outdoor and of indoor origins.
2. Economical cost of single and multi-step filters to filtrate particles in the filter lifetime and optimal choices of filter combinations under different operation environments.
3. The application of ionizer assisted air filtration in a field ventilation system and recommendations regarding this application.

3 Single-fiber air filter theory

Numerous theoretical and experimental studies have been conducted on the filtration of fibrous filters during the past 50 years [6, 65, 87]. Normally, the total filtration efficiency is considered to be built up by five aerosol collection mechanisms: interception, inertial impaction, diffusion, gravitational settling and electrostatic attraction. In general, increasing particle size could enhance the particle collection by the interception and inertial impaction mechanisms, while reducing particle size could enhance particle collection by Brownian diffusion. Additionally, the effects of the five collection mechanisms on the total filtration efficiency are closely related to the characteristics of filter medium and filter operation conditions. This chapter introduces the single-fiber filtration theory from Hinds,1998[65] and compares the measured total filtration efficiency with the theoretical calculated value for three filter medium types: glass fiber filter, charged synthetic filter and uncharged synthetic filter.

3.1 Single-fiber efficiency theory

The filtration efficiency in single fiber efficiency theory is determined by the characteristics of filter media and operation conditions, i.e. fiber diameter (d_f), packing density (α), filter medium thickness (t), face velocity (U_o) and particle diameter (d_p). For fibrous filter, α is defined according to eq. 3.1 and typically between 0.01 and 0.3.

$$\alpha = \frac{fiber\ volume}{total\ volume} = 1 - porosity \qquad (eq.\ 3.1)$$

Face velocity is the air velocity at the filter cross-section perpendicular to the airflow, which is represented by eq. 3.2.

$$U_0 = \frac{\dot{V}}{A} \qquad (eq.\ 3.2)$$

Where $\dot{V}$ is the volumetric flow rate through the filter and A is the cross-sectional area of the filer exposed to the entering airstream. When testing a plane sheet of filter medium, the face velocity is the same as the velocity through the filter medium.

To the above five mechanisms of interception, inertial impaction, diffusion, gravitational settling and electrostatic attraction, the former four mechanisms are mechanical collection mechanisms and the latter one is electrostatic collection mechanisms.

3.1.1 Interception mechanism

Interception occurs when a particle follows a gas streamline that happens to come within one particle radius of the surface of a fiber, see Figure 3.1. Interception is an important collection mechanism in the size range closed to MPPS and is the only mechanism that does not depend on flow velocity U_o.

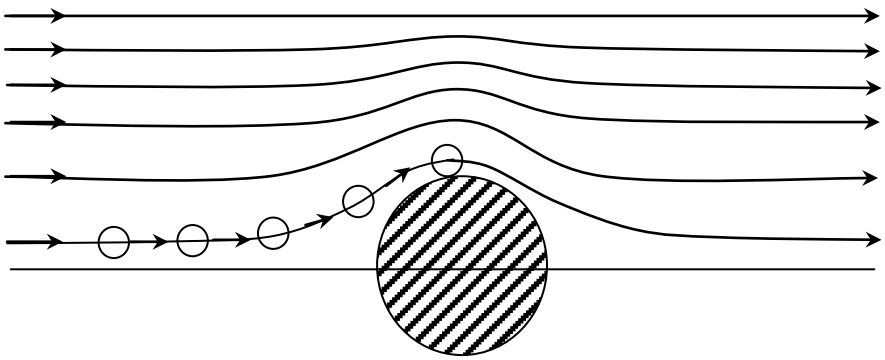

Figure 3.1 Single fiber collection by interception[65]

E_R is the single-fiber efficiency for interception which is defined according to eq.3.3.

$$E_R = \frac{(1-\alpha)R^2}{Ku(1+R)} \qquad \textit{(eq. 3.3)}$$

Where, R and Ku are dimensionless parameters. R describes the ratio of particle diameter to fiber diameter, and Ku represents the compensation for the effect of distortion of the flow field around a fiber because of its proximity to other fibers. They are defined according to eq. 3.4 and 3.5.

$$R = \frac{d_p}{d_f} \qquad \textit{(eq. 3.4)}$$

$$Ku = -\frac{\ln\alpha}{2} - \frac{3}{4} + \alpha - \frac{\alpha^2}{4} \qquad \textit{(eq. 3.5)}$$

3.1.2 Inertial impaction mechanism

Inertial impaction mechanism occurs when the particle is unable to adjust quickly enough to the abruptly changing streamlines near the fiber and crosses those streamlines to hit the fiber because of its inertia (see Figure 3.2).

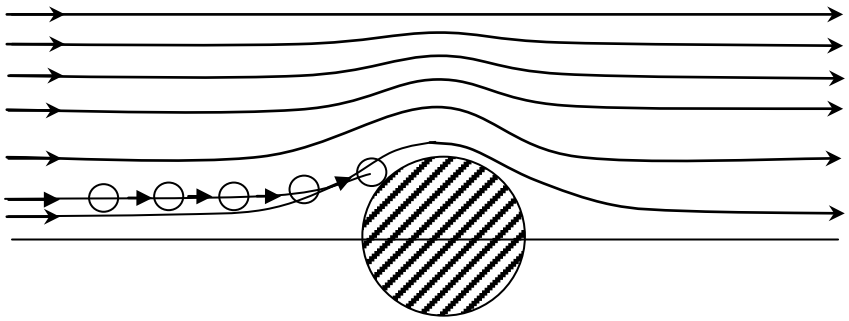

Figure 3.2 Single fiber collection by inertial impaction[65].

The single-fiber efficiency for impaction (E_I) is defined according to eq. 3.6.

$$E_I = \frac{(Stk)J}{2Ku^2} \qquad \textit{(eq. 3.6)}$$

Where, *Stk* is Stokes number which represents the ratio of the "persistence" of a particle to the size of the target. It is defined according to eq. 3.7. τ represents relaxation time; ρ_p is the density of particles; C_c indicates Cunningham correction factor; μ represents viscosity. Additionally, *J* is a symbol representing the results of eq. 3.8 when *R* is less than 0.4. When *R*>0.4, the equation become complex. For approximations the value *J* =2.0 may be used for *R*>0.4.

$$Stk = \frac{\tau U_o}{d_f} = \frac{\rho_p d_p^2 C_c U_o}{18\,\mu d_f} \qquad \textit{(eq. 3.7)}$$

$$J = (29.6 - 28\alpha^{0.62})R^2 - 27.5R^{2.8} \quad \text{for } R<0.4 \qquad \textit{(eq. 3.8)}$$

3.1.3 Diffusion mechanism

The Brownian motion of small particles can greatly enhance the probability of their hitting a fiber while travelling past it on a nonintercepting streamline. The diffusion mechanism is illustrated in Figure 3.3 and defined according to eq. 3.9.

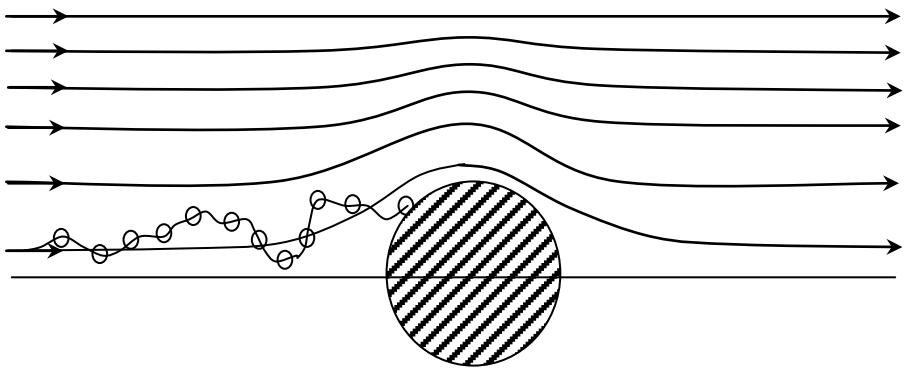

Figure 3.3 Single fiber collection by diffusion mechanism[65].

E_D is the single-fiber efficiency for diffusion, which is defined according to eq.3.9.

$$E_D = 2Pe^{-2/3} \qquad \textit{(eq. 3.9)}$$

Here, *Pe* is the dimensionless Peclet number. It is calculated as:

$$Pe = \frac{d_f U_o}{D} \qquad \textit{(eq. 3.10)}$$

Where, *D* is the particle diffusion coefficient. To determine the collection efficiency near MPPS, it is necessary to include an interaction term to account for enhanced collection to interception of the diffusing particles, see eq. 3.11.

$$E_{DR} = \frac{1.24R^{2/3}}{(KuPe)^{2/3}} \qquad \textit{(eq. 3.11)}$$

3.1.4 Gravitational settling mechanism

Gravitational settling is another mechanism for particle deposit on a fiber. The single-fiber efficiency for gravitational settling (E_G) is defined according to eq. 3.12.

$$E_G \approx G(1+R) \qquad \textit{(eq. 3.12)}$$

Where, G is a dimensionless number controlling deposition due to gravitational settling. Here, V_{TS} represents terminal settling velocity; g is acceleration by gravity; p is the subscript presenting particles.

$$G = \frac{V_{TS}}{U_o} = \frac{\rho_p d_p^2 C_c g}{18\mu U_o} \qquad \textit{(eq. 3.13)}$$

3.1.5 Electrostatic mechanism

Electrostatic deposition is important, but is difficult to quantify because it requires knowing the charge on the fiber and on upstream particles. Usually, electrostatic collection is neglected, unless the particles or fibers have been charged in some quantifiable way. The single-fiber efficiency for electrostatic deposition (E_q) is defined according to eq. 3.14.

$$E_q = 1.5\left[\frac{(\varepsilon_f - 1)}{(\varepsilon_f + 1)}\frac{q^2}{12\pi^2 \mu U_0 \zeta_0 d_p d_f^2}\right]^{1/2} \qquad \textit{(eq. 3.14)}$$

where ε_f is the relative permittivity (dielectric constant) of the fiber; q is the charge on the particle; ζ_0 is the permittivity of a vacuum.

3.1.6 Total filtration efficiency

Finally, the single fiber efficiency (E_Σ) is built up by the above five mechanisms. The definition of E_Σ is represented by eq. 3.15. And a simple calculation in eq. 3.16 is often used.

$$E_\Sigma = 1-(1-E_R)(1-E_I)(1-E_D)(1-E_{DR})(1-E_G) \qquad \textit{(eq. 3.15)}$$

$$E_\Sigma \approx E_R + E_I + E_D + E_{DR} + E_G \qquad \textit{(eq. 3.16)}$$

In conclusion, the overall efficiency of a filter (*EF*) is calculated by e.q. 3.17, in which *EF* is a function of the single-fiber efficiency E_{Σ}. Here, *P* is the overall filter penetration rate.

$$EF = 1 - P = 1 - \exp(\frac{-4\alpha E_{\Sigma} t}{\pi d_f}) \qquad \textit{(eq.3.17)}$$

Figure 3.4 shows the filter size-resolved efficiency for two face velocities based on mechanical filtration mechanisms. It indicates that for non-charged filters, the MPPS increases with decreasing flow rate, and mainly lies within the range of 100-300 nm.

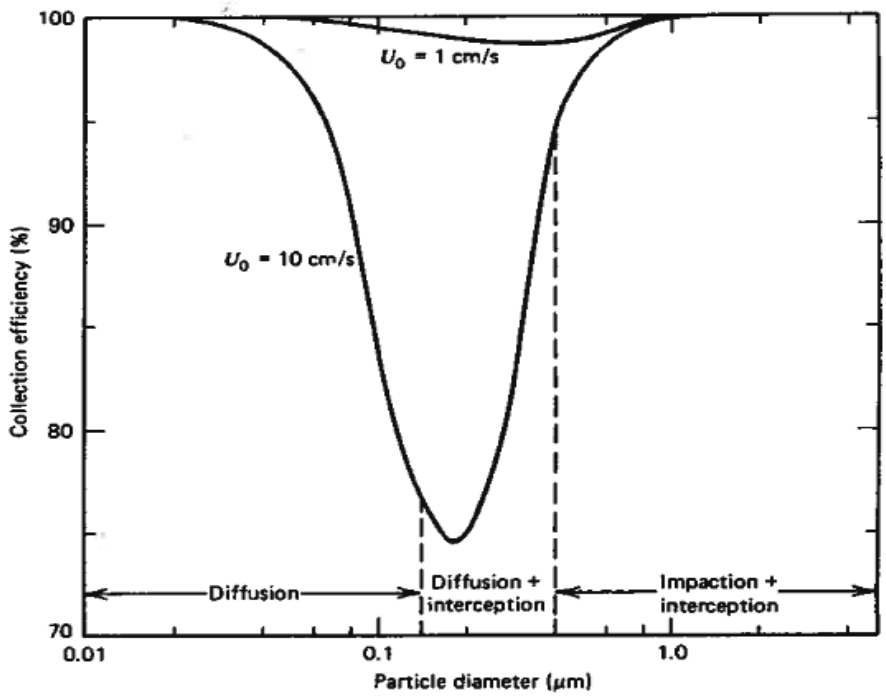

Figure 3.4 Filter efficiency versus particle size for face velocities of 0.01 and 0.1 m/s; t=1 mm, α=0.05, and d_f=2 μm.[65]

3.2 Filter medium measurement and simulation

In this section, three common media of F7 class filters are analyzed for the calculation of filter size-resolved efficiency according to the above single-fiber efficiency theory. Figure 3.5 shows scanning electron microscope (SEM) images for the three F7 class filter media: glass fiber, uncharged synthetic fiber and charged synthetic fiber.

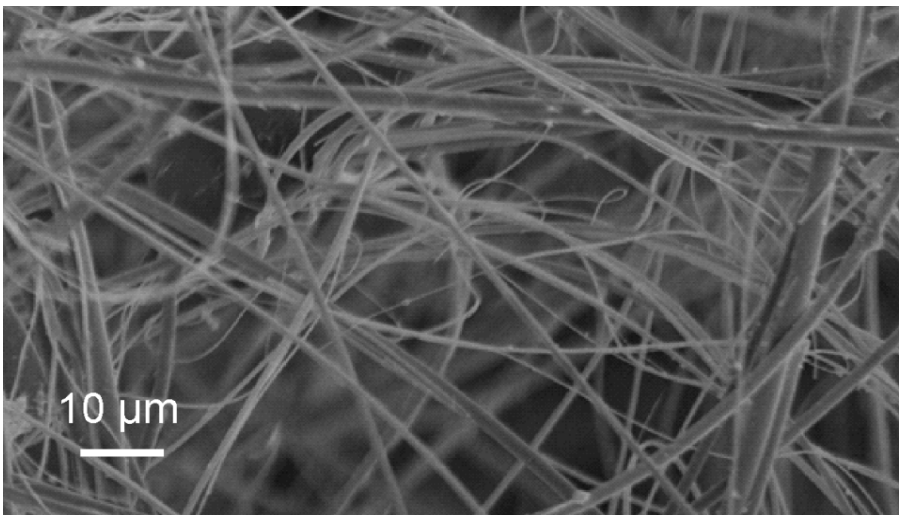

(a)

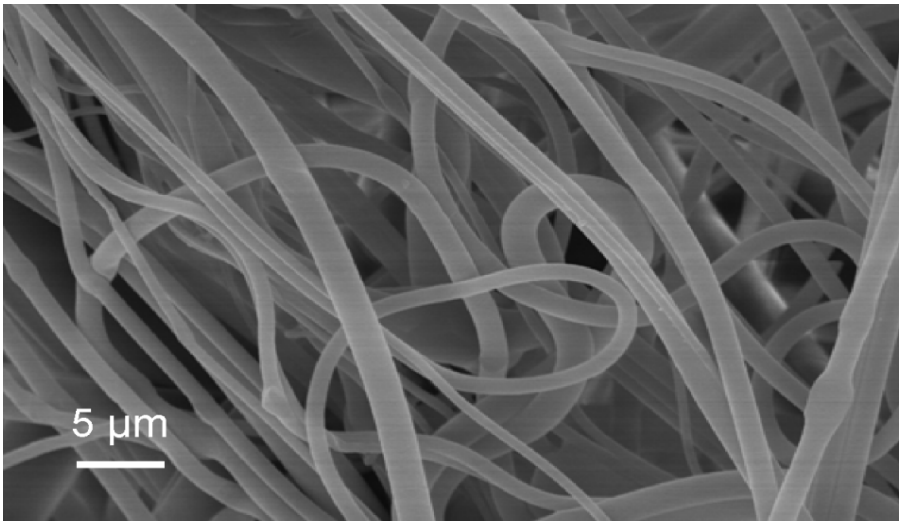

(b)

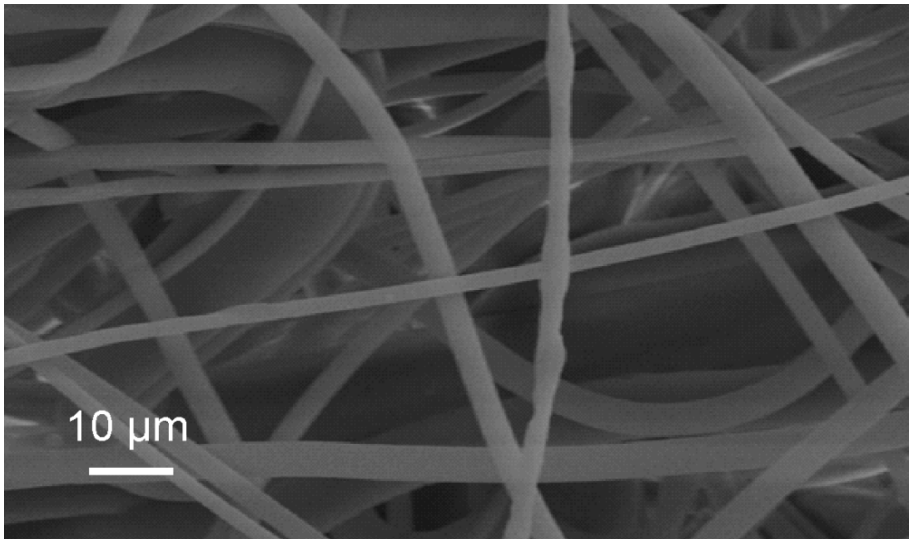

(c)

Figure 3.5 Scanning electron microscope (SEM) images for F7 class filters of three media types (a) glass fiber; (b) uncharged synthetic fiber; (c) charged synthetic fiber.

The characteristics of the three filter media are shown in Table 3.1. The packing density is calculated according to eq. 3.1. Using the data in Table 3.1 as input data to eq. 3.1-3.15, the theoretical efficiencies of the three filter media are calculated. Figure 3.6 shows the calculated efficiencies and the corresponding measured efficiencies.

Table 3.1 Characteristics of the three filter media shown in Figure 3.5.

Filter medium	Class	Thickness (mm)	Fiber diameter (μm)	Calculated packing density
Glass fiber	F7	4.3	2.2	0.010
Uncharged synthetic fiber: Polypropylene	F7	0.4	2.0	0.054
Charged synthetic fiber: Polypropylene	F7	0.6	2.5	0.026

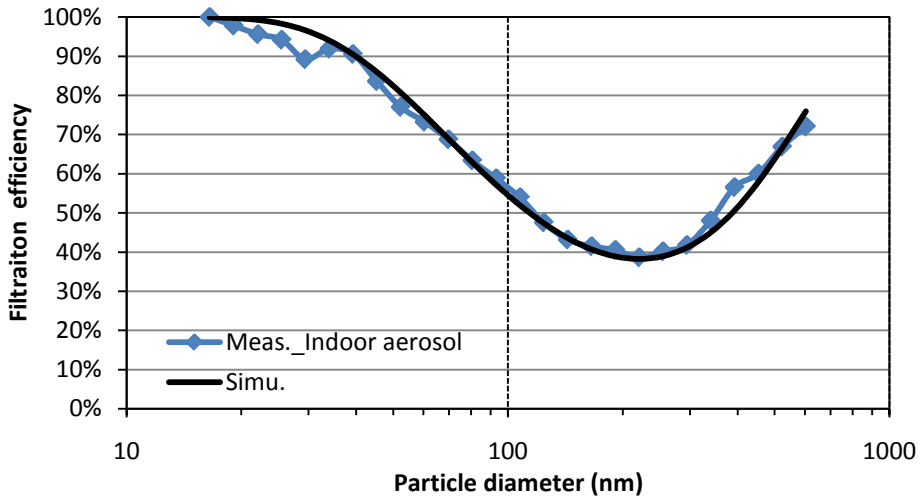

(a)

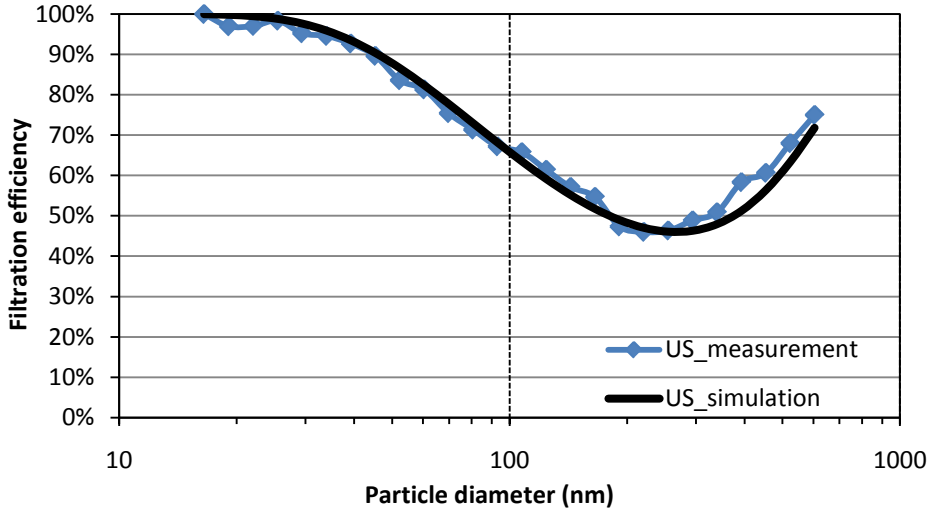

(b)

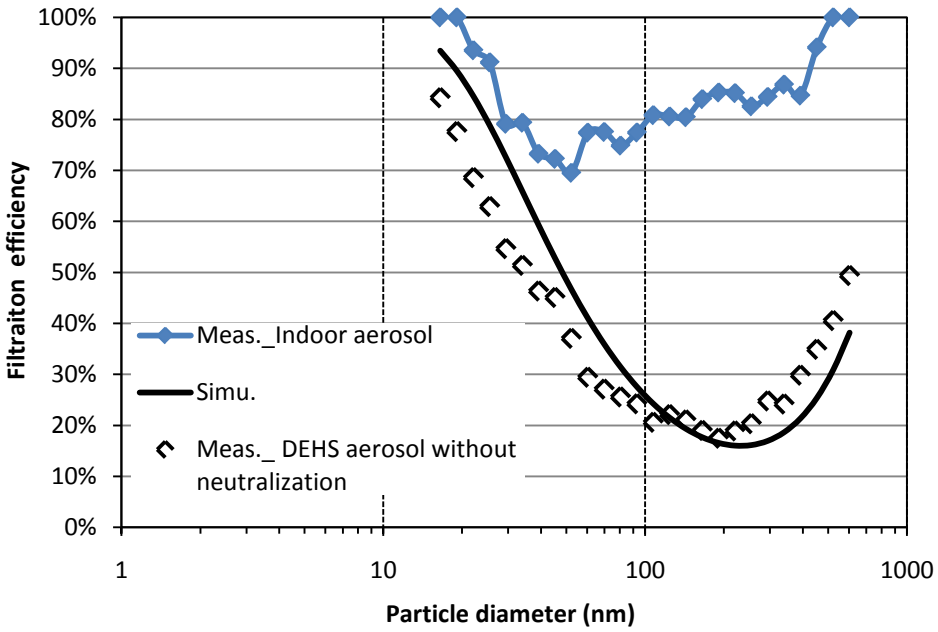

(c)

Figure 3.6 Calculated (simulated) and measured efficiency of F7 class filters of the media: (a) glass fiber (GF), (b) uncharged synthetic fiber (US) and (c) charged synthetic fiber (CS). The simulation air velocity through the filter medium is 0.123 m/s. The measured indoor aerosol data comes from a filter sheet test with indoor aerosol at air velocity of 0.123 m/s. The measured DEHS aerosol data comes from a full scale filter test using non-neutralized DEHS aerosol at an air velocity of 0.12 m/s through the filter medium.

In Figure 3.6 (a) and (b), for glass fiber filter and uncharged synthetic fiber, the measurement and simulation curves are overlapping each other. In Figure 3.6 (c), the calculated efficiency based the mechanical mechanisms is much lower than the efficiency measured with the indoor aerosol. However, the calculated efficiency is close to the efficiency measured in a full scale filter test with non-neutralized Di-Ethyl-Hexyl-Sebacat (DEHS) aerosol. This aerosol can be assumed to have substantially less, or even no, electrostatic charges. This means that the difference between the measured and the calculated efficiency values shown in Figure 3.6(c) probably is the particle collection efficiency due to the electrostatic mechanism. It is also indicated that the electrostatic mechanism has high collection efficiency on the large particles.

Compared to Figure 3.6 (a), Figure 3.7 further demonstrates the contribution to the total particle collection efficiency from the four mechanical filtration mechanisms of the studied F7 glass fiber filter. UFPs are almost completely collected by diffusion; particles with diameter between 0.1μm and 0.4 μm are mainly collected by diffusion and interception; particles with diameter larger than 0.4 μm are mainly collected by interception and impaction; gravitational settling has big impact on coarse particles. In the figure, the total simulation efficiency is the sum of the collection efficiencies for the four mechanisms.

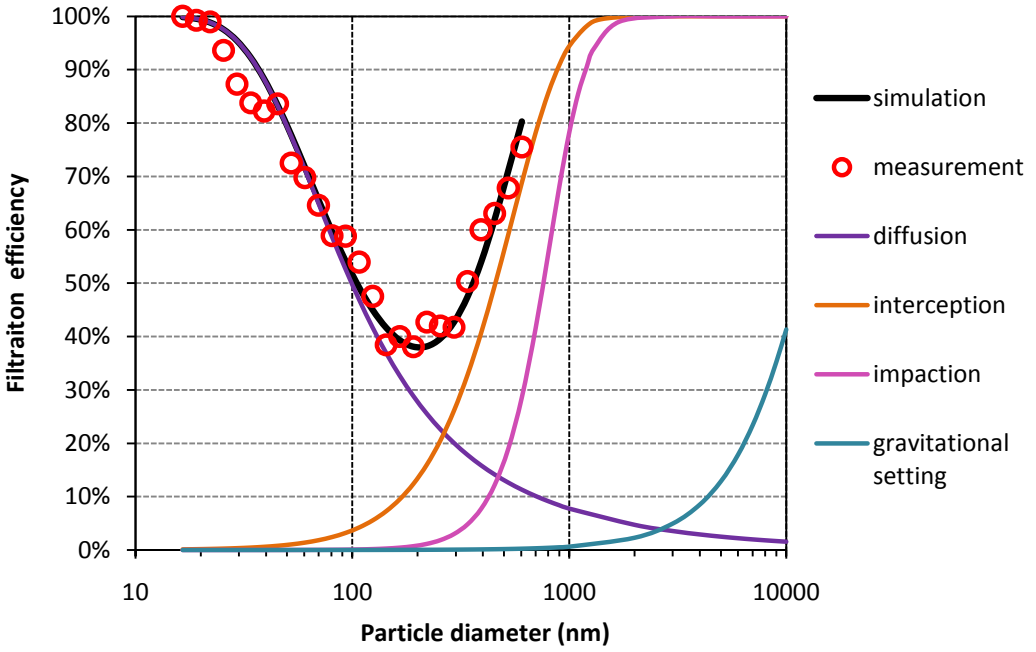

Figure 3.7 Calculated (simulated) and measured efficiency of a glass fiber filter of class F7. The particle collection efficiencies for the four mechanical collection mechanisms are also presented individually.

Figure 3.8 shows the calculated efficiency of a glass fiber filter of class F7 at four air velocities. In the figure, MPPS is reduced with increasing air velocity. Hinds (1998)[65] demonstrated for non-charged fibers, that the MPPS would be reduced with increasing airflow rate.

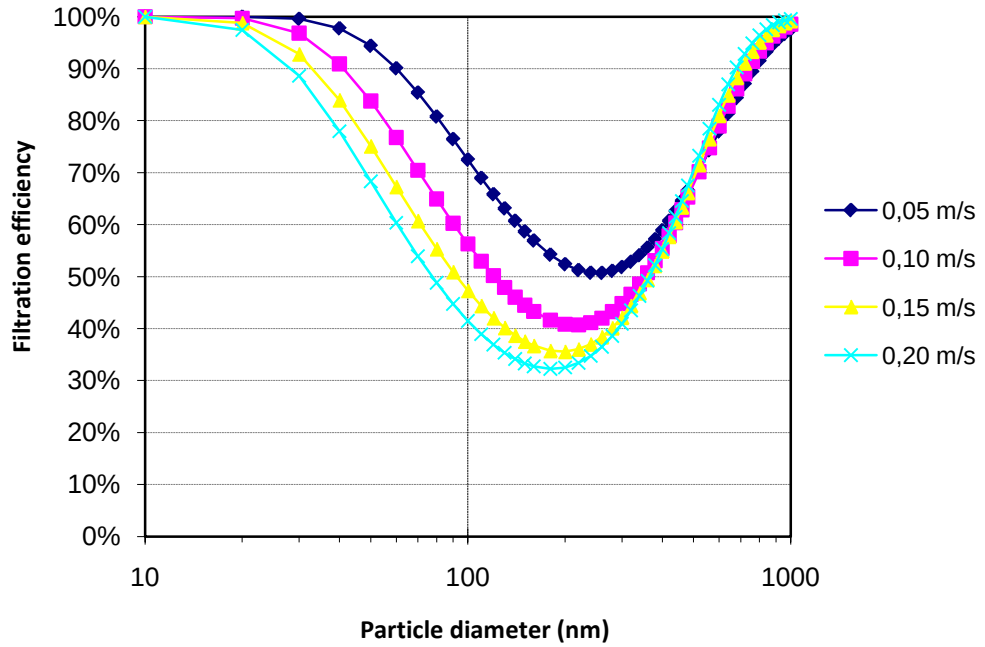

Figure 3.8 Calculated efficiency of a glass fiber filter of class F7 at four air velocities: 0.05 m/s, 0.10 m/s, 0.15 m/s and 0.20 m/s.

3.3 Conclusions

The single-fiber filter theory can predict the size-resolved filtration efficiency well, and the importance of the collection efficiencies from individual mechanisms can be demonstrated. The electrostatic force has big influence on the shape of the efficiency curves of charged synthetic filters. Compared to uncharged filter media, it is difficult to quantify the filtration efficiency of charged filter media, because it is usually hard to know the charge on the fibers and on the upstream particles.

Since the filtration efficiencies of charged synthetic filters can be expected to drop after a short running time[124, 125], the new European standard EN779:2012[42] supplements a minimum requirement on the discharged efficiency. The comparison study in Figure 3.7 (c) demonstrates that the measured efficiency in a test with non-neutralized DEHS aerosol in the upstream air can preliminary predict the discharged efficiency of charged synthetic filters.

4 Experimental methods and equipment

The filtration efficiencies of intermediate air filters in class F5~F9 according to EN779:2002[41] on submicron and UFPs were investigated in full-scale filter experiments and filter sheet experiments. 23 sheet filters of the media of glass fiber filters, charged and uncharged synthetic filters were tested in a small-scale filter test rig. Eight full scale filters of the media of glass fiber filters and charged synthetic filters were measured in a full-scale filter test rig. Two DEHS aerosols and a NaCl aerosol were applied in the full-scale filter experiments. A field indoor aerosol and thermally generated oil aerosol were used in the filter sheet experiments.

4.1 Full Scale Filter experiment

4.1.1 Experiment system

The experiments were conducted in a full-scale filter test rig with the experimental setup shown in Figure 4.1.

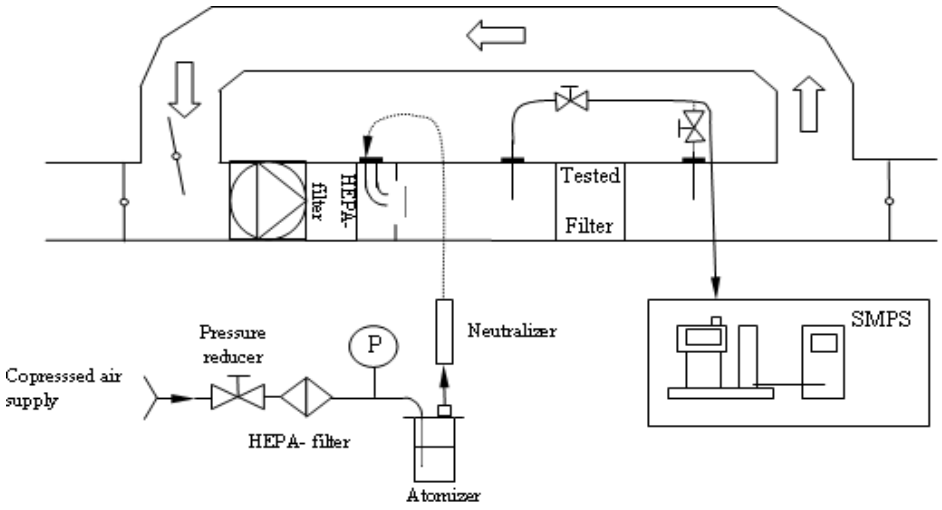

Figure 4.1 Schematic of the full-scale filter testing system in Chalmers laboratory.

The test-rig is located in the laboratory of Building Services Engineering at Chalmers University of Technology, Göteborg, Sweden. The test rig was constructed in accordance with the European filter standard EN779:2002[41]. The duct of the test-rig has the size of 600 mm×600 mm to mount full scale filters. The air was recirculated in the experiments. A HEPA filter of class H14 was used upstream to provide clean air before the test aerosol injection. The air filters were tested under three air flow rates: 0.5 m^3/s, 0.944 m^3/s and 1.3 m^3/s, which are corresponding to the air velocity through filter medium of 0.08m/s, 0.16m/s and 0.22m/s respectively. The air flow rate 0.944m^3/s is the nominal filter test air flow rate according to EN779:2002[41].

4.1.2 Particle measurements

The upstream and downstream particle concentrations and size distributions were measured by a Scanning Mobility Particle Sizer (SMPS) spectrometer (Model:

SMPS 3936, TSI, USA) including a Kr 85 neutralizer (TSI 3077A), a long Differential Mobility Analyzer (DMA) and a Condensation Particle Counter (CPC, TSI 3775). The SMPS was adjusted to measure particles in the size interval 14 nm to 673 nm with 16 channels per decade. Furthermore, the function of the test-rig was verified by a set of measurements as indicated in Table 4.1.

Table 4.1 Full-scale filter test-rig qualification. The reference values are adopted from EN779:2002[41].

Items	Equipment/lab	Measured value	Reference value
Air velocity uniformity	Hot wire anemometer	<8%	<10%
Aerosol uniformity in the test rig	Condensation particle counter (P-Trak)	<12%	<10%
SMPS calibration	TSI annual testing certification	–	–
SMPS zero test	HEPA filter and SMPS	0	<10 pc/cc
100% efficiency test	HEPA filter in test-rig + SMPS	–	>99%
Zero % efficiency test	No filter in test-rig + SMPS	<3%	<3%

4.1.3 Full scale air filters

Eight new intermediate full scale filters provided by three major Swedish filter manufactures were tested. The filter classes and filter media types are shown in Table 4.2. The filters were of class F5-F9 according to the European filter standard, EN 779:2002[41], which roughly corresponds to MERV9-MERV15 according to the US-standard, ASHRAE 52.2[5]. Table 4.3 shows the properties of these full scale air filters.

Table 4.2. Tested full-scale bag filters; filter classes, media types, dimensions and manufactures.

Filter code	Filter class		Filter media type	Filter size, L·H·D (mm)	Nr. of filter bags	Manu. code
	European standard EN 779	US standard ANSI/ASHRAE 52.2				
#1	F5	MERV 9-10	CS	592×592×500	4	B
#2	F6	MERV 11-12	CS	592×592×635	8	B
#3	F6	MERV 11-12	GF	592×592×500	10	C
#4	F7	MERV 13	CS	592×592×635	8	B
#5	F7	MERV 13	GF	592×592×500	10	C
#6	F8	MERV 14	CS	592×592×635	8	B
#7	F8	MERV 14	GF	592×592×450	8	A
#8	F9	MERV 15	CS	592×592×635	8	B

GF: glass fiber filter; CS: charged synthetic filter.

Table 4.3 The properties of the tested full-scale bag filter media. Pressure drop for the full scale filter was measured at 0.944m^3/s.

Filter code	Fiber diameter (µm)	Thickness (mm)	Packing density	Pressure drop (ΔPa)
#1	5-10	1.3	0.013	64
#2	5-10	1.8	0.035	75
#3	5-10	4.1	0.01	118
#4	1-5	3.8	0.026	98
#5	1-5	4.4	0.01	125
#6	1-5	2.6	0.011	152
#7	1-5	4.3	0.011	204
#8	1-5	1.5	0.015	180

4.1.4 Test Aerosols

Two DEHS aerosols and a NaCl aerosol (solution: 1% of NaCl) were generated by an atomizer (Model: ATM 230, Topas, Germany). In parallel experiments, the filters were challenged to the neutralized and unneutralized DEHS and NaCl aerosols. Experiments were made both with and without neutralization of the two aerosols. A Kr-85 neutralizer of model TSI 3012A was used for this purpose.

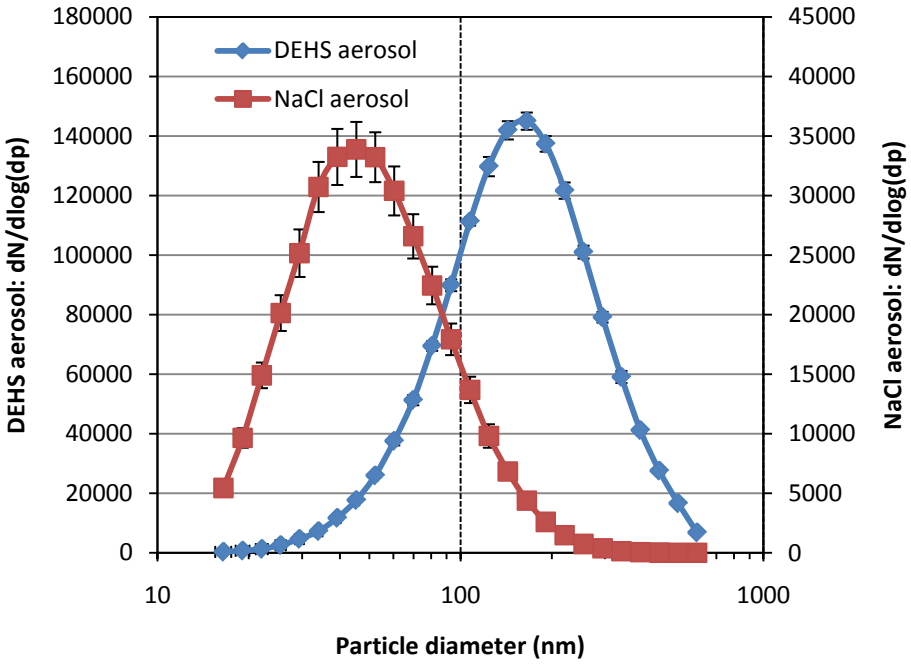

Figure 4.2. Particle size-distributions of DEHS aerosol and NaCl aerosol. The error bar describes the variation of upstream samples in repeatable tests for a filter sample.

Figure 4.2 shows the particle size-distributions of the two aerosols. In the figure, the average value and the standard variation are obtained from 10 continuously measured upstream samples and the standard variation is less than 3%. The peak concentration of the NaCl aerosol is around 40nm, which is much smaller than that of the DEHS aerosol.

4.1.5 Calculation of efficiency values

Based on consecutively taken upstream and downstream aerosol samples, the filtration efficiency (*EF*) was calculated according to eq. 4.1.

$$EF = 1 - n_2/Average(n_1, n_3) \qquad (eq.\ 4.1)$$

The value n_2 represents a downstream sample, while n_1 and n_3 belongs to upstream samples which are taken before and after sampling downstream. The sampling continued until the relative standard deviation of two sequential efficiencies (calculated for the total particle concentration) was less than 15%, and the average efficiency was considered as the qualified efficiency. The uncertainties were established as the standard deviation expressed as efficiency percentage units.

4.2 Filter sheet test

4.2.1 Laboratory and test-rig

The experiments were conducted in an over pressurized laboratory room (5m·7m·3m) at SP The Swedish National Technical Research Institute, located in a suburb of Borås, Sweden. Figure 4.3 shows a sketch of the small-scale filter test-rig that was built up in the laboratory room solely for the purpose of the experiments presented in the next two chapters.

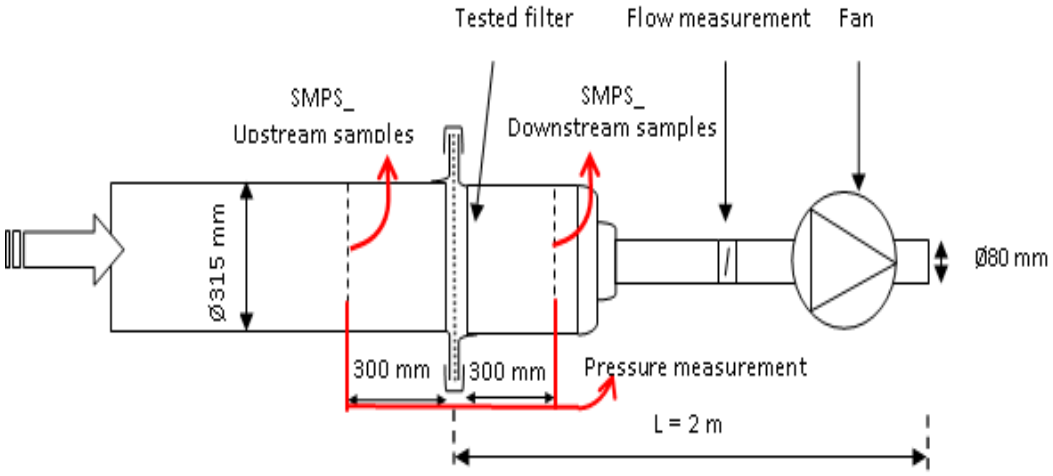

Figure 4.3. Schematic of filter sheet testing system in SP laboratory.

Laboratory room air was supplied to the test-rig by a fan placed at the far downstream side of the rig. The test-rig had a circular duct with the diameter 315 mm, where the filter samples were mounted. All tests were carried out at an air velocity of 0.123 m/s through the filter medium. The function of the test-rig was verified by a set of measurements as indicated in Table 4.4.

Table 4.4. Filter sheet test-rig qualification. The reference values are adopted from EN779:2002[41].

Items	Equipment/method	Measured value	Reference value
Air velocity uniformity	Hot wire anemometer	5%	<10%
Aerosol uniformity in the test rig	Condensation particle counter (P- Trak)	3%	<15%
SMPS calibration	TSI annual testing certification	-	-
SMPS zero test	HEPA filter and SMPS	4 pc/cc	<10 pc/cc
100% efficiency test	HEPA filter in test-rig + SMPS	97%	>99%
Zero % efficiency test	No filter in test-rig + SMPS	0.25%	<3%

4.2.2 Air Filter Samples

A total of 23 new fiber-filter samples from three major Swedish filter manufactures were tested. The filter classes and filter media types are shown in Table 4.5. The filter samples were of the three filter media types: glass fiber, uncharged synthetic fiber and charged synthetic fiber. All of the filter media are intended for use in bag filters – but the filter samples were in the form of plane sheets. During tests, the samples were mounted in the circular cross section of the test-rig (diameter 315 mm). Each of the filter samples presented in Table 4.5 were challenged by an indoor aerosol; a selection of them were also challenged by an oil aerosol. Properties of the filter media are summarized in Table 4.6.

Table 4.5. Tested fine filter samples and their media types

Filter sample	Filter class		Filter media type
	European standard EN 779	US standard ANSI/ASHRAE 52	
#1	F5	MERV 9-10	Glass fiber
#2	F5	MERV 9-10	Charged Synthetic
#3	F6	MERV 11-12	Glass fiber
#4	F6	MERV 11-12	Uncharged synthetic
#5	F6	MERV 11-12	Glass fiber
#6	F6	MERV 11-12	Charged Synthetic
#7	F6	MERV 11-12	Charged Synthetic
#8	F6	MERV 11-12	Charged Synthetic
#9	F7	MERV 13	Glass fiber
#10	F7	MERV 13	Uncharged synthetic
#11	F7	MERV 13	Uncharged synthetic
#12	F7	MERV 13	Glass fiber
#13	F7	MERV 13	Charged Synthetic
#14	F7	MERV 13	Charged Synthetic
#15	F7	MERV 13	Charged Synthetic
#16	F8	MERV 14	Glass fiber
#17	F8	MERV 14	Uncharged synthetic
#18	F8	MERV 14	Glass fiber
#19	F8	MERV 14	Uncharged synthetic
#20	F8	MERV 14	Charged Synthetic
#21	F8	MERV 14	Charged Synthetic
#22	F9	MERV 15	Glass fiber
#23	F9	MERV 15	Charged Synthetic

Table 4.6 The properties of a single fiber layer. Pressure drop was for at 12,3 cm/s.

Filter code	Effective fiber diameter (µm)	Thickness (mm)	Calculated packing density	Calculated pressure drop (ΔPa)
#1	6.2	3.7	0.010	14
#2	6.5	1.3	0.013	37
#3	5	4.1	0.010	24
#4	2.5	0.2	0.044	51
#5	2.5	1.8	0.010	41
#6	2.5	0.6	0.025	41
#7	3.5	0.5	0.040	51
#8	2.5	0.6	0.030	75
#9	2.2	4.3	0.010	126
#10	2	0.4	0.054	59
#11	2	0.6	0.030	116
#12	2.2	3.5	0.010	103
#13	2	0.7	0.014	42
#14	2.5	0.6	0.026	64
#15	2	0.6	0.018	77
#16	2	4.3	0.012	199
#17	1.5	1.2	0.020	219
#18	1.4	2.0	0.010	146
#19	1.6	0.8	0.023	128
#20	1.5	0.9	0.010	57
#21	2.3	1.4	0.011	44
#22	2	4.3	0.011	178
#23	2	1.4	0.015	93

4.2.3 Particle measurements

The upstream and downstream concentrations of airborne particles were monitored by the same Scanning Mobility Particle Sizer (SMPS) as described in a previous section. Both the upstream and the downstream aerosol samples were taken 300 mm from the tested filter. Also in this case the SMPS was adjusted to measure particles from 14 nm to 673 nm, with 16 channels per decade.

4.2.4 Test Aerosols

The tested filters were challenged by the aerosol prevailing in the laboratory. This was repeated for the two situations described below. The two aerosol size-distributions obtained are shown in Figure 4.4.

1) Indoor aerosol test. There were no dominating indoor particle sources in the laboratory, and thus, the indoor aerosol mainly originated outdoors, being supplied to the room through the supply air system. In this case the indoor aerosol had a concentration peak at about 100 nm. The indoor aerosol is assumed to be close to the Boltzmann equilibrium charge state, and it is assumed to have properties close to the aerosols typically challenging a filter during "normal" real-life operation.

2) Oil aerosol test, an oil aerosol was thermally generated and mixed with the room air by the use of a mixing fan. The oil aerosol was thermally generated from Shell Ondina oil 917, and had a peak concentration at 220 nm-sized particles. The oil aerosol was not neutralized and is assumed to be practically without any charges.

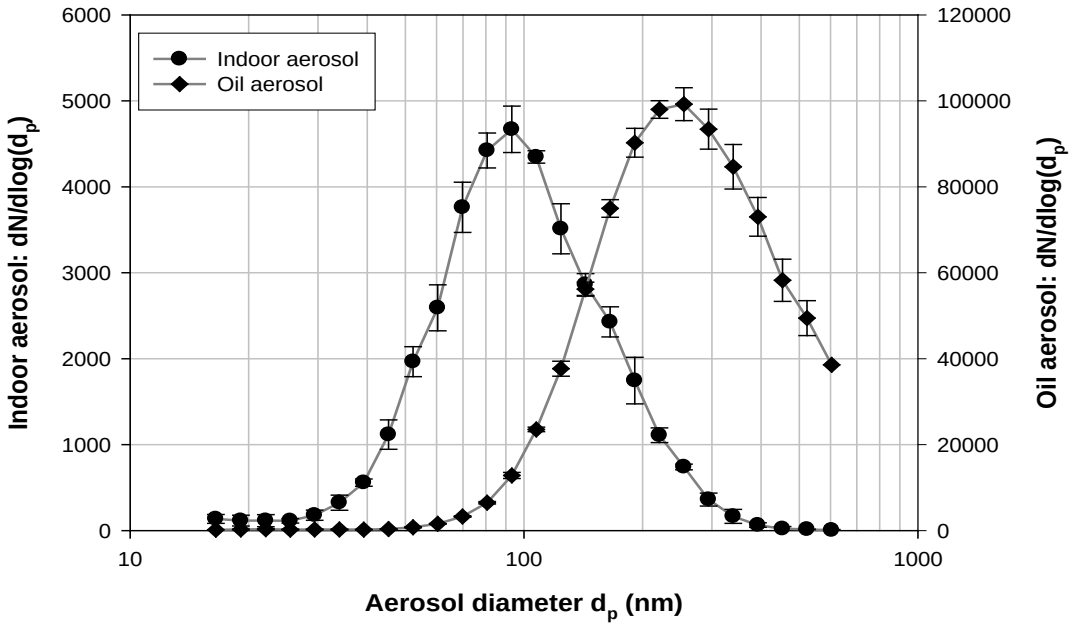

Figure 4.4. Particle size-distributions of the two test aerosols.

4.2.5 Calculation of efficiency values

The calculation method in small scale filter test is the same as that used in the full scale filter test, see chapter 4.1.5 and eq. 4.1.

4.3 Conclusions

In this chapter, the materials and methods of the full-scale filter experiments and filter sheet experiments were presented. Comparing the measured qualification parameters with the requirements in EN779:2002[41], the two testing systems are considered meeting the requirements in general. In the two experiments, multiple upstream aerosols, air velocities and equipments were applied in multiple filter media tests. The motivation is to investigate the influence of the upstream aerosol on the measured efficiencies of different filter media, thus further suggest the proper testing methods.

5 Air filter efficiency measurements

This chapter presents the results of the experiments described in Chapter 4. The data comprise size-resolved efficiency values determined for eight full scale filters in the DEHS aerosol test and 23 filter sheets in the indoor aerosol test. Additionally, the influences of fiber material, air velocity, use of neutralizer and upstream aerosol on the efficiency curves are investigated, respectively.

5.1 Fractional filtration efficiency

5.1.1 Full scale filter test

Figure 5.1 shows the size-resolved filtration efficiency observed for charged synthetic filters and glass fiber filter at the standard air flow rate of 0.944 m^3/s. The corresponding air velocity through filter medium is 0.16 m/s.

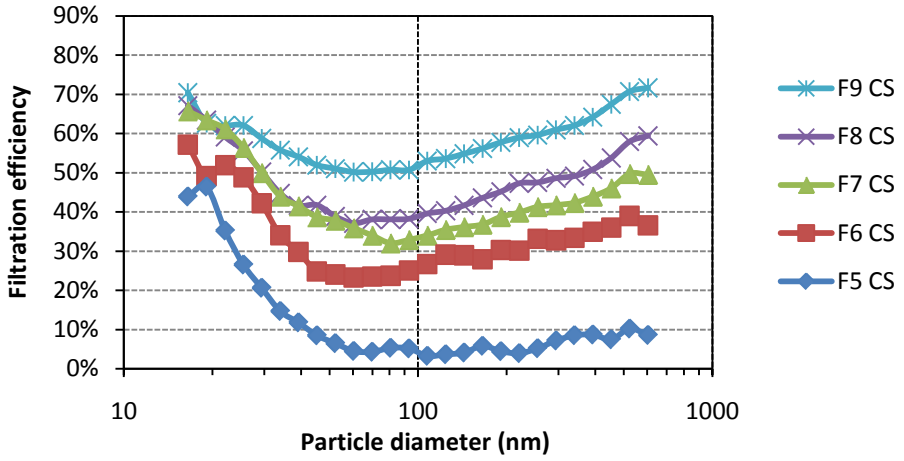

(a)

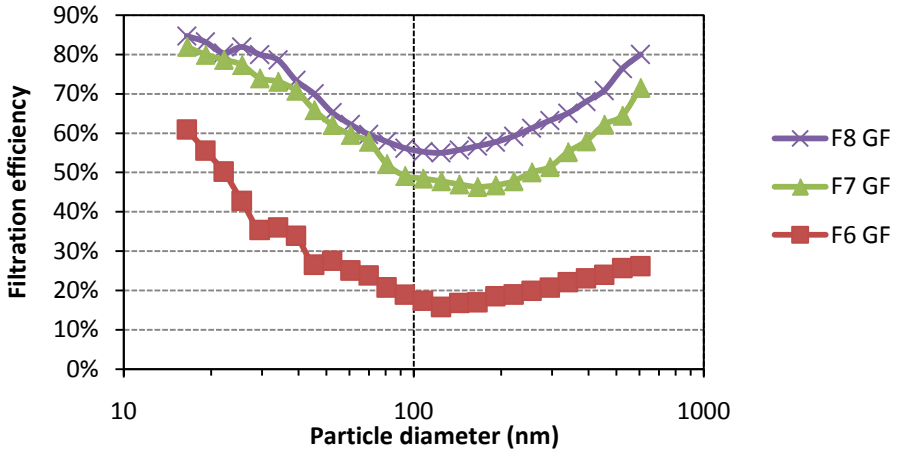

(b)

Figure 5.1 Fractional filtration efficiency at an air velocity of 0.16 m/s through the filter medium: (a) Charged synthetic filters (CS); (b) Glass fiber filters (GF). The data comes from the full scale filter tests when using the neutralized DEHS aerosol.

The measured results at air velocities of 0.08 m/s and 0.22 m/s through the filter medium are presented in Figure 5.2 and 5.3. The curves show that MPPS of charged synthetic filters is smaller than 100 nm, but MPPS of glass fiber filters is larger than 100 nm.

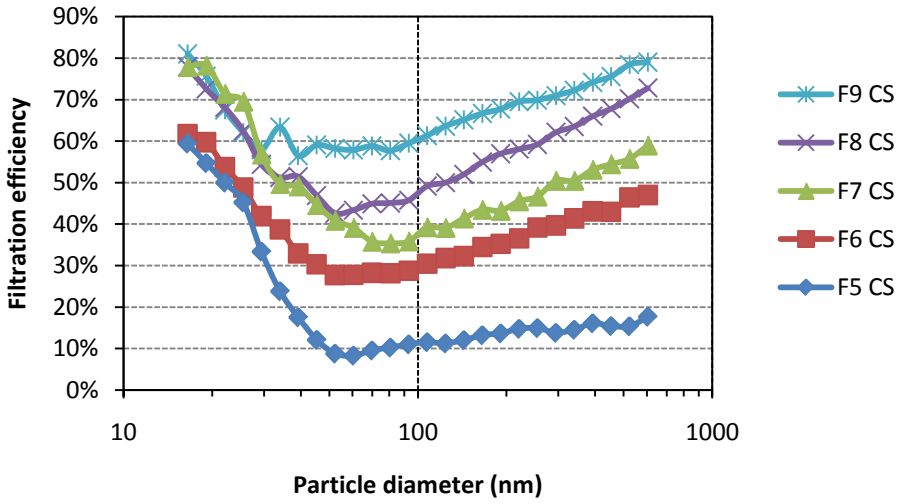

(a)

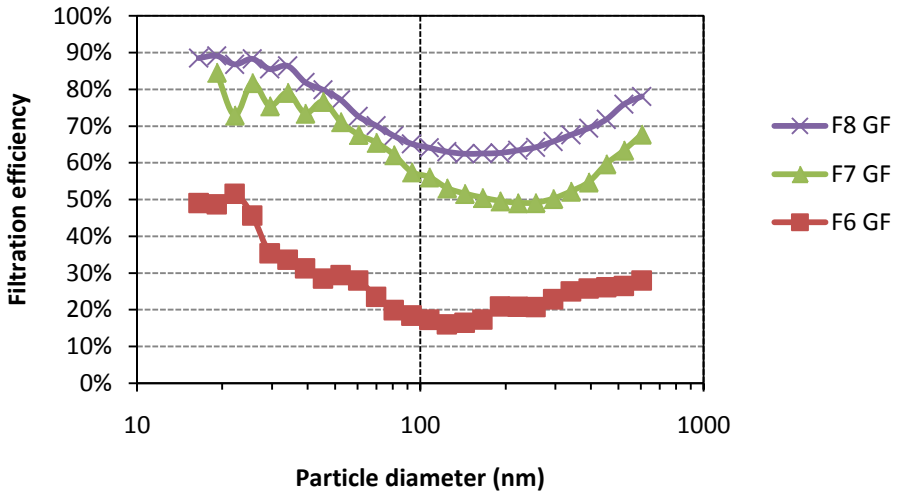

(b)

Figure 5.2 Fractional filtration efficiency at an air velocity of 0.08 m/s through the filter medium: (a) Charged synthetic filters (CS); (b) Glass fiber filters (GF). The data comes from the full scale filter tests when using the neutralized DEHS aerosol.

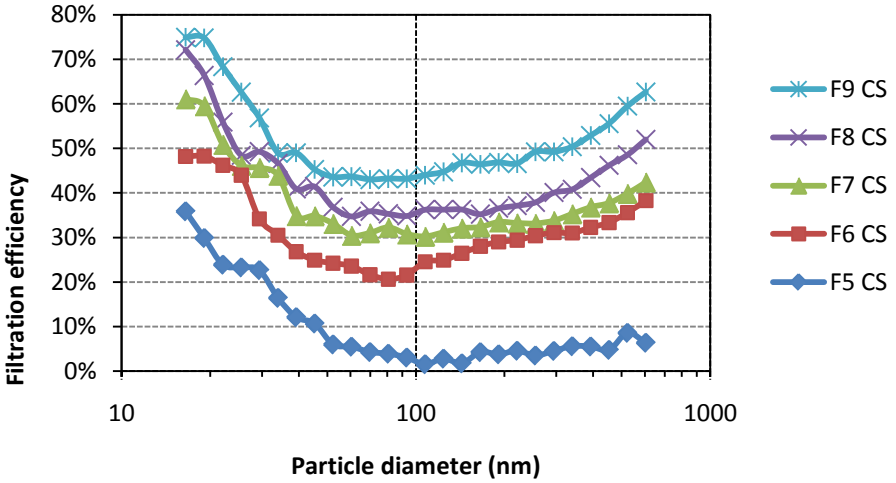

(a)

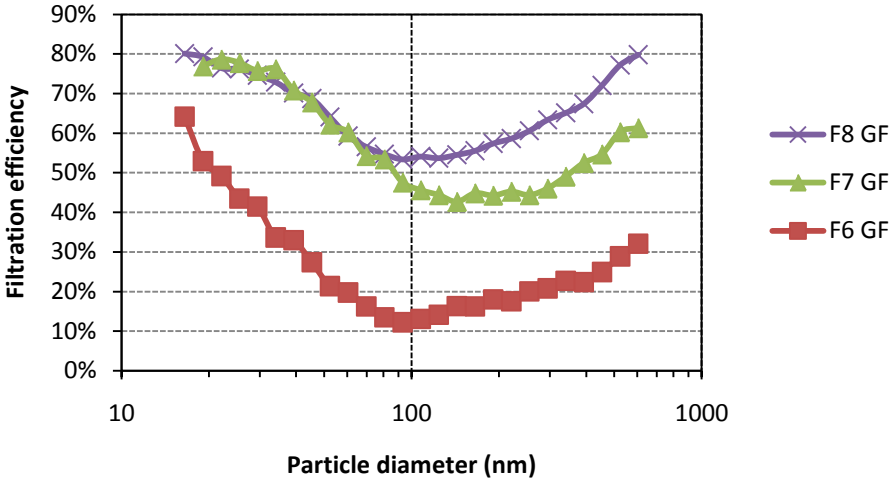

(b)

Figure 5.3 Fractional filtration efficiency at an air velocity of 0.22 m/s through the filter medium: (a) Charged synthetic filters (CS); (b) Glass fiber filters (GF). The data comes from the full scale filter tests when using the neutralized DEHS aerosols.

5.1.2 Sheet filter test

Twenty three filter sheets were tested with the indoor aerosol. Figure 5.4 (a)-(d) shows the size-resolved efficiencies of F5-F9 class filters in these indoor aerosol tests at an air velocity of 0.123 m/s through the filter medium. The figure shows that the filtration efficiencies of charged synthetic filters are much higher than that of glass fiber and uncharged synthetic filters of the same filter class. As the results of the previously presented full scale filter test, the MPPS of glass fiber filter sheets are larger than 100 nm, while the MPPS of charged synthetic filter sheets are smaller than 100 nm.

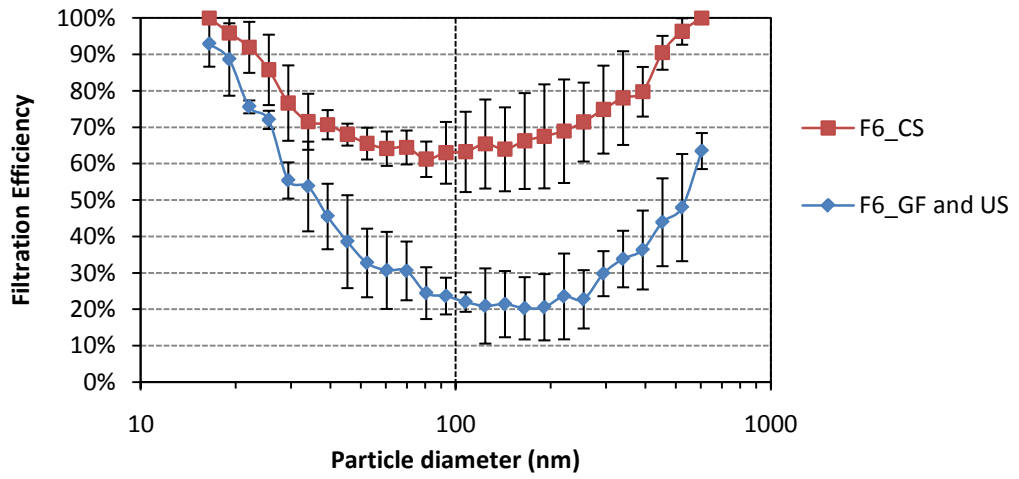
100%
90%
80%
70%
60%
50%
40%
30%
20%
10%
0%
Filtration Efficiency
10
100
1000
Particle diameter (nm)
F6_CS
F6_GF and US

(a)

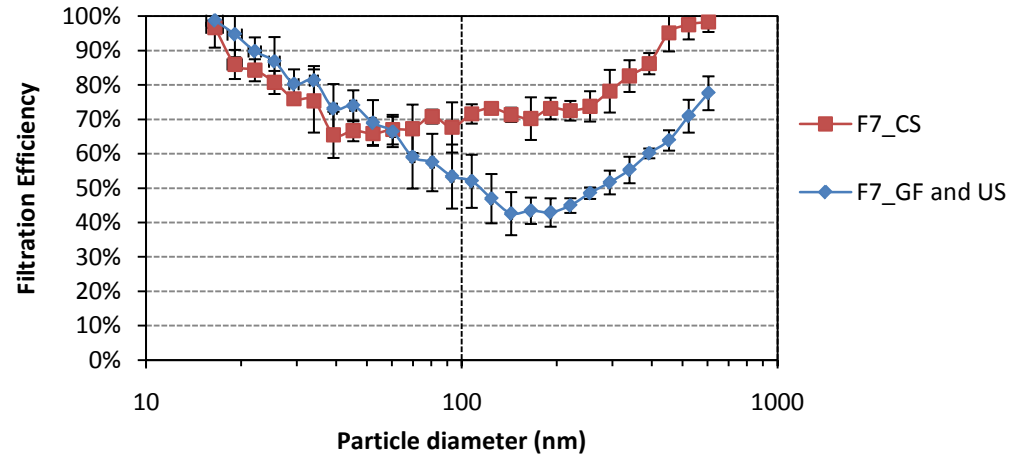
100%
90%
80%
70%
60%
50%
40%
30%
20%
10%
0%
Filtration Efficiency
10
100
1000
Particle diameter (nm)
F7_CS
F7_GF and US

(b)

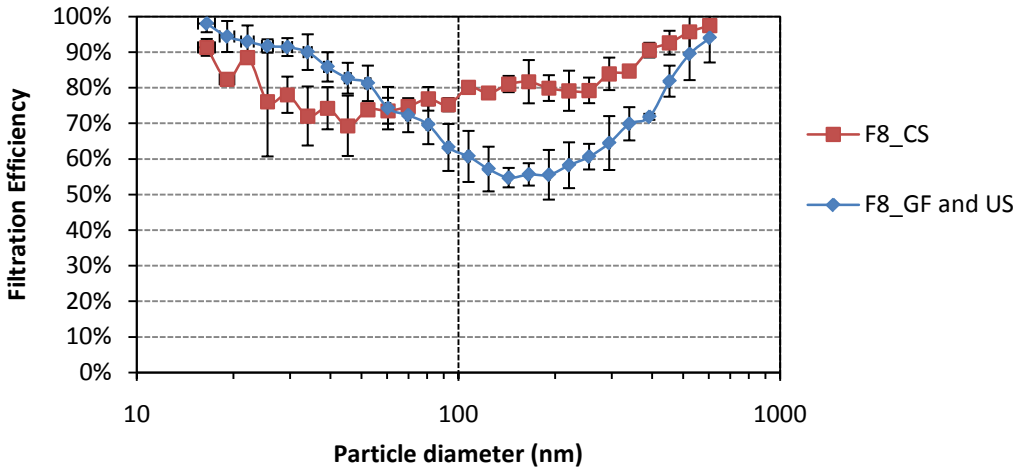
100%
90%
80%
70%
60%
50%
40%
30%
20%
10%
0%
Filtration Efficiency
10
100
1000
Particle diameter (nm)
F8_CS
F8_GF and US

(c)

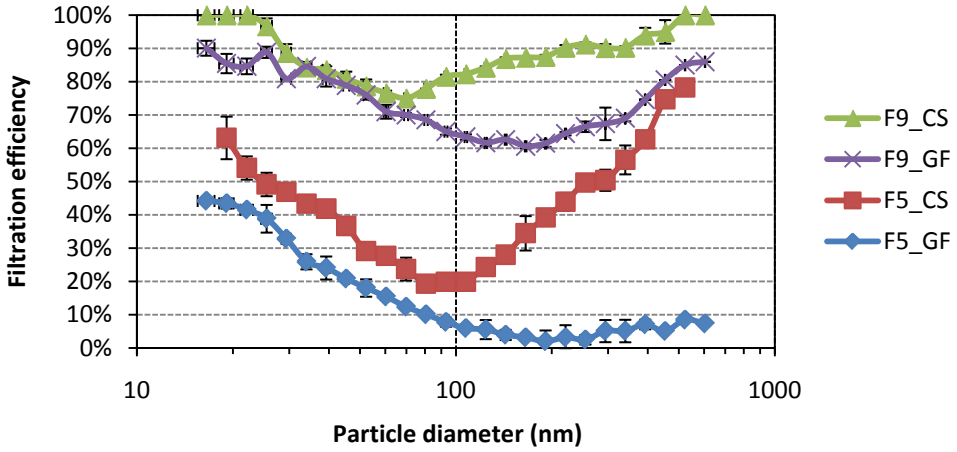

(d)

Figure 5.4 Fractional filtration efficiency for F5-F9 class filters observed in the indoor aerosol test at an air velocity of 0.123 m/s through the filter medium: (a) F6 class filters; (b) F7 class filters; (c) F8 class filters; (d) F5 and F9 class filter. In the legends, CS: charged synthetic filter; US: uncharged synthetic filters; GF: glass fiber filter.

5.2 Influencing factors

5.2.1 Filter medium influence

According to Figure 5.1-5.4, the shape of the size-resolved efficiency curves of glass fiber filters are different compared to that of charged synthetic filters. MPPS of the charged synthetic filters is typically around 50nm, while that of glass fiber filters is larger than 100 nm.

5.2.2 Air velocity influence

Air velocity through the filter medium is another important impact factor on filter size-resolved efficiency curves. Figure 5.5 (a) and (b) show the size-resolved efficiency at three air velocities through charged synthetic filter and glass fiber filters respectively.

In the figure, for both filter media, the filtration efficiency is reduced with increasing air velocity. However, when the air velocity increases, the MPPS for glass fiber filters become smaller, and the MPPS for charged synthetic filters become larger. The variations of MPPS with the air velocity are summarized in Figure 5.6. The figure shows the variation trends of MPPS are clearly different for glass fiber filter and charged synthetic filter.

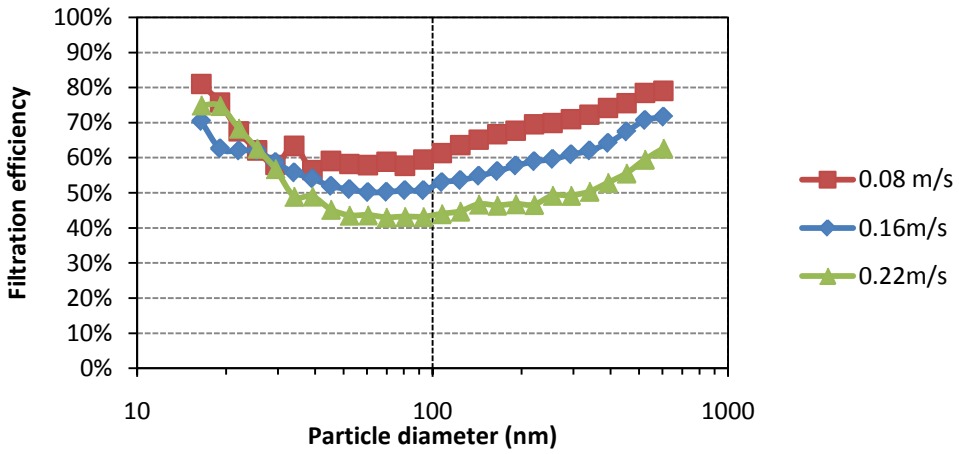

(a)

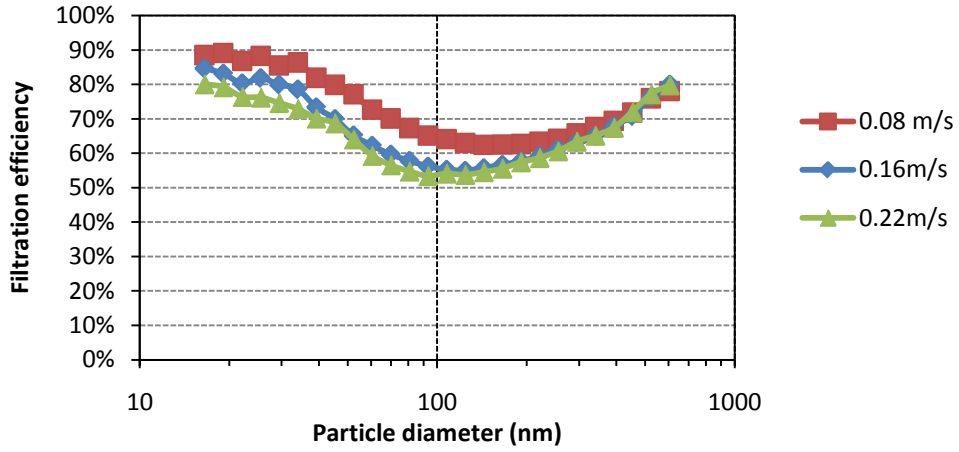

(b)

Figure 5.5 Fractional filtration efficiency at air velocities of 0.08 m/s, 0.16 m/s and 0.22 m/s through the filter medium: (a) F9 class charged synthetic filter; (b) F8 class glass fiber filter. The data comes from the full scale filters challenged neutralized DEHS aerosols.

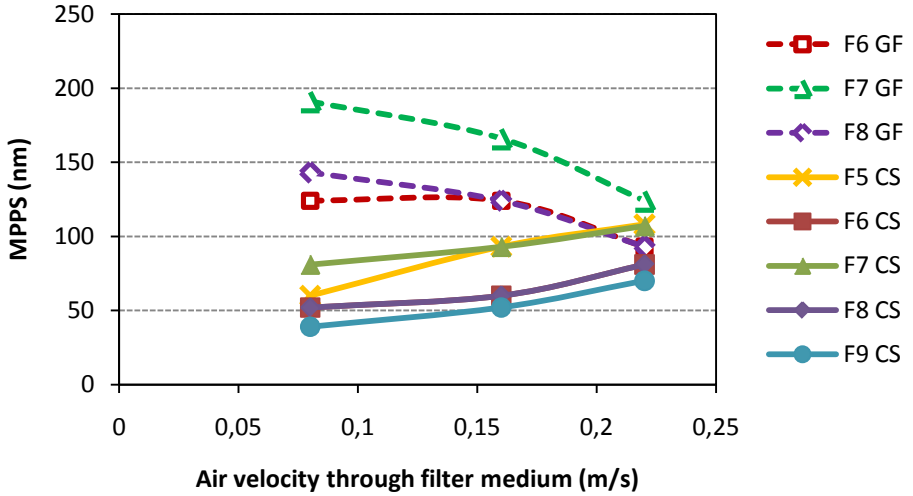

Figure 5.6 MPPS of charged synthetic filters (CS) and glass fiber filters (GF) varied with the air velocity in the full scale filter tests.

5.2.3 Neutralizer influence

A neutralizer is required in a filter testing system according to the European standard EN779:2002[41]. However, the neutralizer among the testing instruments is sometimes thought unimportant, especially for filed filter measurements. Considering that ambient aerosols are normally naturally neutralized, the neutralizer might be neglected for saving instrument cost. Figure 5.7 shows the influence of a neutralizer on the size-resolved efficiency of glass fiber filters and charged synthetic filters. The results come from the full scale filter test with the DEHS aerosol.

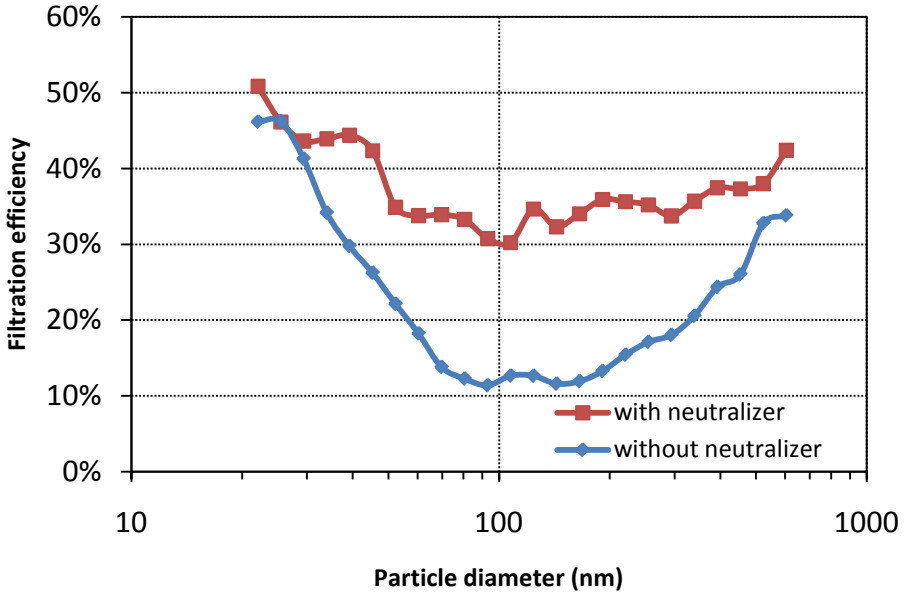

(a)

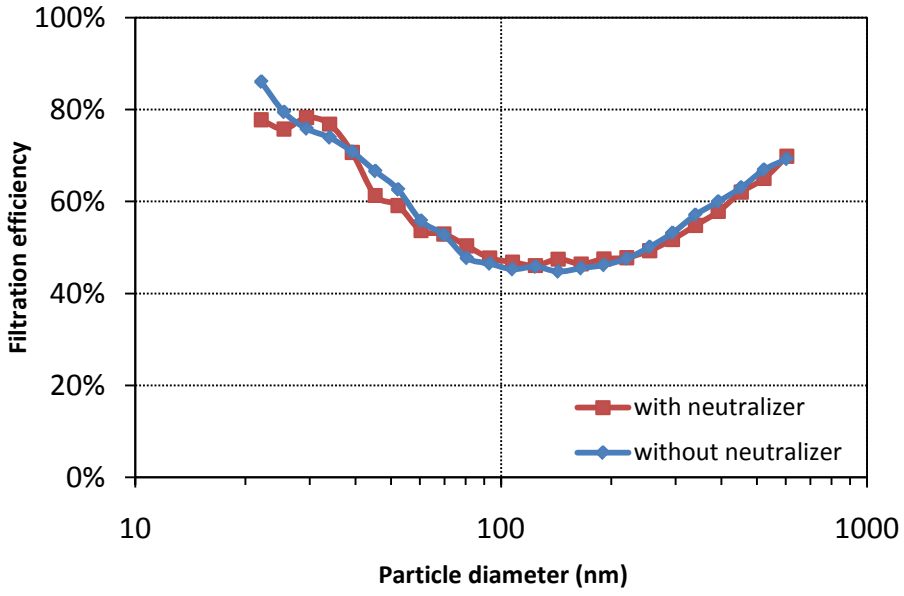

(b)

Figure 5.7 F7 class filter at an air velocity of 0.22 m/s with and without neutralizer in the full scale filter tests with DEHS aerosol. (a) Charged synthetic filter; (b) Glass fiber filter.

The figure shows that the neutralizer does not influence the efficiency of a glass fiber filter, but that it significantly influences the efficiency of a charged synthetic filter. The DEHS aerosol generated by an atomizer is almost not charged at all. When the air flow passes the neutralizer, this aerosol is charged with theoretically an equal number of negative and positive ions at the atmospheric aerosol level[65]. A neutralized upstream aerosol is required according to the European standard EN779. The results confirm that this is necessary especially for charged synthetic filter tests.

5.2.4 Upstream aerosol influence

In the European standard EN779:2002[41], a DEHS aerosol is recommended as the test aerosol, while in US standard ASHRAE 52.2[5], KCl aerosol is the corresponding testing aerosol. The two aerosols are different at the charge ability and particle size range. The DEHS aerosol is a kind of oil aerosol which is not easily being charged. The size distribution is hard to adjust and the peak concentration is usually around the particle diameter of 250 nm. Instead, KCl aerosol is a kind of salt liquid aerosol, which is easily being charged during the generation and transfer. The size distribution can be adjusted by varying the concentration of KCl in the liquid. NaCl aerosol has similar characteristics as that of KCl aerosol, and is commonly used in filter tests at present. In the full-scale filter test, both a NaCl (1% NaCl solution) and a DEHS aerosol are used as upstream aerosol to investigate any differences between these as regards the filter test result. The size distributions of the two testing aerosols are shown in Figure 4.2.

Figure 5.8 (a) and (b) show the size-resolved efficiencies of glass fiber filters and charged synthetic filters respectively when the filters are challenged with DEHS aerosols and NaCl aerosols in the full scale filter test. For the same filter, the measurement results with NaCl and DEHS aerosols are shown on the opposite sides of 100 nm. Figure 5.8 (a) indicates that, for glass fiber filters, the filtration efficiencies are not influenced by the neutralizer or charge level of the upstream aerosols, as expected from the previous section. Figure 5.8 (b) shows that the filtration efficiency of charged synthetic filters challenged with the NaCl aerosol is higher than that observed with the DEHS aerosol. This may be because the NaCl aerosol, also after it has passed the neutralizer, is still more charged than the neutralized DEHS aerosol. Although, according to the manual, the used neutralizer should have enough capacity to neutralize the aerosols generated in the experiments, it may not have enough capacity to completely neutralize the highly charged NaCl aerosol.

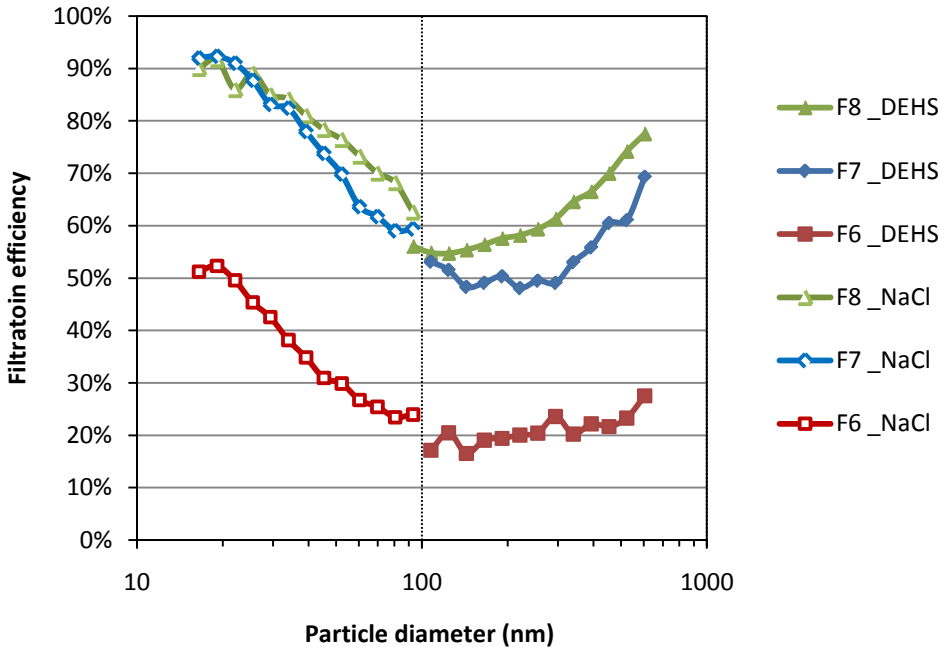

(a)

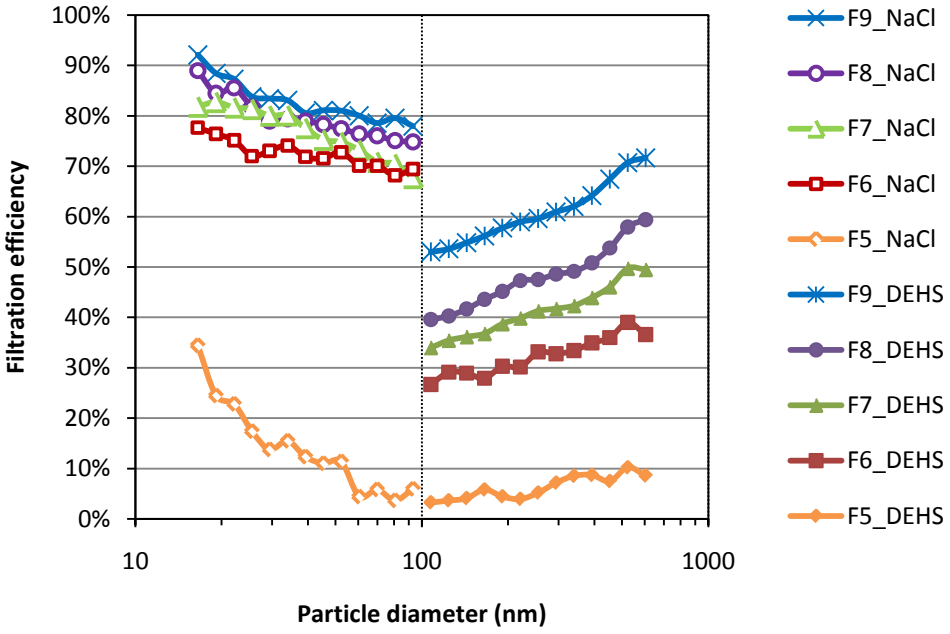

(b)

Figure 5.8 Fractional filtration efficiency challenged with DEHS and NaCl aerosols at an air velocity of 0.16 m/s through the filter medium: (a) glass fiber filter; (b) charged synthetic filters. The data comes from the full scale filter tests.

Figure 5.9 (a) and (b) shows the size-resolved efficiencies of glass fiber filters and charged synthetic filters challenged with indoor aerosol and oil aerosol in the filter sheet test. The oil aerosol is a Shell Ondina oil aerosol without neutralizer. The indoor aerosol mainly comes from ambient air. It is considered to be a neutralized aerosol, having the same charge state as atmospheric aerosol.

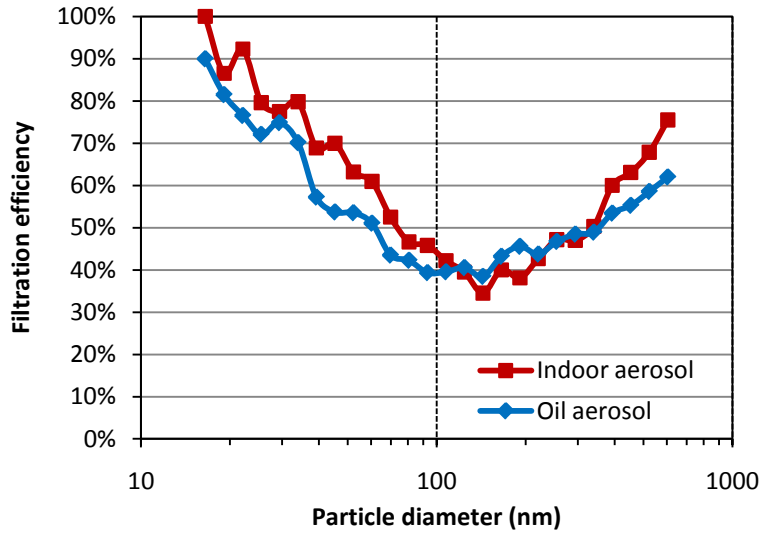

(a)

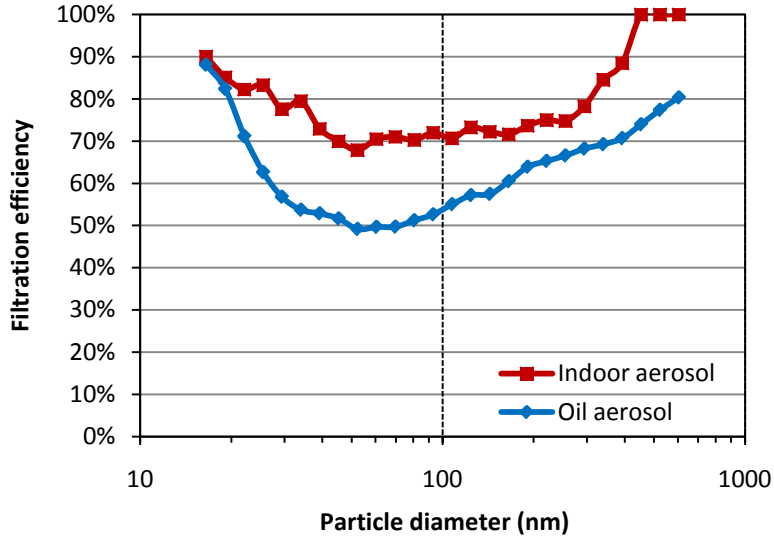

(b)

Figure 5.9 Fractional filtration efficiency of F7 class filters challenged with indoor aerosol and oil aerosol in the filter sheet tests: (a) Glass fiber filter; (b) Charged synthetic filter.

For the charged synthetic filters, the filtration efficiencies observed in the indoor aerosol tests are obviously higher than those observed in the oil aerosol tests. However, for glass fiber filters, the efficiencies measured with the two aerosols are almost the same. Since the oil aerosol without neutralization is almost completely uncharged, the efficiency of charged synthetic filters in the oil aerosol test can be considered as the efficiency when charged synthetic filters lose their charge.

5.3 Conclusions

For charged synthetic filters, the efficiencies measured with the neutralized DEHS aerosol and the indoor aerosol is higher than the efficiency measured with oil aerosol without neutralization. The main reason should be that the oil aerosol without neutralization is almost not electrically charged at all. Therefore, oil aerosol tests without neutralization may indicate the mechanical efficiency of charged synthetic fibers when they lose their charge. It is valuable to further study

this as an alternative to the neutralizing method of iso-propanol (IPA) as prescribed in EN779.

In the study of influencing factors, the size-resolved efficiency is reduced with increasing air velocity. However, the MPPS are changed in a different way for the different filter media. When the air velocity is increased, the MPPS for glass fiber filters become smaller, while the MPPS for charged synthetic filters become larger. The neutralizer is an important component in the laboratory test for charged synthetic filters, while it can be neglected in glass fiber filter tests. When the charged synthetic filters are challenged with a NaCl aerosol, it is important to use a large capacity neutralizer, because NaCl aerosols are normally charged to a higher level than DEHS aerosols are.

6 Air filter efficiency relations

One efficient way to include EF_{MPPS} and EF_{UFPs} in the filter classification would be to calculate EF_{MPPS} and EF_{UFPs} from a standardized efficiency, such as $EF_{0.4\mu m}$ in EN779:2002[41]. A critical background research is to investigate the correlations between EF_{UFPs}, EF_{MPPS} and $EF_{0.4\mu m}$ for different intermediate filter media and classes. However, there are few studies carried out to investigate such relationship and the influential factors.

Filter operation conditions, such as air velocities, fiber media and upstream aerosols could influence the correlations between EF_{MPPS}, EF_{UFPs} and $EF_{0.4\mu m}$. Firstly, since previous studies [65, 87] have presented that MPPS varies with air velocity, it is natural to expect that the correlations between such three efficiencies varies with air velocity. Secondly, glass fiber filters and charged synthetic filters have different MPPS, so the above correlations could be different for glass fiber filters and charged synthetic filters respectively. Finally, because the integrated efficiency for UFPs can be influenced by the upstream aerosol size distribution [38], it is reasonable to compare the correlations obtained in the tests with different upstream aerosol size distributions. In this study, the results from the field indoor aerosol test are compared to the results from laboratory DEHS aerosol test. The peak concentration of DEHS aerosols is for particles with the diameter about 200nm, while the peak concentration of indoor aerosols is for particles with the diameter around 100 nm. The ambient traffic pollution probably contributed to a large amount of UFPs to the indoor aerosol tested.

In summary, the purpose of the study is to explore the relationship between EF_{UFPs}, EF_{MPPS} and $EF_{0.4\mu m}$ for intermediate filters of class F5-F9, and the influence of the potential impact factors. This study is based on the test of full scale glass fiber filters and charged synthetic filters challenged with neutralized DEHS aerosol at three air velocities through the filter medium, 0.08 m/s, 0.16 m/s and 0.22 m/s. The test of filter sheets challenged with indoor aerosol is presented to analyse upstream aerosol influence.

6.1 Correlations between three efficiencies

6.1.1 EF_{MPPS}, EF_{UFPs} and $EF_{0.4\mu m}$ for DEHS aerosol test

Filtration efficiencies on MPPS-sized particles, UFPs and 0.4 μm particles in the full scale DEHS aerosol filter test are summarized in Table 6.1-6.3 for three air velocities. The uncertainties are expressed as the standard deviation (efficiency percentage units). In Table 6.1-6.3, the filtration efficiency is reduced with air velocity.

Table 6.1 EF_{MPPS}, EF_{UFPs} and $EF_{0.4\mu m}$ at an air velocity of 0.08 m/s through the filter medium. (GF – glass fiber, CS – charged synthetic). The neutralized DEHS aerosol was used in the tests.

Filter			EF_{MPPS}		$EF_{0.4\mu m}$		EF_{UFPs}	
			Ave.	**SD**	**Ave.**	**SD**	**Ave.**	**SD**
F5	GF		—	—	—	—	—	—
	CS	C1	8%	0%	16%	0%	10%	1%
F6	GF	C2	17%	3%	26%	1%	25%	2%
	CS	C3	28%	3%	43%	5%	34%	2%
F7	GF	C4	49%	2%	60%	1%	60%	2%
	CS	C5	35%	1%	53%	3%	39%	1%
F8	GF	C6	62%	1%	70%	1%	68%	1%
	CS	C7	43%	7%	66%	4%	46%	5%
F9	GF		—	—	—	—	—	—
	CS	C8	57%	5%	74%	3%	59%	4%

Table 6.2 EF_{MPPS}, EF_{UFPs} and $EF_{0.4\mu m}$ at an air velocity of 0.16 m/s through the filter medium. (GF – glass fiber, CS – charged synthetic). The neutralized DEHS aerosol was used in the tests.

Filter		EF_{MPPS}		$EF_{0.4\mu m}$		EF_{UFPs}	
		Ave.	**SD**	**Ave.**	**SD**	**Ave.**	**SD**
F5	GF	—	—	—	—	—	—
	CS	3%	0%	9%	3%	3%	2%
F6	GF	16%	2%	23%	1%	21%	1%
	CS	23%	3%	35%	4%	31%	1%
F7	GF	46%	2%	57%	2%	54%	3%
	CS	32%	2%	44%	2%	35%	3%
F8	GF	55%	1%	68%	2%	58%	1%
	CS	37%	2%	51%	3%	38%	1%
F9	GF	—	—	—	—	—	—
	CS	49%	1%	62%	2%	50%	2%

Table 6.3 EF_{MPPS}, EF_{UFPs} and $EF_{0.4\mu m}$ at an air velocity of 0.22 m/s through the filter medium. (GF – glass fiber, CS – charged synthetic). The neutralized DEHS aerosol was used in the tests.

Filter			EF_{MPPS}		$EF_{0.4\mu m}$		EF_{UFPs}	
			Ave.	**SD**	**Ave**	**SD**	**Ave**	**SD**
F5	GF		—	—	—	—	—	—
	CS	C1	2%	2%	6%	0%	2%	2%
F6	GF	C2	12%	1%	22%	1%	18%	1%
	CS	C3	21%	1%	32%	3%	30%	1%
F7	GF	C4	43%	3%	55%	2%	51%	3%
	CS	C5	30%	2%	37%	4%	32%	2%
F8	GF	C6	53%	1%	67%	3%	56%	1%
	CS	C7	35%	4%	43%	3%	35%	2%
F9	GF		—	—	—	—	—	—
	CS	C8	43%	5%	53%	1%	43%	2%

6.1.2 Regression analysis

Figure 6.1 and 6.2 respectively show the correlations between $EF_{MPPS,}$ EF_{UFPs} and $EF_{0.4\mu m}$ at the three air velocities in the full scale filter test. In general, they show linear relationships within the observed efficiency ranges. Least squares regression analysis is used to estimate linear relationships between $EF_{MPPS,}$ EF_{UFPs} and $EF_{0.4\mu m}$. The squares of the Pearson correlation coefficients (R^2) are above 0.95 in all cases. T-tests of the correlation coefficients show p-values lower than 0.025 for all cases in Figure 6.1 and 6.2. Therefore, the analysis indicates that both EF_{MPPS} and EF_{UFPs} are linearly related to $EF_{0.4\mu m}$ at $p<0.025$, within the measured efficiency interval.

For the glass fiber filters, EF_{MPPS} is lower than $EF_{0.4\mu m}$ by 10%~15%-units, while EF_{UFPs} is close to $EF_{0.4\mu m}$ and only slightly lower by 0%~6%-units. For the charged synthetic fiber filters, EF_{MPPS} and EF_{UFPs} are lower than $EF_{0.4\mu m}$ by 6%~20%-units and 1%~16%-units respectively.

The cause of the filter medium influence is probably that the MPPS of glass fiber filters is larger than 100 nm, while the MPPS of charged synthetic filters is normally smaller than 100 nm (see Figure 5.1 and 5.4). Thus for glass fiber filters, because the diameter of UFPs and 0.4μm-sized particles are located at each side of the MPPS on the X-axis and with similar distances, EF_{UFPs} and $EF_{0.4\mu m}$ on the size-resolved efficiency curves have similar value on the Y-axis. However, for charged synthetic filters, because their MPPS are in the diameter range of UFPs, EF_{MPPS} is integrated into EF_{UFPs}. This probably can explain why EF_{UFPs} is substantially less than $EF_{0.4\mu m}$ for charged synthetic filters.

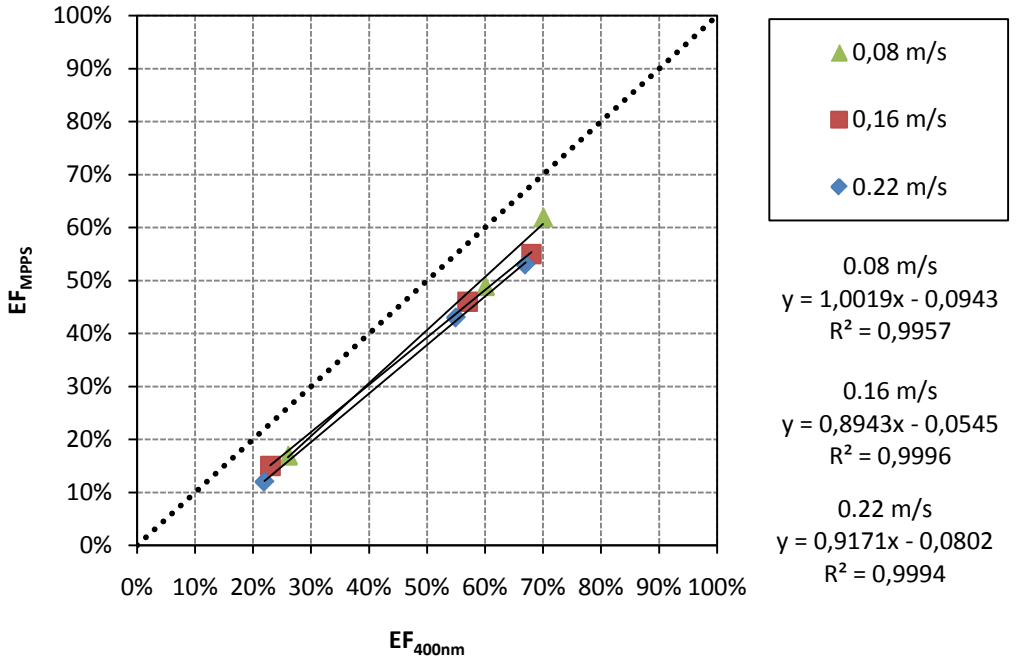

(a)

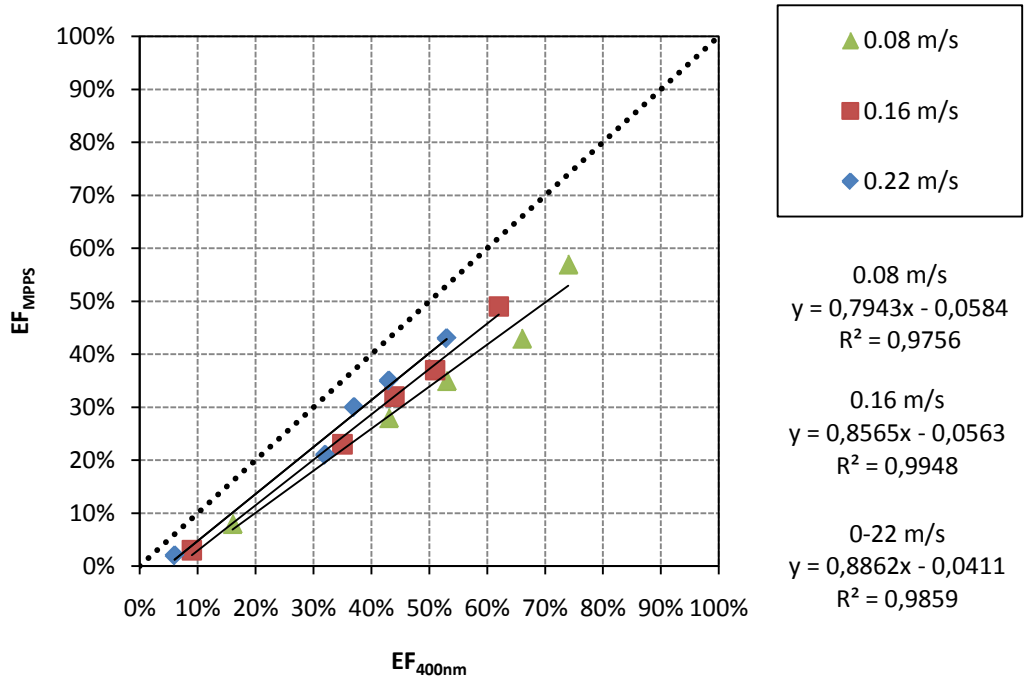

(b)

Figure 6.1 Filtration efficiency based on MPPS plotted against the efficiency based on 0.4 μm-sized particles for three velocities in the neutralized DEHS aerosol test: (a) glass fiber filters; (b) charged synthetic filters.

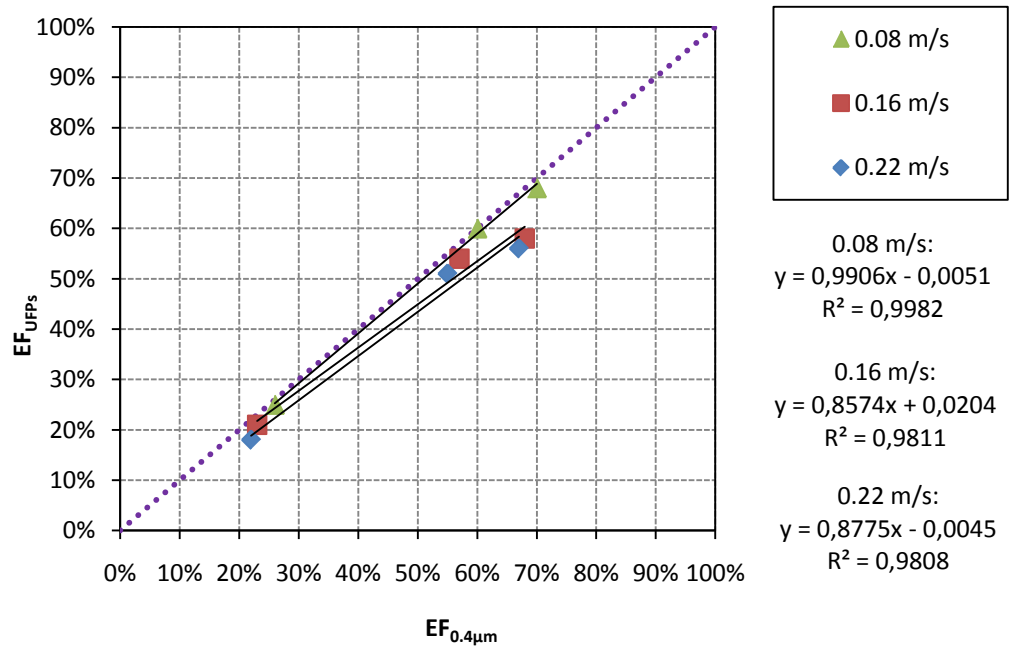

(a)

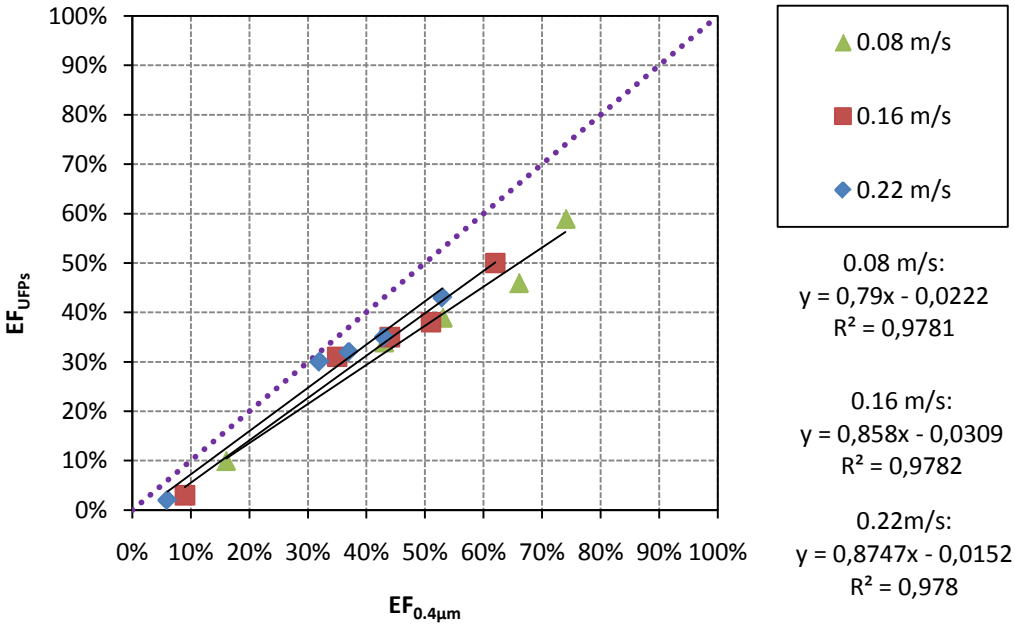

(b)

Figure 6.2 Filtration efficiency based on UFPs plotted against the efficiency based on 0.4 µm-sized particles for three velocities in the neutralized DEHS aerosol test: (a) glass fiber and uncharged synthetic filters; (b) charged synthetic filters.

In Figure 6.1 and 6.2, the regression equations can be considered as example equations to calculate $EF_{MPPS,}$ EF_{UFPs} from $EF_{0.4µm}$. The figures show that the slopes of the regression curves slightly reduces with increasing air velocity for glass fiber filters, and slightly increases with increasing air velocity for charged synthetic filters. Moreover, there is a slight tendency that, the higher the efficiency, the larger the deviation between the EF_{MPPS} and the $EF_{0.4µm}$. The above phenomena could be further explained in Figure 6.4 and 6.5.

6.2 Air velocity and filter media influence

The observed $EF_{MPPS,}$ EF_{UFPs} and $EF_{0.4\mu m}$ vary with air velocity. Figure 6.3 shows that $EF_{0.4\mu m}$ of all tested filters is reduced with increasing air velocities. The rates of this reduction for the charged synthetic filters are larger than that for the glass fiber filters.

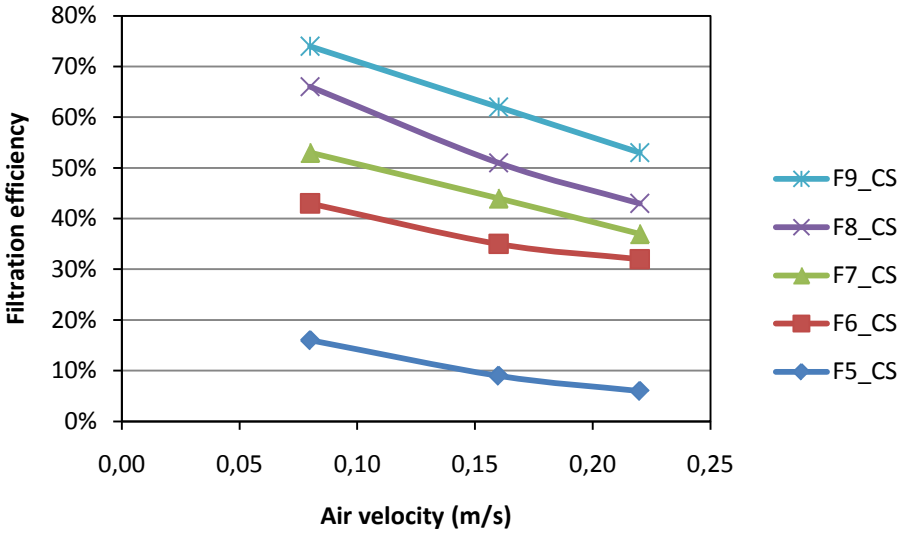

(a)

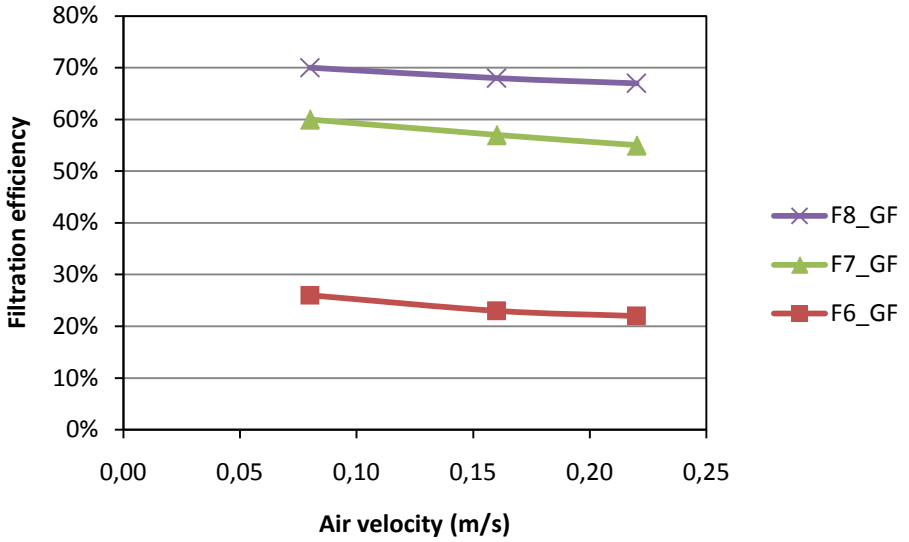

(b)

Figure 6.3 $EF_{0.4\mu m}$ varied with the air velocity through the filter medium: (a) charged synthetic filter (CS); (b) glass fiber filter (GF). The tests used the neutralized DEHS aerosol.

Furthermore, Figure 6.4 and 6.5 show the ratio of EF_{MPPS} to $EF_{0.4\mu m}$ ($EF_{MPPS}/EF_{0.4\mu m}$) and the ratio of EF_{UFPs} to $EF_{0.4\mu m}$ ($EF_{UFPs}/EF_{0.4\mu m}$) respectively with increasing air velocities. The $EF_{MPPS}/EF_{0.4\mu m}$ and the $EF_{UFPs}/EF_{0.4\mu m}$ roughly correspond with the slope of the regression curves in Figure 6.1 and 6.2 respectively. For glass fiber filters, the $EF_{MPPS}/EF_{0.4\mu m}$ and the $EF_{UFPs}/EF_{0.4\mu m}$ decrease with the air velocity for all filter classes. However, for charged synthetic filters, the $EF_{MPPS}/EF_{0.4\mu m}$ and $EF_{UFPs}/EF_{0.4\mu m}$ increase with increasing air velocity

except for the F5 class filter. This means that, for glass fiber filters, the EF_{MPPS} and EF_{UFPs} are reduced more than that of $EF_{0.4\mu m}$ with increasing air velocity. However, for charged synthetic filters except the F5 class filter, the EF_{MPPS} and EF_{UFPs} are reduced less than that of $EF_{0.4\mu m}$ with increasing air velocity. This is because the efficiency curves of the two filter media types are varying differently with varying air velocity, see Figure 5.5. It is also shown in Figure 5.6 that the MPPS increases with air velocity for the charged synthetic filters, while it reduces with air velocity for the glass fiber filters.

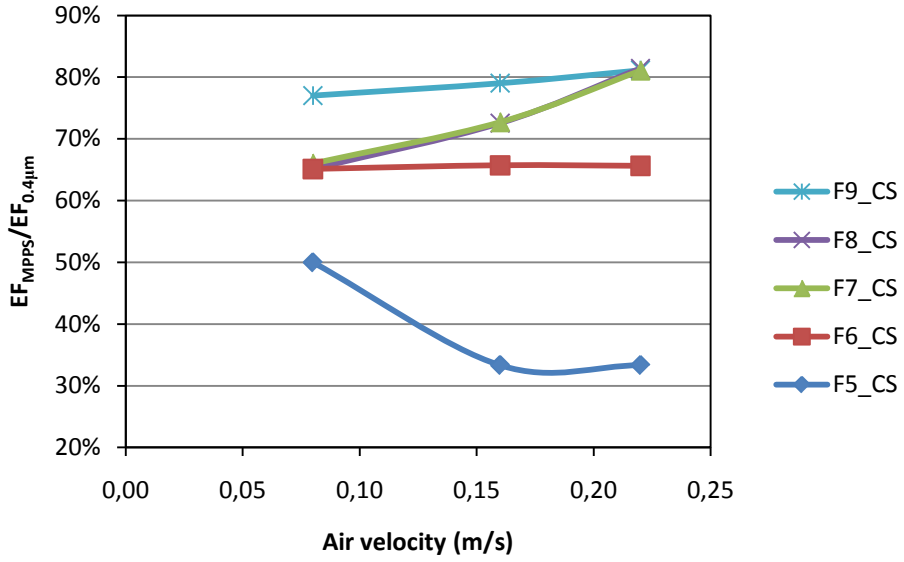

(a)

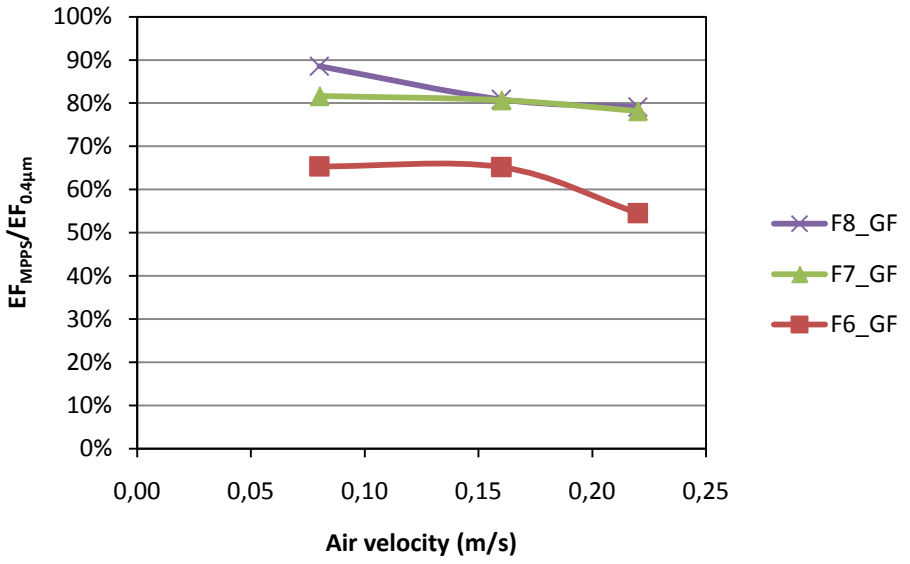

(b)

Figure 6.4 Ratio of EF_{MPPS} to $EF_{0.4\mu m}$ with increasing air velocity: (a) charged synthetic filter (CS); (b) glass fiber filter (GF). The tests used the neutralized DEHS aerosol.

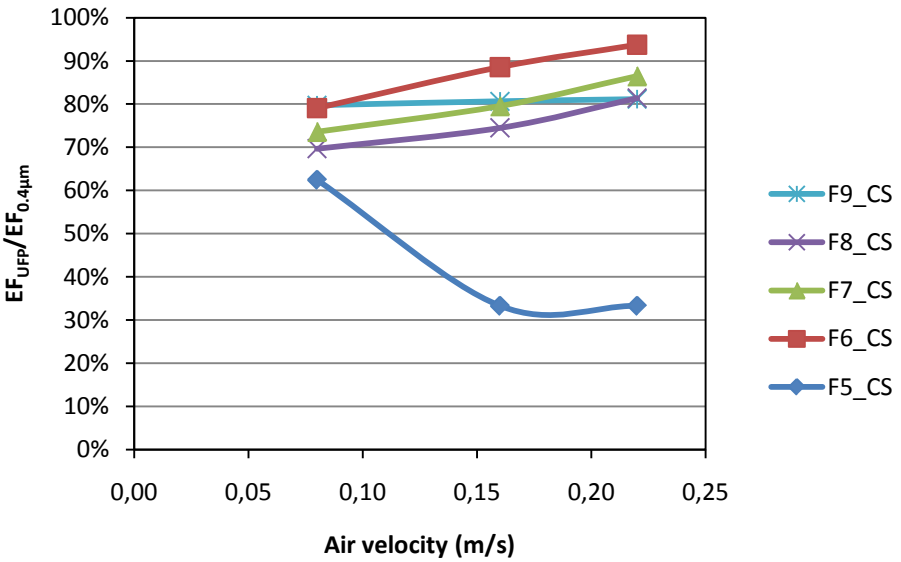

(a)

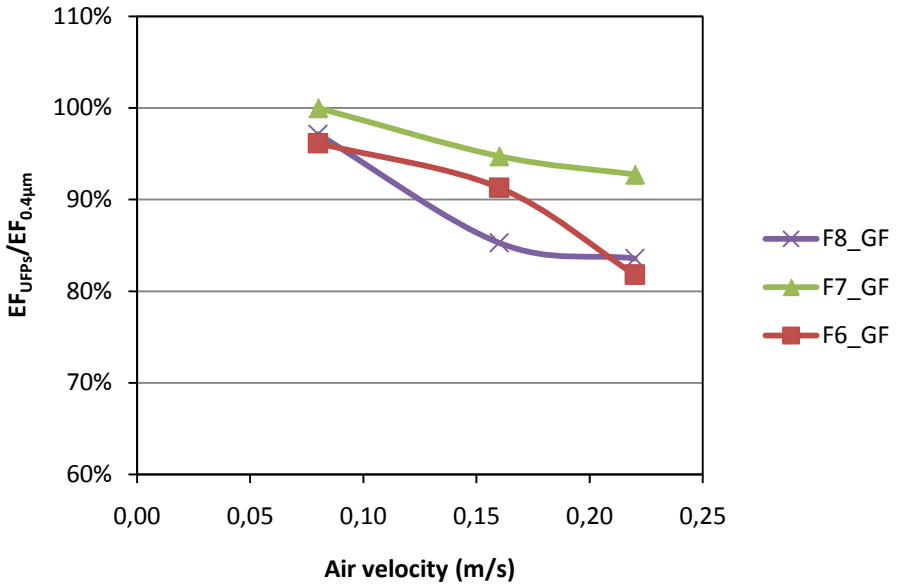

(b)

Figure 6.5 Ratio of EF_{UFPs} to $EF_{0.4\mu m}$ with increasing air velocity: (a) charged synthetic filter (CS); (b) glass fiber filter (GF). The tests used the neutralized DEHS aerosol.

6.3 Aerosol influence

6.3.1 EF_{MPPS}, EF_{UFPs} and $EF_{0.4\mu m}$ in indoor aerosol test

The results of the filter sheets tested in the small scale filter test rig and challenged by the indoor aerosol at an air velocity of 0.123 m/s through the filter medium are summarized in Table 6.4. The uncertainties are expressed as the standard deviation (efficiency percentage units). The results for the charged synthetic filters are different from the results for the glass fiber filters and uncharged synthetic filters. Since the latter two filter media showed similar results, they are grouped into one filter category. Comparing Table 6.4 with both

Table 6.1 and 6.2, shows that for glass fiber filters, the three filtration efficiencies in the two tests are similar. However, for charged synthetic filters, the three filtration efficiencies observed in the indoor aerosol test are obviously higher than those observed in the DEHS aerosol test. One probable reason is that the indoor aerosol is more charged than the neutralized DEHS aerosol used in the full scale filter test.

Table 6.4 EF_{MPPS}, EF_{UFPs} and $EF_{0.4\mu m}$ observed in the indoor aerosol test at an air velocity of 0.123 m/s through the filter medium: GF – glass fiber, US-uncharged synthetic, CS – charged synthetic. The indoor aerosol was used in the tests.

Filter			EF_{MPPS}		$EF_{0.4\mu m}$		EF_{UFPs}	
			Ave.	**SD**	**Ave.**	**SD**	**Ave.**	**SD**
F5	GF	#1	3%	0%	11%	0%	15%	6%
	CS	#2	28%	1%	41%	3%	31%	4%
F6	GF and US	#3	12%	1%	25%	2%	21%	2%
		#4	18%	1%	36%	1%	38%	2%
		#5	25%	2%	40%	0%	42%	2%
	CS	#6	60%	5%	83%	2%	69%	2%
		#7	66%	3%	80%	5%	70%	0%
		#8	51%	3%	74%	6%	60%	2%
F7	GF and US	#9	47%	5%	61%	1%	57%	2%
		#10	47%	4%	58%	2%	67%	1%
		#11	44%	0%	62%	8%	64%	1%
		#12	41%	5%	60%	4%	62%	1%
	CS	#13	63%	0%	88%	0%	73%	3%
		#14	68%	3%	88%	5%	71%	2%
		#15	56%	4%	84%	2%	67%	0%
F8	GF and US	#16	51%	5%	64%	1%	71%	6%
		#17	57%	1%	69%	4%	76%	3%
		#18	55%	5%	72%	6%	71%	2%
		#19	54%	3%	72%	0%	77%	4%
	CS	#20	74%	6%	89%	0%	77%	2%
		#21	70%	4%	92%	4%	74%	0%
F9	GF	#22	61%	1%	75%	5%	72%	1%
	CS	#23	73%	4%	94%	4%	77%	3%

6.3.2 Regression curves comparison

The indoor aerosol is different from the oil aerosol as regards particle size distribution, see Figure 6.7.

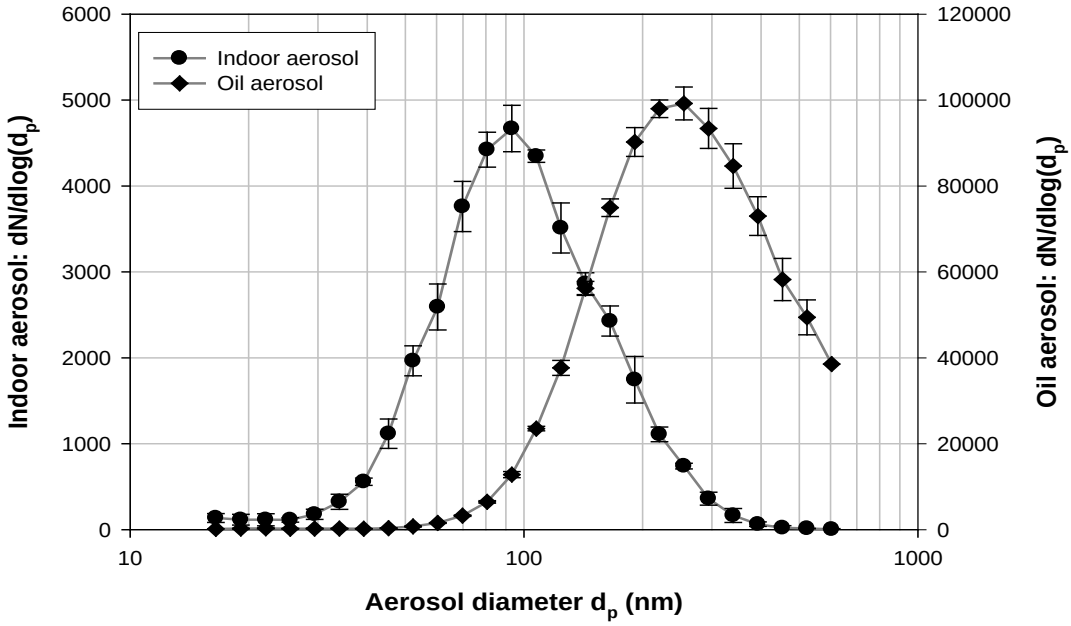

Figure 6.7 Size distributions of oil aerosol and indoor aerosol.

In the figure, the peak concentration of the oil aerosol is found for particles with the diameter about 250 nm, while the peak concentration in the indoor aerosol is found for particles with the diameter less than 100 nm. It is probably because the indoor aerosol mainly came from outdoor pollution since there was no strong indoor aerosol source during the experiments.

Figure 6.8 and 6.9 present the regression curves between $EF_{MPPS,}$ EF_{UFPs} and $EF_{0.4\mu m}$ observed in both the oil aerosol test and the indoor aerosol test. The indoor aerosol resulted in a general shift towards higher efficiency values for the charged synthetic filters, although the filter classes were the same. For the indoor aerosol results, least squares regression analysis shows that the R^2 values are above 0.89 in all cases. T-tests of the correlation coefficients in Figure 6.8 and 6.9 show p-values lower than 0.025 for all cases. Additionally, the Student's t-test was applied to the filtration efficiencies of the same filters, tested with such two aerosols, and with the null hypothesis indicating no difference between the two measurement efficiencies. The analysis shows that the p-value for charged synthetic filters is less than 0.05 ($p<0.05$), while the p-value for glass fiber filters is larger than 0.18 ($p>0.18$). If the null hypothesis is judged at a significance level of 5%, the null hypothesis is rejected at a p-value lower than 0.05 for charged synthetic filters, while is accepted at p-value above 0.18 for glass fiber filters. In other words, the two aerosols gave efficiency values that are significantly different for charged synthetic filters at $p<0.05$, but not significantly different for glass fiber filters.

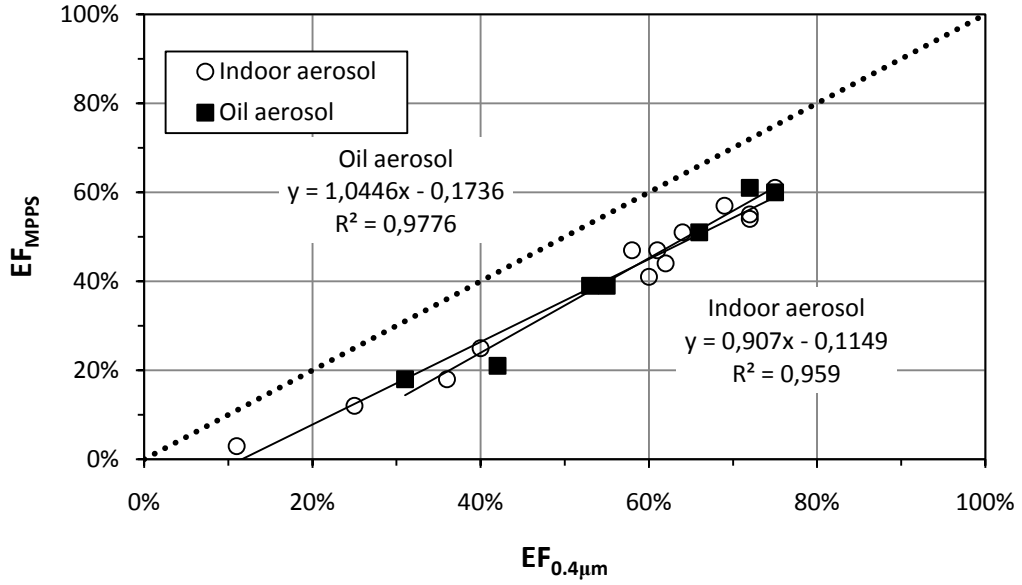

(a)

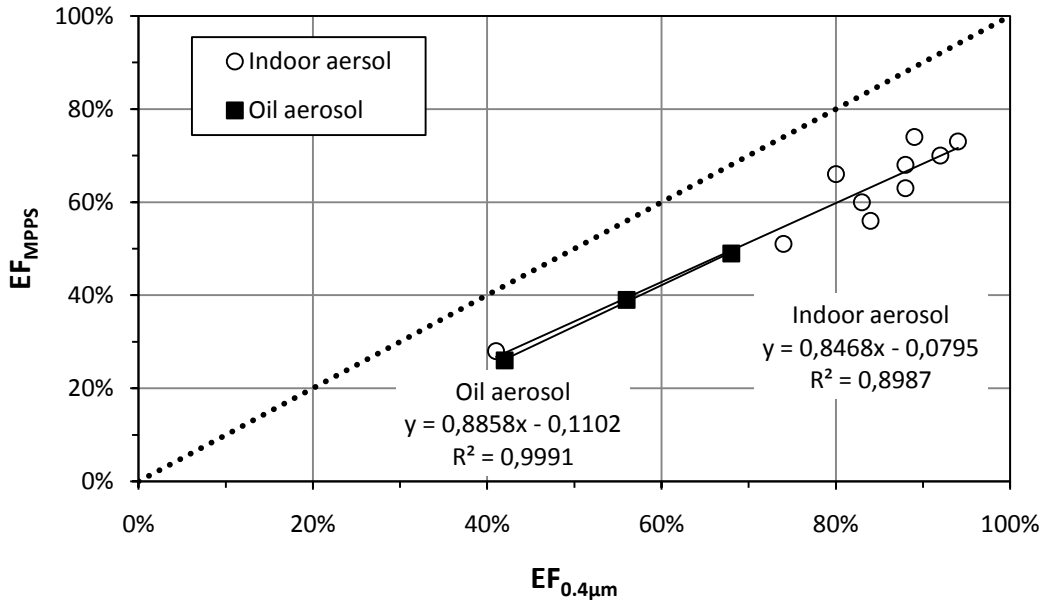

(b)

Figure 6.8 Filtration efficiency based on MPPS-sized particles plotted against the efficiency based on 0.4 µm-sized particles in the indoor aerosol test and the oil aerosol test. (a) Glass fiber and uncharged synthetic filters; (b) charged synthetic filters.

In Figure 6.8, the regression curves between EF_{MPPS} and $EF_{0.4\mu m}$ in two aerosol tests are close to each other and have similar slopes. Especially for charged synthetic filters, the curves are almost overlapping each other. The data show that experiments with an indoor aerosol and an oil aerosol can lead to similar regression curves between EF_{MPPS} and $EF_{0.4\mu m}$.

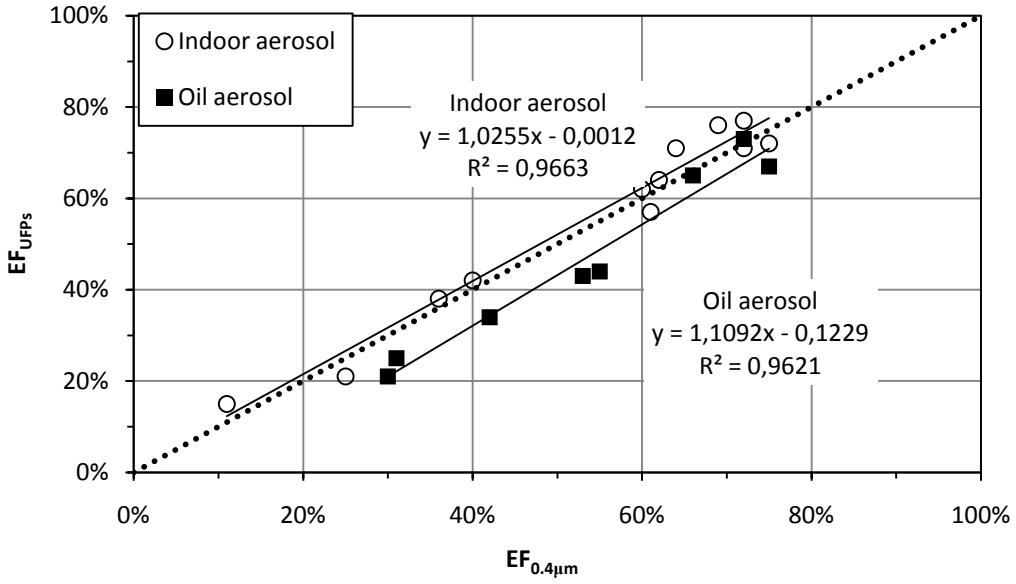

(a)

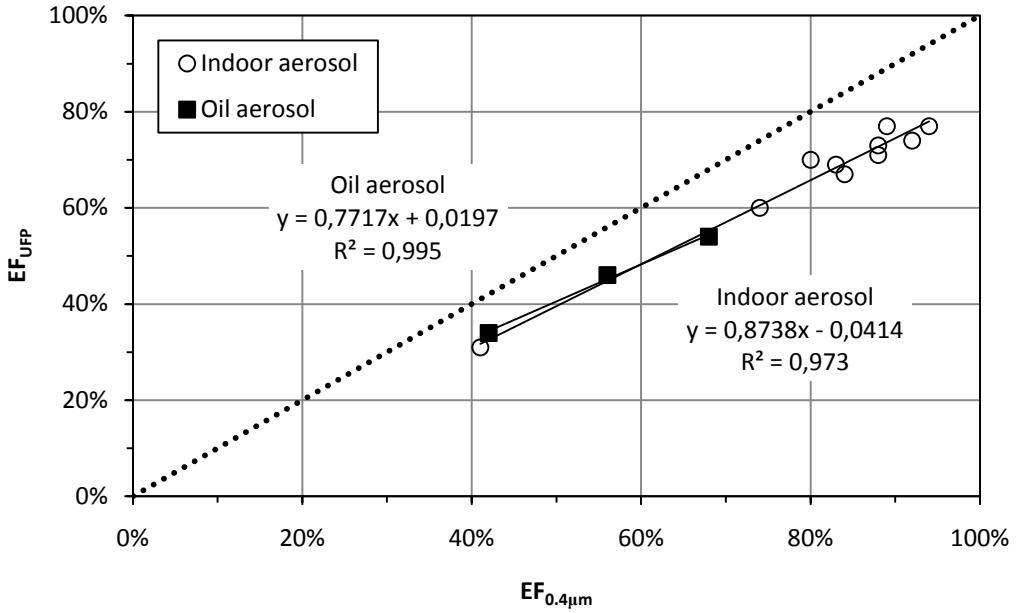

(b)

Figure 6.9 Filtration efficiency based on UFPs plotted against the efficiency based on 0.4 µm-sized particles in the indoor aerosol test and the oil aerosol test. (a) Glass fiber and uncharged synthetic filters; (b) charged synthetic filters.

Figure 6.9 shows the correlation between EF_{UFPs} and $EF_{0.4\mu m}$. For the glass fiber filters in Figure 6.9(a), the regression curve obtained from the indoor aerosol test is above the regression curve from the oil aerosol test. However, for charged synthetic filter in Figure 6.9(b), the regression curves almost overlap each other. This is because the upstream particle size distribution can influence the integrated efficiency on UFPs. Here, regression curves of glass fiber filters are influenced by the size distribution of the two aerosols.

6.4 Discussion

According to the regression analysis presented, the relation between EF_{MPPS} and $EF_{0.4\mu m}$ appear to be linear within the observed efficiency range ($EF_{0.4\mu m}$ between about 10% and 75%). However, single fiber theory reveals that the relationship is non-linear, as indicated in Figure 6.10. The calculation results shown in the figure were obtained by using the theory presented by Hinds (1999). The filter parameters for sheet filter #9 were used as input data. Varying efficiency values were then simulated by varying the packing density over a wide range. Another set of simulations made by varying the filter depth gave practically identical curves.

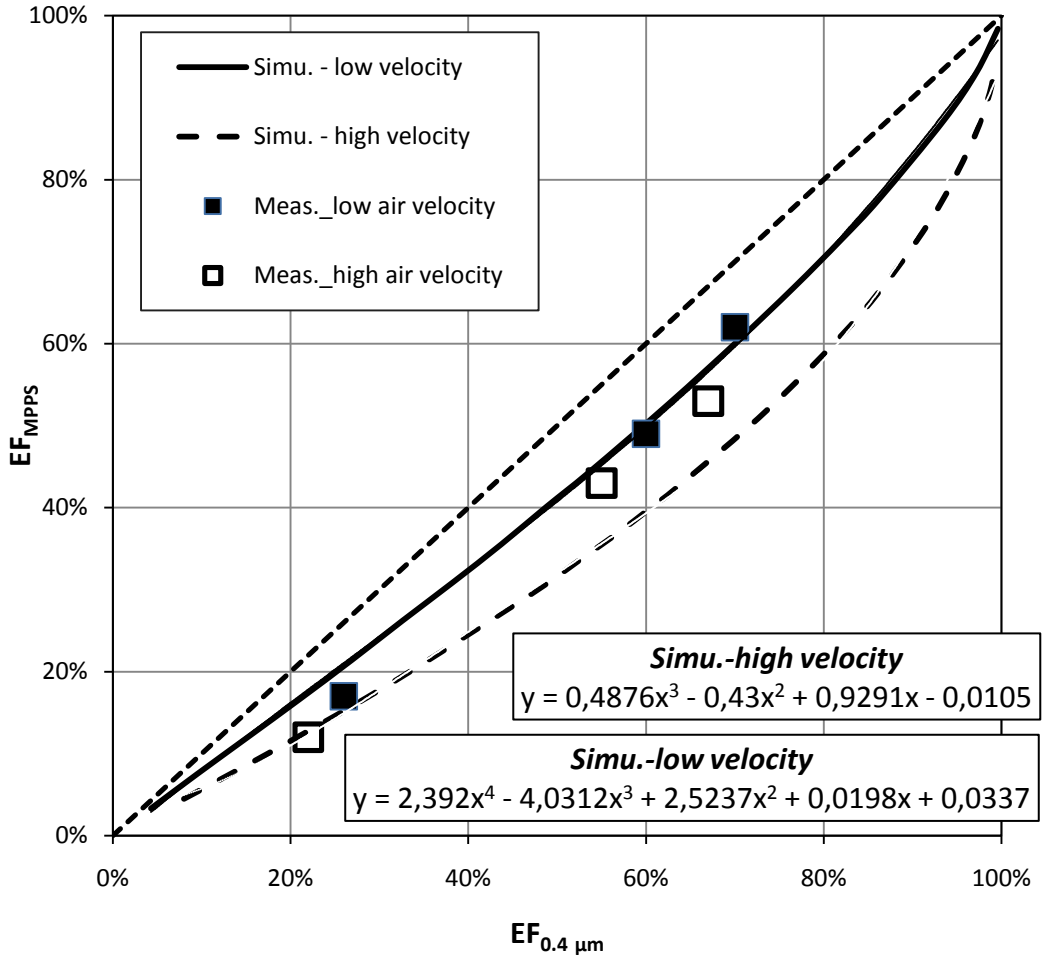

Figure 6.10 Comparison of the measured efficiency and the simulated efficiency for a glass fiber filter. The simulation efficiency in the range of 0%-100% is produced through the theory simulation on #9 filter media with varied parking density. Low air velocity: 0.08 m/s; High velocity: 0.22 m/s.

Experimental data for glass fiber filters tested at the low and the high air velocity have been added to Figure 6.10. There is fair agreement between the simulation results and the experimental results. However, single fiber theory indicates a somewhat stronger influence from velocity variations. Additionally, as long as the $EF_{0.4\mu m}$-value is below 65-70%, the increase of the slope is almost negligible.

The above relationship study between EF_{MPPS}, EF_{UFPs} and $EF_{0.4\mu m}$, shows the results for intermediate air filters under normal operation air velocity. It also shows the influence of filter media type and testing aerosol. Based on the regression curves, it is possible to briefly estimate EF_{MPPS} and EF_{UFPs} based on the $EF_{0.4\mu m}$ announced from filters manufactures or obtained from measurements made according to current filter standards. Additionally, it is possible that the estimation could be made somewhat more precise if a substantially higher number of filters were tested and included in the analysis. However, most likely, still the data should be regarded as rough estimations, reflecting the behaviour of intermediate filters on average. To include MPPS, EF_{MPPS} and EF_{UFPs} in future filter performance criteria, for the sake of precision, there is a need to include the determination of them for each and every filter being tested/classified. There is reason to consider inclusion of this in future revisions of both EN 779 and ASHRAE 52.2. It needs to be noticed that the EF_{UFPs} is influenced by field aerosol diameter of peak concentration.

6.5 Conclusions

The study investigated the correlations between EF_{UFPs}, EF_{MPPS} and $EF_{0.4\mu m}$ and the influential factors of air velocities, filter media and upstream aerosols. The full scale filter measurements indicate linear relationships between EF_{UFPs}, EF_{MPPS} and $EF_{0.4\mu m}$ in the range of $EF_{0.4\mu m}$ less than 70%. The indoor aerosol test and oil aerosol test obtain similar regression curves between EF_{UFPs}, EF_{MPPS} and $EF_{0.4\mu m}$. EF_{MPPS} and EF_{UFPs} are closer to $EF_{0.4\mu m}$ for glass fiber filters than for charged synthetic filters.

The air velocity limitedly influences the efficiency regression curves. Additionally, when air velocity increases, the EF_{MPPS} and EF_{UFPs} are reduced more than $EF_{0.4\mu m}$ for glass fiber filters, while reduced less than $EF_{0.4\mu m}$ for charged synthetic filters. This is because the variation of MPPS with air velocity is different for glass fiber filters and charged synthetic filters. Although, the charge of the aerosol could influence the filtration efficiency of charged synthetic filters, the aerosol type almost has no influence on the regression curve between EF_{MPPS} and $EF_{0.4\mu m}$ for the two filter media. However, the size-distribution of the aerosol could influence on the regression curve between EF_{UFPs} and $EF_{0.4\mu m}$.

The investigation also shows the possible way to compose EF_{UFPs} and EF_{MPPS} into a future filter standard. The regression equation provides a simple way to make a brief estimation, while for an accurate estimation, individual determination is necessary for each and every filter being tested/ classified.

7 Modelling of particle transport in buildings

Knowledge of indoor dynamics of outdoor infiltrated particles and indoor emitted particles is important to be able to control indoor particle personal exposure and to choose a suitable ventilation mode. The purposes of the analysis are to evaluate the effect of air filtration and ventilation mode on indoor particles of indoor and outdoor origins and to understand the influence of air filtration locations on the effects of the indoor removal mechanisms. The study is based on a balance model of indoor particles. The dynamical mechanisms include outdoor and recirculated air filtration, indoor deposition, outdoor particle infiltration and indoor particle exfiltration and exhaustion. The evaluation is conducted using the parameters of indoor particles proportion of outdoor origin ($C_{i,o}/C_o$) and the time constant for removal of indoor emitted particles ($C_{i,s}/(S_i/V)$).

7.1 Introduction

According to previous literature studies [4, 7, 30, 40, 79, 98, 103, 133, 150, 154, 165], the toxicity of the particles probably greatly depends on particle chemical composition and size-resolved number concentration, which are further decided by particle sources and formation processes. Furthermore, particle properties studies reviewed in Chapter 2.1 and 2.3 show that particle chemical composition is closely related with particle size and particle formation process. Therefore, there is a high possibility that when particles are controlled specifically with respect to indoor and outdoor origins on specific size ranges, the health risks of the breathable particles in indoor air could be substantially under control.

In many studies, the small particles from combustion were considered to be more closely associated with adverse health effects. However, when tobacco smoking exists indoors, outdoor particle infiltration becomes to be negligible. To control indoor particles of indoor and outdoor origins and reduce indoor personal exposure to “real” harmful particles at the right time, choosing a suitable air filtration and ventilation mode is important. A critical study is to analyse the performance of air filtration and ventilation to remove indoor particles of indoor and outdoor origins respectively. For this, the knowledge of indoor particle fate is the basis.

Indoor particles are removed by the mechanisms of outdoor and recirculation air filtration, indoor particle exfiltration and exhaustion and particle deposition. Additionally, indoor particles are contributed to by outdoor particle infiltration and indoor source generation. The outdoor particle infiltration includes the penetration of outdoor particles through the building envelope and by outdoor supply air. All the above mechanisms are depending on particle size. They could modify the indoor particle percentage of outdoor origins and the time constant of indoor emitted particles.

Many current studies have investigated the suitable (or optimal) ventilation rate for the sake of energy saving and for “securing” indoor air quality. The outdoor air flow rate directly influences outdoor particle infiltration and indirectly influences indoor particle exhaustion. Additionally, recirculation air through an air filter could remove indoor particles. Here, outdoor air flow and recirculating air flow compose the supply air flow. As an important basic knowledge, it is

necessary to understand how the supply air flow rate and outdoor air flow rate affect the concentration of indoor particles from indoor generation and outdoor particle infiltration respectively.

Additionally, the removal of indoor particles of indoor and outdoor origins is also decided by the application of air cleaners for airborne particles. The air cleaners would be air filters installed in a ventilation system to capture particles from outdoor air flow, or recirculation air flow or both of them. It also could be a room air cleaner to capture indoor particles. Their application could play a critical role in the reduction of the personal exposure to indoor particles of indoor and outdoor origins.

At present, many studies investigated the relative contributions of indoor generated particles and outdoor particle infiltration to indoor environments, while few of them discussed how to control indoor particles according their origins [1, 92, 128]. In addition, many researchers have studied advanced ventilation measures to control total indoor particles, however few of them have investigated the efficiencies of these systems to remove indoor particles of indoor and outdoor origins respectively [93, 107]. The motivation of the study is to fill in the gap between the above two topics.

7.2 Methodology

7.2.1 Mathematics model

A mathematical model is developed based on an indoor particle mass balance, as illustrated in Figure 7.1. A filter is installed in one of four possible locations A-D in the ventilation system to filtrate outdoor air, supply air, recirculation air and indoor air respectively. The C_i and C_o are indoor and outdoor particle concentration; k_v, k_d, k_{inf}, k_{exf} and k_c are outdoor air exchange rate, deposition rate, infiltration rate, exfiltration rate and recirculation rate respectively, with the unit of h^{-1}, p_{inf} is the particle penetration rate of the infiltration (%), EF is the filter filtration efficiency (%). In the model, the sum of k_{exf} and k_v is considered to be the total exhaust air exchange rate from the building, which is equal to the total infiltration air exchange rate, i.e. the sum of k_{inf} and k_v.

The model study focuses on the indoor fate of ultrafine and submicron particles, since normally the number concentrations of ambient particles and combustion particles are mainly distributed in this size range. Additionally, previous studies have shown that particle loss in ventilation ducts are negligible for submicron and ultrafine particles, but become important for particles larger than 5 μm in diameter [140, 164]. So, the model does not include any particle loss due to the deposition in ventilation duct system. However, this is a simplification since the calculations include particles up to 10 μm. Furthermore, the model does not include the influence from resuspension of particles.

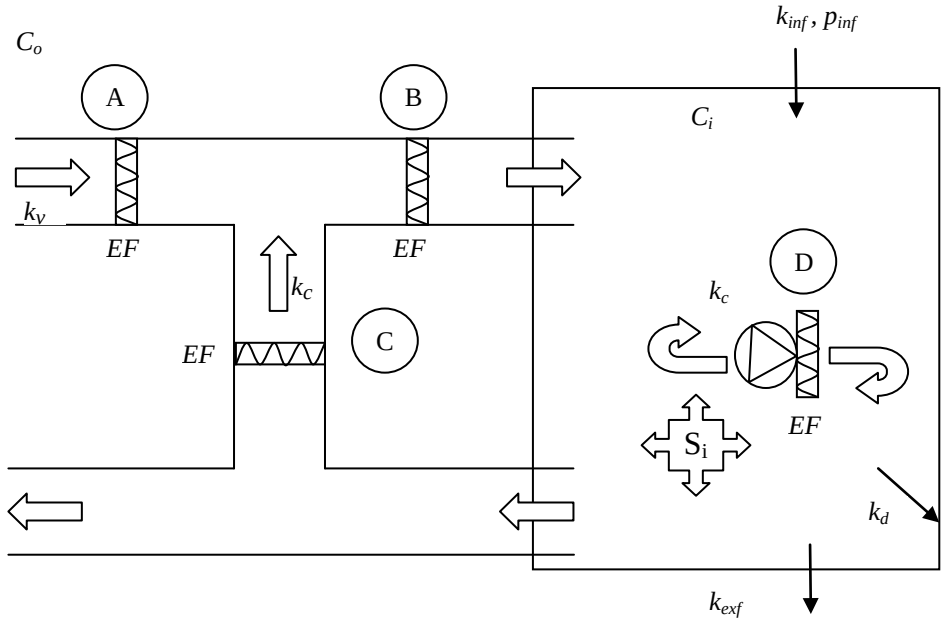

Figure 7.1 Schematic of indoor particle transportation and four air filtration locations A-D.

The indoor particle balance equation is presented in eq. 7.1[128]. C_o and C_i could be particle number, mass or surface area concentration. In this study they represent the particle number concentration (particles/cm^3).

$$\frac{dC_i}{dt} = \left(\frac{S_i}{V} + (1 - EF_{OA}) * k_v * C_o + k_{inf} * p_{inf} * C_o\right) - \left(k_d + k_v + k_{exf} + k_c * EF_{IA}\right) * C_i \qquad \textit{(eq. 7.1)}$$

Where:

V is the volume of the room (cm^3); S_i is the indoor source strength (particles/h), EF is the filter filtration efficiency. To investigate the filtration efficiency on particles in outdoor air and return or indoor air, EF is written as EF_{OA} and EF_{IA}.

This equation can also be presented as eq. 7.2 and 7.3

$$\frac{dC_i}{dt} = \beta - KC_i \qquad \textit{(eq. 7.2)}$$

$$C_i(t) = C_{i,t=o}e^{\frac{-t}{T}} + \frac{\beta}{K}(1 - e^{\frac{-t}{T}}) \qquad \textit{(eq. 7.3)}$$

Where:

The symbol β represents the increased particles from indoor particle generation and the total outdoor particle infiltration. Here $\beta = \frac{S_i}{V} + (1 - EF_{OA}) * k_v * C_o + k_{inf} * p_{inf} * C_o$. K represents the total sink rate. Here $K=k_v+k_d+k_{exf}+k_c*EF_{IA}$. T is

the time constant of indoor particles (h). Here $T=1/K=1/(k_v+k_d+k_{exf}+k_c*EF_{IA})$. $C_{i,t=0}$ is the initial indoor particle concentration.

Thus, the first part on the right side represents the initial indoor particles under decay; and the second part represents the indoor generated particles and outdoor infiltrated particles (β) under decay. Under stable conditions, $\frac{dC_i}{dt}$ is equivalent to 0, thus eq. 7.1 becomes eq. 7.4.

$$C_i = \frac{\frac{S_i}{V}}{k_d+k_v+k_{exf}+k_c*EF_{IA}} + \frac{[(1-EF_{OA})*k_v+k_{inf}*p_{inf}]*C_o}{k_d+k_v+k_{exf}+k_c*EF_{IA}} \qquad \textit{(eq. 7.4)}$$

On the right hand of eq. 7.4, the first part represents the indoor particles contributed to by indoor generated particles, and the second part represents indoor particles contributed to by the outdoor particles infiltration. If we separate indoor particles into outdoor infiltrated particles ($C_{i,o}$) and indoor generated particles ($C_{i,s}$), then the concentration of $C_{i,o}$ and $C_{i,s}$ can be calculated according to eq. 7.5 and 7.6, respectively.

$$C_{i,o} = \frac{[(1-EF_{OA})*k_v+k_{inf}*p_{inf}]*C_o}{k_d+k_v+k_{exf}+k_c*EF_{IA}} \qquad \textit{(eq. 7.5)}$$

$$C_{i,s} = \frac{\frac{S_i}{V}}{k_d+k_v+k_{exf}+k_c*EF_{IA}} \qquad \textit{(eq. 7.6)}$$

Furthermore, the indoor particles proportion of outdoor origin ($C_{i,o}/C_o$), indoor particle proportion of indoor origin ($C_{i,s}/(S_i/\dot{Q})$), and the time constant of indoor particles T = $C_{i,s}/(S_i/V)$ are presented in eq. 7.7-7.9 respectively.

$$\frac{C_{i,o}}{C_o} = \frac{(1-EF_{OA})*k_v+k_{\inf}*p_{\inf}}{k_d+k_v+k_{exf}+k_c*EF_{IA}} \ (\%) \qquad \textit{(eq. 7.7)}$$

$$\frac{C_{i,s}}{(\frac{S_i}{\dot{Q}})} = \frac{ACR}{(k_d+k_v+k_{exf}+k_c*EF_{IA})} \ (\%) \qquad \textit{(eq. 7.8)}$$

$$\frac{C_{i,s}}{(\frac{S_i}{V})} = \frac{1}{k_d+k_v+k_{exf}+k_c*EF_{IA}} \ (\text{h}) \qquad \textit{(eq. 7.9)}$$

Where:

ACR is the outdoor air exchange rate (h^{-1}) and $\dot{Q}$ is the outdoor air flow rate (m^3/h). When *ACR* is 1 h^{-1}, $C_{i,s}/(S_i/\dot{Q})$ has the same value as $C_{i,s}/(S_i/V)$. In addition, the definition of $C_{i,s}/(S_i/V)$ in eq. 7.9 is the same as the definition of the time constant "*T*" in eq. 7.3. In practice, this confirms that $C_{i,s}/(S_i/V)$ is the time constant of indoor particles. When $C_{i,s}/(S_i/V)$ is small, it means that indoor generated particles, $C_{i,s}$, are rapidly removed and stay indoors for a short time.

In eq. 7.7-7.9 about $C_{i,o}/C_o$, $C_{i,s}/(S_i/Q)$ and $C_{i,s}/(S_i/V)$ there is no influence of the ambient particle concentration, the indoor source strength or their size distributions. .

Table 7.1 The specific setting of the studied cases.

Cases	Filter location	k_v (h^{-1})	k_c (h^{-1})	EF_{OA} *and* EF_{IA}
Base case	None	1	1	$EF_{OA}= EF_{IA} =0$
Case A	A	1	1	$EF_{OA}=EF$; $EF_{IA} =0$
Case B	B	1	1	$EF_{OA}= EF_{IA}=EF$
Case C	C	1	1	$EF_{OA}=0$; $EF_{IA}=EF$
Case D	D	1	1	$EF_{OA}=0$; $EF_{IA}=EF$

One base case and cases A-D with different air filter locations and air exchange rates are studied, see Table 7.1. The filter in the locations C and D equally works to remove particles from indoor air. Thus, both Case C and D are represented by Case C.

7.2.2 Parameters

The filter size-resolved filtration efficiencies are illustrated in Figure 7.2, which includes data from the laboratory measurements, theory simulations, and the study of Hanley [58]. The measurement data shown in Figure 7.2 were obtained by the methodology described in Chapter 4. The testing air flow rate was 0.944m^3/s for the measured efficiencies of F5-F9 class filters. The filters are corresponding to MERV 9-13 in ASHRAE 52.2. Based on the fibrous filtration theory described by Hinds [65], a set of simulations were conducted in the full diameter range used in the study. Considering the good agreement between the data from the three studies, the simulation efficiencies are utilized in the model.

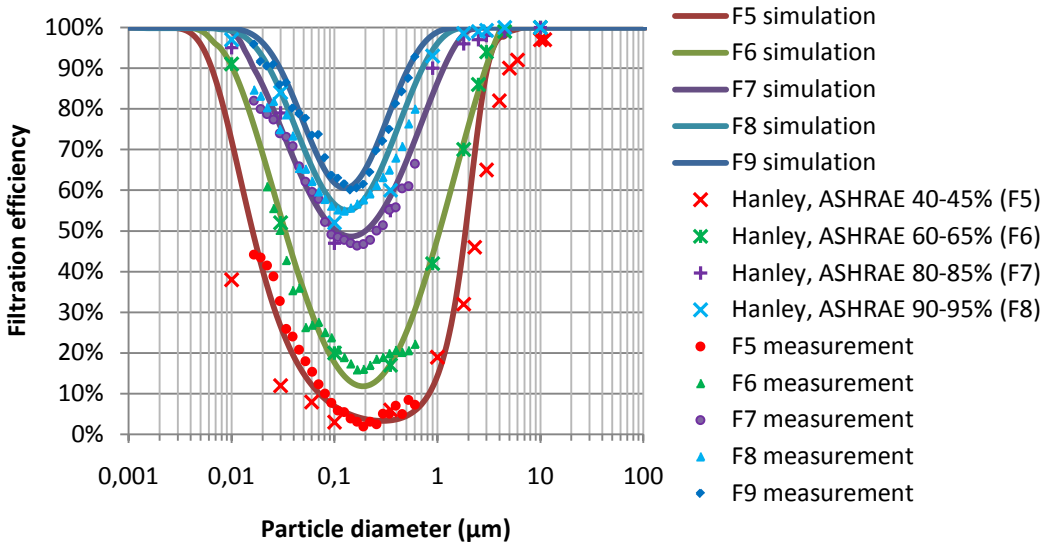

Figure 7.2 The size-resolved efficiency for F5~F9 class filters.

For other parameters, the building envelope penetration rate (p_{inf}) and indoor particle deposition rate (k_d) are referring to the studies of Liu and Nazaroff, 2001 [90] and Riley et al. 2002[128] respectively. See Figure 7.3 and 7.4. The air

infiltration rate, k_{inf}, and exfiltration rate, k_{exf}, are assumed to be 0.2 h^{-1} for normal office buildings

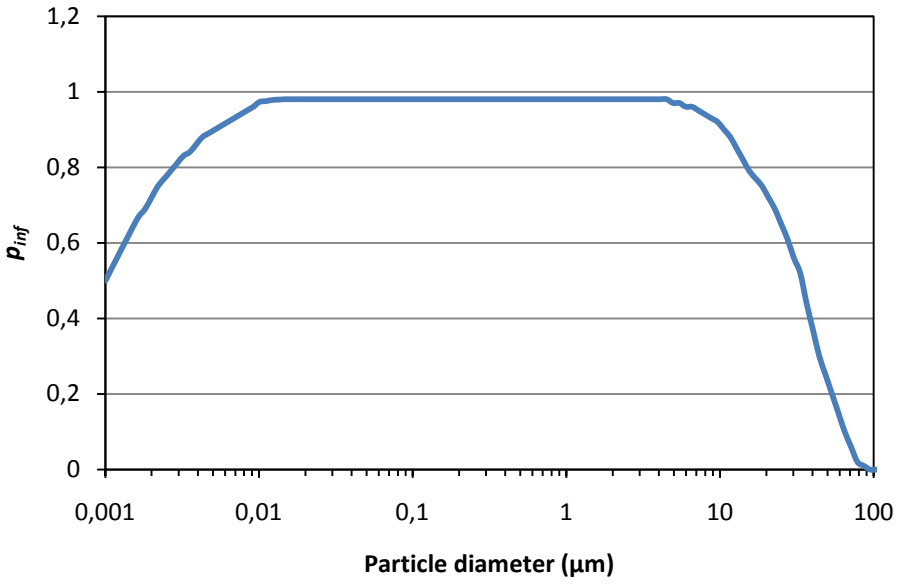

Figure 7.3 Penetration rate (p_{inf}) vs aerosol diameter. The diagram is adopted from Liu and Nazaroff, 2001[90]. This overall penetration rate is for a building with crack area distributed uniformly with respect to crack height of 0.05-2.0 mm and crack length of 3 cm under a pressure difference of 4 Pa.

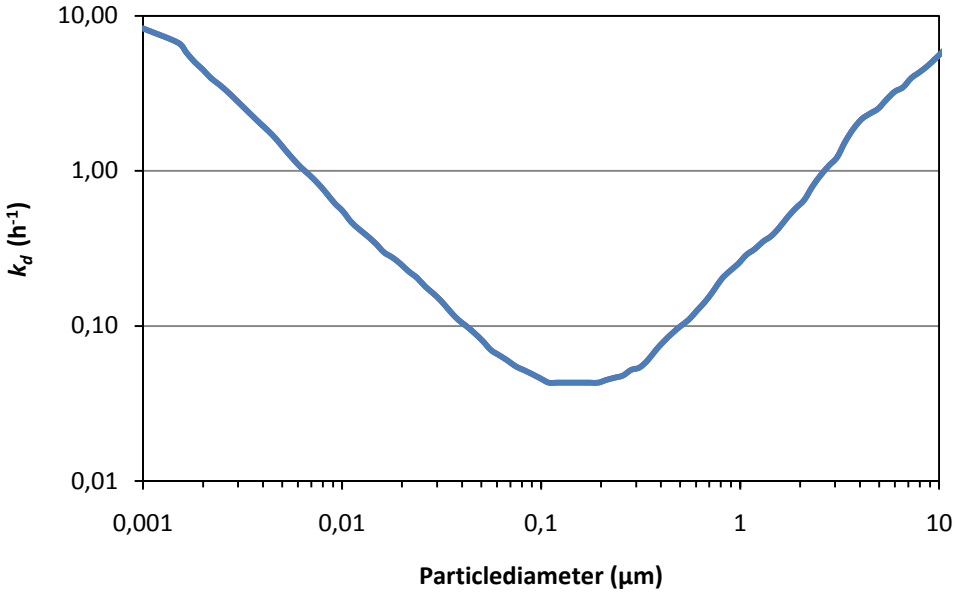

Figure 7.4 Deposition rate (k_d) vs aerosol diameter. The diagram is adopted from Riley et al., 2002[128].

7.2.3 Theory of the mechanisms effect

Installing filters in different locations would influence the mechanisms effects to reduce $C_{i,o}/C_o$ and $C_{i,s}/(S_i/V)$. The influences of these mechanisms are described by eq. 7.10 and 7.11. In eq. 7.10, the variation of $C_{i,o}/C_o$ is induced by the

variation of the total outdoor particle infiltration and the particle sink mechanisms of k_v, k_d, k_{exf} , k_c, EF_{IA} and EF_{OA}. As the particle sink mechanisms, k_v and EF_{OA} work as exhaust air removal and outdoor air filtration respectively. Unlike them, k_c and EF_{IA} work together as recirculating air filtration. In the calculations presented in section 7.3, the partial differential item of EF_{IA} represents the mechanism effect of recirculating air filtration, and k_c is considered as a constant parameter. Both k_{exf} and k_v can be considered as exhausted air mechanisms, so the sum of their effects is the effect of the total exhaust air.

$$
\begin{aligned}
d\frac{C_{i,o}}{C_o} = &\left[\frac{1-EF_{OA}}{k_v+k_d+k_{exf}+EF_{IA}*k_c}dk_v + \frac{p_{inf}}{k_v+k_d+k_{exf}+EF_{IA}*k_c}dk_{inf}\right] \\
&-\left[\frac{(1-EF_{OA})*k_v+k_{inf}*p_{inf}}{\left(k_v+k_d+k_{exf}+EF_{IA}*k_c\right)^2}dk_v\right. \\
&+\frac{(1-EF_{OA})*k_v+k_{inf}*p_{inf}}{\left(k_v+k_d+k_{exf}+EF_{IA}*k_c\right)^2}dk_d \\
&+\frac{(1-EF_{OA})*k_v+k_{inf}*p_{inf}}{\left(k_v+k_d+k_{exf}+EF_{IA}*k_c\right)^2}dk_{exf} \\
&+\frac{\left[(1-EF_{OA})*k_v+k_{inf}*p_{inf}\right]*EF_{IA}}{\left(k_v+k_d+k_{exf}+EF_{IA}*k_c\right)^2}dk_c \\
&+\frac{\left[(1-EF_{OA})*k_v+k_{inf}*p_{inf}\right]*k_c}{\left(k_v+k_d+k_{exf}+EF_{IA}*k_c\right)^2}dEF_{IA} \\
&\left.+\frac{k_v}{k_v+k_d+k_{exf}+EF_{IA}*k_c}dEF_{OA}\right] \qquad \textit{(eq. 7.10)}
\end{aligned}
$$

The corresponding analysis for $C_{i,s}/(S_i/V)$ is described by the differential equation below.

$$
\begin{aligned}
&d\left(\frac{C_{i,s}}{\frac{S_i}{V}}\right) \\
&= -\frac{1}{\left(k_d+k_v+k_{exf}+EF_{IA}*k_c\right)^2}dk_d - \frac{1}{\left(k_d+k_v+k_{exf}+EF_{IA}*k_c\right)^2}dk_v \\
&-\frac{1}{\left(k_d+k_v+k_{exf}+EF_{IA}*k_c\right)^2}dk_{exf} - \frac{EF_{IA}}{\left(k_d+k_v+k_{exf}+EF_{IA}*k_c\right)^2}dk_c \\
&-\frac{k_c}{\left(k_d+k_v+k_{exf}+EF_{IA}*k_c\right)^2}dEF_{IA} \qquad \textit{(eq. 7.11)}
\end{aligned}
$$

Eq. 7.11 shows how the variation of $C_{i,s}/(S_i/V)$ is contributed to by the variation of the mechanisms of k_v, k_d, k_{exf}, k_c and EF_{IA}. The increase of k_v, k_d, k_{exf}, k_c and EF_{IA} could result in the decrease of $C_{i,s}/(S_i/V)$. Thus, the partial differential items of these mechanisms represents the mechanisms reduction effects on $C_{i,s}/(S_i/V)$. In the calculations presented in section 7.3, k_c is considered as a constant parameter. And the integration on the partial differential item of EF_{IA} represents the mechanism effect of recirculating air filtration

7.2.4 Study objects

According to the definition of $C_{i,o}/C_o$ and $C_{i,s}/(S_i/V)$ in eq. 7.7-7.9, the effects of particle indoor removal mechanisms on $C_{i,o}/C_o$ and $C_{i,s}/(S_i/V)$ are identified

through the partial differential equations. Then, the outcomes are used to investigate the following objects:

- *Mechanisms effects on $C_{i,o}/C_o$ and $C_{i,s}/(S_i/V)$ in Case A-C;*
- *Comparing the influence of air filtration location on $C_{i,o}/C_o$ and $C_{i,s}/(S_i/V)$;*
- *Influence of the air filter class on $C_{i,o}/C_o$ and $C_{i,s}/(S_i/V)$;*
- *Influence of outdoor air flow percentage on $C_{i,o}/C_o$ and $C_{i,s}/(S_i/V)$;*
- *Influence of supply air flow exchange rate on $C_{i,o}/C_o$ and $C_{i,s}/(S_i/V)$.*

Based on the above analysis method, the expected outcomes are indications about the adequate filter locations and ventilation modes to remove $C_{i,o}$ and $C_{i,s}$.

7.3 Mechanisms effects

Figure 7.5 and 7.6 show how the individual mechanisms remove $C_{i,o}$ and $C_{i,s}$ in Case A-C. The percentages of the mechanisms on the removal of $C_{i,o}$ are shown in Figure 7.5. The effects of on the removal of $C_{i,o}$ are calculated from the partial differential items of k_v, k_d, k_{exf}, EF_{IA} and EF_{OA} in eq. 7.10.

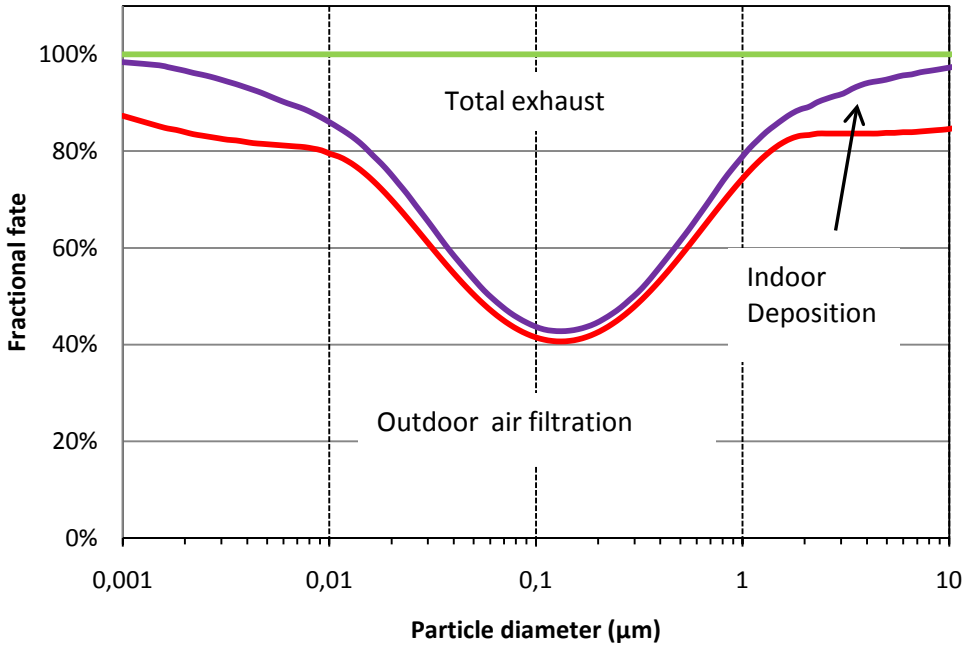

(a)

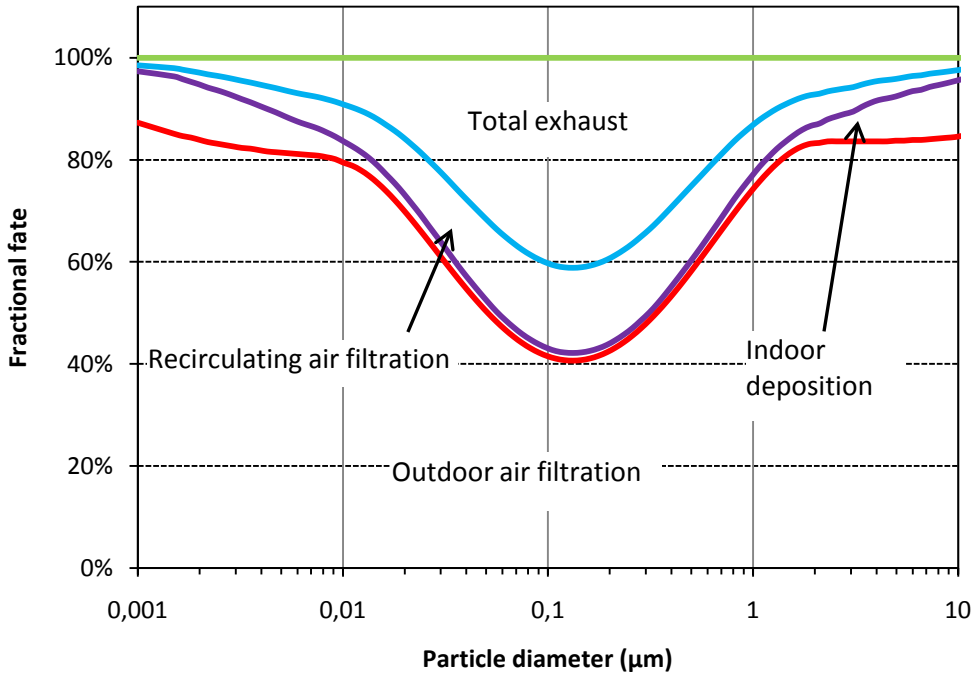

(b)

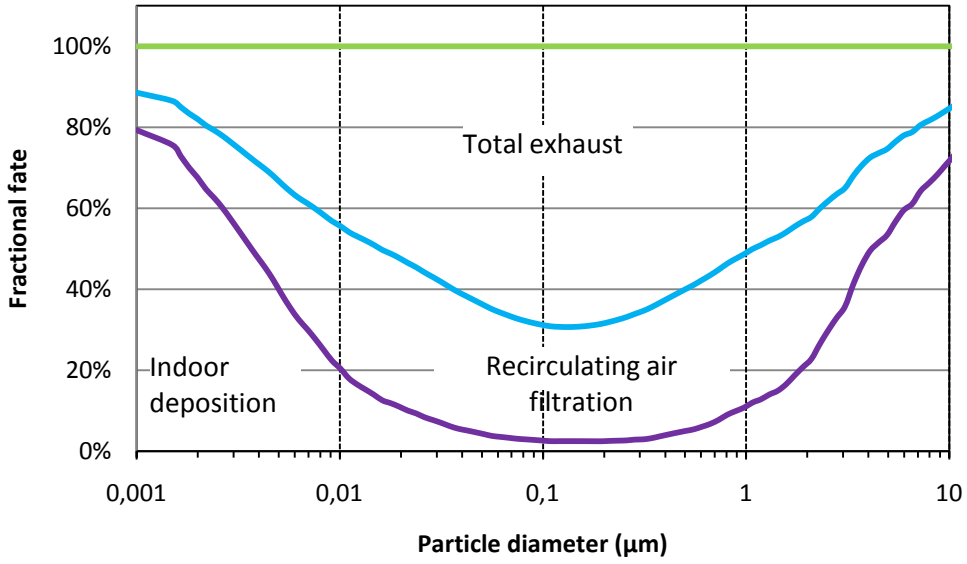

(3)

Figure 7.5 Predicted fractional fates of $C_{i,o}$ for (a) Case A; (b) Case B; (c) Case C. The filter class is set to F7.

The figure shows that, for indoor particles, in Case A and B, with the diameter less than 0.01µm and larger than 2µm, more than 80% of $C_{i,o}$ are filtrated by an F7 class filter and only about less than 10% of $C_{i,o}$ deposit on the indoor surfaces. Both outdoor air filtration and indoor deposition have significant effects on the removal of small particles (e.g. <0.01 µm) and large particles (e.g. >1 µm). However, total exhaust accounts for a substantial part of the removal of particles with a diameter close to 0.1 µm. Without outdoor air filtration, the percentage of $C_{i,o}$ depositing indoors is substantial in Case C. Especially, these percentage is higher than 20% for the particles with diameters less than 0.01µm or larger than 2

μm. In the size ranges of <0.004μm and >4μm in Case C, the recirculating air filtration or a room air cleaner capture less $C_{i,o}$ than indoor deposition does. This phenomenon could be explained by the decay rate of k_d being larger than $EF_{IA} \cdot k_c$ in the size ranges of <0.004μm and >4μm.

Similarly, the percentage of the mechanisms on the removal of $C_{i,s}$ are calculated from the partial differential items k_v, k_d, k_{exf} and k_c in e.q. 7.11. The figure shows that filter locations in Case A-C slightly affect the percentage of indoor depositions. It is self evident that outdoor air filtration has no effect at all on $C_{i,s}$ in Case A-C. Similar to the effect on $C_{i,o}$, recirculating air filtration is most efficient to remove $C_{i,s}$ within the diameter range 0.01 μm to1 μm.

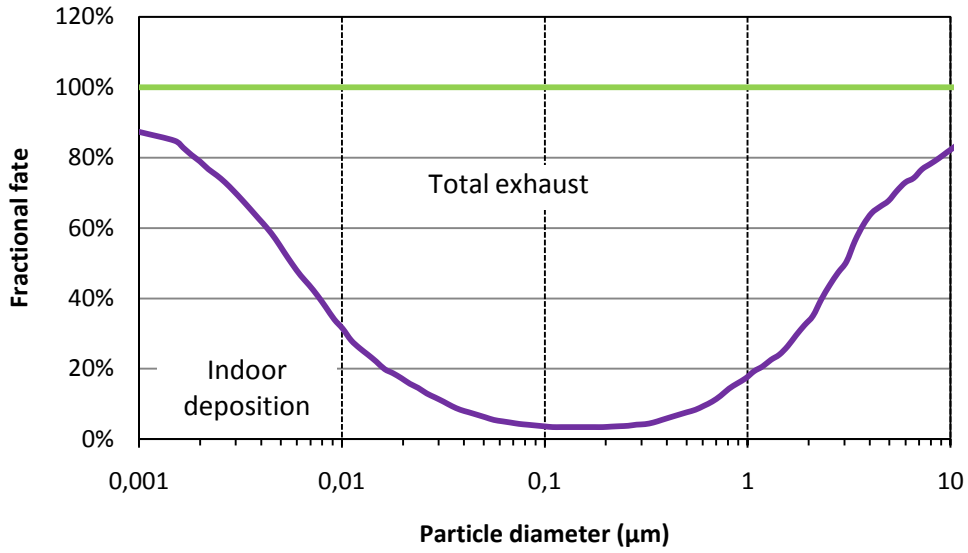

(a)

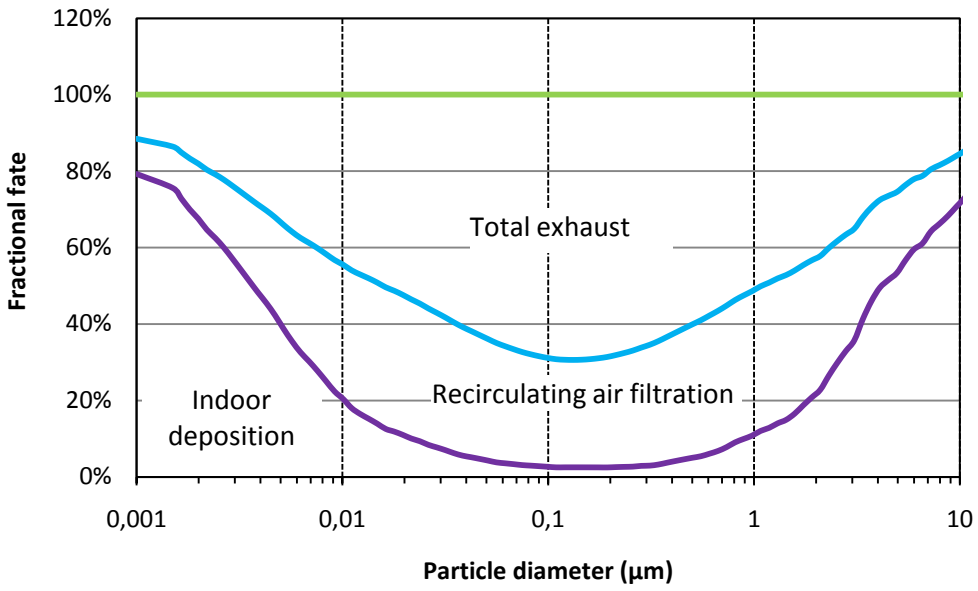

(b)

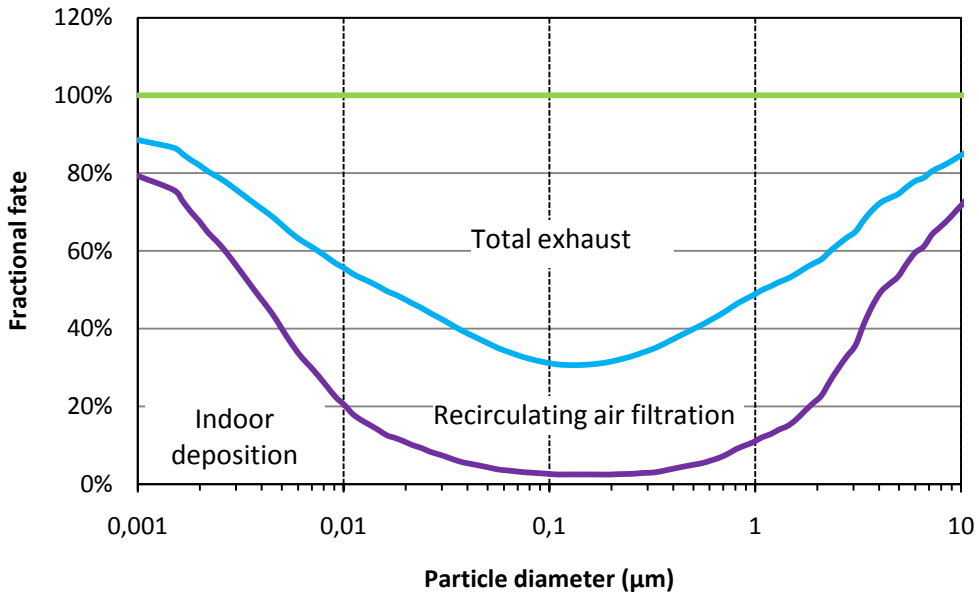

(c)

Figure 7.6 Predicted fractional fates of $C_{i,s}$ for (a) Case A; (b) Case B; (c) Case C. The filter class is set to F7.

7.4 Air filtration influence

To further investigate the effect of air filtration location, Figure 7.7 presents the reduction of $C_{i,o}/C_o$ of Case A-C compared to the Base case. Both k_v and k_c of the above four cases are set to 1 h^{-1}. Additionally, Case A at k_v of 2 h^{-1} and k_c of 0 h^{-1} and Case C at k_v of 0 h^{-1} and k_c of 2 h^{-1} are compared with the same Base case to show the situations with the same filtrated air flow rate as Case B.

For the comparison with k_v of 1 h^{-1} and k_c of 1 h^{-1}, the cases reducing $C_{i,o}/C_o$ from high to low are Case B> Case A > Case C; reducing $C_{i,s}/(S_i/V)$ from high to low are Case C= Case B > Case A.

Comparing Case A at k_v of 2 h^{-1} and k_c of 0 h^{-1} with Case C at k_v of 0 h^{-1} and k_c of 2 h^{-1}, it shows that the $C_{i,o}/C_o$ reduction in Case A is lower than that in Case C on the whole size range, especially in the size range of 0.01-2 µm. However, the corresponding study on the reduction of $C_{i,s}/(S/V)$ shows that Case A with k_v of 2 h^{-1} and k_c of 0 h^{-1} performs better than Case C does at the whole particle size range, especially in the size range of 0.01-2 µm. It needs to be noticed that the size range of 0.01-2 µm includes the most penetrating particle size (MPPS) of most filters.

In Figure 7.7, for particles larger than a few micrometers, the filtration efficiency rapidly approaches its maximum of 100%. However, for the same particle sizes the deposition in the room continues to increase dramatically with increasing particle size (the filter still having about 100% efficiency). The deposition is the same in all cases (A-C), including the Base case. Thus, the marginal effect of the filters becomes smaller with increasing particle size. The same is true for the really small particles (smaller than about 20 nm).

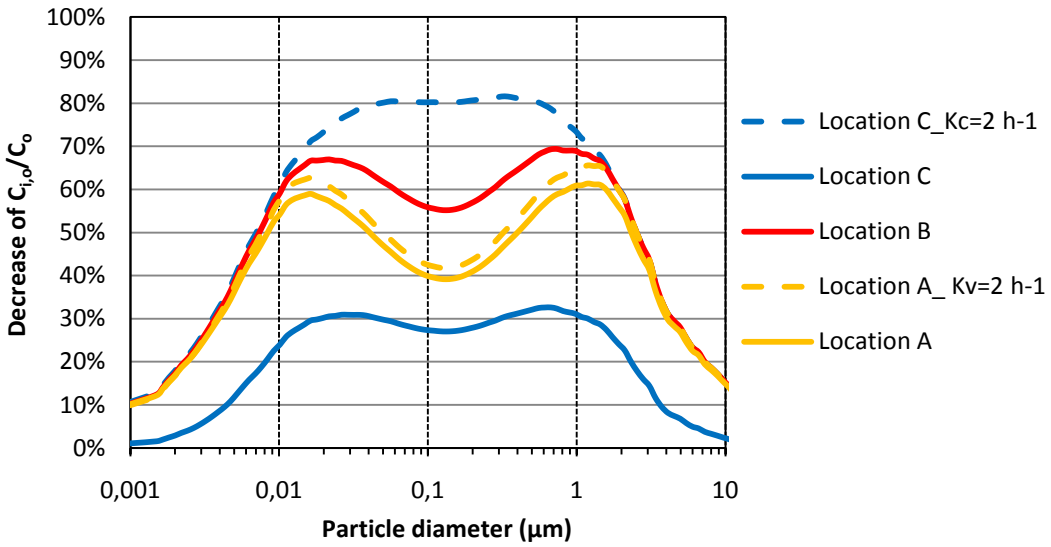

(a)

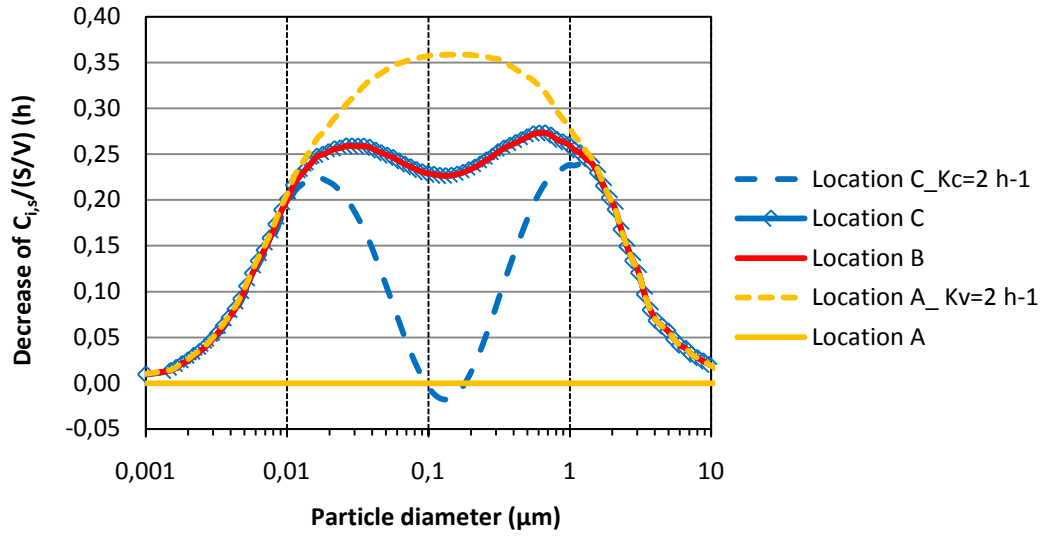

(b)

Figure 7.7 Air filtration influence on $C_{i,o}/C_o$ and $C_{i,s}/(S_i/V)$ in Case A-C. The calculation is based on an F7 class filter, and unless otherwise specified with k_v=1 h^{-1} and k_c=1 h^{-1}. (a) $C_{i,o}/C_o$; (b) $C_{i,s}/(S/V)$.

The same calculations were also conducted on F5 and F9 class filters, see Figure 7.8-7.9. The figures show that, the performance order of filter location for F5 and F9 class filters is the same as obtained for the F7 class filter. The reductions of $C_{i,o}/C_o$ and $C_{i,s}/(S_i/V)$ slightly increase in the F9 class filter application, while they are substantially reduced in the F5 class filter application.

There is a negative decrease of $C_{i,s}/(S_i/V)$ for the Case C with filter class F5 and k_c of 2 h^{-1} and k_v of 0 h^{-1}. Such negative decrease means that the time constant of indoor particles is longer in Case C than in the Base case. With the application of F7 class filter in this case, the time constant of indoor particles is almost the same as that of the base case. However, with the application of F5 class filter, the time constant of indoor particle removal is prolonged by 2.5 hours compared to the base case. Furthermore, this negative reduction of $C_{i,s}/(S_i/V)$ in the F5 class filter

case would not disappear until k_c is larger than 30 h^{-1}. Therefore, F5 class filter is not recommended in recirculating air filtration.

According to the above filter class performance study, it is suggested to avoid the low class filter application in the recirculating air filtration. And the filter class is better no less than F7 class.

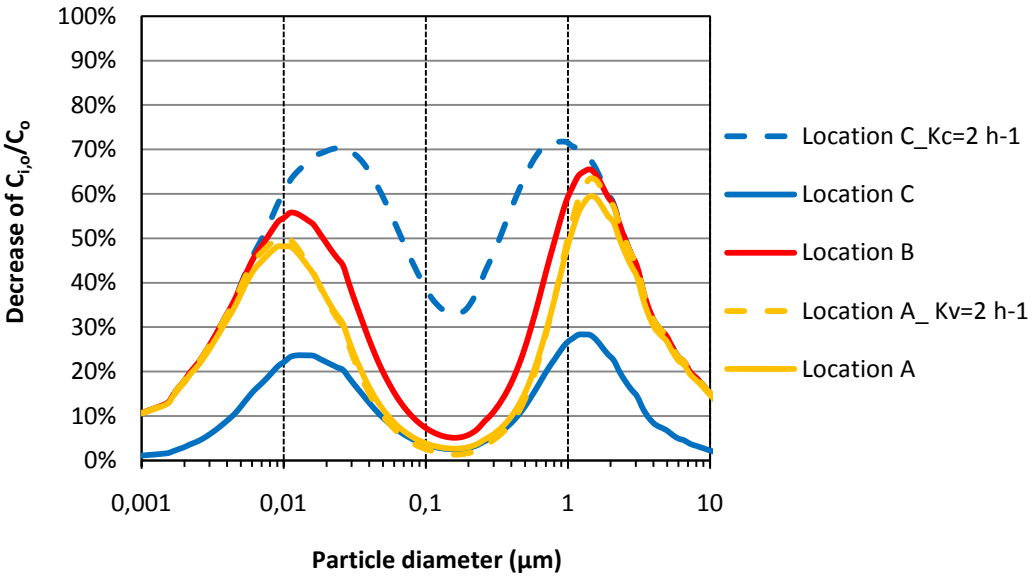

(a)

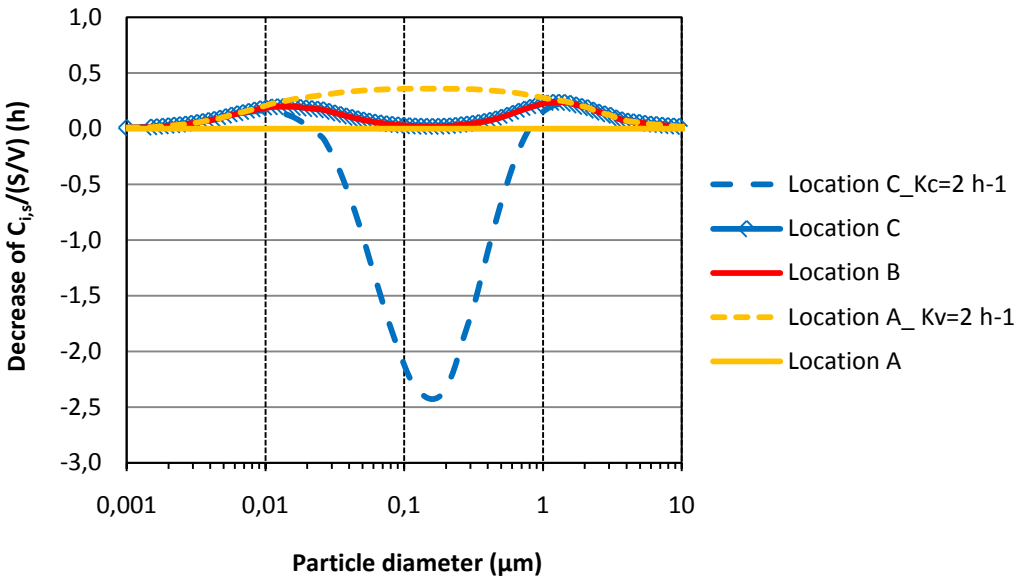

(b)

Figure 7.8 Air filtration influence on $C_{i,o}/C_o$ and $C_{i,s}/(S_i/V)$ in Case A-C. It based on a F5 class filter, and unless otherwise specified with k_v=1 h^{-1} and k_c=1 h^{-1}. (a) $C_{i,o}/C_o$; (b) $C_{i,s}/(S/V)$.

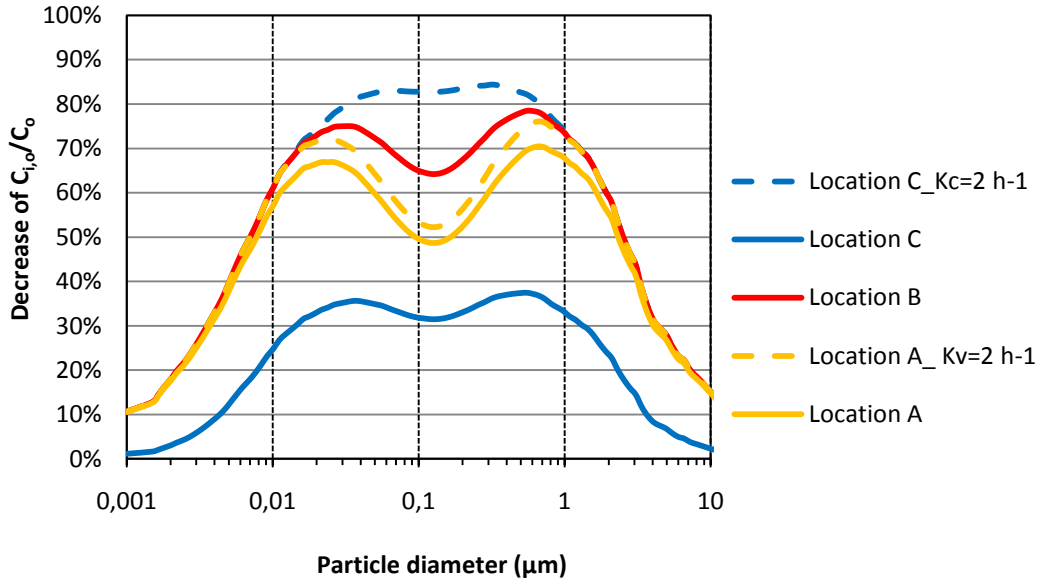

(a)

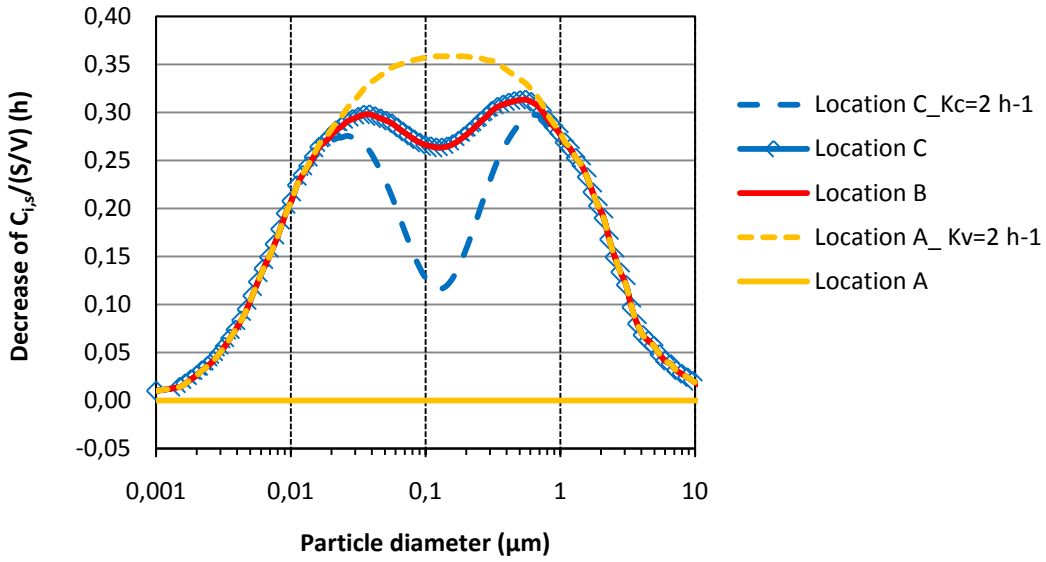

(b)

Figure 7.9 Air filtration influence on $C_{i,o}/C_o$ and $C_{i,s}/(S_i/V)$ in Case A-C. It based on a F9 class filter, and unless otherwise specified with k_v=1 h^{-1} and k_c=1 h^{-1}. (a) $C_{i,o}/C_o$; (b) $C_{i,s}/(S/V)$.

7.5 Air flow influence

Figure 7.10 shows $C_{i,o}/C_o$ and $C_{i,s}/(S_i/V)$ in Case B with the outdoor air flow percentage varied from 0% to 100% at a constant supply air flow rate of 5 h^{-1}. In the figure, $C_{i,o}/C_o$ increases with outdoor air percentage, while $C_{i,s}/(S_i/V)$ decreases with outdoor air percentage. To reasonably control indoor concentration of $C_{i,o}$ and $C_{i,s}$ together, the suitable outdoor air percentage should be dependent on the relative source strength of the outdoor particle infiltration and indoor particle emission. $C_{i,o}/C_o$ and $C_{i,s}/(S_i/V)$ at 0.132 µm have largest variation when

$k_v/(k_v+k_c)$ is varied from 0% to 100%. It could be explained by that the MPPS of the filtration efficiency of the cited F7 class filter is also at 0.132 μm.

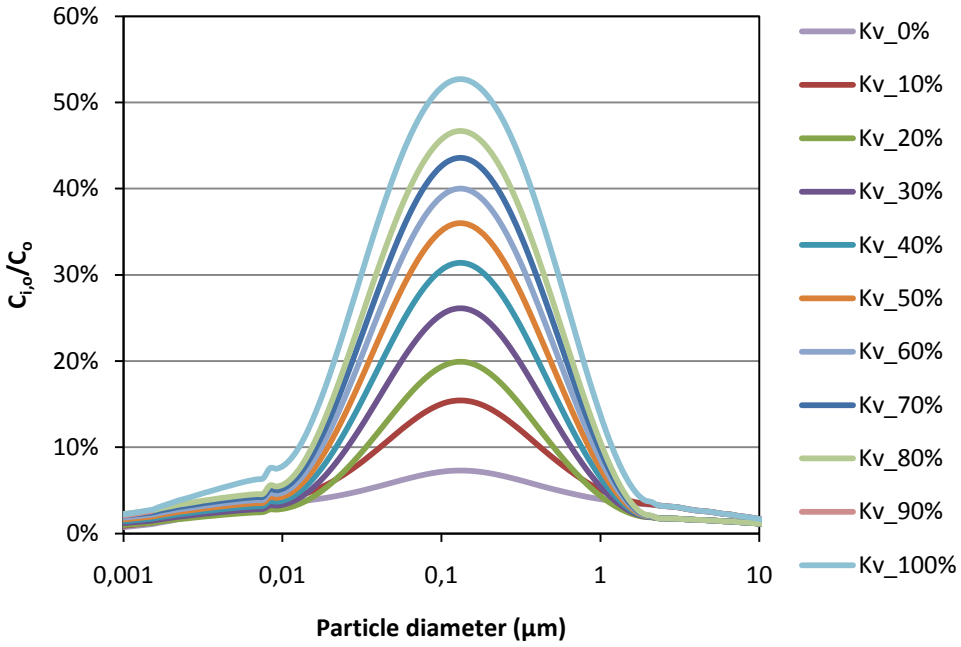

(a)

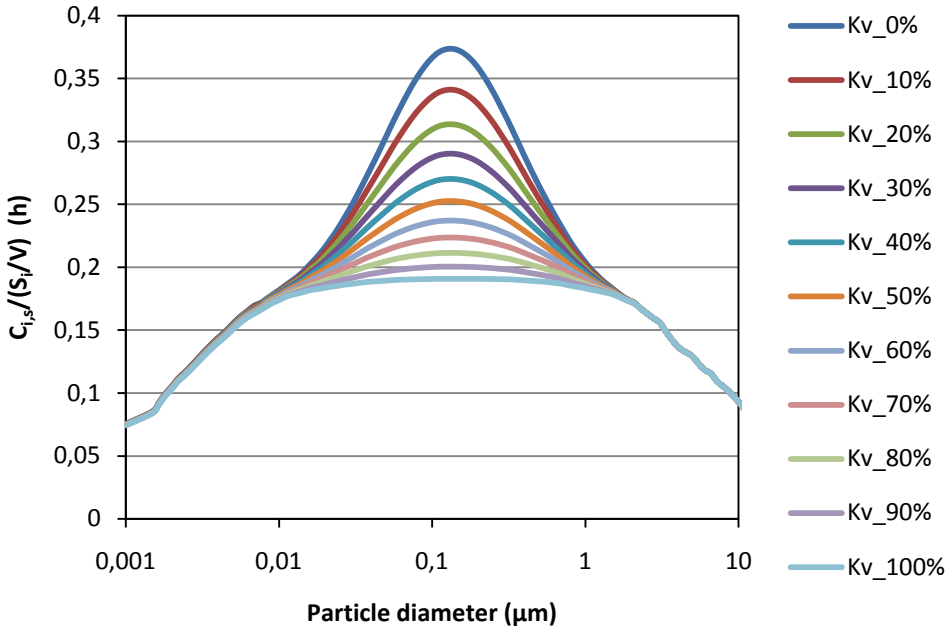

(b)

Figure 7.10 $C_{i,o}/C_o$ and $C_{i,s}/(S_i/V)$ in Case B with varied outdoor air percentage at a supply air flow rate of 5 h^{-1} and with filter class F7. (a) $C_{i,o}/C_o$; (b) $C_{i,s}/(S_i/V)$.

Additionally, the model study has been applied to a building with ambient particles in Figure 7.1[73] and with indoor particles generated from perfumed candle burning[51].

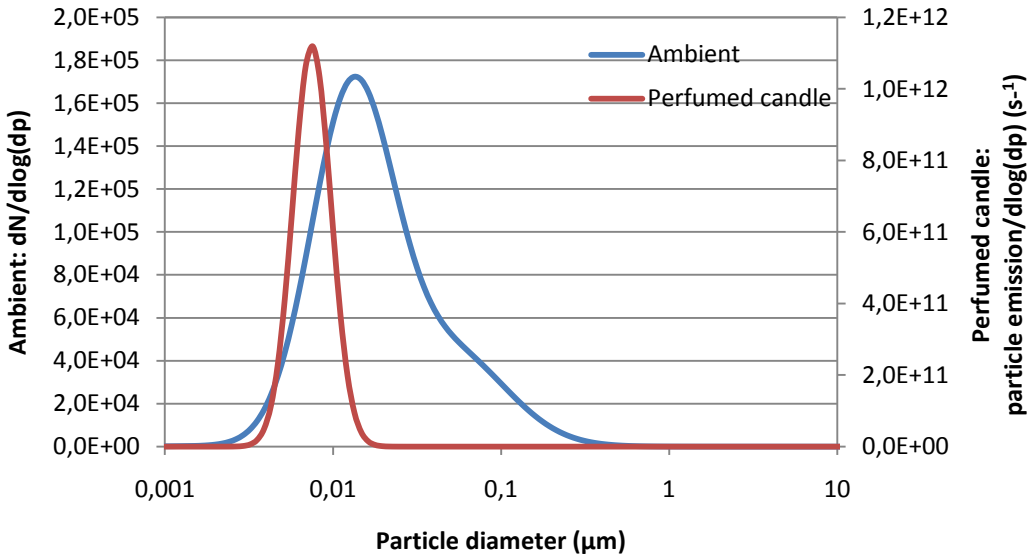

Figure 7.11 Adopted size-resolved number concentration of ambient particles[73] and particles emission from perfumed candle burning[51]. The candle is assumed to burn for 1 hour in a room with a volume of 30 m^3.

Figure 7.11 shows the size distributions of ambient particles[74] and particle emission from perfumed candle burning[51]. Based on the size distributions of the above two particle origins, the size-resolved $C_{i,o}/C_o$ and $C_{i,s}/(S_i/V)$ in Figure 7.10 could be integrated to be the results for particles in a specific size range. Figure 7.12 shows the integrated $C_{i,o}/C_o$, $C_{i,s}/(S_i/V)$ in the size range of $PM_{0.01}$, $PM_{0.1}$, PM_1, $PM_{2.5}$ and PM_{10} when outdoor air flow percentage in the supply air is varied from 0% to 100%. Here, the PM refers to number concentrations, not mass concentrations. Additionally, considering the big variation of $C_{i,o}/C_o$, $C_{i,s}/(S_i/V)$ on MPPS (0.132 µm) in Figure 7.10, it is reasonable to include the results on MPPS in the Figure 7.12.

Both the cited ambient particles and the particle emission by perfumed candle in Figure 7.11 have the peak concentrations at a size less than 0.1 µm. Due to the similar number concentration of PM_1, $PM_{2.5}$ PM_{10} and even $PM_{0.1}$, the integrated $C_{i,o}/C_o$ and $C_{i,s}/(S_i/V)$ are similar for $PM_{0.1}$, PM_1, $PM_{2.5}$ and PM_{10}, while they are lowest for $PM_{0.01}$ and largest for MPPS. Furthermore, MPPS curves practically present the largest variation for all possible particle size distributions to leave indoors. The results in Figure 7.12 could be different for particle sources with different size distributions.

Another calculation based on a different size-distribution is presented in Figure A2-A4 in Appendix C. In Figure A2, the size of peak concentration of the new ambient particles and indoor particle emission is around 0.1 µm, which is close to the MPPS of the filter class F7. Figure A3-A4 show that the size integrated $C_{i,o}/C_o$ and $C_{i,s}/(S_i/V)$ in a diameter range including MPPS would be close to the two parameters values on MPPS.

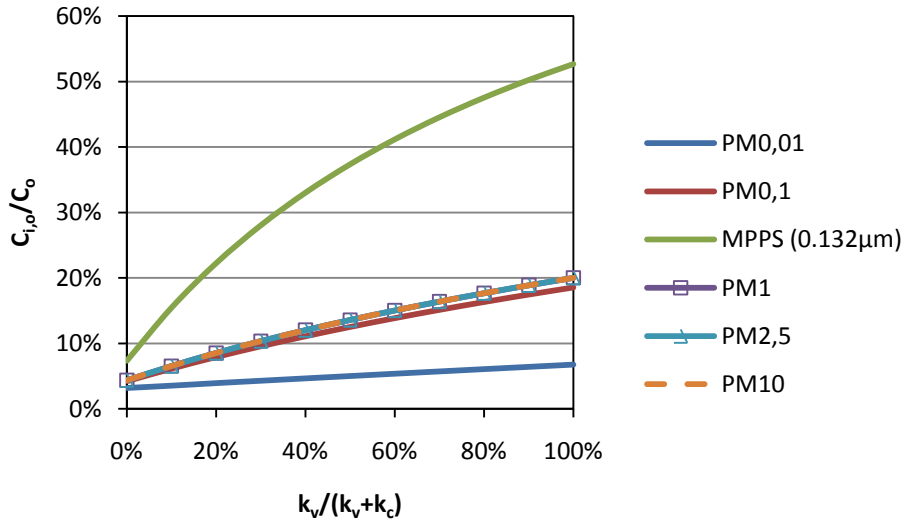

(a)

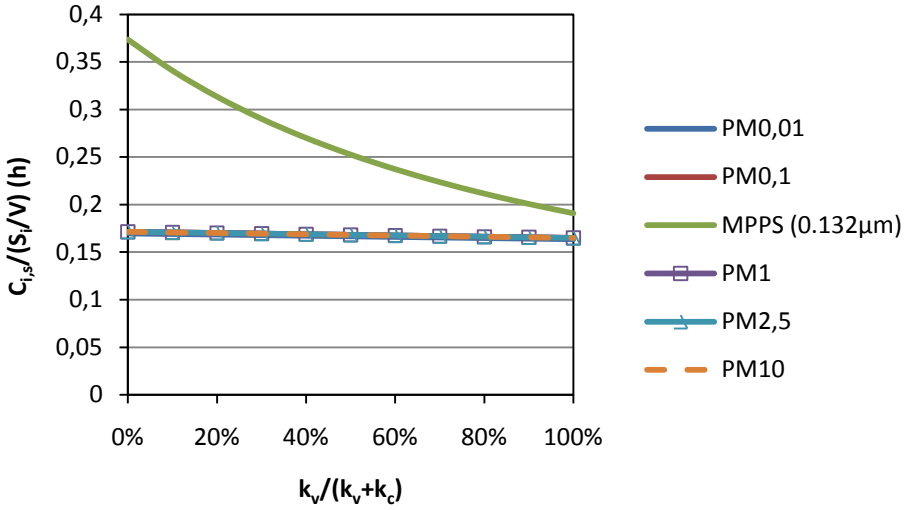

(b)

Figure 7.12 Integrated $C_{i,o}/C_o$, $C_{i,s}/(S_i/V)$ in the size range of $PM_{0.01}$, $PM_{0.1}$, PM_1, $PM_{2.5}$, PM_{10} and MPPS (0.132µm) at varied outdoor air flow percentage with filter class F7. The supply air flow rate is 5 h^{-1}. (a) $C_{i,o}/C_o$; (b) $C_{i,s}/(S_i/V)$.

According to Figure 7.12, among the above six particle sizes, $PM_{0.01}$ is hardest to penetrate into indoors and easiest to leave indoors, while MPPS-sized particles is easiest to penetrate into indoors and hardest to leave indoors. To investigate the influence of supply air flow exchange rate, outdoor air percentage is assumed to be 50% in the following study.

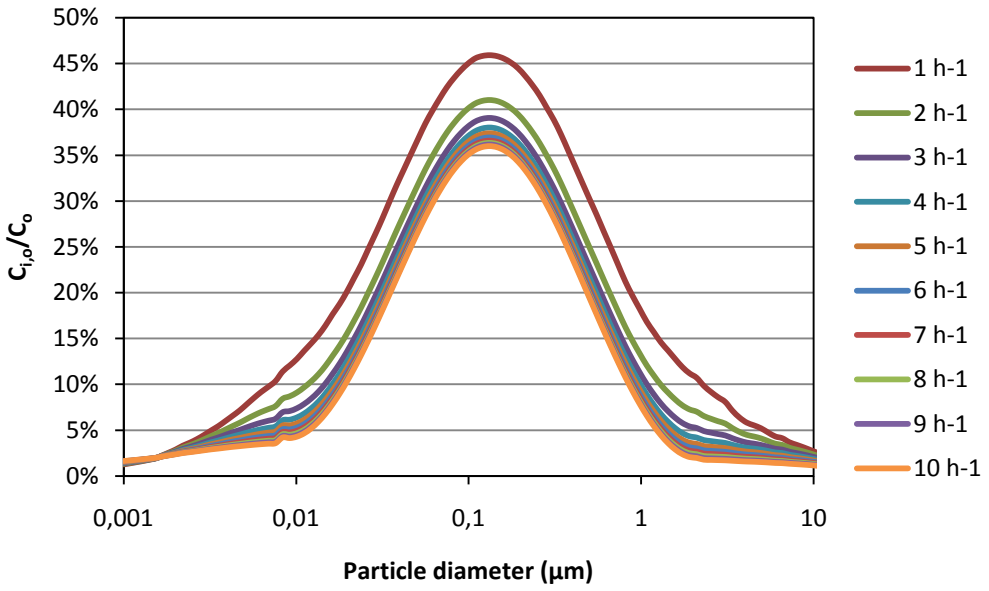

(a)

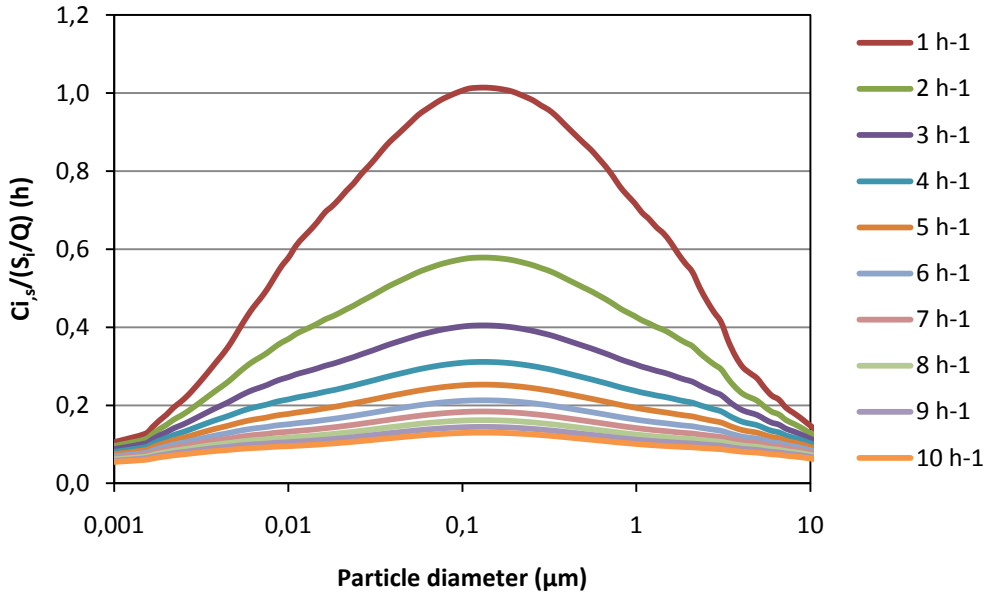

(b)

Figure 7.13 $C_{i,o}/C_o$ and $C_{i,s}/(S_i/V)$ in Case B with different supply air exchange rates and with filter class F7. The outdoor air flow percentage is constant at 50%, i.e. $k_v/(k_v+k_c)=50\%$. (a) $C_{i,o}/C_o$; (b) $C_{i,s}/(S_i/V)$.

Figure 7.13 shows the $C_{i,o}/C_o$ and $C_{i,s}/(S_i/V)$ in Case B with the supply air exchange rate increasing from 1 h^{-1} to 10 h^{-1}. The percentage of outdoor air flow in the supply air flow is 50%. The figure shows that both $C_{i,o}/C_o$ and $C_{i,s}/(S_i/V)$ decrease with supply air exchange rate. The suitable supply air flow rate is based on the required/recommended $C_{i,o}/C_o$ and $C_{i,s}/(S_i/V)$. For the sake of energy saving, it is reasonable to use the minimum air flow meeting the indoor air quality requirement.

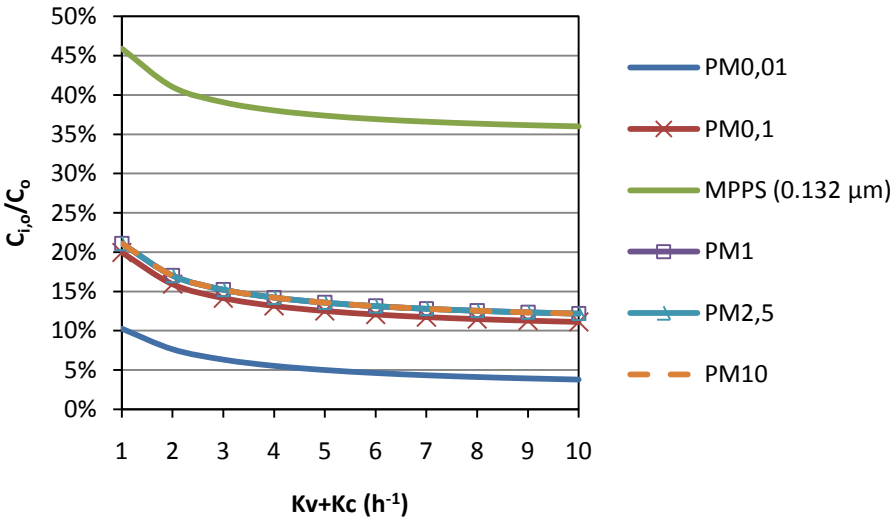

(a)

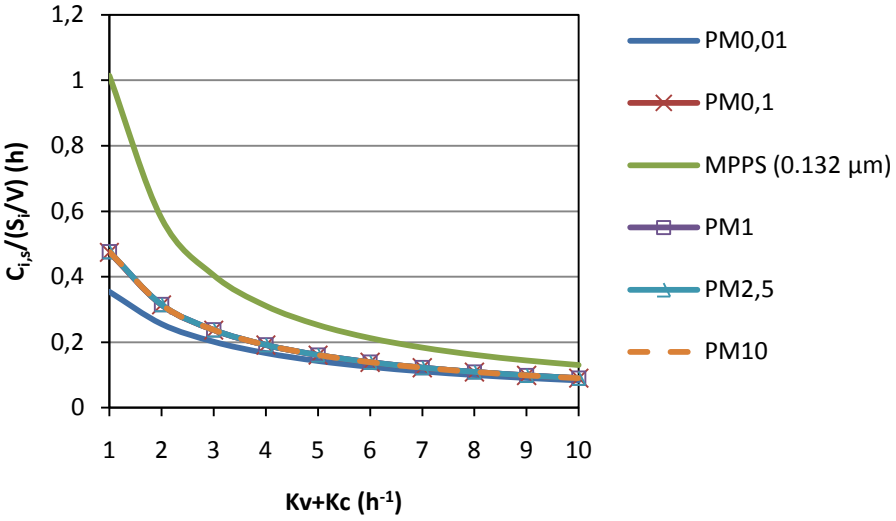

(b)

Figure 7.14 Integrated $C_{i,o}/C_o$, $C_{i,s}/(S_i/V)$ in the size range of $PM_{0.01}$, $PM_{0.1}$, PM_1, $PM_{2.5}$, PM_{10} and MPPS (0.132µm) at with different supply air exchange rates and with filter class F7. The outdoor air flow percentage is constant at 50%, i.e. $k_v/(k_v+k_c)=50\%$. (a) $C_{i,o}/C_o$; (b) $C_{i,s}/(S_i/V)$.

Figure 7.14 show the corresponding integration results based on the size distributions of the above two particle origins in Figure 7.11. In the figure, $C_{i,o}/C_o$, $C_{i,s}/(S_i/V)$ is integrated in the size range of $PM_{0.01}$, $PM_{0.1}$, PM_1, $PM_{2.5}$, PM_{10} and MPPS (0.132µm) when the supply air flow increases from 1 h^{-1} to 10 h^{-1}. The percentage of outdoor air flow in the supply air is 50%. Similar to Figure 7.12, the integrated $C_{i,o}/C_o$ and $C_{i,s}/(S_i/V)$ are similar for $PM_{0.1}$, PM_1, $PM_{2.5}$ and PM_{10}, while they are largest for MPPS-sized particles and smallest for $PM_{0.01}$. The results are also depending on size-distributions. Moreover, the figure shows that when the supply air exchange rate is less than 2 h^{-1}, increasing supply air exchange rate leads to a substantial decrease of $C_{i,o}/C_o$ and $C_{i,s}/(S_i/V)$, while further increasing the supply air exchange rate, the above decrease becomes less and less.

7.6 Conclusion

The study investigates the sink fate of indoor particles influenced by indoor particle dynamical mechanisms, various air filter locations and ventilation modes. The mechanism effect on indoor particle removal are evaluated by the indoor particle proportion of outdoor origin $(C_{i,o}/C_o)$, and the time constant of indoor emitted particles, $(C_{i,s}/(S_i/V))$. The two parameters have been investigated by a method that eliminates consideration of the source strengths and size distributions of C_o and S. The dynamical mechanisms are considered as outdoor air and recirculated air filtration, indoor deposition, outdoor particle infiltration and indoor particle exfiltration and exhaustion. Filters in four locations to filtrate outdoor air, supply air, recirculated air and indoor air are evaluated, respectively. The four air filtration cases are compared with a base case with no air filtration.

As expected, the mechanism model shows that reducing outdoor particle infiltration through the building envelope and reducing the outdoor air flow rate, can greatly reduce $C_{i,o}/C_o$. As also expected, increasing recirculating air filtration can substantially reduce $C_{i,s}/(S_i/V)$. Furthermore, outdoor air filtration have significant effects on the removal of particles with diameter less than 0.01 μm and larger than 1 μm, while recirculating air filtration has good ability to remove particles with a diameter between 0.1 μm and 1 μm. Additionally, small particles (<0.01 μm) and large particles (>1 μm) apparently have a high possibility to deposit on indoor surfaces.

The filter location study shows, for a case with equal outdoor air flow and recirculating air flow, that outdoor air filtration shows better performance than recirculating air filtration does on the reduction of $C_{i,o}/C_o$, while the opposite phenomenon appears in the $C_{i,s}/(S_i/V)$ reduction. However, in a constant supply air flow, filtrating a high percentage recirculating air flow can more efficiently reduce $C_{i,o}/C_o$ than filtrating a high percentage outdoor air flow. And filtrating a high percentage outdoor air flow can more efficiently reduce $C_{i,s}/(S_i/V)$ than filtrating a high percentage recirculating air flow.

The comparison between the performance of F5, F7 and F9 class filters shows that low class filters, such as F5 class filters, has much lower decrease effect on $C_{i,o}/C$ and $C_{i,s}/(S_i/V)$ than F7 class filter does. And high class filters, such as F9 class filters, further decrease $C_{i,o}/C$ and $C_{i,s}/(S_i/V)$ by almost no more than 10%-unit from the level of F7 class filters. Furthermore, it needs to be noticed that low class filters used for recirculating air filtration probably would prolong the time constant of indoor particles compared to the case without air filters and no recirculating air. It is better to avoid using a filter less than F7 class in recirculating air filtration.

The air flow mode study shows that to reduce $C_{i,o}/C_o$, the percentage of outdoor air flow in the supply air is better to be small. However, to reduce $C_{i,s}/(S_i/V)$, the percentage of outdoor air in the supply air flow is better to be large. Additionally, the variation of the percentage of outdoor air flow in the supply air is more sensitive to $C_{i,o}/C_o$ than to $C_{i,s}/(S_i/V)$, while the supply air flow has bigger impact on the variation of $C_{i,s}/(S_i/V)$ than on the variation of $C_{i,o}/C_o$. Therefore, a probably reasonable consideration in the ventilation system design is the capacity to provide a suitable $C_{i,s}/(S_i/V)$ and $C_{i,o}/C_o$ to against the typical indoor and outdoor original pollutants for the designed building.

In a case study with a polluted ambient air[73] and an indoor source of perfumed candle[51], the integrated $C_{i,o}/C_o$, $C_{i,s}/(S_i/V)$ at the size range of $PM_{0.01}$, $PM_{0.1}$, PM_1, $PM_{2.5}$ and PM_{10} shows that $C_{i,o}/C_o$ and $C_{i,s}/(S_i/V)$ are largest for MPPS-sized particles, while they are smallest for $PM_{0.01}$. Moreover, increasing the supply air exchange rate and outdoor air percentage, the variation of $C_{i,o}/C_o$ and $C_{i,s}/(S_i/V)$ are also largest for MPPS-sized particles and smallest for $PM_{0.01}$. Although the integrated results of $C_{i,o}/C_o$ and $C_{i,s}/(S_i/V)$ are depended on the size-distributions of particle sources, MPPS curves practically present the potentially largest variation for all possible particle size distributions to leave indoors When the size distributions of outdoor and indoor particle emissions are unpredictable, it is reasonable to consider the risk of system of air filtration and ventilation to remove indoor particles should be evaluated based on MPPS curves.

Considering the big influence of EF_{MPPS} on the $C_{i,o}/C_o$ and $C_{i,s}/(S_i/V)$, it can be predicted that the variation $C_{i,s}/(S_i/V)$ would become sharp for low class filters, and become slight for high class filters. See Figure A4-A5 in Appendix C. However, it needs to be noticed that the variation of $C_{i,o}/C_o$ is also limited to be within 0%-100%.

In summary, motivated to control personal exposure to “harmful” particles, a potential application of the model is to analyze the routes of transportation and indoor occurrence of particle from specific sources. $C_{i,o}/C_o$ and $C_{i,s}/(S_i/V)$ are two critical parameters to evaluate the system performance on indoor particles removal. Based on a pre-study of the major particle sources in a building and in the surrounding environment, the results from model calculations can be used to recommend suitable air filters and ventilation rates/modes or to predict the existing system performances. There may be a potential to control the ventilation rate and mode based on one or more particle sensors.

8 Two-step air filtration

According to Chapter 7, the filter MPPS has an important effect on indoor personal exposure to particulate air pollution. It is meaningful to study measures to ensure the filtration efficiency of intermediate air filtration without a substantial increase of the cost of the filtration. Two-step filtration could enhance filtration efficiency and pro-long main filter lifetime. A model study was done to evaluate the filtration efficiency and economical cost of two-step filtration compared to single-step filtration. The filter pressure drop increase rate was based on long-term measurements on field filters. The clean air flow cost based on the filtration efficiencies of full-scale filters on UFPs, PM_1, $PM_{2.5,}$ PM_{10} and MPPS-sized particles were investigated in the model.

8.1 Introduction

Total cost of two-step filtration is affected by filter lifetime, filter class, electricity price, and ambient particle concentration. Filter lifetime is critical to the annual filtration cost. European standard EN 779:2012 [42] states 450 Pa as the final pressure drop when testing intermediate (M5-M6 and F7-F9) filters. US standard ASHRAE 52.2 [5] uses 250 Pa and 350 Pa as the minimum final pressure drops for MERV 9-12 (M5-M6) and MERV 13-16 (F7-F9) filters to identify when a filter minimum efficiency occurs. In many real applications, filters are replaced at 300 Pa to keep the energy cost low [56]. Reducing the final pressure drop would shorten the filter lifetime, thus increasing the filter investment cost. Additionally, due to the by-products emitted from used filters, the filter replacement interval usually is based on the running time instead of the pressure drop in many cases. Standard EN 13779:2007 [45] recommends that pre-filters and main filters should be replaced within one year and two years, respectively. Some studies have found that when moisture deposits on the filter surface, microbiology can grow up quickly on the filter and emit microbial volatile organic compounds (MVOC) [116]. However, if the local climate is dry, the filter running time could be reasonably extended.

Filters of different classes have different filtration efficiencies and initial pressure drops. Combining suitable filter classes is important to apply two-step filtration. Therefore, it is meaningful to analyse the economical cost of two-step filtration under the trend of energy cost increasing. In addition, the local ambient particle concentration can greatly influence the dust loading on filters. Boldo et al. (2006)[14] investigated ambient concentration of PM_{10} and $PM_{2.5}$ in 23 European cities. In their study, PM_{10} concentrations in the most studied cities were about 20 $\mu g/m^3$ and in few urban cities they were about 40 $\mu g/m^3$. Dingenen et al. (2004) [32] demonstrated that European annual average concentrations of PM_{10} in nature and rural areas were about 10 $\mu g/m^3$. Therefore, 20 $\mu g/m^3$ and 10 $\mu g/m^3$ are considered as typical urban and rural PM_{10} mass concentrations in the model. Because of the high urban particle concentration, the dust deposited on urban filters is probably more than that on rural filters after the same running time. Thus, the filter pressure drop increase in urban areas is expected to be higher than that in rural areas.

The purpose of this model study is to compare the annual total cost between single-step filtration and two-step filtration with similar or higher filtration efficiency, especially on submicron particles and UFPs. The influences of filter

lifetime, electricity price, filter class, and ambient particle concentration on the filtration cost are investigated. The analysis compares single-step filtration and two-step filtration based on G4, M5-M6 and F7-F9 class filters according to the European standard EN779:2012 [42]. These filters are corresponding to MERV 7-15 class filters in ASHRAE standard 52.2[5]. The filters are utilized in HVAC supply-air streams with 100% of outdoor air.

8.2 Methodology

The model is about the annual air flow costs and annual clean air flow cost of single-step filtrations and two-step filtrations. The annual cost includes energy cost and the cost for filter and labor.

8.2.1 Modelling annual total cost of air filtration

The annual total cost of air filtration consists of the cost of interval filter maintenance (filter and labor), the fan electricity consumption and the initial investment for the filter frame in the air handling unit [56, 99]. The labor cost includes the cost for installation, replacement and disposal of filters. The cost of filters and labor can be considered as the cost for filter maintenance, which could be reduced by filter lifetime extension. The fan electricity consumption is greatly influenced by the initial pressure drop and the pressure drop increase during the operation. The initial investment for the filter frame is not considered in the model, because it is judged to be much smaller than energy cost and filter maintenance cost.

The fan electrical power (W) per unit volumetric air flow is extracted from eq. 8.1, where $\overline{\Delta P}$ is the average value of filter pressure drop during the lifetime (Pa), η is the total efficiency of the fan and motor (%), $\dot{V}$ is the volumetric air flow rate through the filter (m^3/s), EF is the filtration efficiency (%). The filter prices (filter cost) in eq. 8.3 and 8.4 are cited from in the website of BELOK [12].

$$Fan\ power = \frac{(Air\ flow\ rate) \times (Average\ \ pressure\ \ drop)}{Total\ \ fan\ \ and\ \ motor\ \ efficiency} = \frac{\dot{V} \times \overline{\Delta P}}{\eta} \qquad (eq.\ 8.1)$$

The energy cost during the operating time is expressed as:

$$Lifetime\ energy\ cost =$$

$$(Fan\ power) \times (Operating\ hours\ over\ filter\ life) \times (Electricity\ Price) \qquad (eq.\ 8.2)$$

The costs per unit of volumetric air flow and per clean air flow are obtained from in eq. 8.3 and 8.4.

$$Annual\ Cost\ per\ unit\ air\ flow = \frac{Filter\ cost + Labor\ cost\ per\ filter\ installation + Lifetime\ energy\ cost}{Airflow\ \ rate * life\ \ time\ \ (year)} \qquad (eq.\ 8.3)$$

$$Annual\ Cost\ per\ unit\ clean\ air\ flow = \frac{Filter\ cost + Labor\ cost\ per\ filter\ installation + Lifetime\ energy\ cost}{Air\ \ flow\ \ rate * EF * life\ \ time\ \ (year)} \qquad (eq.\ 8.4)$$

8.2.2 Modelling particle mass deposition rate on filters

The particle size-resolved mass loading rate per unit volume air flow through the filters are calculated by eq. 8.5-8.8.

The dust load on the single filter is calculated as:

$$m_{f0} = m_{out} \times EF_0 \qquad \textit{(eq. 8.5)}$$

The dust loads on the two combined filters are calculated as:

For pre-filter

$$m_{f1} = m_{out} \times EF_1 \qquad \textit{(eq. 8.6)}$$

For main filter

$$m_{f2} = m_{pre} \times EF_2 = (1 - EF_1) \times m_{out} \times EF_2 \qquad \textit{(eq. 8.7)}$$

where m_{f0}, m_{f1} and m_{f2} are the particle size-resolved mass depositions per unit volume air flow [$mg/(\mu m \cdot m^3)$] on the single filter, pre-filter and main filter respectively; m_{out} and m_{pre} are the particle size-resolved mass concentrations [$mg/(\mu m \cdot m^3)$] in outdoor air and the downstream air of the pre-filter; EF_0, EF_1 and EF_2 are the size-resolved efficiency of the single filter, pre-filter and main filter. The size-resolved mass depositions, m_{f0}, m_{f1} and m_{f2}, are calculated from a function of the size-resolved number concentration and the particle density. In the model, the particles density is assumed to be 1g/cm^3 and the particles are assumed to be spherical.

All the above parameters are depending on the particle diameter d_p, which is in the range of 0.001~100 μm in this study. The total dust load on a filter, $M_{f,\,tot}$, is calculated through integrating the particle size-resolved mass loading rate over d_p between 0.001~100 μm, then multiplying the total volumetric air flow during the filter operation time. This calculation is presented as eq. 8.8.

$$M_{f,tot} = \int_{d_p} m_{f_i} d(d_p) \times \dot{V} \times \tau_{HVAC} \times 3600 \qquad \textit{(eq. 8.8)}$$

where τ_{HVAC} is the filter operation time (h). For a given airflow rate, $M_{f,\,tot}$ increases with filter filtration efficiency and filter operation time.

In the model, some assumptions were made: the electricity price is 1 *SEK/(kW/h*); the labor cost per filter is 50 SEK; the total efficiency of fan and motor is 70% at an air flow rate of 3400 m^3/h; the filter efficiency during the lifetime is constant. Because the running time of HVAC systems in commercial buildings usually is 12 hours/day, we assume filter operation time is 365 hours/month. The annual total cost is the sum of energy cost and the cost of filter and labor.

8.2.3 Ambient particle size-resolved concentration

The particle size-resolved concentrations in urban and rural atmosphere from Jaenicke [73] are utilized in the model. Figure 8.1 shows the particle size-resolved number and volume concentrations, dN/dlogDp and dV/dlogDp in urban and rural atmospheres. The mass concentration, m_{out}, is calculated by multiplying the

volume concentration with the particle density. However, the calculated particle mass concentration is substantially higher compared to the general particle concentrations in Europe [14, 32]. According to the general PM_{10} concentration in European rural and urban in the study of Boldo et al. [14] and Dingenen et al. [32], the particle size-resolved concentrations in Figure 8.1 are adjusted to the concentrations with the integrated PM_{10} mass concentration of 20 $\mu g/m^3$ for urban areas and 10 $\mu g/m^3$ for rural areas. Moreover, to investigate the cases in seriously polluted urban areas, the urban particle mass concentration is increased from 10 $\mu g/m^3$ to 80$\mu g/m^3$.

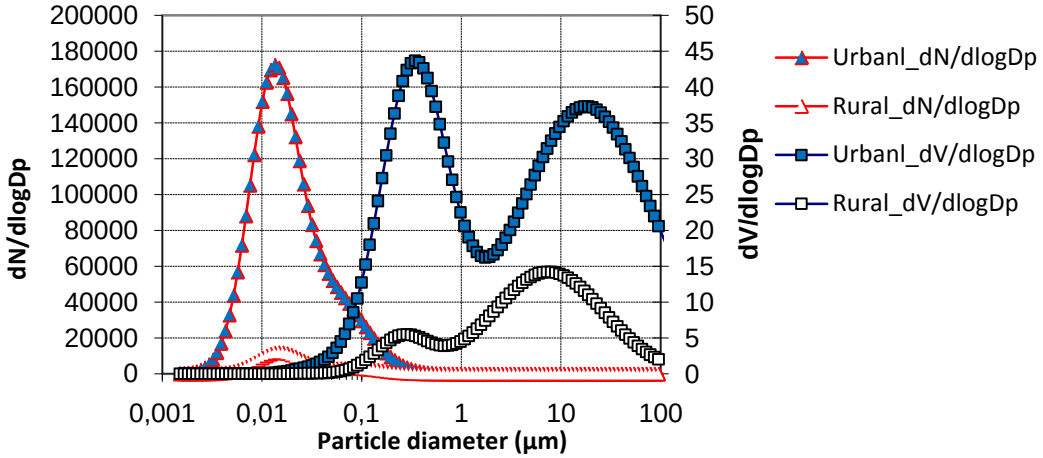

Figure 8.1 Particle size-resolved number and volume concentration in urban and rural atmosphere. The size distributions are adopted from Jaenicke (1993) [73].

8.2.4 Filtration

The filter size-resolved filtration efficiencies are illustrated in Figure 8.2, which includes the data from the laboratory measurements, the theory simulation, and the study of Hanley [58].

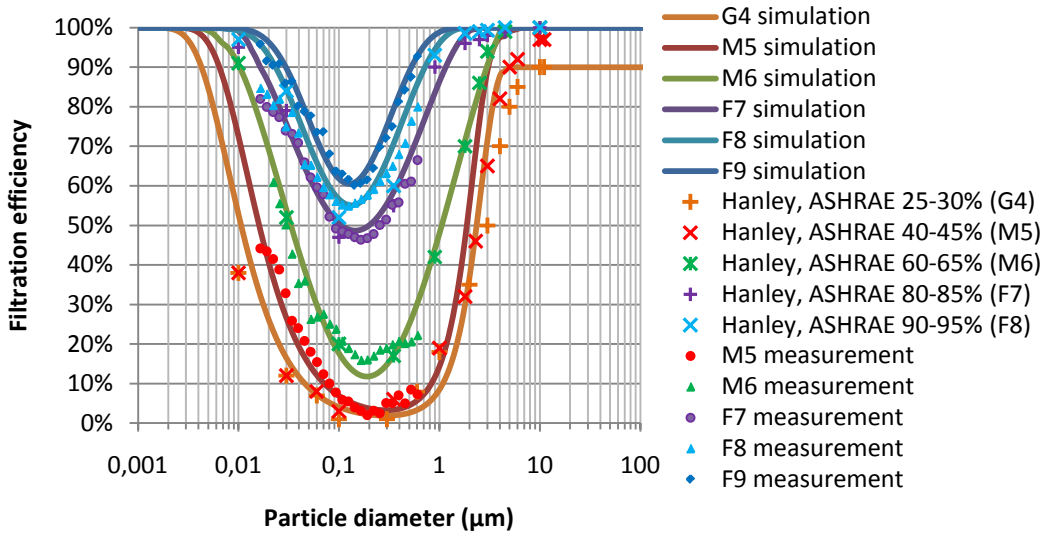

Figure 8.2 The size-resolved efficiency for G4, M5-M6 and F7-F9 class filters.

The ASHRAE class filters in Hanley's study are roughly corresponding to the European filter classes in the brackets. The measurement data shown in Figure 8.2 were obtained by the methodology described in Chapter 4. The testing air flow rate was 0.944m^3/s for the measured efficiencies given in Figure 8.2. Based on the fibrous filtration theory described by Hinds [65], and summarized in Chapter 3, a set of simulations were conducted in the full diameter range of the study. Considering the good agreement between the data from the three sources, the simulation efficiencies are utilized in the model.

For the ambient particle size distribution shown in Figure 8.1, the filtration efficiencies integrated on UFPs, PM_1, $PM_{2.5}$ and PM_{10} are very similar, while the efficiency on MPPS-sized particles is much lower than them. In the following model study, the clean air flow costs according to eq. 8.4 are calculated based on the filtration efficiency on UFPs (EF_{UFPs}) and MPPS-sized particles (EF_{MPPS}).

8.2.5 Filter pressure drop

The average pressure drop during the running time is calculated as the average value of the initial and final pressure drops. In the experiments, the filter initial pressure drops were measured to the following values: G4 (58Pa), M5 (64Pa), M6 (75Pa), F7 (98Pa), F8 (152Pa) and F9 (180Pa) at an air flow rate of 3400m^3/h. Figure 7.3 shows how the pressure drops (ΔP-$\Delta P_{initial}$) of the G4, M5-M6 and F7-F8 class filters increase with the normalized dust load on filter cross section area (m^2). The data are obtained from field filter experiments in Borås, Sweden [37].

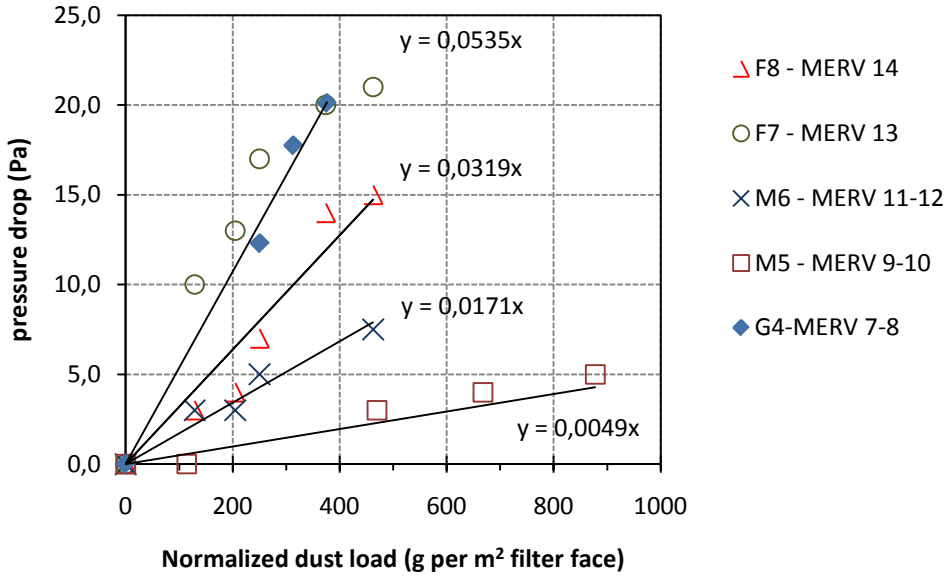

Figure 8.3 Effect of normalized dust load (g/m^2) on relative pressure drop (ΔP-$\Delta P_{initial}$) of G4, M5-M6 and F7-F8 class filters [37].

In the figure, the G4, M6 and F7-F8 class filters were operated for 6 months and M5 filter was operated for 14 months. The increase of the pressure drop with the dust load was obviously less than the laboratory measurements according to EN779, while very close to another field measurement presented by Bekö et.al [9]. Although the figure shows a linearly increasing relationship, it would be a non-linear relationship when the normalized dust load extends to a big range [41]. Since

many filter manufactures may sell the same filter medium both as F9 and F8 filters, the regression function of F9 class filters is assumed to be the same as that of F8 class filters.

8.2.6 Filter lifetime

The recommended filter lifetime in HVAC systems according to the standard EN 13779:2007[45] and the REHVA guidebook (2009) [57] is 2000 h or a maximum of one year for pre-filters/single filters, and 4000 h or a maximum of two years for main-filters. According to the operation time of 365h/month, this lifetime corresponds to half a year for pre-filters/single filters and one year for main filters. The influence of filter lifetime is investigated through separately increasing the lifetime of the main filter and the pre-filter, see Figure 8.4 (a)-(c).

Figure 8.4 (a)-(c) shows the annual air flow costs of two-step filtration of G4+F9 and M6+F7 when pre-filter and main filter lifetime are varied separately, from 3 months to 42 months, in urban areas (PM_{10}: 20 μg/m^3), rural areas (PM_{10}: 10 μg/m^3) and polluted urban areas (PM_{10}: 40 μg/m^3). To the two-step filtration, extending the main filter lifetime would reduce the cost more than the pre-filter does. Furthermore, the cost decrease with the extended filter lifetime is more obvious on "G4+F9" than that on "M6+F7". This means that, to reduce the annual cost, prolonging the main filter lifetime is more effective when such two filters have a larger class difference.

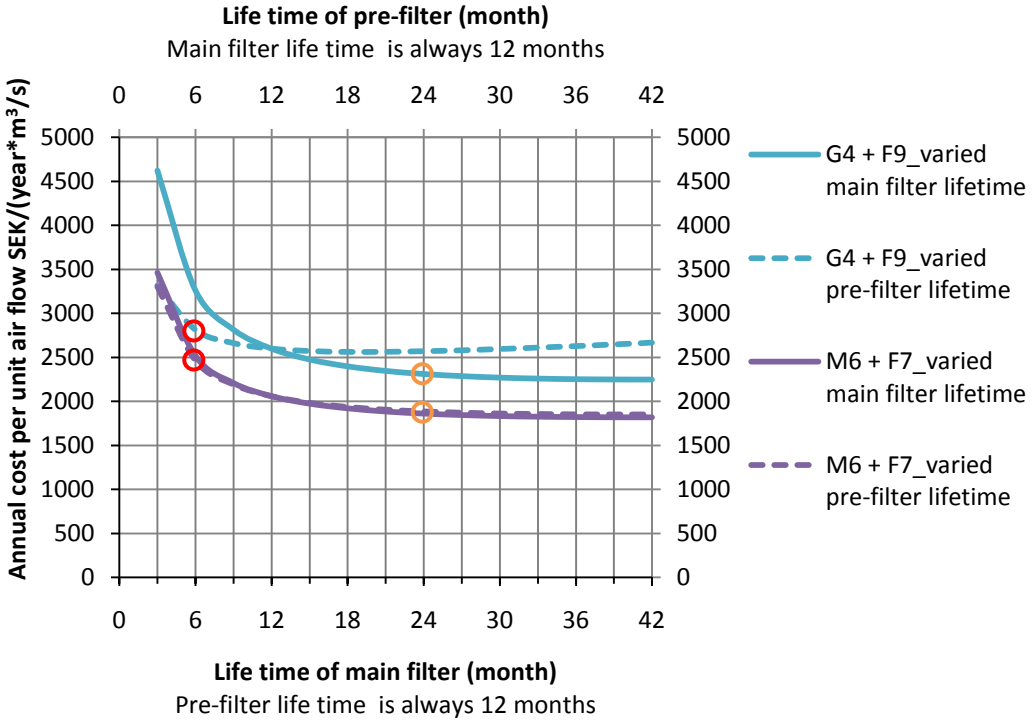

(a)

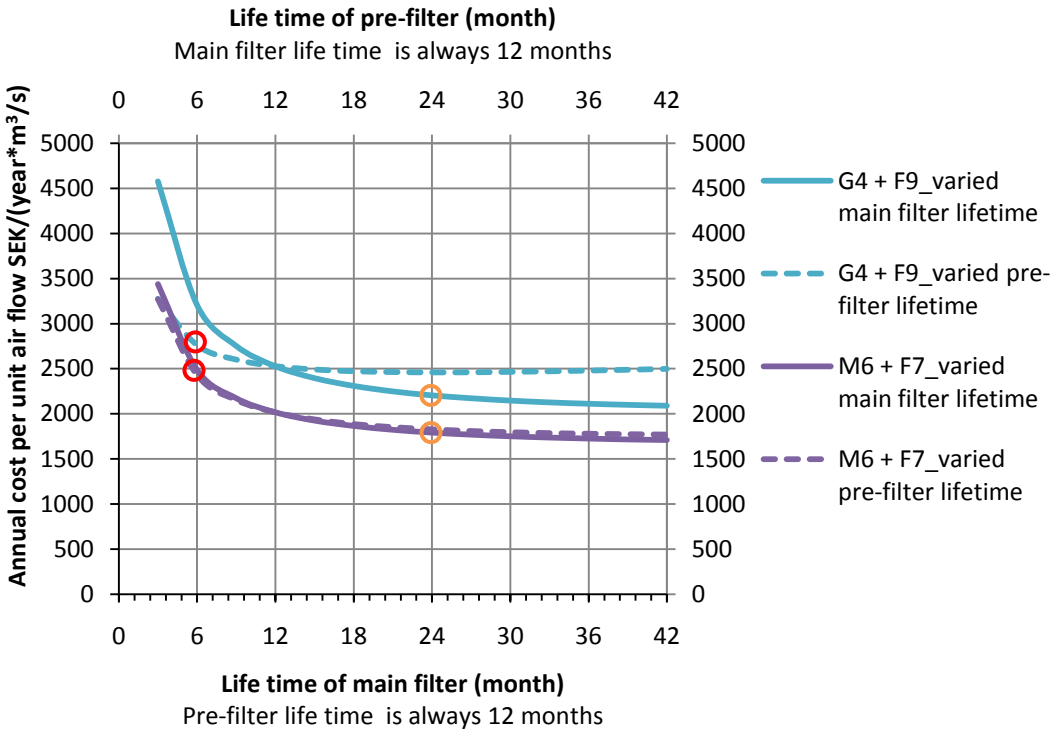

(b)

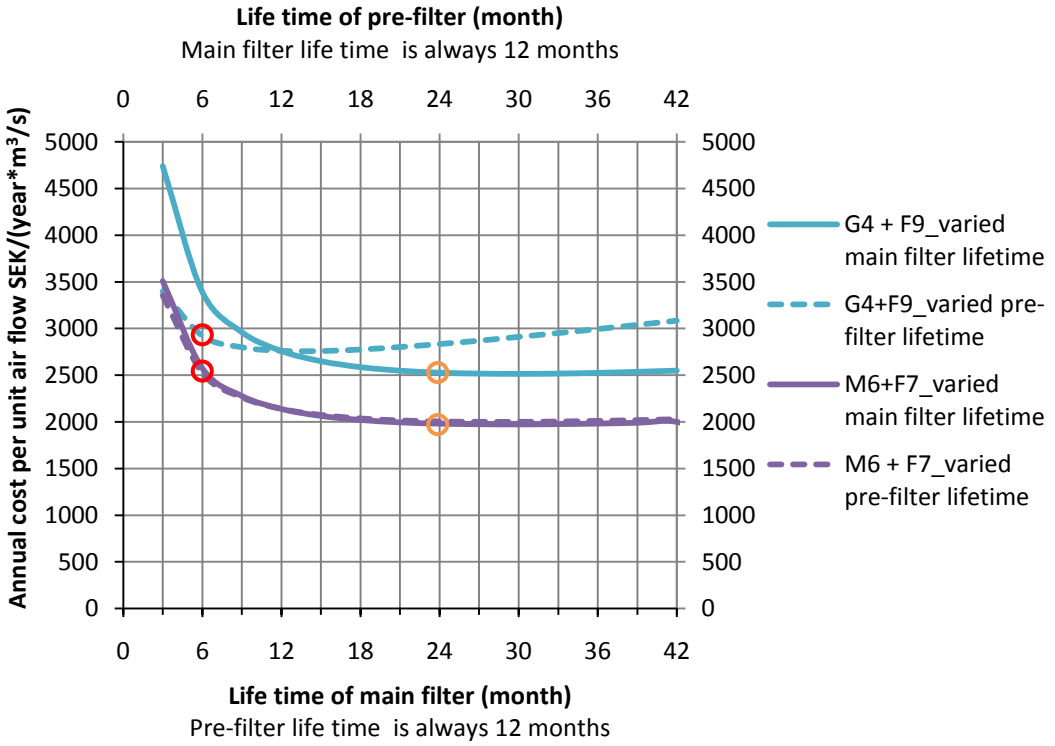

(c)

Figure 8.4 Annual air flow cost of two-step filtration of M6+F7 and G4+F9 varied with pre-filter and main filter lifetime. (a) Urban areas: PM_{10} is 20 μg/m^3; (b) Rural areas: PM_{10} is 10 μg/m^3; (c) Polluted urban areas: PM_{10} is 40 μg/m^3.

In the figure, when main or pre-filter lifetime is less than 6 months, the annual cost is substantially high. When main or pre-filter lifetime is prolonged from 6 months to 24 months, the annual cost is not reduced much. When the lifetime is extended above 24 months, the reduction of annual cost is very small. The red circles marked cost is for the case with the lifetime of 6 months for pre-filter and 12 months for main filter [45, 57]. The orange circle marked cost is for the case with the lifetime of 12 months for pre-filter and 24 months for main filter. In the calculation, the cost in orange circle is close to the minimum cost and 500 SEK less than the cost in red circle. Therefore, the lifetime in the following study is 12 months for pre-filter and 24 months for main filter. Additionally, to make a parallel comparison, the single filter lifetime is also set to 12 months as same as the pre-filter lifetime.

In Figure 8.4 (a)-(c), to reduce the cost, extending the main filter lifetime is more useful in low PM_{10} concentration areas than in high PM_{10} concentration areas. In Figure 8.4 (c), when ambient PM_{10} concentration and filter class is high, the long lifetime of the main filter would result in a high cost due to high dust load induced high pressure drop.

8.3 Results

Suitable combinations of filter classes are important to control two-step filtration cost. Figure 8.5 (a)-(b) shows the average pressure drops of pre-filters and main filters applied in urban areas (PM_{10}: 20 μg/m^3) and rural areas (PM_{10}: 10 μg/m^3).

In the figure, the total pressure drop of low class combined filters could be even lower than that of a high class single filter, such as M6+F7 versus F9. The pressure drop of high class combined filters is obviously higher than other two-step and single-step filtration, which results in high cost for electricity consumption. In the study, the modelled final pressure drops of main and pre-filters are less than the limitation of 250 Pa for pre-filters and for 350 Pa for main filters. In Figure 8.5 (a)-(b), for the same filter the pressure drop in rural areas is somewhat lower than that in urban areas.

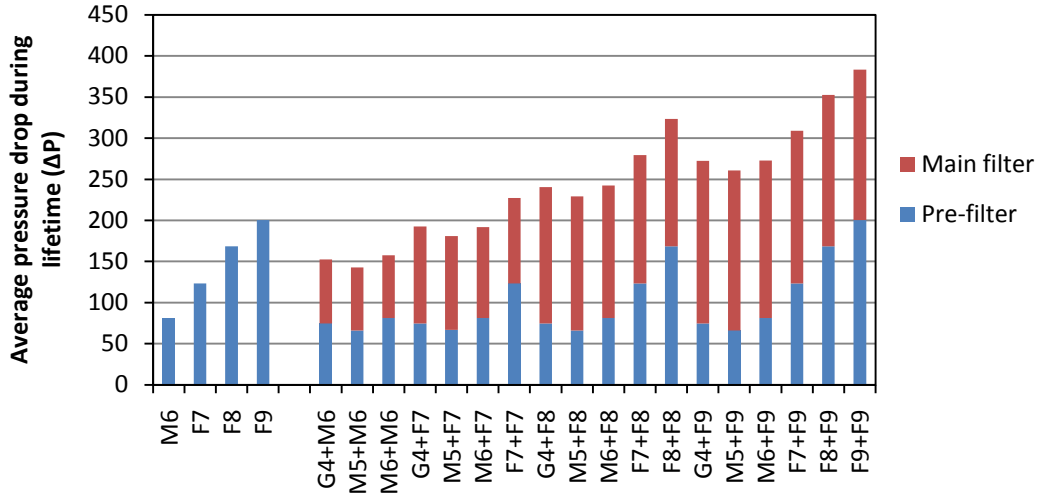

(a)

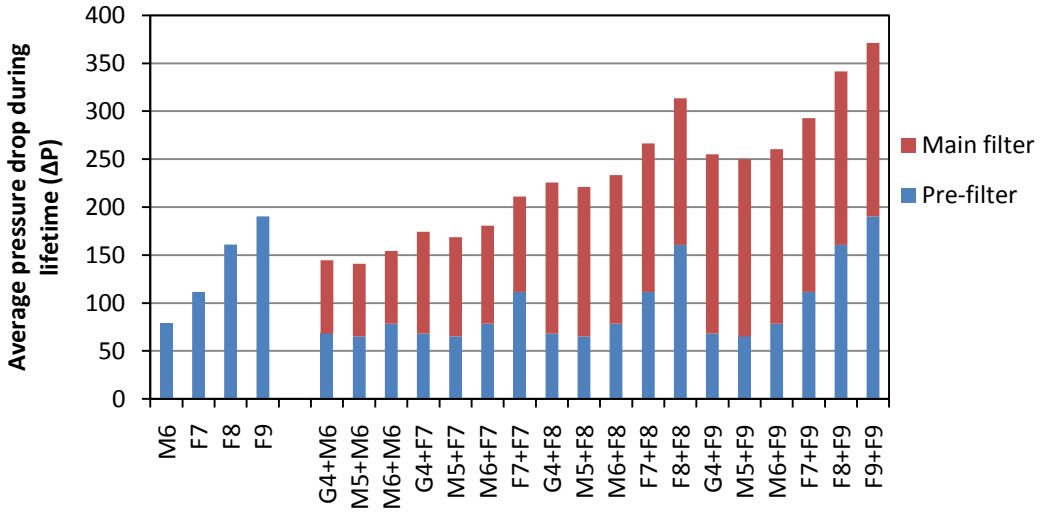

(b)

Figure 8.5. Average pressure drops of pre-filter and main filter. (a) Urban areas; (b) Rural areas.

Figure 8.6 (a)-(b) shows the annual cost per unit volumetric air flow (including energy, filter and labor) in urban areas (PM_{10}: 20 μg/m^3) and rural areas (PM_{10}: 10 μg/m^3). The high cost cases in Figure 8.6(a)-(b) also have high pressure drops in Figure 8.5 (a)-(b). This is because the energy cost contributes about 60 % of total cost in both urban and rural areas. For single-step filtration, this percentage is 62 % in urban areas and 61 % in rural areas. However, for two-step filtration, the above percentage is increased to 69 % in urban areas and 68 % in rural areas. This means that, when a single filer is replaced by two combined filters, the percentage of energy cost of the total cost increases. In summary, when the indoor environment only needs an F7, or less than F7 class filter, two-step filtration is not attractive in the view of economical cost. However, for indoor environments with high air quality requirements, some two-step filtrations probably are cost competitive with an F8/F9 class single-step filtration.

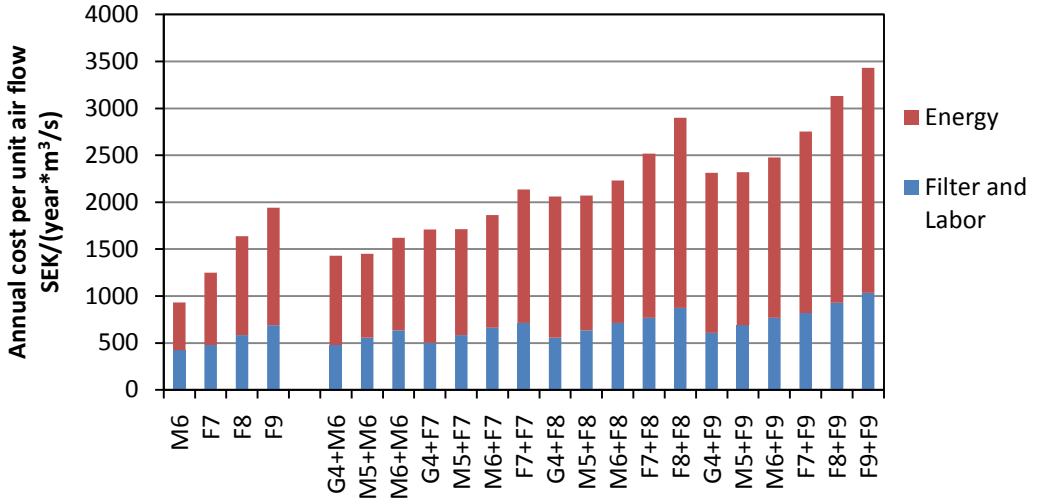

(a)

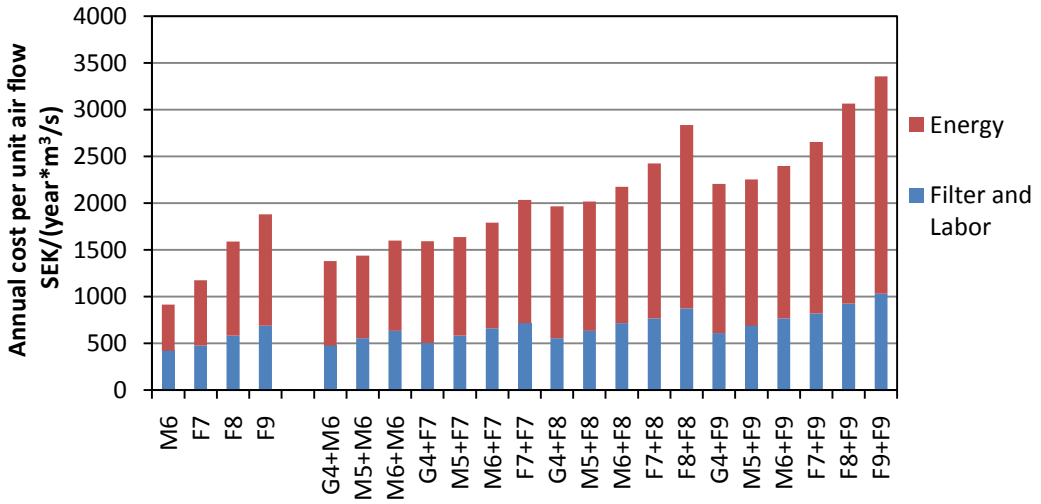

(b)

Figure 8.6 The annual costs for per unit volumetric air flow. (a) Urban areas; (b) Rural areas.

The clean air flow cost comparisons between single-step and two-step filtrations are displayed in Figure 8.7 (a)-(b), which are based on EF_{UFPs} and EF_{MPPS} respectively. Here, the relative clean air cost is the cost ratio of the two-step filtration to the single-step filtration. Because the value of EF_{UFPs}, EF_{PM1}, $EF_{PM2.5}$ and EF_{PM10} are similar for the studied aerosol size distribution, the results of EF_{UFPs} in Figure 8.7 (a) also indicate the results based on EF_{PM1}, $EF_{PM2.5}$ and EF_{PM10}. Additionally, because EF_{MPPS} is substantially lower than EF_{UFPs}, EF_{PM1}, $EF_{PM2.5}$ and EF_{PM10} in the study, Figure 8.7 (b) is obviously different from Figure 8.7 (a). The bars with values below 100% in Figure 8.7 (a)-(b) indicates that the two-step filtration cost is lower than the compared cost of single-step filtration. The purple bars mean that the two-step filtration has lower filtration efficiency than the compared single-step filtration.

In Figure 8.7 (a), the many cases of two-step filtration cost about 20% more than an F9 class single-step filtration does. The same situation also appears for some two-step cases compared to the case of a single F8 class filter. Furthermore, the two-step filtration of M6+F7 costs even less than the F9 class single-step filtration does. However, compared to the cost of an M6 or F7 class single-step filtration, the costs of many two-step filtration cases are about 50% higher. When the evaluation is based on EF_{MPPS}, two-step filtration seems to be a bit more economical. In Figure 8.7 (b), almost all efficient two-step filtration cases cost up to 20% more than F8 or F9 class single-step filtration, and less than 50% of the cost for F7 class single-step filtration. Because M6 class filters have very low EF_{MPPS}, its clean air flow cost is much higher than that of most combined filters cases. Additionally, the cost of two-step filtration of F7+F7 is lower than that of F9 class single-step filtration in Figure 8.7 (b). Note that the evaluation based on EF_{MPPS} presents the worst filtration case that most upstream particles are size distributed in the size range with minimum filtration efficiency.

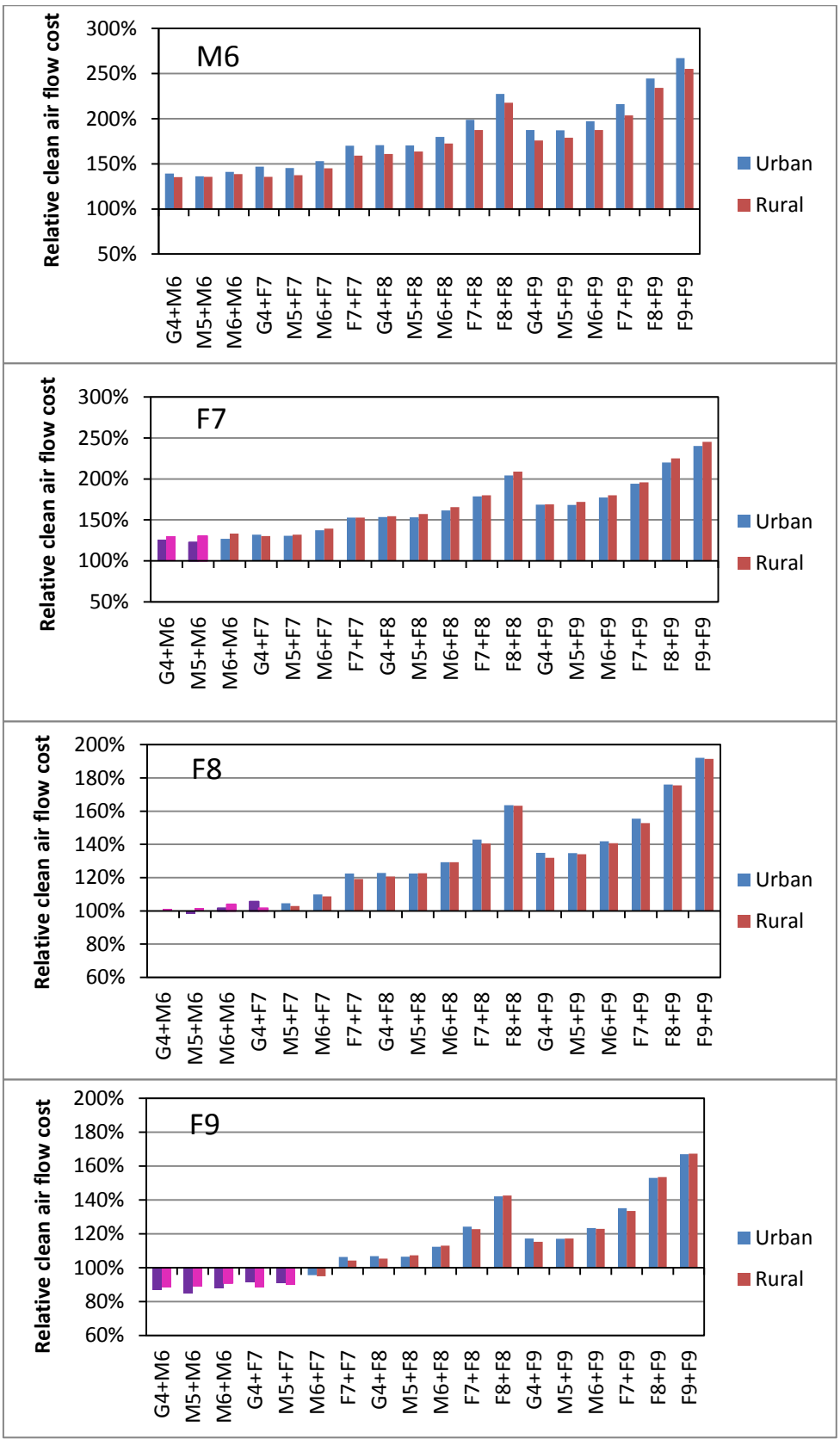
M6
F7
F8
F9
Relative clean air flow cost
Urban
Rural
G4+M6
M5+M6
M6+M6
G4+F7
M5+F7
M6+F7
F7+F7
G4+F8
M5+F8
M6+F8
F7+F8
F8+F8
G4+F9
M5+F9
M6+F9
F7+F9
F8+F9
F9+F9

(a)

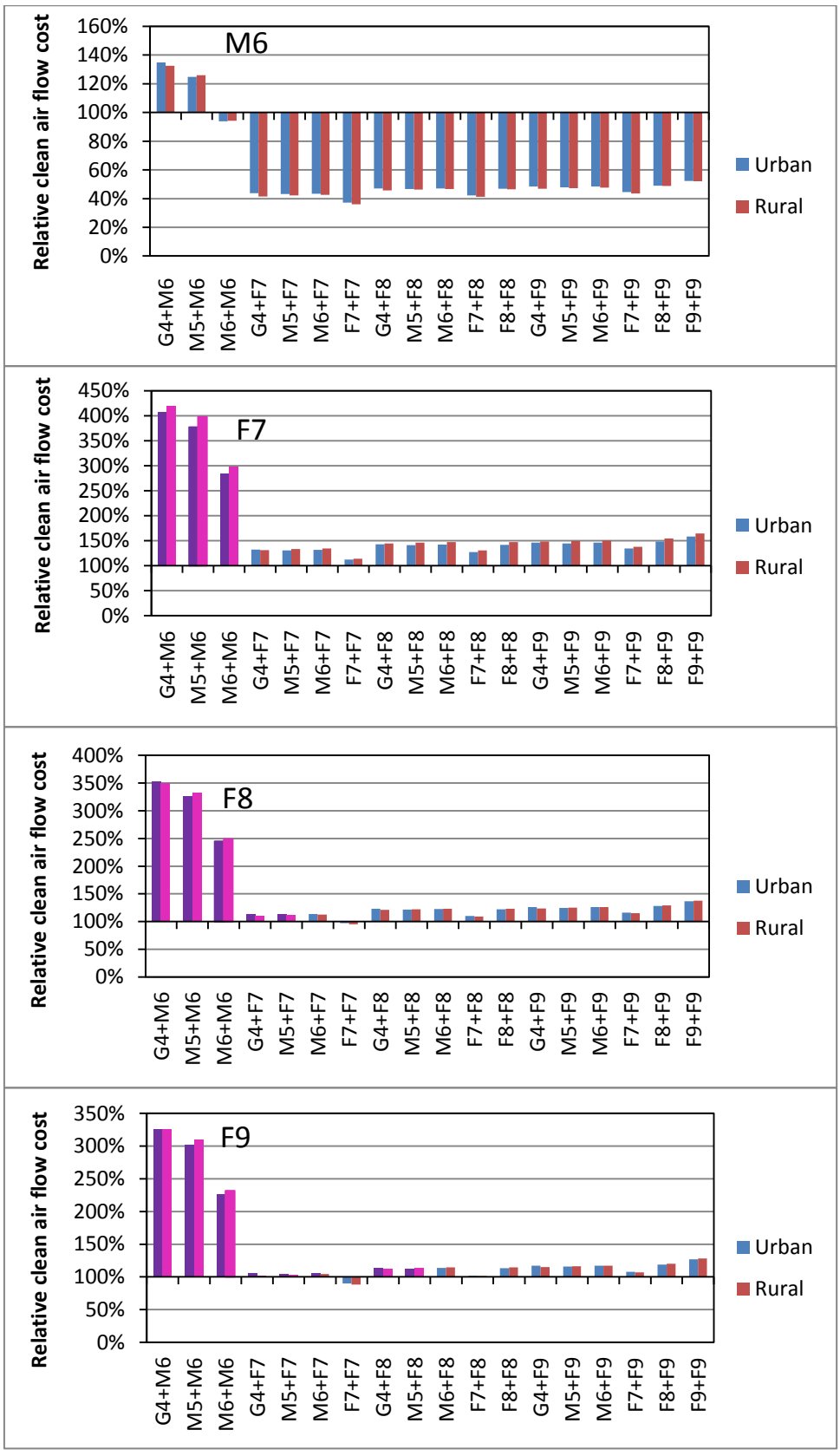

(b)

Figure 8.7 Relative clean air flow cost of combined filters compared to single filters. (a) Clean air flow for UFPs; (b) Clean air flow for MPPS-sized particle.

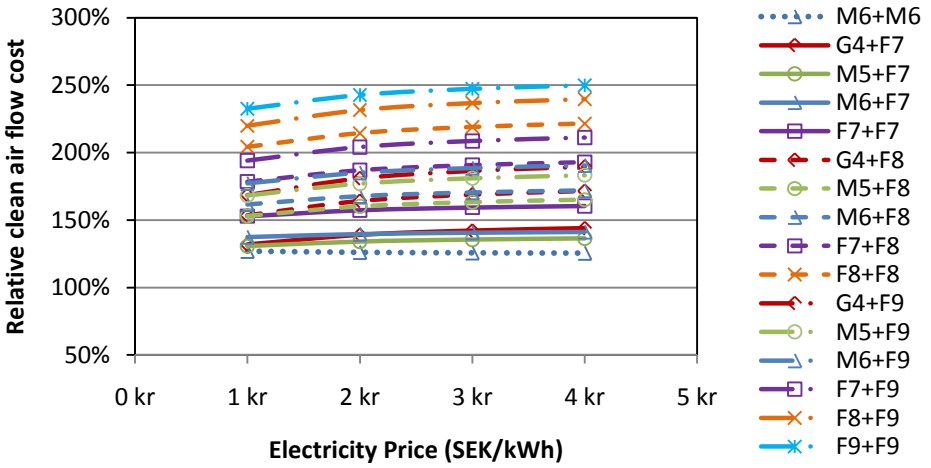

(a)

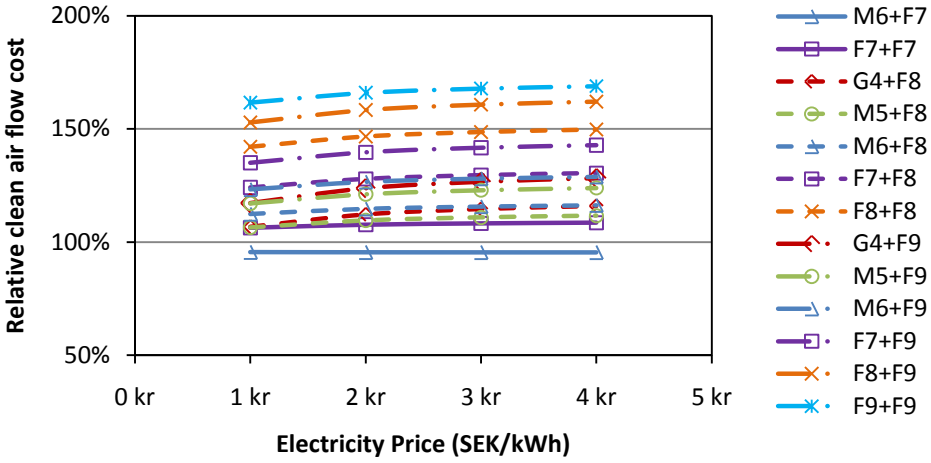

(b)

Figure 8.8 Relative clean air flow cost of two-step filtration compared to single-step filtration with varied electricity price. The calculations are made for the urban environment. (a) Versus an F7 filter; (b) Versus an F9 filter.

Considering the model ambient particle size distribution as shown in Figure 8.1, the following results in Figure 8.8-8.10 are based on EF_{UFPs}. And the figures only present the two–step filters obtaining the same or higher efficiency than that of the compared single-step filter. Figure 8.8 shows the effect of electricity price on the clean air flow cost ratio of single-step filtration to two-step filtration. The figure indicates that, the ratio is almost constant with the increase of electricity price. However, the absolute cost difference is still probably enlarged at the electricity price increase rate. An exception is the two-step filtration of M6+F7 versus a F9 class single-step filtration, whose ratio is less than one. Additionally, if two combined filters are used to replace a high class single filter, the relative cost ratio is more stable than the case if the filter combination replaces a single filter of lower class.

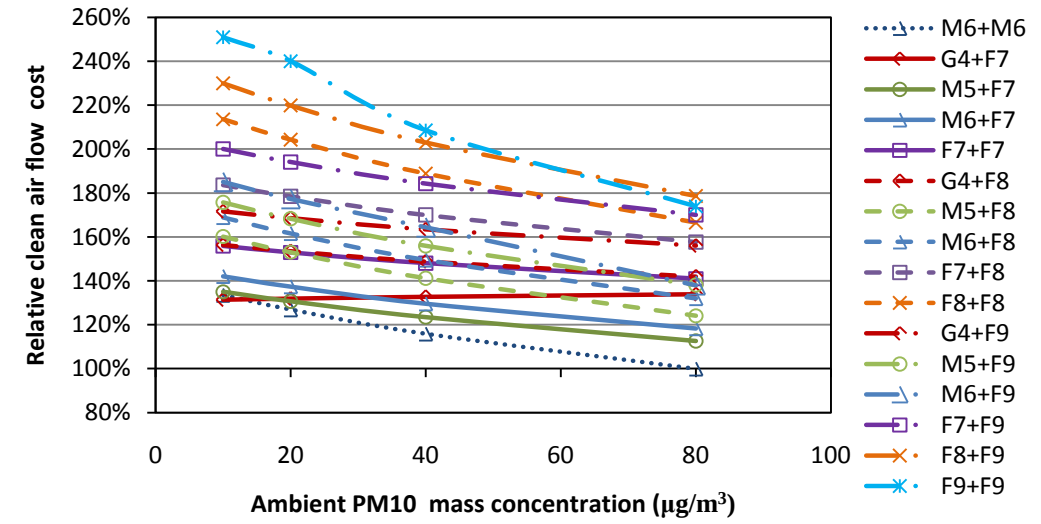

(a)

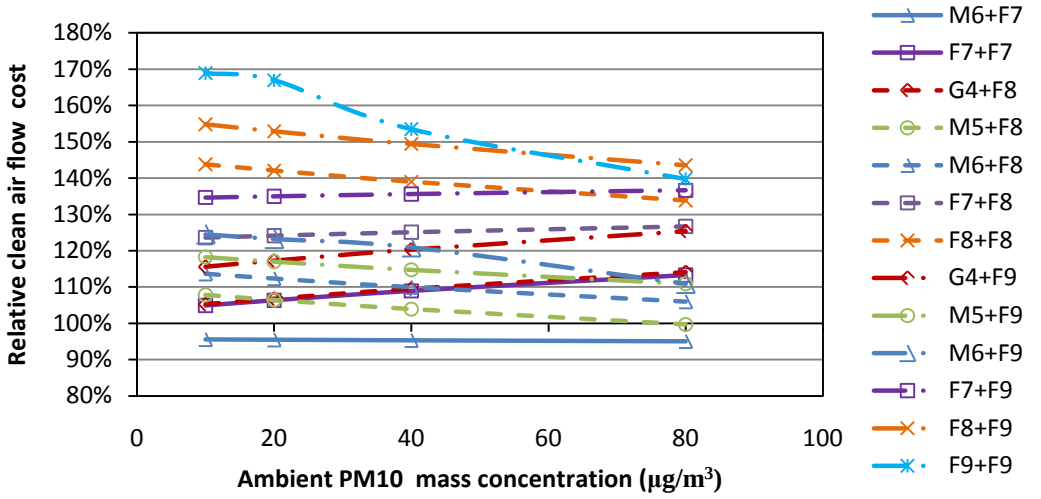

(b)

Figure 8.9 Relative annual cost per unit clean air flow on UFPs between single filters and combined filters for varied ambient PM_{10} mass concentration. (a) Versus an F7 class filter; (b) Versus an F9 class filter.

Figure 8.9 shows the relative clean air flow cost varied with the ambient PM_{10} mass concentration. The relative clean air flow cost is the clean air flow cost ratio of two-step filtration to single-step filtration. In the figure, for most two-step filtration cases, the relative clean air cost slowly decreases with ambient particle concentration. This demonstrates that, compared to a single filter, two-step filtration is more economical in heavy particle polluted areas. Especially, this phenomenon seems to be clearer when compared to low class single-step filtration.

Figure 8.10 shows a comparison between the cost when using the short filter lifetimes (pre-filter: 6 months; main filter: 12 months)[l] to the cost with the above investigated lifetimes. The relative clean air flow cost, which is the ratio of the cost with the short lifetime to the cost with the lifetime investigated above. The figure shows that the cost with the short lifetime is about 30% higher than the cost

with the investigated lifetime. However, compared to the cost of single-step filtration with a lifetime of 6 months, the cost ratio of two-step filtration to single-step filtration is reduced at the short lifetime. And there are more economical benefit two-step filtration cases. See Appendix B. This short lifetime is set in order to reduce the risk of by-products generation from used filters. The results indicate the magnitude of the costs associated with this risk reduction.

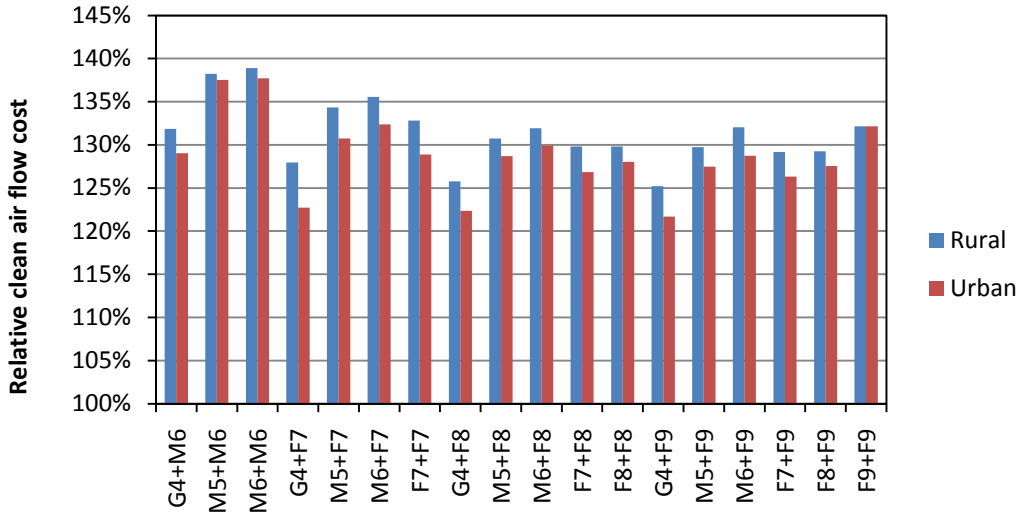

Figure 8.10 Relative annual clean air cost between the cost with the short lifetime (pre-filter: 6 months; main filter: 12 months) and the cost with the investigated lifetime (pre-filter: 12 months; main filter: 24 months).

8.4 Discussion and conclusion

In summary, the study shows that two-step filtration is not obviously more expensive than single-step filtration. Low class two-step filtration probably costs less than high class single-step filtration does and obtains the same or even higher filtration efficiency, for example M6+F7 filters cost less than a single F9 class filter does per volumetric clean air flow.

As a general filtration comparison, when judging clean air flow cost based on EF_{UFPs}, many two-step filtration cases cost about 20 % more than F8/F9 class single-step filtration does; and many two-step filtration cases cost about 50 % more than an M6/F7 single-step filtration does. However, when judging clean air cost based on EF_{MPPS}, almost all two-step filtration cases cost less than 20% of the compared single filter does, except for the comparison to a single F7 class filter.

Suitable lifetime of main filter and pre-filter is needed to reduce two-step filtration cost to the minimum cost level. The study shows that extending the main filter lifetime can reduce the cost more than extending the pre-filter lifetime does. This solution is more effective when the combined two filters have larger difference in class.

Extending filter lifetime relies on the ambient particle concentration. Special attention should be paid when extending the life time of the main filter in

seriously particle polluted areas, because extending the main filter lifetime has the risk to substantially increase the energy cost.

The relative economical benefit of two-step filtration compared to single-step filtration increases with the ambient particle concentration. Thus in general, it is more economical to use combined filters in urban areas than in rural areas. Due to uncertainties regarding energy supply and energy prices, the influence of electricity price was investigated. And the results show that the clean air flow cost ratio is almost constant with the electricity price increase.

The potential economical benefit on air flow and clean air flow can be attributed to the following reasons: (a) the lifetime of the main filter can be extended because a large amount of coarse particles are blocked by the pre-filter; (b) low class filters have lower initial pressure drop than that of high class filters; (c) the increased filtration efficiency on UFPs and MPPS-sized particles can relatively reduce the clean air flow cost of two-step filtration.

To reasonably apply two-step filtration, some suggestions are summarized according to the study:

1. Suitable low class two-step filtration is cost competitive compared to high class single-step filtration, without any reduction of the filtration efficiency of UFPs and MPPS.
2. Reasonably extending the main filter lifetime can reduce the total cost. This extension relies on the ambient particle concentration.
3. It is more economical to apply two-step filtration in areas with high ambient particle concentration.
4. The cost ratio of two-step filtration to single-step filtration is almost constant with the electricity price increase.
5. The annual cost with the short lifetime (pre-filter: 6 months; main filter: 12 months) is about 30% higher than the cost with the investigated lifetime (pre-filter: 12 months; main filter: 24 months).

In conclusion, the study evaluated the economical cost and filtration efficiency of two-step filtration compared to single-step filtration in different ambient air; and investigated the effect of the main influencing factors. The priority between them is closely related with filter lifetimes, filter classes, ambient particle concentrations and electricity prices. To limit the by-products generation from used filters, the filter lifetime at a specific location probably needs to be designed according to the local climate and the local ambient particle concentration.

The analysis is an example and the results rely on a number of assumptions. For example, the data on the increase of the pressure drop over time are based on a few measurements made in one location only. Thus, the assumed relation between accumulated dust and pressure drop increase is judged to be uncertain. In general, reliable data are scarce. In order to sharpen the precision of analyses of the type presented here, there is an urgent need to establish better data from the field.

Another assumption is that the filtration efficiency is constant over time. Also in this case it is hard to establish reliable data valid for filters in real operation in buildings. The analysis was made using the initial filtration efficiency observed for one individual filter of each class studied.

Of these reasons the study must be considered as an indication of tendencies rather than en establishment of generally valid relationships.

9 Ionizer assisted air filtration

An ionizer applied at the upstream of a ventilation air filter could enhance the particle collection efficiency of the filter, without affecting the pressure drop. This chapter is to investigate the magnitude of the filtration efficiency enhancement when using an ionizer on charged synthetic and glass fiber ventilation air filters.

9.1 Introduction

This study investigates the influence of the fiber material, filter class and ion concentration on the enhanced efficiency obtained by ionization before the filter. Besides the enhanced efficiency, the risk of emission of by-products, e.g. ozone, is another important issue that has been considered in the experiments. The study was carried out at laboratory full-scale filter test rig, a small-scale filter test rig and a field demand controlled ventilation (DCV) system.

9.2 Full scale filter laboratory experiments

9.2.1 Methods

The ventilation filter experiment was conducted in a full-scale filter test rig with the experimental setup shown in Figure 9.1. In the laboratory filter test rig experiments, seven ventilation filters of class F5-F9 (MERV11-15), made of three types of fiber materials were tested.

The measurement equipment and methods are basically the same as the ones presented in chapter 4. The upstream and downstream aerosol concentrations and size distributions were measured by a Scanning Mobility Particle Sizer (SMPS) spectrometer (Model: SMPS 3936, TSI, USA) including a long Differential Mobility Analyzer (DMA) and a Condensation Particle Counter (CPC). The test rig was constructed in accordance with the European filter standard EN779. A HEPA filter of class H14 was used upstream to provide clean air. Downstream the HEPA filter, a Di-Ethyl-Hexyl-Sebacat (DEHS) aerosol was generated by an atomizer (Model: ATM 230, Topas, Germany) and negative ions were generated by a carbon fiber ionizer (Transjoinc AB, Sweden) with the working voltage of 7 kV. The ion concentration was measured by an ion meter (Transjoinc AB, Sweden).

The tests were done with an average ion concentration about $3.2 \cdot 10^5$ ion^-/cm^3, and $1.2 \cdot 10^6$ ion^-/cm^3. The corresponding face velocities of the two air flow rates are 0.7 m/s and 2.6 m/s. The air flow rate $0.944 m^3/s$ is the nominal filter test air flow rate according to EN779. The air flow rate of $0.25 m^3/s$ was chosen in order to increase the contact time between ions and particles.

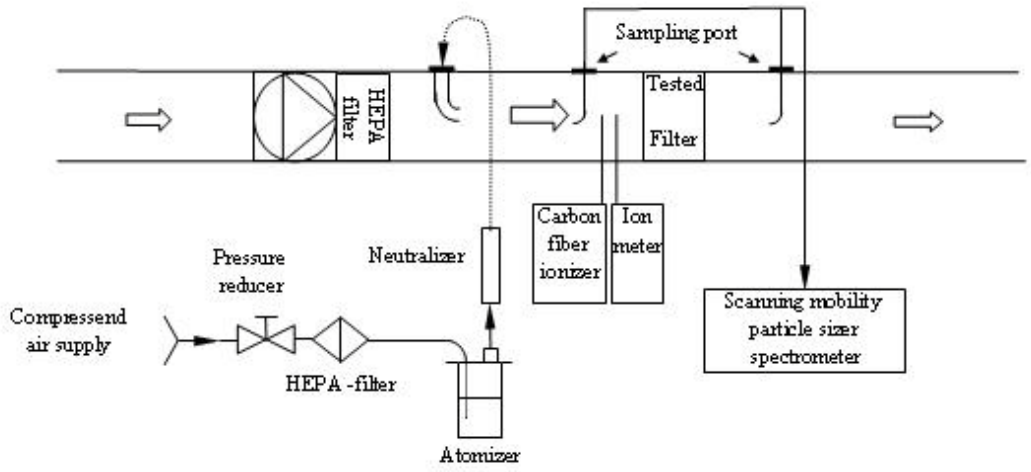

Figure 9.1 Experimental setup of the test in the full-scale filter test rig.

Table 9.1 lists the specification of the filters tested in the experiments. Filter #4 is designated a "nano-fiber filter" by the manufacturer. It is made of charged synthetic fibers, which, also according to the manufacturer, incorporates submicron fibers.

Table 9.1. Specifications of the Filters Tested in the Filter Test Rig.

Tested filters	Filter class		Filter media type	Filter size
	EN 779	ASHRAE 52.2		
#1	F6	MERV 11-12	Charged Synthetic	592*592*635mm_8 bags
#2	F7	MERV 13	Charged Synthetic	592*592*635mm_8bags
#3	F7	MERV 13	Glass Fiber	592*592*500mm_10 bags
#4	F7	MERV 13	Nano-fiber	592*592*635mm_8 bags
#5	F8	MERV 14	Charged Synthetic	592*592*635mm_8 bags
#6	F8	MERV14	Glass Fiber	592*592*450mm_8 bags
#7	F9	MERV 15	Charged Synthetic	592*592*635mm_8 bags

Additionally, the increase of the efficiency obtained by assisting the filter with the ionizer is defined by eq. 9.1. Here, EF with ionizer and EF without ionizer are the filtration efficiencies of a filter assisted with an ionizer and without an ionizer, respectively.

Enhanced efficiency= EF with ionizer- EF without ionizer *(eq.9.1)*

9.2.2 Results

The enhanced efficiency is investigated for different filter materials, classes and ion concentrations. Figure 9.2 shows the results for glass fiber filter #3 under ion concentrations $3.2 \cdot 10^5$ ions$^-$/cm^3 and $1.2 \cdot 10^6$ ions$^-$/cm^3. By comparing Figure 9.2 (a) and (b), it is clear that the enhanced efficiency is higher with a higher ion concentration. Additionally, both Figure 9.2 (a) and (b) show that the efficiency is enhanced more for ultrafine particles than for particles of other sizes. This is expected because the particles are influenced by the Coulombic force, which increases with decreasing particle size [78, 129].

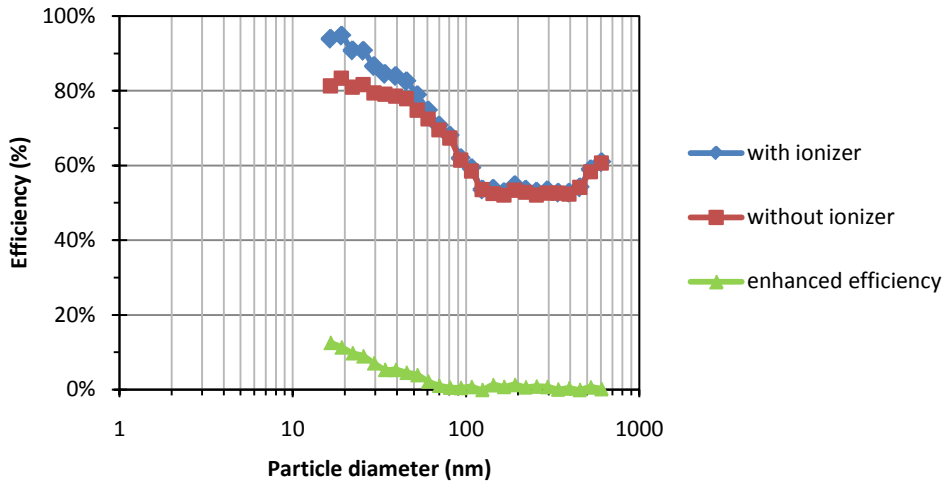

(a)

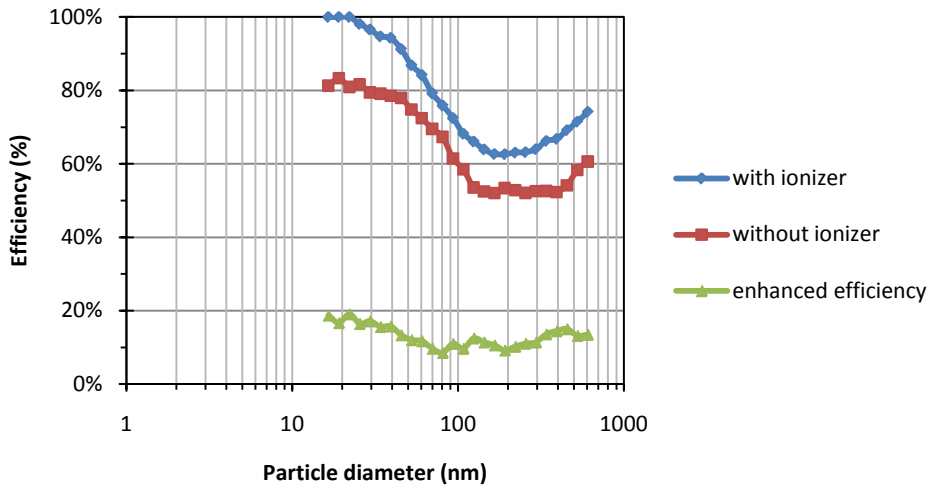

(b)

Figure 9.2 Particle removal efficiency of F7 glass fiber filter #3 at the face velocity 0.7 m/s and ion concentration of (a) $3.2 \cdot 10^5$ ions$^-$/cm^3; (b) $1.2 \cdot 10^6$ ions$^-$/cm^3.

Figure 9.3 shows the enhanced efficiencies of three fiber materials under the same low ion concentration and the face velocity 0.7 m/s. In the ultrafine size-range both the synthetic fiber filter #2 and the nano-fiber filter #4 showed higher enhanced efficiencies than the glass fiber filter #3 did. The differences were quite

small for other particle sizes. The curves are almost identical for the nano-fiber filter #4 and the synthetic fiber filter #2, which may have been expected since also the nano-fiber material is made of synthetic fibers. The main difference between these filter materials is assumed to be the fiber size. However, this has not been investigated to date.

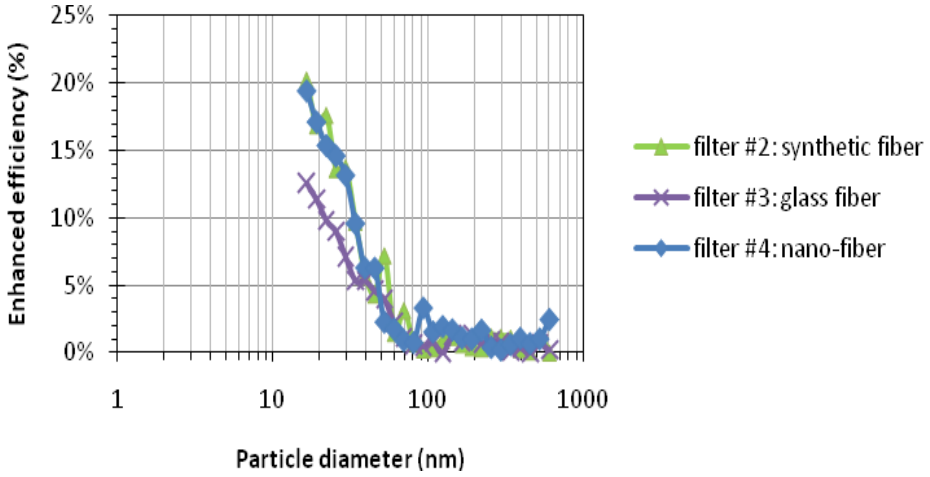

Figure 9.3 Enhanced efficiency by the ionizer for three F7 filters #2, #3 and #4 at the face velocity 0.7 m/s and ion concentration of $3.2 \cdot 10^5$ ions$^-$/cm^3.

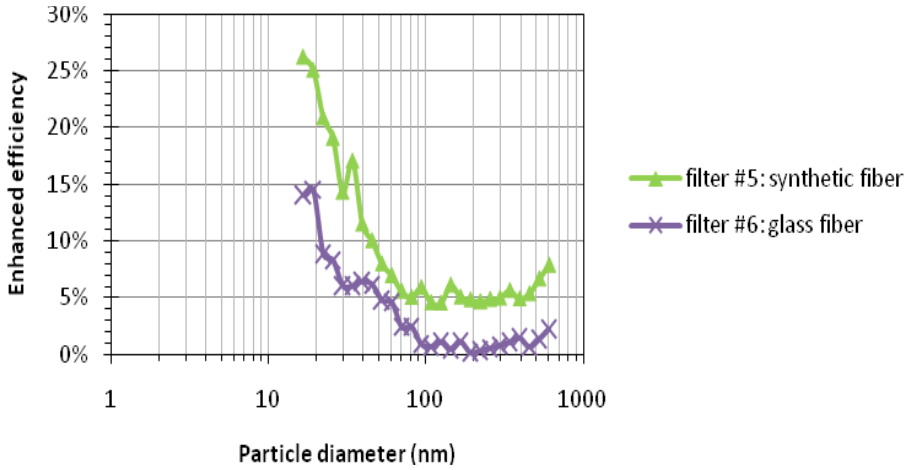

Figure 9.4 Enhanced efficiency with ionizer for two F8 filters #5 and #6 at the face velocity of 2.6 m/s and ion concentration of $1.2 \cdot 10^6$ ions$^-$/cm^3.

Figure 9.4 shows the results of the corresponding experiments on F8 filters # 5 and #6 under an ion concentration of $1.2 \cdot 10^6$ ions$^-$/cm^3 and at the face velocity 2.6 m/s. Also in this experiment the synthetic filter showed a higher enhanced efficiency than the glass fiber filter. Moreover, the higher ion concentration probably promoted the enhanced efficiency of the case presented in Figure 9.4, compared to the case presented in Figure 9.3. However, the substantially higher face velocity is expected to have counteracted the enhanced efficiency for the case in Figure 9.4. Despite this expected negative effect of the higher face velocity, the synthetic F8 filter showed a higher enhanced efficiency than the synthetic F7 filter did.

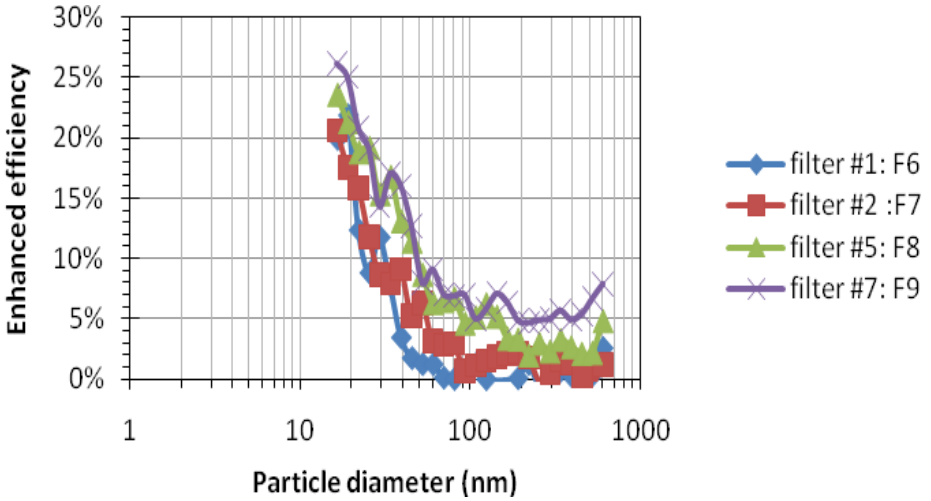

Figure 9.5 Enhanced efficiency for filters #1, #2, #5 and #7 obtained at the face velocity 2.6 m/s and an ion concentration of $1.2 \cdot 10^6$ ions$^-$/cm^3.

Figure 9.5 shows that the enhanced efficiency for the charged synthetic filters increases somewhat from filter F6 to filter F9. It is supposed that the filters of higher class have more charged fibers and higher packing density than the filters of lower class. Thus, the higher class filters may impose a stronger electric field on the charged particles than the lower class filters can.

When the ionizer was turned off the ozone concentration downstream of the tested filter was below the detection limit of 1 ppb. At the ion concentrations $3.2 \cdot 10^5$ ions$^-$/cm^3 and $1.2 \cdot 10^6$ ions$^-$/cm^3, the ozone concentration increased to 1.2 ppb±0.5 ppb and 2.8 ppb±1.7 ppb, respectively. In both cases the face velocity was 0.25 m^3/s.

9.3 Field DCV system experiments

9.3.1 Methods

The experiments were conducted in a DCV system of a hospital office building in Göteborg, Sweden. The air handling unit has a design supply airflow rate of 4.8 m^3/s, and exhaust air flow rate of 4.6 m^3/s. However, due to the DCV-function it operates at substantially lower flow rates most of the time. The particle number concentrations were measured by two instruments: A TSI P-TRAK Ultrafine Particle Counter was used to measure in the size range between 0.02µm and 1.0µm, and a CLiMET CI-500 optical particle counter was used for the following size ranges: 0.3-0.5, 0.5-1.0, 1.0-5.0, 5.0-10.0, 10.0-25.0 and >25µm. Additionally, a TSI Dust-Trak photometer was used to measure the total mass concentration of particles with diameters less than 10 µm (PM_{10}). Ozone concentration was measured by an Environics Series 300 UV-photometry instrument, with the detection limit of 1 ppb by volume. The outdoor air intake is located at the roof of the building. Figure 9.6 and 9.7 shows the experimental set up and the ionization system. The ionization system includes multiple carbon fiber brushes and a plasma field ionizer. The ion emission was controlled by the supply electricity voltage and the number of carbon fiber brushes.

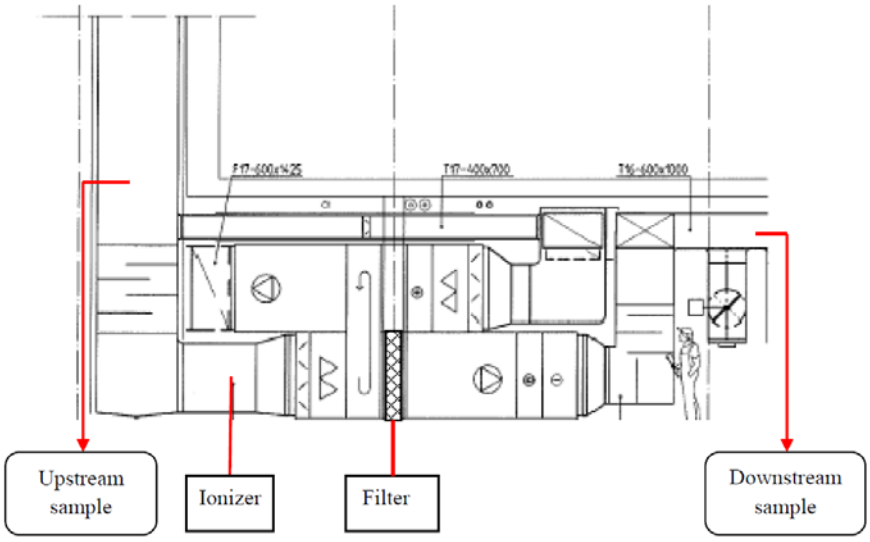

Figure 9.6 Experimental setup of the test in the DCV system.

Figure 9.7 Image of the ionization system.

Two ventilation air filters were tested in the experiments. Table 9.2 lists the specification of the tested filters. The effect of the ionizer on the filtration efficiency is also described by the enhanced efficiency with the definition in eq. 9.1.

Table 9.2 Specifications of the Filters Tested in the DCV system. The F7 filter had been in operation for about one year. The G4 filter was new.

Tested filters	Filter class		Filter media type	Filter size	Number
	EN 779	ASHRAE 52.2			
#8	F7	MERV 13	Glass fiber	592×592 mm	3
				592×287 mm	3
				592×490 mm	3
#9	G4	MERV 7-8	Synthetic	592×592 mm	3
				592×287 mm	3
				592×490 mm	3

9.3.2 Results

9.3.2.1 F7 dirty filters

The experiments on the F7 dirty filters (1 year operation) were conducted with the ionizer providing an ion concentration of $3.4 \cdot 10^5$ ions$^-$/cm^3. The filtration efficiency values and the enhanced efficiency are presented, see Figure 9.8 (a)-(c). The white bar represents the original filtration efficiency without ionizers. The stacked black bar represents the enhanced efficiency under the testing ion concentration.

The figures show that the filtration efficiency of the F7 class filter is increased by about 20%-units for particles in the size range of 0.3-0.5µm. Comparing the results with data presented in Chapter 4 indicates that the filtration efficiency of the tested F7 class filter assisted with an ionizer is similar to the efficiency level of using an F8 or even F9 class filter alone.

Additionally, the original filtration efficiency slowly increases with the reduced air velocity. The enhanced efficiency increases a bit with the reduced air velocity in Figure 9.8 (a) and (b). However, the enhanced efficiency in Figure 9.8 (c) reduces a bit and the total efficiency is similar to the level in Figure 9.8 (a) and (b). The cause is supposed to be the high original efficiency.

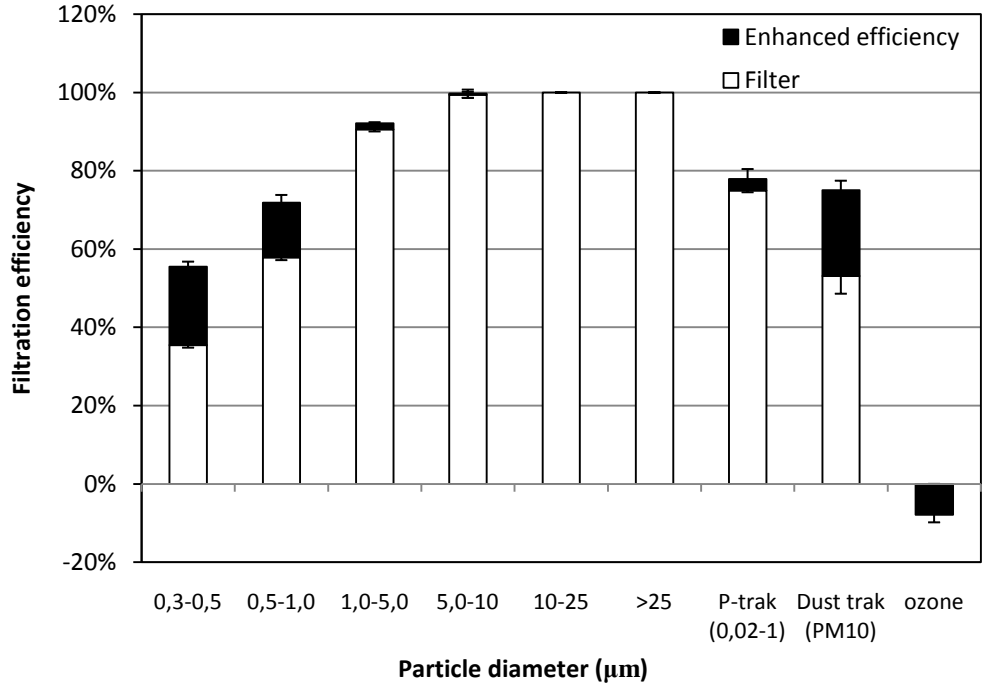
120%
100%
80%
60%
40%
20%
0%
-20%
Enhanced efficiency
Filter
Filtration efficiency
0,3-0,5
0,5-1,0
1,0-5,0
5,0-10
10-25
>25
P-trak (0,02-1)
Dust trak (PM10)
ozone
Particle diameter (µm)

(a)

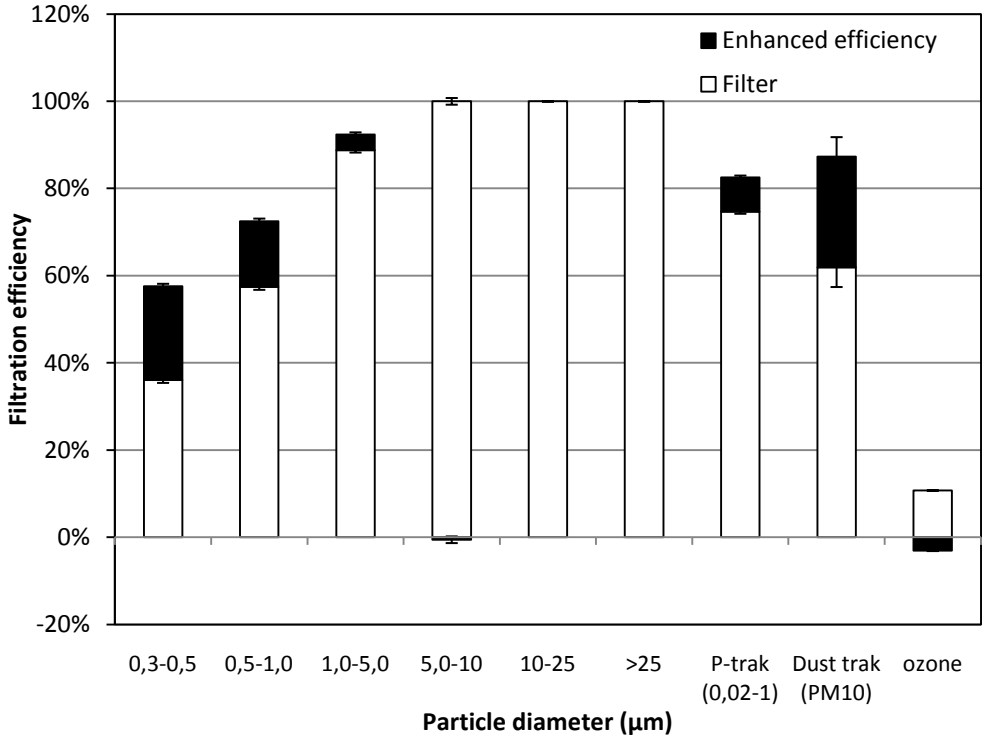
120%
100%
80%
60%
40%
20%
0%
-20%
Enhanced efficiency
Filter
Filtration efficiency
0,3-0,5
0,5-1,0
1,0-5,0
5,0-10
10-25
>25
P-trak (0,02-1)
Dust trak (PM10)
ozone
Particle diameter (µm)

(b)

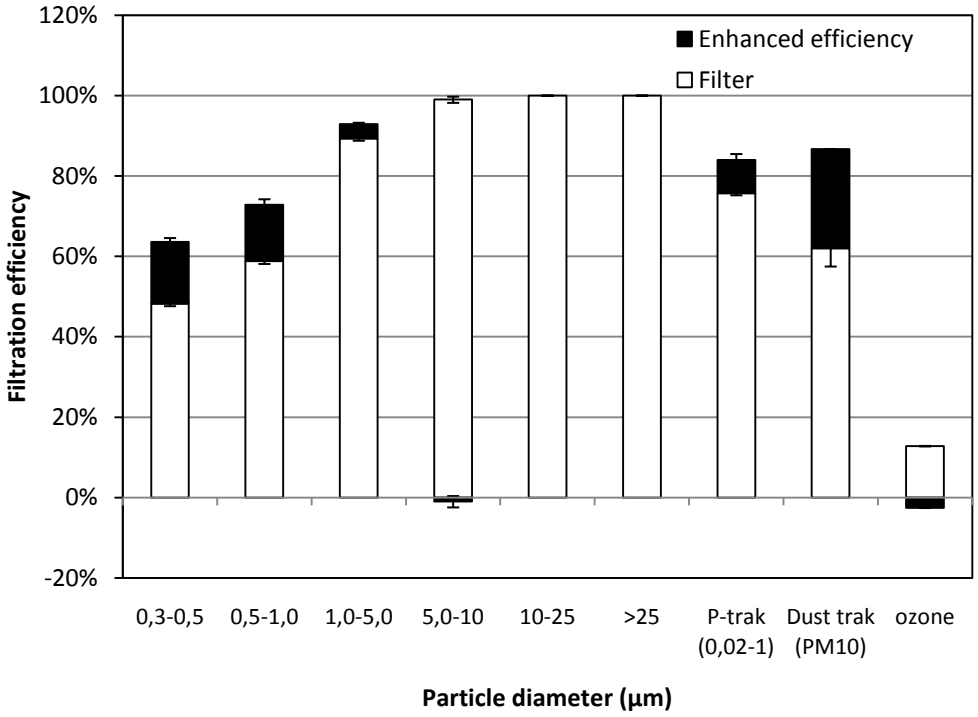

Figure 9.8 Original filtration efficiency without ionization and ionizer enhanced efficiency for the glass fiber F7 filter with an ion concentration of $3.4 \cdot 10^5$ ions$^-$/cm^3 at (a) 1.5 m/s, (b) 1.1m/s and (c) 0.9 m/s.

9.3.2.2 G4 new filters

The potential to substantially reduce the use of electrical energy for fan operation would be high if a low class filter, e.g. class G4, used together with ionization, could replace a traditional filter of higher class, e.g. an F7 filter. Therefore, a G4 class synthetic filter was also investigated.

Figure 9.9 shows its original filtration efficiency and enhanced efficiency tested at the face air velocity of 1.1 m/s with the ion concentration of $3.4 \cdot 10^5$ ions$^-$/cm^3. The figure shows that the enhanced efficiency for the tested G4 filter is much lower than for the F7 filter at the same air velocity and ion concentration. Furthermore, the filtration efficiency of the G4 class filter with ionizer is still much lower than the filtration efficiency of the F7 class filter alone.

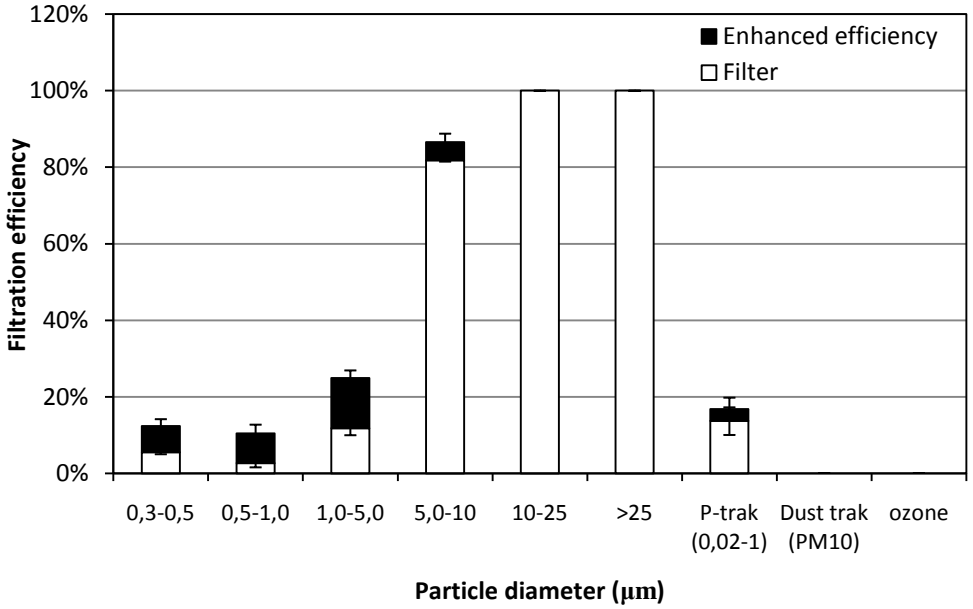

Figure 9.9 Original filtration efficiency without ionization and ionizer enhanced efficiency for the G4 class synthetic filter at 1.1 m/s with $3.4 \cdot 10^5$ ions$^-$/cm^3.

Similarly, the G4 filter was also tested at two air velocities, 1.1 m/s and 1.3 m/s. Figure 9.10 shows the enhanced efficiency in the two tests. In the figure, when the air velocity increases from 1.1 m/s to 1.3 m/s, the enhanced efficiency clearly appears to be reduced. Furthermore, this reduction is clearer for the G4 class filter than for the F7 class filter, when Figure 9.10 is compared with Figure 9.8.

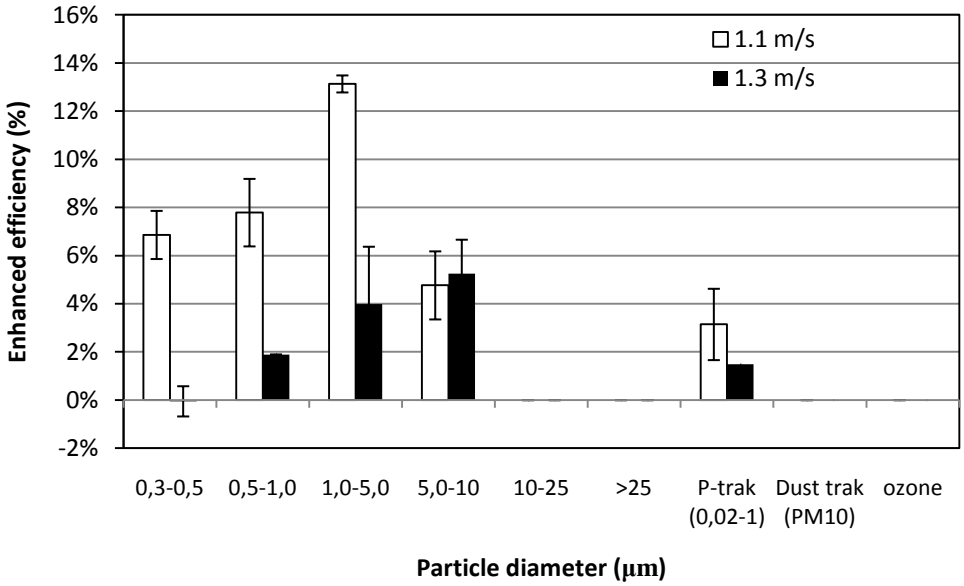

Figure 9.10 Enhanced filtration efficiency for the G4 filter at 1.1 m/s and 1.3 m/s with $3.4 \cdot 10^5$ ions$^-$/cm^3.

For the purpose of increasing the enhanced efficiency for G4 class filters, the ion concentration was increased up to $7 \cdot 10^5$ ions$^-$/cm^3. The enhanced efficiencies

observed under the two ion concentrations are shown in Figure 9.11. The figure shows that the enhanced filtration efficiency is almost zero under the low ion concentration ($3.0 \cdot 10^5$ ions$^-$/cm^3). However, increasing the ion concentration, the enhanced filtration efficiency obviously increased.

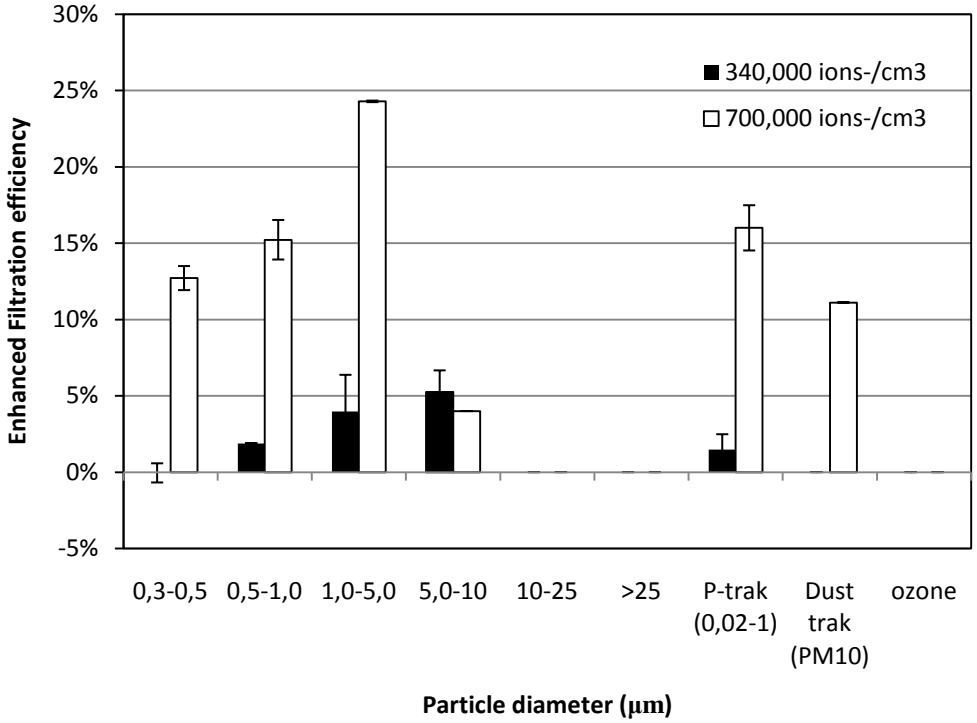

Figure 9.11 Enhanced filtration efficiency for the synthetic G4 filter at 1.3 m/s with $3.0 \cdot 10^5$ ions$^-$/cm^3 and $7.0 \cdot 10^5$ ions$^-$/cm^3.

The G4 class synthetic filter is a coarse filter and completely without electrostatic charges according to the manufacturer, which is expected to be the reason why the enhanced filtration efficiency is lower for this filter than for the F7 class filter. Furthermore, the results show that the filtration efficiency of the G4 class filter assisted with ionizer is lower than the filtration efficiency of the F7 class filter. In the above two filters tests, the ozone concentrations in the downstream air, with and without ionizers, were close to the upstream air concentration level within ± 3ppb. Therefore, at and below the ion concentration of $7.0 \cdot 10^5$ ions$^-$/cm^3, the G4 class filter cannot be used together with an ionizer to replace the commonly used F7 class filter.

9.4 Flat sheet test for charged synthetic filter

9.4.1 Methods

The filter media type and class have an important influence on the enhanced efficiency. To find a suitable filter in this application, three flat sheet filters were tested in a small scale filter test rig. Figure 9.12 shows the schematic of the experimental setup. As can be seen in the figure, the test rig is the same as the one used for the small scale experiments presented in Chapters 4-6.

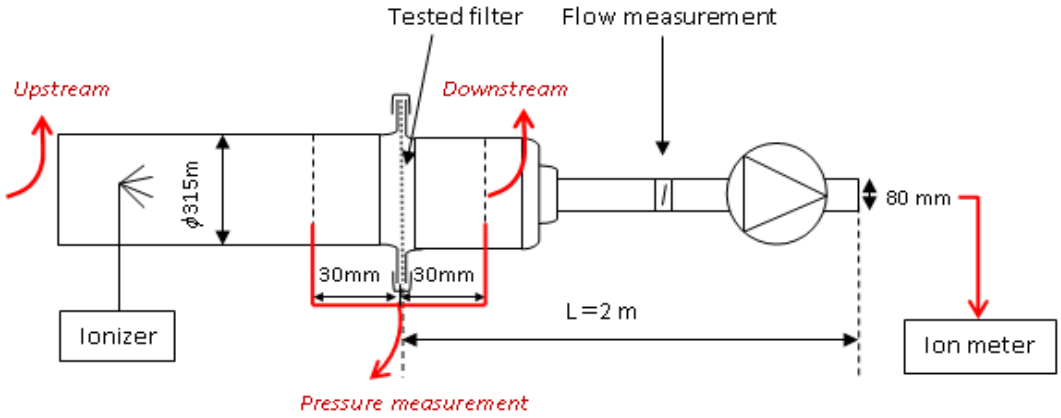

Figure 9.12 Experimental setup of the test in the small scale filter test rig.

The number particle concentrations were measured by a TSI P-TRAK Ultrafine Particle Counter for particles in the size range between 0.02µm and 1.0µm, and a CLiMET CI-500 optical particle counter for particles in the following size ranges: 0.3-0.5, 0.5-1.0, 1.0-5.0, 5.0-10.0, 10.0-25.0 and >25µm. Similarly, a TSI Dust-Trak photometer was used to measure the mass concentration of PM_{10}. Ozone concentration was measured by the same Environics Series 300 UV-photometry instrument. A carbon fiber ionizer provided an ion concentration of about $2.0 \cdot 10^6$ ions$^-$/cm^3. The ion concentration in the exhaust air was measured by an ion meter. The three flat sheet filters were provided by a Swedish filter manufacturer. The specifications of the flat sheet filters are listed in Table 9.3.

Table 9.3 Specifications of the flat filter sheets.

Filter code	Filter class		Filter media type	Electrostatic Charged state
	EN 779	ASHRAE 52.2		
#10	G4	MERV 7-8	Polyester	No charged
#11	F6	MERV 11-12	Polypropylene	Charged
#12	F7	MERV 13	Polypropylene	Highly charged

9.4.2 Results

The filtration efficiencies of the three flat sheet filters were tested at two air velocities through the filter medium, 0.16 m/s and 0.36 m/s. The ion concentration in the exhaust air was observed to vary between 700 ion$^-$/cm^3 and 1000 ion$^-$/cm^3. The ozone concentration in the downstream air was below 5 ppb during the experiments.

Figure 9.13 shows the results from the G4 class filter sample. The enhanced efficiency the figure is substantially higher than that in Figure 9.11. However, the efficiency with ionizer working is still lower than the efficiency of the F7 class filter alone, as shown in Figure 9.8. Additionally, the increases of air velocity from 0.16 m/s to 0.36 m/s results in a reduction of the enhanced efficiency by more than 20%-units.

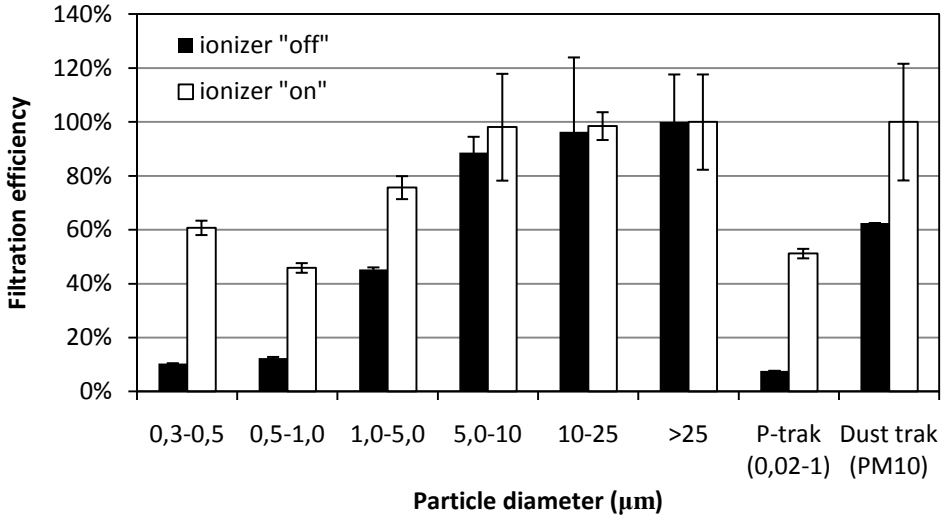

(a)

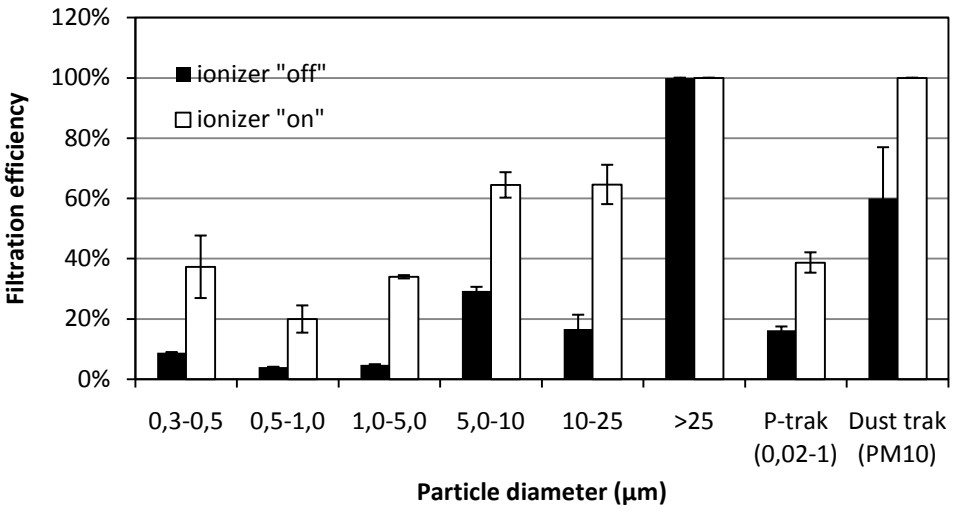

(b)

Figure 9.13 Filtration efficiency of G4 class filter with an ionizer on and off. (a) 0.16 m/s; (b) 0.36 m/s.

Figure 9.14 and 9.15 show the results for the F6 and F7 class sheet filters. Because the two filter sheets are charged, the original filtration efficiencies are extremely high. Thus, the enhanced efficiency is greatly limited by the high original efficiency. The ionizer increases the filtration efficiency up to 100% in all particle size ranges. Because the electrostatic charge normally disappears after some time of operation (e.g. a few months), it is meaningful to investigate the long-term performance of the ionizer assisted filtration system. The efficiency of the tested F6 class filter with ionizer is apparently higher than the efficiency of an F7 filter alone, without ionization. Long term tests are required to investigate if this would be the case for extended periods of time.

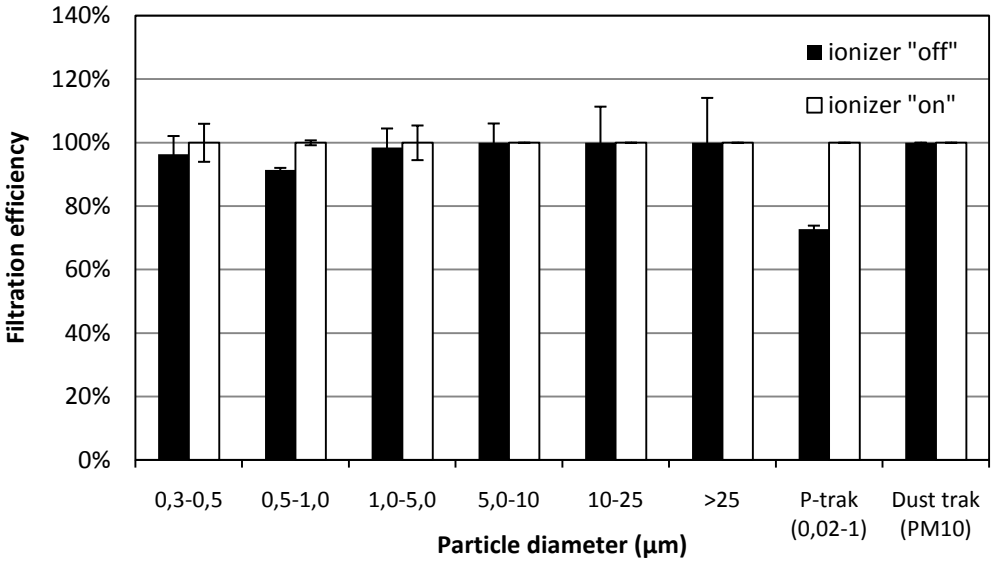

(a)

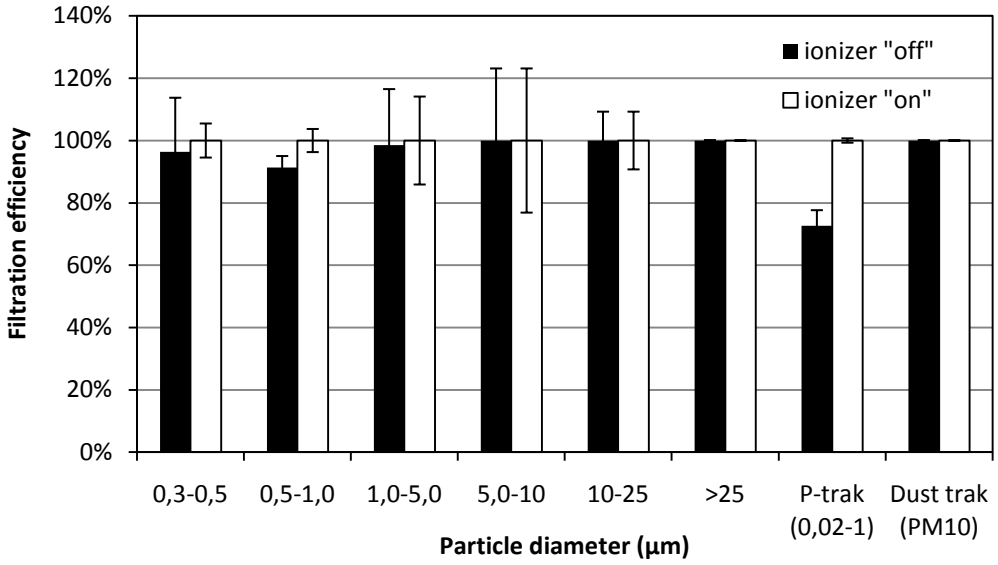

(b)

Figure 9.14 Filtration efficiency of M6 class filter with an ionizer on and off. (a) 0.16 m/s; (b) 0.36 m/s.

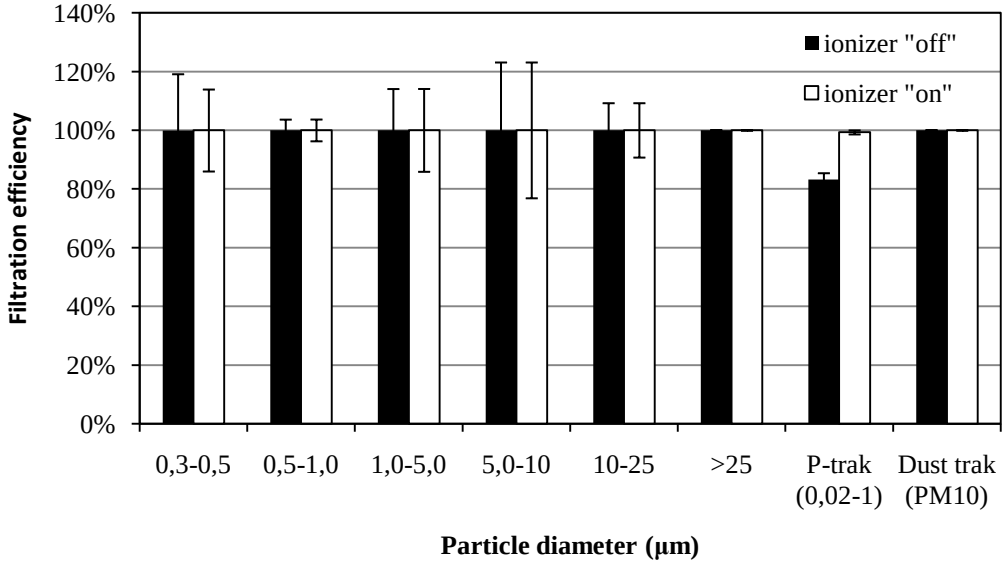

(a)

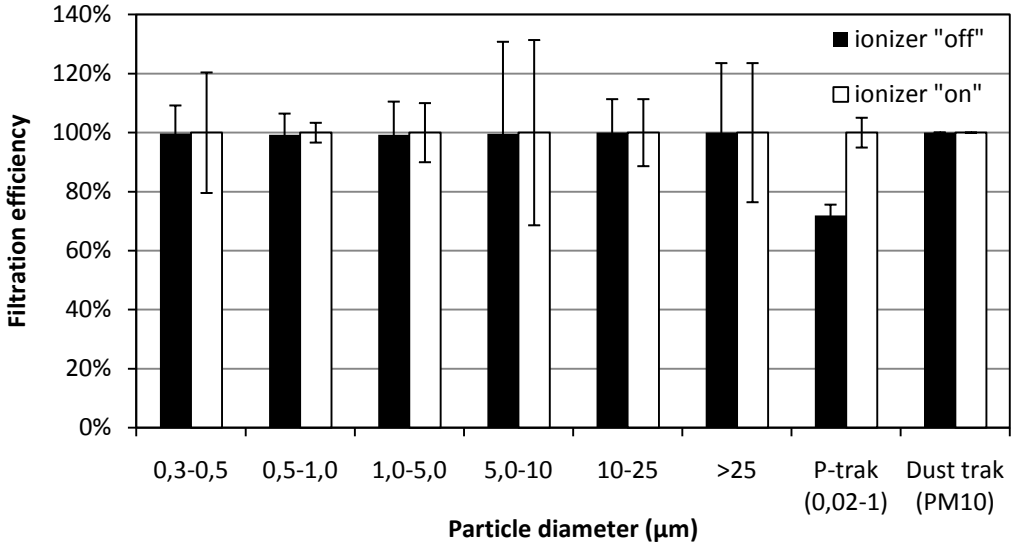

(b)

Figure 9.15 Filtration efficiency of F7 class filter with an ionizer working and non working. (a) 0.16 m/s; (b) 0.36 m/s.

9.5 Discussion and conclusion

The results show that the effect on filtration efficiency of ionizer assisted filtration depending on the ion concentration, air velocity, filter class and filter medium type. Because the supply air flow rate in a DCV system varies quite frequently, it is important that the ionizer can provide a stable high ion concentration to keep the enhanced efficiency. The setting of the system should be examined by measuring the enhanced filtration efficiency and the downstream ozone concentration at the design minimum and maximum air flow rate.

In general, their effects on the enhanced efficiency are as follows.

- With the same ion concentration, the enhanced efficiency of charged synthetic filters is higher than that of glass fiber filters, especially in the ultrafine particle size fraction.
- With the ion concentration of $3.2 \cdot 10^5$ ions$^-$/cm^3, the dirty glass fiber F7 filter showed an enhanced efficiency about 15 to 20 %-units for submicron particles, and reached an efficiency level approximately corresponding to F9 class filters.
- The enhanced efficiency for the G4 class filter increased from 0 to 50 %-units for submicron particles when the ion concentration was raised from $3.4 \cdot 10^5$ ions$^-$/cm^3 to $2 \cdot 10^6$ ions$^-$/cm^3. But this total efficiency is still lower than the filtration efficiency of a F7 class filter alone.
- Measurements showed a negligible generation of ozone in all experiments.
- With the same ion concentration, the higher class filters showed higher enhanced efficiencies than the lower class filters did.
- With a constant air velocity, the enhanced efficiency was increased with the ion concentration. However, with a constant ion concentration, the enhanced efficiency did not always increase with decreasing air velocity. According to the measurements, with decreasing air velocities, the enhanced efficiency is supposed to increase up to a certain level and then decrease when the filtration efficiency is close to 100%.
- When the enhanced efficiency decreased with increasing air velocity, the reduction of the enhanced efficiency was larger for low class filters than for high class filters.
- Ion concentration in the supply air increased to a little extent only, compared to the case without ionization. In the test, the downstream ion concentration was 0.05% of the upstream ion concentration.

According to the above findings, some recommendations are obtained for the application of ionizer assisted air filtration.

- An enough high ion concentration is important for the system to obtain an obvious increase on the filtration efficiency.
- With an enough high ion concentration, an F7 class filter assisted with an ionizer may reach the filtration efficiency of an F9 class filter alone.
- G4 class filter is not recommended for the application of ionizer assisted air filtration, to replace an F7 class filter alone, unless it works under an extremely high ion concentration.
- M6 class filter is supposed to be a suitable filter assisted with an ionizer to possibly replace a single F7 or F8 class filter.
- The generation of ozone could be negligible with a suitable ionizer and supply electricity voltage.
- For field applications in a ventilation system of DCV or VAV, the increased filtration efficiency and downstream ozone concentration should be tested under both the minimum and maximum air flow rates.

Additionally, it is of great interest to measure the long-term performance of ionizer assisted air filtration. However, due to limitation of the time available, the experiment of the long-term performance study has not been finished yet.

10 Conclusions and future research

To investigate methods to substantially reduce indoor personal exposure to UFPs, the thesis was developed in three parts. The first part is a literature study on health effects of UFPs, indoor UFPs sources, and common particle removal techniques and their applications. The second part is an investigation of the UFP removal performance of intermediate air filters available on the Swedish market. The third part is dedicated to applications of air filtration, and is focusing on the subjects of source specific control, ionizer assisted filtration and two-step air filtration.

10.1 Summary

The thesis mainly focuses on investigations around two important questions. Firstly, how to describe the filtration efficiency of intermediate air filters for UFPs and MPPS-sized particles? To objectively describe the filter performance, multiple experiments assisted with simulation studies were conducted. As expected, a finding is that the charge of filter fiber and the charge of the challenge aerosol greatly influence the shape of the efficiency curve. The relationships between EF_{UFPs}, EF_{MPPS} and $EF_{0.4\mu m}$ (EN779 classification efficiency) were investigated, and regression equations between these three expressions of the filtration efficiency were estimated. The regression equations provide a simple way to make a brief estimation, while for an accurate estimation, individual determinations are necessary for each and every filter being tested/ classified. This would be necessary if UFPs or MPPS were to be included in future filter standards.

Secondly, motivated to control indoor personal exposure to “harmful” particles, a model study was developed to analyze transport and indoor occurrence of particles from specific sources. The model forms the basis of a method to find suitable air filters and ventilation rates/modes to efficiently remove particles from indoor and outdoor sources. Based on a pre-study of the major particle sources in a building and in the surrounding environment, the results from model calculations can be used to recommend suitable air filters and ventilation rates/modes or to predict the existing system performances.

In addition, two investigations were conducted to contribute regarding how to economically and efficiently filtrate “small particles”. One solution is to use two-step filters instead of single filters. To determine the “right” applications, the economical annual cost and filtration efficiency were compared between two-step and single-step air filtration. The filter lifetime, filter class, local outdoor particle concentration and electricity price differently influence on the economical benefit of two-step filtration. Another study was made to investigate how to enhance filter efficiency through ionizer assisted air filtration. Laboratory tests and field experiments were conducted to provide guidance on the suitable air filters and ion concentrations for a certain ventilation rate.

10.2 Specific conclusions

Corresponding to the research objectives presented in the beginning of the thesis, the following specific conclusions can be made.

Literature study

- Up to now, several epidemiological and toxicological studies have shown that UFPs generated by combustion (e.g. traffic exhaust, smoking and cooking) are probably the most hazardous particles considering their size distribution and chemical composition. Since air filtration is the current widest applied technique for particle removal, the investigation of air filtration of UFPs from the indoor and outdoor combustion sources should be given top priority.

Intermediate filter efficiency

- In general, EF_{MPPS} was 10-20% lower than $EF_{0.4\mu m}$. Given the particle size distributions used in the tests, EF_{UFPs} was close to $EF_{0.4\mu m}$ for glass fiber filters, and lower than $EF_{0.4\mu m}$ for charged synthetic filters.
- Linear relationships were found between EF_{UFPs}, EF_{MPPS} and $EF_{0.4\mu m}$ within the observed efficiency range, for both glass fiber and charged synthetic filters. The relationships were influenced by the face air velocity and related with filter media.
- Single-fiber efficiency theory is a useful tool to simulate filter size-resolved efficiency values. The electrical force has big influence on the shape of the efficiency curves of charged synthetic filters.
- The neutralizer is an important component in the laboratory test of charged synthetic filters, while it appears to be of negligible influence in glass fiber filter tests. The filtration efficiency obtained when using a non-neutralized oil aerosol probably represents the mechanical efficiency of charged synthetic fibers when they lose their charge.
- The full-scale filter experiments showed that the MPPS of glass fiber filters decreased with the increase of the air velocity, while the MPPS of charged synthetic filters increased with the increase of the air velocity.
- An increase of the air velocity differently influences the filtration efficiency of different filter media. For glass fiber filters, the efficiency values clearly decreased with increased air velocity within the UFP size range, while particles in the upper end of the measured size range were practically not affected at all. However for charged synthetic filters, the efficiency values for large particles decreased substantially with velocity, while particles in the lower end of the measured size range were practically not affected at all.

Indoor particle model

- Outdoor air filtration has significant effects on the removal of particles with diameters less than 0.01 μm and larger than 1 μm, while recirculating air filtration mainly removes particles within a size range between 0.01 μm and 1 μm. Additionally, small particles (<0.01 μm) and large particles (>1 μm) apparently have a high possibility to deposit on indoor surfaces.
- Low class filters used for recirculating air filtration probably would prolong the time constant of indoor particles compared to the case without air filters and no recirculating air. It is better to avoid using a filter less than F7 class in recirculating air filtration.
- The case study shows that the integrated $C_{i,o}/C_o$ and $C_{i,s}/(S_i/V)$ are largest for MPPS-sized particles, while they are smallest for $PM_{0.01}$. Moreover, increasing the supply air flow rate and outdoor air percentage, the variation of $C_{i,o}/C_o$ and $C_{i,s}/(S_i/V)$ are also largest for MPPS-sized particles and smallest for

$PM_{0.01}$. If no specific particle size is in focus, it appears reasonable to evaluate the system performance of air filtration and ventilation to remove indoor particles on MPPS curves.
- The multi-case studies show that when the size of particle peak concentration is close to the MPPS of filters, the parameters $C_{i,o}/C_o$ and $C_{i,s}/(S_i/V)$ integrated over a diameter range including MPPS would be close to the two parameters values on MPPS.

Two-step air filtration

- Suitable two-step filtration is not necessarily more expensive than single-step filtration. Low class two-step filtration may even cost less than high class single-step filtration. For example, among the studied cases, M6+F7 filters cost less than a single F9 class filter does per volumetric clean air flow.
- Reasonably extending the main filter lifetime can reduce the total cost. This extension relies on the ambient particle concentration. It is more economical to apply two-step filtration in areas with high ambient particle concentration.

Ionizer assisted air filtration

- A suitable ionizer system can provide a high ion concentration and emit negligible amounts of ozone. Supply electricity voltage is critical to the ion generation.
- Under reasonable operation conditions, an F7 class filter assisted with an ionizer may reach the efficiency level of a single F8 or F9 class filter. A G4 class filter is not recommended for the ionizer assisted air filtration. M6 class filter is supposed to be a suitable filter assisted with an ionizer to replace a single F7 or F8 class filter.

10.3 Future work

According to the work carried out, valuable directions of future work are prospected in the following.

- Alternative methods for de-electrification of charged synthetic filter media should be investigated in more detail.
- An intervention study on efficient removal of traffic related UFPs should be carried out in the field.
- The long term performance of ionizer assisted air filtration should be further evaluated, when the short-term experiments are finished.
- The results of the particle fate model needs to be demonstrated by an experimental study.
- The influence of multi-step filtration on by-products generation should be investigated experimentally. By-products generation is hopefully greatly decreased by proper design and operation of multi-step filtration under proper air temperature and humidity in supply air.
- Measurements should be carried out in order to establish the pressure drop increase of intermediate class filters, as a function of service life and dust load under real operating conditions

References

1. Abt, E, Suh, H, Catalano, P, Koutrakis, P, 2000. Relative contribution of outdoor and indoor particles sources to indoor concentrations. Environ. Sci. Technol., vol. 34, no. 17, pp. 3579-3587.

2. Afshari, A, Matson, U, Ekberg, L E, 2005. Characterization of indoor sources of fine and ultrafine particles: a study conducted in a full-scale chamber. Indoor air, vol. 15, no. 2, Apr, pp. 141-150.

3. Agranovski, I E, Huang, R, Pyankov, O V, Altman, I S, Grinshpun, S A, 2006. Enhancement of the Performance of Low-Efficiency HVAC Filters Due to Continuous Unipolar Ion Emission. Aerosol Science and Technology, vol. 40, no. 11, pp. 963-968.

4. Araujo, J A, Nel, A E, 2009. Particulate matter and atherosclerosis: role of particle size, composition and oxidative stress. Particle and Fibre Toxicology, vol. 6, no. 24, pp. 1-19.

5. ASHRAE52.2, 2007. Method of Testing General Ventilation Air-Cleaning Devices for Removal Efficiency by Particle Size. Atlanta: American Society of Heating, Refrigerating and Air-Conditioning Engineers.

6. Baron, P A, Willeke, K, 2001. Aerosol Measurement - Principles, Techniques, and Applications. John Wiley & Sons.

7. Becker, S, Soukup, J, 2003. Coarse(PM(2.5-10)), fine(PM(2.5)), and ultrafine air pollution particles induce/increase immune costimulatory receptors on human blood-derived monocytes but not on alveolar macrophages. J Toxicol Environ Health A, vol. 66, no. 9, pp. 847-59.

8. Bekö, G, Clausen, G, Weschler, C J, 2008. Is the use of particle air filtration justified? Costs and benefits of filtration with regard to health effects, building cleaning and occupant productivity. Building and Environment, vol. 43, no. 10, pp. 1647-1657.

9. Bekö, G, Clausen, G, Weschler, C J, 2008. Sensory pollution from bag filters, carbon filters and combinations. Indoor air, vol. 18, no. 1, pp. 27-36.

10. Bekö, G, Halas, O, Clausen, G, Weschler, C J, 2006. Initial studies of oxidation processes on filter surfaces and their impact on perceived air quality. Indoor air, vol. 16, no. 1, Feb, pp. 56-64.

11. Bell, M L, Davis, D L, Fletcher, T, 2004. A retrospective assessment of mortality from the London smog episode of 1952: The role of influenza and pollution. Environmental Health Perspectives, vol. 112, no. 1, Jan, pp. 6-8.

12. BELOK, 2011. Procurement Group for Public and Commercial Buildings (In Sweden). www. belok.se.

13. BIPM/ISO, 1993. Guide to the Expression of Uncertainty in Measurement. (International Organization for Standardization) Geneva, Switzerland.

14. Boldo, E, Medina, S, LeTertre, A, Hurley, F, et al., 2006. Apheis: Health impact assessment of long-term exposure to PM2.5 in 23 European cities. European Journal of Epidemiology, vol. 21, no. 6, pp. 449-458.

15. Borja-Aburto, V H, Castillejos, M, Gold, D R, Bierzwinski, S, Loomis, D, 1998. Mortality and ambient fine particles in southwest Mexico City, 1993-1995. Environ Health Perspect., vol. 106, pp. 849-855.

16. Brauner, E V, Forchhammer, L, Moller, P, Simonsen, J, Glasius, M, Wahlin, P, Raaschou-Nielsen, O, Loft, S, 2007. Exposure to ultrafine particles from ambient air and oxidative stress-induced DNA damage. Environ Health Perspect, vol. 115, no. 8, Aug, pp. 1177-1182.

17. Breitner, S, Stolzel, M, Cyrys, J, Pitz, M, Wolke, G, Kreyling, W, Kuchenhoff, H, Heinrich, J, Wichmann, H E, Peters, A, 2009. Short-term mortality rates during a decade of improved air quality in Erfurt, Germany. Environ Health Perspect, vol. 117, no. 3, Mar, pp. 448-454.

18. Brouwer, D H, Gijsbers, J H, Lurvink, M W, 2004. Personal exposure to ultrafine particles in the workplace: exploring sampling techniques and strategies. Ann Occup Hyg, vol. 48, no. 5, Jul, pp. 439-453.

19. Brown, D M, Stone, V, Findlay, P, MacNee, W, Donaldson, K, 2000. Increased inflammation and intracellular calcium caused by ultrafine carbon black is independent of transition metals or other soluble components. Occup Environ Med, vol. 57, no. 10, Oct, pp. 685-691.

20. Burtscher, H, 2005. Physical characterization of particulate emissions from diesel engines: a review. Journal of Aerosol Science, vol. 36, no. 7, Jul, pp. 896-932.

21. Calderon-Garciduenas, L, Solt, A C, Henriquez-Roldan, C, Torres-Jardon, R, Nuse, B, Herritt, L, Villarreal-Calderon, R, Osnaya, N, Stone, I, Garcia, R, et al., 2008. Long-term Air Pollution Exposure Is Associated with Neuroinflammation, an Altered Innate Immune Response, Disruption of the Blood-Brain Barrier, Ultrafine Particulate Deposition, and Accumulation of Amyloid beta-42 and alpha-Synuclein in Children and Young Adults. Toxicologic Pathology, vol. 36, no. 2, Feb, pp. 289-310.

22. Carbone, F, Beretta, F, D'Anna, A, 2010. Factors Influencing Ultrafine Particulate Matter ($PM_{0.1}$) Formation under Pulverized Coal Combustion and Oxyfiring Conditions. Energy Fuels, vol. 24, Dec, pp. 6248-6256.

23. Carbone, F, Beretta, F, D'Anna, A, 2010. Multimodal ultrafine particles from pulverized coal combustion in a laboratory scale reactor. Combustion and Flame, vol. 157, no. 7, Jul, pp. 1290-1297.

24. Cheng, Y H, Chao, Y C, Wu, C H, Tsai, C J, Uang, S N, Shih, T S, 2008. Measurements of ultrafine particle concentrations and size distribution in an iron foundry. J Hazard Mater, vol. 158, no. 1, Oct 1, pp. 124-130.

25. Cheng, Y H, Huang, C H, Huang, H L, Tsai, C J, 2010. Concentrations of ultrafine particles at a highway toll collection booth and exposure implications for toll collectors. Science of the Total Environment, vol. 409, no. 2, Dec 15, pp. 364-369.

26. Cho, Y S, Lee, J T, Jung, C H, Chun, Y S, Kim, Y S, 2008. Relationship between particulate matter measured by optical particle counter and mortality in Seoul, Korea, during 2001. J Environ Health, vol. 71, no. 2, Sep, pp. 37-43.

27. Clausen, G, 2004. Ventilation filters and indoor air quality: a review of research from the International Centre for Indoor Environment and Energy. Indoor air, vol. 14 no. 7, pp. 202-207.

28. Clausen, G, Alm, O, Fanger, P O, 2002. The impact of air pollution from used ventilation filters on human comfort and health. 9th International Conference on Indoor Air Quality and Climate, Monterey, California,Proceedings of Indoor Air 2002 vol. 1, pp. 338-343.

29. Cullen, R T, Tran, C L, Buchanan, D, Davis, J M C, Searl, A, Jones, A D, Donaldson, K, 2000. Inhalation of poorly soluble particles. I. Differences in inflammatory response and clearance during exposure. Inhalation Toxicology, vol. 12, no. 12, Dec, pp. 1089-1111.

30. Davidson, C I, Phalen, R F, Solomon, P A, 2005. Airborne Particulate Matter and Human Health: A Review. Aerosol Science and Technology, vol. 39, no. 8, pp. 737-749.

31. Delfino, R J, Sioutas, C, Malik, S, 2005. Potential role of ultrafine particles in associations between airborne particle mass and cardiovascular health. Environ Health Perspect, vol. 113, no. 8, Aug, pp. 934-946.

32. Dingenen, R V, Raes, F, Putaud, J P, Baltensperger, U, Charron, A, Facchini, M C, et al., 2004. A European aerosol phenomenology-1: physical characteristics of particulate matter at kerbside, urban, rural and background sites in Europe. Atmospheric Environment, vol. 38, no. 16, pp. 2561-2577.

33. Donaldson, K, Brown, D, Clouter, A, Duffin, R, MacNee, W, Renwick, L, Tran, L, Stone, V, 2002. The pulmonary toxicology of ultrafine particles. Journal of Aerosol Medicine-Deposition Clearance and Effects in the Lung, vol. 15, no. 2, Sum, pp. 213-220.

34. Donaldson, K, Tran, C L, 2002. Inflammation caused by particles and fibers. Inhalation Toxicology, vol. 14, no. 1, Jan, pp. 5-27.

35. Douglas W. Dockery, C A P, Xiping Xu, John D. Spengler, James H. Ware, Martha E. Fay, Benjamin G. Ferris, and Frank E. Speizer, 1993. An Association between Air Pollution and Mortality in Six U.S. Cities. The New England Journal of Medicine, vol. 329, pp. 1739-1759.

36. EAL-R2, 1997. Expression of the Uncertainty of Measurement in Calibration. European cooperation for Accreditation of Laboratories.

37. Ekberg, L, Flyckt, A, 2006. Evaluation of air filters in connection with procurement: A pre-study, BELOK, Stockholm. (In Swedish). www.belok.se.

38. Ekberg, L E, Shi, B, 2009. Removal of ultrafine particles by ventilation air filters. Proceeding of 9th International Conference on Healthy Buildings, 2009, Syracuse, NY, USA,

39. Elder, A, Gelein, R, Silva, V, Feikert, T, Opanashuk, L, Carter, J, Potter, R, Maynard, A, Finkelstein, J, Oberdorster, G, 2006. Translocation of inhaled ultrafine manganese oxide particles to the central nervous system. Environmental Health Perspectives, vol. 114, no. 8, Aug, pp. 1172-1178.

40. Elder, A C P, Gelein, R, Finkelstein, J N, Cox, C, Oberdorster, G, 2000. Endotoxin priming affects the lung response to ultrafine particles and ozone in young and old rats. Inhalation Toxicology, vol. 12, no. s1, pp. 85-98.

41. EN779, 2002. Particulate air filters for general ventilation – Determination of the filtration performance. (CEN: European Committee for Standardization).

42. EN779, 2012. Particulate air filters for general ventilation – Determination of the filtration performance. (CEN: European Committee for Standardization).

43. EN1822-1, 1998. High efficiency particulate air filters (HEPA and ULPA): Classification, performance testing, marking. (CEN: European Committee for Standardization).

44. EN1822-1, 2009. High efficiency air filters (HEPA and ULPA):Classification, performance test, marking. (CEN: European Committee for Standardization).

45. EN13779, 2007. Ventilation for non-residential buildings - Performance requirements for ventilation and room-conditioning systems. (CEN: European Committee for Standardization).

46. Evans, D E, Heitbrink, W A, Slavin, T J, Peters, T M, 2008. Ultrafine and respirable particles in an automotive grey iron foundry. Ann Occup Hyg, vol. 52, no. 1, Jan, pp. 9-21.

47. Fisk, W J, Faulkner, D, Palonen, J, Seppanen, O, 2002. Performance and costs of particle air filtration technologies. Indoor air, vol. 12, pp. 223-234.

48. Fisk, W J, Faulkner, D, Sullivan, D, Mandell, M J, 2000. Particle concentration and sizes with normal and high efficiency air filtration in a sealed air-conditioned office building. Aerosol Science and Technology, vol. 32, pp. 527-544.

49. Flannigan, B, 1992. Indoor Microbiological Pollutants - Sources, Species, Characterization and Evaluation. Chemical, Microbiological, Health and Comfort Aspects of Indoor Air Quality - State of the Art in SBS, ed. Knöppel, H., Wolkoff, P., pp. 73-98. (Kluwer Academic Publishers.) Dordrecht.

50. Gaydos, T M, Stanier, C O, Pandis, S N, Pandis, S N, 2005. Modeling of in situ ultrafine atmospheric particle formation in the eastern United States. Journal of Geophysical Research-Atmospheres, vol. 110, no. D07S12.

51. Gehin, E, Ramalho, O, Kirchner, S, 2008. Size distribution and emission rate measurement of fine and ultrafine particle from indoor human activities. Atmospheric Environment, vol. 42, no. 35, Nov, pp. 8341-8352.

52. Gilmour, P S, Ziesenis, A, Morrison, E R, Vickers, M A, Drost, E M, Ford, I, Karg, E, Mossa, C, Schroeppel, A, Ferron, G A, et al., 2004. Pulmonary and systemic effects of short-term inhalation exposure to ultrafine carbon black particles. Toxicol Appl Pharmacol, vol. 195, no. 1, Feb 15, pp. 35-44.

53. Gravesen, S, Larsen, L, Gyntelberg, F, Skov, P, 1986. Demonstration of Microorganisms and Dust in Schools and Offices - an Observational Study of Nonindustrial Buildings. Allergy, vol. 41, no. 7, Sep, pp. 520-525.

54. Gravesen, S, Larsen, L, Skov, P, 1983. Aerobiology of schools and public institutions--part of a study. Ecology of Disease, vol. 2, no. 4, pp. 411-3.

55. Grinshpun, S A, Mainelis, G, Trunov, M, Adhikari, A, Reponen, T, Willeke, K, 2005. Evaluation of ionic air purifiers for reducing aerosol exposure in confined indoor spaces. Indoor air, vol. 15, no. 4, Aug, pp. 235-245.

56. Gustavsson, J, 2002. Software programme that calculates the life cycle cost of air filters. Filtration and separation, vol. 39, pp. 22-26.

57. Gustavsson, J, Ginestet, A, Tronville, P, Hyttinen, M, 2009. Air filtration in HVAC systems. REHVA guidebook No.11.

58. Hanley, J T, Ensor, D S, Smith, D D, Sparks, L E, 1994. Fractional Aerosol Filtration Efficiency of in-Duct Ventilation Air Cleaners. Indoor Air-International Journal of Indoor Air Quality and Climate, vol. 4, no. 3, pp. 169-178.

59. Harris, S J, Maricq, M M, 2001. Signature size distributions for diesel and gasoline engine exhaust particulate matter. Journal of Aerosol Science, vol. 32, no. 6, pp. 749-764.

60. Harris, S J, Maricq, M M, 2002. The role of fragmentation in defining the signature size distribution of diesel soot. Journal of Aerosol Science, vol. 33, no. 6, pp. 935-942.

61. Harrison, R M, Giorio, C, Beddows, D C, Dall'Osto, M, 2010. Size distribution of airborne particles controls outcome of epidemiological studies. Science of the Total Environment, vol. 409, no. 2, Dec 15, pp. 289-293.

62. Harrison, R M, Yin, J, 2000. Particulate matter in the atmosphere: which particle properties are important for its effects on health? Sci Total Environ, vol. 249, no. 1-3, Apr 17, pp. 85-101.

63. He, C, Morawska, L, Taplin, L, 2007. Particle emission characteristics of office printers. Environ Sci Technol, vol. 41, no. 17, Sep 1, pp. 6039-6045.

64. Hertel, S, Viehmann, A, Moebus, S, Mann, K, Brocker-Preuss, M, Mohlenkamp, S, Nonnemacher, M, Erbel, R, Jakobs, H, Memmesheimer, M, et al., 2010. Influence of short-term exposure to ultrafine and fine particles on systemic inflammation. European Journal of Epidemiology, vol. 25, no. 8, Aug, pp. 581-592.

65. Hinds, W C, 1998. Aerosol Technology: Properties, Behavior, and Measurement of Airborne Particles. pp. 183-205. (Jonh Wiley & Sons.) Los Angeles.

66. Hunt, A, Abraham, J L, Judson, B, Berry, C L, 2003. Toxicologic and epidemiologic clues from the characterization of the 1952 London smog fine particulate matter in archival autopsy lung tissues. Environmental Health Perspectives, vol. 111, no. 9, Jul, pp. 1209-1214.

67. Hussein, T, Hameri, K, Aalto, P, Asmi, A, Kakko, L, Kulmala, M, 2004. Particle size characterization and the indoor-to-outdoor relationship of atmospheric aerosols in Helsinki. Scandinavian Journal of Work Environment & Health, vol. 30, pp. 54-62.

68. Hussein, T, Hameri, K, Heikkinen, M S A, Kulmala, M, 2005. Indoor and outdoor particle size characterization at a family house in Espoo-Finland. Atmospheric Environment, vol. 39, no. 20, pp. 3697-3709.

69. Hyttinen, M, Pasanen, N, Kalllokoski, P, 2006. Removal of ozone on clean, dusty and sooty supply air filters. Atmospheric Environment, vol. 40, no. 2, Jan, pp. 315-325.

70. Hyttinen, M, Pasanen, P, Bjorkroth, M, Kalliokoski, P, 2007. Odors and volatile organic compounds released from ventilation filters. Atmospheric Environment, vol. 41, no. 19, Jun, pp. 4029-4039.

71. Hyttinen, M, Pasanen, P, Salo, J, Bjorkroth, M, Vartiainen, M, Kalliokoski, P, 2003. Reactions of ozone on ventilation filters. Indoor and Built Environment, vol. 12, no. 3, pp. 151-158.

72. Ibald-Mulli, A, Wichmann, H E, Kreyling, W, Peters, A, 2002. Epidemiological evidence on health effects of ultrafine particles. Journal of Aerosol Medicine-Deposition Clearance and Effects in the Lung, vol. 15, no. 2, pp. 189-201.

73. Jaenicke, R, 1993. Tropospheric aerosols. Aerosol- Cloud- Climate Interactions, pp. 1-31. Ed. P Hobbs, New York Academic Press.

74. Jamriska, M, Morawska, L, Clark, B A, 2000. Effect of ventilation and filtration on submicrometer particles in an indoor environment. Indoor air, vol. 10, no. 1, Mar, pp. 19-26.

75. Janssen, N A H, Schwartz, J, Zanobetti, A, Suh, H H, 2002. Air conditioning and source-specific particles as modifiers of the effect of PM10 on hospital admissions for heart and lung disease. Environ Health Perspect, vol. 110, no. 1, pp. 43-49.

76. Jarvis, D, Chinn, S, Luczynska, C, Burney, P, 1996. Association of respiratory symptoms and lung function in young adults with use of domestic gas appliances. The Lancet, vol. 347, no. 8999, pp. 426-431.

77. Johnston, C J, Finkelstein, J N, Mercer, P, Corson, N, Gelein, R, Oberdorster, G, 2000. Pulmonary effects induced by ultrafine PTFE particles. Toxicology and Applied Pharmacology, vol. 168, no. 3, Nov 1, pp. 208-215.

78. Kim, J C, Qtani, Y, Noto, D, Namiki, N, Kimura, K, 2005. Initial collection performance of Resin Wool Filters and Estimation of Charge Density. Aerosol Science and Technology vol. 39, no. 6, pp. 501-508

79. Kittelson, D B, 1998. Engines and nanoparticles: A review. Journal of Aerosol Science, vol. 29, no. 5-6, pp. 575-588.

80. Ko, Y-C, Cheng, L S-C, Lee, C-H, Huang, J-J, Huang, M-S, Kao, E-L, Wang, H-Z, Lin, H-J, 2000. Chinese Food Cooking and Lung Cancer in Women Nonsmokers. American Journal of Epidemiology, vol. 151, no. 2, January 15, 2000, pp. 140-147.

81. Koponen, I K, Asmi, A, Keronen, P, Puhto, K, Kulmala, M, 2001. Indoor air measurement campaign in Helsinki, Finland 1999 - the effect of outdoor air pollution on indoor air. Atmospheric Environment, vol. 35, no. 8, pp. 1465-1477.

82. Korpi, A, Kasanen, J P, Alarie, Y, Kosma, V M, Pasanen, A L, 1999. Sensory irritating potency of some microbial volatile organic compounds (MVOCs) and a mixture of five MVOCs. Archives of Environmental Health, vol. 54, no. 5, pp. 347-352.

83. Kreyling, W G, Semmler, M, Erbe, F, Mayer, P, Takenaka, S, Schulz, H, Oberdorster, G, Ziesenis, A, 2002. Translocation of ultrafine insoluble iridium particles from lung epithelium to extrapulmonary organs is size dependent but very low. J Toxicol Environ Health A, vol. 65, no. 20, Oct 25, pp. 1513-1530.

84. Langer, S, Moldanová, J, Arrhenius, K, Ljungström, E, Ekberg, L, 2008. Ultrafine particles produced by ozone/limonene reactions in indoor air under low/closed ventilation conditions. Atmospheric Environment, vol. 42, no. 18, pp. 4149-4159.

85. Lee, B U, Yermakov, M, Grinshpun, S A, 2004. Removal of fine and ultrafine particles from indoor air environments by the unipolar ion emission. Atmospheric Environment, vol. 38, no. 29, Sep, pp. 4815-4823.

86. Lee, C-W, Hsu, D-J, 2007. Measurements of fine and ultrafine particles formation in photocopy centers in Taiwan. Atmospheric Environment, vol. 41, no. 31, pp. 6598-6609.

87. Lee, K W, Liu, B Y H, 1980. On the minimum efficiency and the most penetrating particle size for fibrous filters. Journal of the air pollution Control association. Journal of the air pollution Control association, vol. 30, no. 4, pp. 377-381.

88. Li, N, Sioutas, C, Cho, A, Schmitz, D, Misra, C, Sempf, J, Wang, M Y, Oberley, T, Froines, J, Nel, A, 2003. Ultrafine particulate pollutants induce oxidative stress and mitochondrial damage. Environmental Health Perspectives, vol. 111, no. 4, Apr, pp. 455-460.

89. Li, W, Hopke, P K, 1993. Initial Size Distributions and Hygroscopicity of Indoor Combustion Aerosol-Particles. Aerosol Science and Technology, vol. 19, no. 3, Oct, pp. 305-316.

90. Liu, D, Nazaroff, W W, 2001. Modeling pollutant penetration across building envelopes. Atmos. Environ., vol. 35, no. 26, pp. 4451-4462.

91. Long, C M, Suh, H H, Kobzik, L, Catalano, P J, Ning, Y Y, Koutrakis, P, 2001. A pilot investigation of the relative toxicity of indoor and outdoor fine particles: in vitro effects of endotoxin and other particulate properties. Environ Health Perspect, vol. 109, no. 10, pp. 1019-1026.

92. Long, C M, Sun, H H, Catalano, P, Koutrakis, P, 2001. Using Time- and Size-Resolved Particulate Data To Quantify Indoor Penetration and Deposition Behavior. Environ. Sci. Technol., vol. 35, no. 10, pp. 2089-2099.

93. Marsik, T, Johnson, R, 2008. HVAC air-quality model and its ust to test a PM2.5 control strategy. Building and Environment, vol. 43, no. 11, pp. 1850-1857.

94. Matson, U, 2005. Indoor and outdoor concentrations of ultrafine particles in some Scandinavian rural and urban areas. Science of the Total Environment, vol. 343, no. 1-3, May 1, pp. 169-176.

95. Matson, U, Ekberg, L E, 2005. Prediction of ultrafine particle concentration in various indoor environments. Indoor Air 2005: Proceedings of the 10th International Conference on Indoor Air Quality and Climate, Vols 1-5, pp. 1581-1885.

96. McAuley, T R, Fisher, R, Zhou, X, Jaques, P A, Ferro, A R, 2010. Relationships of outdoor and indoor ultrafine particles at residences downwind of a major international border crossing in Buffalo, NY. Indoor air, vol. 20, no. 4, Aug, pp. 298-308.

97. McMillen, R C, Winickoff, J P, Klein, J D, Weitzman, M, 2003. US adult attitudes and practices regarding smoking restrictions and child exposure to environmental tobacco smoke: changes in the social climate from 2000-2001. Pediatrics, vol. 112, no. 1 Pt 1, Jul, pp. e55-60.

98. Melia, R J W, du V Florey, C, Chinn, S, 1979. The Relation between Respiratory Illness in Primary Schoolchildren and the Use of Gas for Cooking. International Journal of Epidemiology, vol. 8, no. 4, pp. 333-338.

99. Montgomery, J F, Green, S I, Rogak, S N, Bartlett, K, 2012. Predicting the energy use and operation cost of HVAC air filters. Energy and Buildings, vol. 47, April, pp. 643–650.

100. Morawska, L, He, C, Johnson, G, Guo, H, Uhde, E, Ayoko, G, 2009. Ultrafine particles in indoor air of a school: possible role of secondary organic aerosols. Environ Sci Technol, vol. 43, no. 24, Dec 15, pp. 9103-9109.

101. Morawska, L, He, C, Johnson, G, Jayaratne, R, Salthammer, T, Wang, H, Uhde, E, Bostrom, T, Modini, R, Ayoko, G, et al., 2009. An investigation into the characteristics and formation mechanisms of particles originating from the operation of laser printers. Environ Sci Technol, vol. 43, no. 4, Feb 15, pp. 1015-1022.

102. Morawska, L, Thomas, S, Bofinger, N, Wainwright, D, Neale, D, 1998. Comprehensive characterization of aerosols in a subtropical urban atmosphere: Particle size distribution and correlation with gaseous

pollutants. Atmospheric Environment, vol. 32, no. 14-15, Aug, pp. 2467-2478.

103. Nel, A, 2005. Atmosphere. Air pollution-related illness: effects of particles. Science, vol. 308, no. 5723, pp. 804-806.

104. Nevalainen, A, 1993. Microbial contamination of buildings. Indoor Air 1993: Proceedings of the 6th International Conference on Indoor Air Quality and Climate, vol. 4, pp. 3-13.

105. Nicolas, P, Jocelyne, P, Michel, F, Sophie, G-C, Pascal, R, Émilien, P, 2008. Oxidative stress and immunologic responses following a dietary exposure to PAHs in Mya arenaria. Chem Cent J., vol. 2, no. 23, pp. 1-11.

106. Ning, Z, Cheung, C S, Fu, J, Liu, M A, Schnell, M A, 2006. Experimental study of environmental tobacco smoke particles under actual indoor environment. Sci Total Environ, vol. 367, no. 2-3, Aug 31, pp. 822-830.

107. Noh, K C, Hwang, J, 2010. The Effect of ventilation Rate and Filter Performance on Indoor Particle Concentration and Fan Power Consumption in a Residential Housing Unit. Indoor Built Environ, vol. 19, no. 4, pp. 444-452.

108. Oberdörster, G, 2000. Pulmonary effects of inhaled ultrafine particles. International Archives of Occupational and Environmental Health, vol. 74, no. 1, pp. 1-8.

109. Oberdörster, G, Sharp, Z, Atudorei, V, Elder, A, Gelein, R, Kreyling, W, Cox, C, 2004. Translocation of Inhaled Ultrafine Particles to the Brain. Inhalation Toxicology, vol. 16, no. 6-7, pp. 437-445.

110. Oberdörster, G, Sharp, Z, Atudorei, V, Elder, A, Gelein, R, Lunts, A, Kreyling, W, Cox, C, 2002. Extrapulmonary translocation of ultrafine carbon particles following whole-body inhalation exposure of rats. J Toxicol Environ Health A, vol. 65, no. 20, Oct 25, pp. 1531-1543.

111. Oberdörster, G, Utell, M J, 2002. Ultrafine particles in the urban air: to the respiratory tract--and beyond? Environ Health Perspect, vol. 110, no. 8, Aug, pp. A440-A441.

112. OEHHA, 1997. Health effects of exposure to environmental tobacco smoke: Final report and Appendices. The California Environmental Protection Agency, Office of Environmental Health Hazard Assessment.

113. Pagels, J, Wierbicka, A, Nilsson, E, Isaxon, C, Dahl, A, Gudmundsson, A, Swietlicki, E, Bohgard, M, 2009. Chemical composition and mass emission factors of candle smoke particles. Journal of Aerosol Science, vol. 40, no. 3, Mar, pp. 193-208.

114. Park, J H, Yoon, K Y, Hwang, J, 2011. Removal of submicron particles using a carbon fiber ionizer-assisted medium air filter in a heating,

ventilation, and air-conditioning (HVAC) system Building and Environment, vol. 46, no. 8, Aug, pp. 1699-1708.

115. Park, J H, Yoon, K Y, Kim, Y S, Byeon, J H, Hwang, J, 2009. Removal of submicron aerosol particles and bioaerosols using carbon fiber ionizer assisted fibrous medium filter media. Journal of Mechanical Science and Technology, vol. 23, no. 7, Jul, pp. 1846-1851.

116. Pasanen, P O, Teijonsalo, J, Seppanen, O, Ruuskanen, J, Kalliokoski, P, 1994. Increase in Perceived Odor Emissions with Loading of Ventilation Filters. Indoor Air-International Journal of Indoor Air Quality and Climate, vol. 4, no. 2, pp. 106-113.

117. Pejtersen, J, 1996. Sensory pollution and microbial contamination of ventilation filters. Indoor Air, vol. 6, no. 4, Dec, pp. 239-248.

118. Pejtersen, J, Clausen, G, Fanger, P O, 1992. Olf og Energi, Fase 2: Olf-værdier før og efter rensning af ventilationsanlæg. Danmarks Tekniske Højskole, Laboratoriet for Varme- og Klimateknik, København, pp. 1-43.

119. Peters, A, Ruckerl, R, Cyrys, J, 2011. Lessons From Air Pollution Epidemiology for Studies of Engineered Nanomaterials. Journal of Occupational and Environmental Medicine, vol. 53, no. 6, Jun, pp. S8-S13.

120. Peters, A, Veronesi, B, Calderón-Garcidueñas, L, Gehr, P, Chen, L C, 2006. Translocation and potential neurological effects of fine and ultrafine particles a critical update. Particle and Fibre Toxicology, vol. 3, pp. 1-13.

121. Peters, A, Wichmann, H, Tuch, T, Heinrich, J, Heyder, J, 1997. Respiratory effects are associated with the number of ultrafine particles. Am. J. Respir. Crit. Care Med., vol. 155, no.4, pp. 1376-1383.

122. Pietropaoli, A P, Frampton, M W, Hyde, R W, Morrow, P E, Oberdorster, G, Cox, C, Speers, D M, Frasier, L M, Chalupa, D C, Huang, L S, et al., 2004. Pulmonary function, diffusing capacity, and inflammation in healthy and asthmatic subjects exposed to ultrafine particles. Inhalation Toxicology, vol. 16, pp. 59-72.

123. Pope, C A, Burnett, R T, Thun, M J, Calle, E E, Krewski, D, Ito, K, Thurston, G D, 2002. Lung cancer, cardiopulmonary mortality, and long-term exposure to fine particulate air pollution. Jama-Journal of the American Medical Association, vol. 287, no. 9, pp. 1132-1141.

124. Raynor, P C, Chae, S J, 2004. The long-term performance of electrically charged filters in a ventilation system. Journal of Occupational and Environmental Hygiene, vol. 1, no. 7, Jul, pp. 463-471.

125. Raynor, P C, Kim, B G, Ramachandran, G, Strommen, M R, Horns, J H, Streifel, A J, 2008. Collection of biological and non-biological particles by

new and used filters made from glass and electrostatically charged synthetic fibers. Indoor air, vol. 18, no. 1, Feb, pp. 51-62.

126. Reich, B J, Fuentes, M, Burke, J, 2008. Analysis of the effects of ultrafine particulate matter while accounting for human exposure. Environmetrics, vol. 20, no. 2, Apr 24, pp. 131-146.

127. Reponen, T, Grinshpun, S A, Trakumas, S, Martuzevicius, D, Wang, Z M, LeMasters, G, Lockey, J E, Biswas, P, 2003. Concentration gradient patterns of aerosol particles near interstate highways in the Greater Cincinnati airshed. J Environ Monit, vol. 5, no. 4, Aug, pp. 557-62.

128. Riley, W J, Mckone, T E, Lai, A K, Nazaroff, W W, 2002. Indoor Particulate Matter of Outdoor Origin: Importance of Size-Dependent Removal Mechanisms. Environ. Sci. Technol., vol. 36, no. 2, pp. 200-207.

129. Romay, F J, Liu, B Y H, Chae, S, 1998. Experimental study of electrostatic capture mechanisms in commercial electret filters Aerosol Science and Technology vol. 28, no. 3, pp. 224-234

130. Ruckerl, R, Phipps, R P, Schneider, A, Frampton, M, Cyrys, J, Oberdorster, G, Wichmann, H E, Peters, A, 2007. Ultrafine particles and platelet activation in patients with coronary heart disease--results from a prospective panel study. Part Fibre Toxicol, vol. 4, pp. 1-14.

131. Ruckerl, R, Schneider, A, Breitner, S, Cyrys, J, Peters, A, 2011. Health effects of particulate air pollution: A review of epidemiological evidence. Inhalation Toxicology, vol. 23, no. 10, Aug, pp. 555-592.

132. Sarwar, G, Corsi, R, 2007. The effects of ozone/limonene reactions on indoor secondary organic aerosols. Atmospheric Environment, vol. 41, no. 5, Feb, pp. 959-973.

133. Sasco, A J, Secretan, M B, Straif, K, 2004. Tobacco smoking and cancer: a brief review of recent epidemiological evidence. Lung Cancer, vol. 45, Supplement 2, no. 0, pp. S3-S9.

134. Schripp, T, Wensing, M, Uhde, E, Salthammer, T, He, C, Morawska, L, 2008. Evaluation of ultrafine particle emissions from laser printers using emission test chambers. Environmental Science & Technology, vol. 42, no. 12, Jun 15, pp. 4338-4343.

135. Schuster, M A, Franke, T, Pham, C B, 2002. Smoking Patterns of Household Members and Visitors in Homes With Children in the United States. Arch Pediatr Adolesc Med, vol. 156, no. 11, November 1, 2002, pp. 1094-1100.

136. Schwartz, J, Dockery, D W, Neas, L M, 1996. Is daily mortality associated specifically with fine particles? Journal of the Air & Waste Management Association (1995), vol. 46, no. 10, pp. 927-39.

137. Seaton, A, Soutar, A, Crawford, V, Elton, R, McNerlan, S, Cherrie, J, Watt, M, Agius, R, Stout, R, 1999. Particulate air pollution and the blood. Thorax, vol. 54, no. 11, Nov, pp. 1027-1032.

138. Shiue, A, Hu, S C, 2011. Contaminant particles removal by negative air ionic cleaner in industrial minienvironment for IC manufacturing processes. Building and Environment, vol. 46, no. 8, Aug, pp. 1537-1544.

139. Sioutas, C, Delfino, R J, Singh, M, 2005. Exposure assessment for atmospheric ultrafine particles (UFPs) and implications in epidemiologic research. Environ Health Perspectives, vol. 113, no. 8, pp. 947-955.

140. Sippola, M R, Nazaroff, W W, 2003. Modeling particle loss in ventilation ducts. Atmos Environ, vol. 37, pp. 5597-5609.

141. Slama, R, Darrow, L, Parker, J, Woodruff, T J, Strickland, M, Nieuwenhuijsen, M, Glinianaia, S, Hoggatt, K J, Kannan, S, Hurley, F, et al., 2008. Meeting report: Atmospheric pollution and human reproduction. Environmental Health Perspectives, vol. 116, no. 6, Jun, pp. 791-798.

142. Stolzel, M, Breitner, S, Cyrys, J, Pitz, M, Wolke, G, Kreyling, W, Heinrich, J, Wichmann, H E, Peters, A, 2007. Daily mortality and particulate matter in different size classes in Erfurt, Germany. J Expo Sci Environ Epidemiol, vol. 17, no. 5, Aug, pp. 458-67.

143. Tamas, G, Weschler, C J, Toftum, J, Fanger, P O, 2006. Influence of ozone-limonene reactions on perceived air quality. Indoor air, vol. 16, no. 3, Jun, pp. 168-178.

144. Thornburg, J, Ensor, D S, Rodes, C E, Lawless, P A, Sparks, L E, Mosley, R B, 2001. Penetration of Particles into Buildings and Associated Physical Factors. Part I: Model Development and Computer Simulations. Aerosol Science and Technology, vol. 34, no. 3, pp. 284-296.

145. Urciuolo, M, Barone, A, D'Alessio, A, Chirone, R, 2008. Fine and Ultrafine Particles Generated During Fluidized Bed Combustion of Different Solid Fuels. Environmental Engineering Science, vol. 25, no. 10, Dec, pp. 1399-1405.

146. USEPA, 2004. Air quality criteria for particulate matter (Final report, Oct 2004). U.S. Environmental Protection Agency. Washington, DC.

147. Wainman, T, Zhang, J F, Weschler, C J, Lioy, P J, 2000. Ozone and limonene in indoor air: A source of submicron particle exposure. Environ Health Perspect, vol. 108, no. 12, pp. 1139-1145.

148. Wake, D, Mark, D, Northage, C, 2002. Ultrafine Aerosols in the Workplace. Annals of Occupational Hygiene, vol. 46, no. suppl 1, January 1, 2002, pp. 235-238.

149. Wallace, L, 2006. Indoor sources of ultrafine and accumulation mode particles: Size distributions, size-resolved concentrations, and source strengths. Aerosol Science and Technology, vol. 40, no. 5, May, pp. 348-360.

150. Wallace, L A, Emmerich, S J, Howard-Reed, C, 2004. Source Strengths of Ultrafine and Fine Particles Due to Cooking with a Gas Stove. Environ. Sci. Technol., vol. 38, no. 8, pp. 2304-2311.

151. Wallace, L A, Mitchell, H, O'Connor, G T, Neas, L, Lippmann, M, Kattan, M, Koenig, J, Stout, J W, Vaughn, B J, Wallace, D, et al., 2003. Particle concentrations in inner-city homes of children with asthma: the effect of smoking, cooking, and outdoor pollution. Environ Health Perspect, vol. 111, no. 9, Jul, pp. 1265-1272.

152. Wang, Y G, Hopke, P K, Chalupa, D C, Utell, M J, 2010. Long-Term Characterization of Indoor and Outdoor Ultrafine Particles at a Commercial Building. Environmental Science & Technology, vol. 44, no. 15, Aug 1, pp. 5775-5780.

153. Ward, M, Siegel, J, 2005. Modeling filter bypass: Impact on filter efficiency. ASHRAE Transactions, pp. 1091-1100.

154. Warnatz, J, Maas, U, Dibble, R W, 1999. Combustion: Physical and Chemical Fundamentals, Modeling and Simulation, Experiments, Pollutant Formation. (Springer.) Berlin.

155. Wasson, S J, Guo, Z, McBrian, J A, Beach, L O, 2002. Lead in candle emissions. Science of the Total Environment, vol. 296, no. 1-3, pp. 159-174.

156. WECCDoc19-1990, 1990. Guideline for the Expression of the Uncertainty of Measurement in Calibration. (Western European Calibration Conference.).

157. Wei, Y, Han, I K, Shao, M, Hu, M, Zhang, O J, Tang, X, 2009. PM2.5 constituents and oxidative DNA damage in humans. Environ Sci Technol, vol. 43, no. 13, Jul 1, pp. 4757-4762.

158. Venkatachari, P, Hopke, P K, Grover, B D, Eatough, D J, 2005. Measurement of particle-bound reactive oxygen species in Rubidoux aerosols. Journal of Atmospheric Chemistry, vol. 50, no. 1, Jan, pp. 49-58.

159. Wensing, M, Schripp, T, Uhde, E, Salthammer, T, 2008. Ultra-fine particles release from hardcopy devices: Sources, real-room measurements and efficiency of filter accessories. Science of the Total Environment, vol. 407, no. 1, pp. 418-427.

160. Wichmann, H E, Spix, C, Tuch, T, Wolke, G, Peters, A, Heinrich, J, Kreyling, W G, Heyder, J, 2000. Daily mortality and fine and ultrafine particles in Erfurt, Germany part I: role of particle number and particle

mass. Research report (Health Effects Institute), no. 98, pp. 5-86; discussion 87-94.

161. Wilson, M R, Lightbody, J H, Donaldson, K, Sales, J, Stone, V, 2002. Interactions between ultrafine particles and transition metals in vivo and in vitro. Toxicology and Applied Pharmacology, vol. 184, no. 3, Nov 1, pp. 172-179.

162. Wilson, W E, Mage, D T, Grant, L D, 2000. Estimating separately personal exposure to ambient and nonambient particulate matter for epidemiology and risk assessment: why and how. J Air waste Manag Assoc, vol. 50, no. 7, Jul, pp. 1167-1183.

163. Wolkoff, P, Clausen, P A, Larsen, K, Hammer, M, Larsen, S T, Nielsen, G D, 2008. Acute airway effects of ozone-initiated d-limonene chemistry: Importance of gaseous products. Toxicology Letters, vol. 181, no. 3, Oct 1, pp. 171-176.

164. Zhao, B, Wu, J, 2009. Modeling particle fate in ventilation system- Part II: Case study. Building and Environment, vol. 44, no. 3, pp. 612-620.

165. Zhu, Y, Hinds, W C, Kim, S, Shen, S, Sioutas, C, 2002. Study of ultrafine particles near a major highway with heavy-duty diesel traffic. Atmospheric Environment, vol. 36, no. 27, pp. 4323-4335.

166. Zhu, Y F, Hinds, W C, Krudysz, M, Kuhn, T, Froines, J, Sioutas, C, 2005. Penetration of freeway ultrafine particles into indoor environments. Aerosol Science, vol. 36, pp. 303-322.

167. Zimmer, A T, Maynard, A D, 2002. Investigation of the aerosols produced by a high-speed, hand-held grinder using various substrates. Ann Occup Hyg, vol. 46, no. 8, Nov, pp. 663-672.

Appendix A

Measurement uncertainty for filter filtration efficiency measurement

The uncertainty of the measured filtration efficiency, *EF*, is analyzed in the following uncertainty budget. The EF is calculated according to eq. A.1.

$$EF = 1 - \frac{C_{down,2}}{\frac{(C_{up,1} + C_{up,3})}{2}} = 1 - \frac{C_{down}}{\overline{C_{up}}} \qquad \textit{(eq. A.1)}$$

C_{down} and C_{up} are downstream and upstream particle concentration in the testing rig. They were taken in the time serial 1, 2 and 3. $\overline{C_{up}}$ is the average of $C_{up,1}$ and $C_{up,3}$. The particle concentration was measured by a SMPS 3936, TSI. The measurable range of aerosol concentration is from 1 to 10^8 particles/ cm^3.In this study, the SMPS measured the particle from 14 nm to 673 nm in 32 channels/ decade. The measured uncertainty is calculated using the differentiating *eq. A.2*.

$$\frac{\Delta EF}{EF} = \frac{\Delta C_{down}}{C_{down}} - \frac{\Delta\overline{C_{up}}}{\overline{C_{up}}} = \frac{\Delta C_{down}}{C_{down}} - \frac{\Delta C_{up}}{\sqrt{2}C_{up}} \qquad \textit{(eq. A.2)}$$

The above equation could be written as.

$$\frac{\Delta EF}{EF} = P_1 * \frac{\Delta C_{down}}{C_{down}} + P_2 * \frac{\Delta C_{up}}{C_{up}} \qquad \textit{(eq. A.3)}$$

Here,

$$P_1 = 1 \text{ and } P_2 = -\frac{1}{\sqrt{2}}$$

The uncertainty of *EF* is contributed by the uncertainty of particle concentration measures due to calibration, reading, operating point, operating conditions and conditions of installation. Depending on the type of uncertainty of *EF*, the above equation would be in the following appearances. According to the model of BIPM/ISO[13], the uncertainty from one source could be grouped as random/estimated uncertainties (type A) and systematic/expected uncertainty (type B). Therefore, the eq. A.3 could be developed as follows.

Type A:

$$\frac{s_{EF}}{EF} = \sqrt{P_1{}^2 * \frac{\left(s_{cal}{}^2 + s_{read}{}^2 + s_{opt}{}^2 + s_{opc}{}^2 + s_{inst}{}^2\right)_{down}}{C_{down}{}^2} + P_2{}^2 * \frac{(s_{cal}{}^2 + s_{read}{}^2 + s_{opt}{}^2 + s_{opc}{}^2 + s_{inst}{}^2)_{up}}{C_{up}{}^2}}$$

(eq. A.4)

Type B:

$$\frac{w_{EF}}{EF} = \sqrt{P_1{}^2 * \frac{(w_{cal}{}^2 + w_{read}{}^2 + w_{opt}{}^2 + w_{opc}{}^2 + w_{inst}{}^2)_{down}}{C_{down}{}^2} + P_2{}^2 * \frac{(w_{cal}{}^2 + w_{read}{}^2 + w_{opt}{}^2 + w_{opc}{}^2 + w_{inst}{}^2)_{up}}{C_{up}{}^2}}$$

(eq. A.5)

Then, the combined uncertainty is presented as,

$$\frac{u_{EF}}{EF} = \sqrt{\left(\frac{s_{EF}}{EF}\right)^2 + \left(\frac{w_{EF}}{EF}\right)^2} \qquad \textit{(eq. A.6)}$$

$$\frac{U_{EF}}{EF} = k * \frac{u_{EF}}{EF} \qquad \textit{(eq. A.7)}$$

where *k* is a numerical factor. To achieve a confidence level equivalent to 95% for this normal distributed random variable, *k* is assigned as 2.0 according to WECC[156] and EAL[36].

Here, because P_2^2 is less than P_1^2 and C_{down} is smaller than C_{up}, C_{down} contributed more uncertainty than C_{up} does. Since C_{down} is closely related with the filter class in the test, we take the case of a F9 class filter test of at low face air velocity of 0.08m/s as an example. This case is considered has the largest uncertainty in the experiments. Here, C_{down}=94582 pc/cc and C_{up}= 230000pc/cc.

Calibration

Type A: The calibration of the CPC in the SMPS-system was conducted by the manufacturer, TSI, through the calibration of sheath flow, orifice pressure drop of bypass flow, pressure drop of impactors. The report show extremely small fitting errors (<0.3%) in ten repeated samples, so this uncertainty is neglected in the total uncertainty calculations. This uncertainty estimation is same for C_{down} and C_{up}.

Type B: The calibration is made under the same installation and environment condition as during the measurements. Furthermore, the same instrument was used for both the upstream and downstream measurements. So, the type B uncertainty is neglected in this analysis.

Particle concentration reading

Type A: The uncertainty for each reading is $\frac{\sqrt{N}}{N}$. Here, *N* is the total particle number concentration. During the test, we continuously took 5 samples of C_{down} and $\overline{C_{up}}$ respectively.

$$\frac{s_{C,up}}{C_{up}} = \frac{\sqrt{94582}}{94582} = 0.21\%$$

$$\frac{s_{\overline{C,up}}}{\overline{C_{up}}} = \frac{\frac{\sqrt{230000}}{\sqrt{5}}}{230000} = 0.09\%$$

$$\frac{s_{C,down}}{C_{down}} = \frac{\sqrt{94582}}{94582} = 0.33\%$$

$$\frac{s_{\overline{C,down}}}{\overline{C_{down}}} = \frac{\frac{\sqrt{94582}}{\sqrt{5}}}{94582} = 0.15\%$$

Type B: The particle counter solution is 0.1particle /cm^3, therefore,

$$\frac{w_{Cu}}{C_{up}} < \frac{\frac{0.1}{\sqrt{5}}}{230000} = 0.000019\% \approx 0$$

$$\frac{w_{C_d}}{C_{down}} < \frac{\frac{0.1}{\sqrt{5}}}{94582} = 0.000047\% \approx 0$$

Operating Point

The measurement range of SMPS 3936 is from 1 to 10^8 particles/cm^3. Because the maximum particle concentration during the experiments was 230 000pc/cc, which was much less than 10^8 particles/cm^3, it is reasonable to assume that the particle concentration measured by the SMPS follows a linear relationship with the real particle concentration. Thus, the operation point uncertainty could be neglected.

Variations in the operating conditions

Random variations of air flow rate and particle emission rate could cause random variation of the particle concentration. Therefore, to the standard deviation of an upstream sample and down sample, the type A uncertainty is as follows,

$$\frac{s_{C,up}}{C_{up}} = \frac{3285}{230000} = 1.43\%$$

$$\frac{s_{\overline{C,up}}}{\overline{C_{up}}} = \frac{\frac{3285}{\sqrt{5}}}{230000} = 0.64\%$$

$$\frac{s_{C,down}}{C_{down}} = \frac{1303}{94582} = 1.38\%$$

$$\frac{s_{\overline{C,down}}}{\overline{C_{down}}} = \frac{\frac{1303}{\sqrt{5}}}{94582} = 0.62\%$$

Type B: no contributions

Conditions of installation

Type A: No contributions

Type B: All possible particle loss on the sample tube added up to the total type B component. Because in the experiments, the down- and up-stream sample tube were the dedicated Pitot static tubes provided by TSI, the uncertainty due to the particle loss on the sample tube could be neglected.

Budget of uncertainty for the air filtration efficiency measurement

Uncertainty budget of the air filtration efficiency measurements is given in Table A1. The combined uncertainty and total uncertainty were calculated according to eq. A.4-A.7. As the above analysis, the uncertainty of other filtration testing cases was considered less than the uncertainty in this case.

Table A.1 Uncertainty budget for the air filtration efficiency

Cause of the uncertainty	Propagation constant, P_j	Uncertainty type (A)	Uncertainty type (B)
Calibration	P_1=1 $P_2 = -\frac{1}{\sqrt{2}}$	-	-
Meter reading	P_1=1 $P_2 = -\frac{1}{\sqrt{2}}$	$\frac{s_{C,up}}{C_{up}} = 0.21\%$ $\frac{s_{\overline{C,up}}}{\overline{C_{up}}} = 0.09\%$ $\frac{s_{\overline{C,down}}}{\overline{C_{down}}} = 0.15\%$ $\frac{s_{C,down}}{C_{down}} = 0.33\%$	$\frac{w_{Cu}}{C_{up}} \approx 0$ $\frac{w_{C_d}}{C_{down}} \approx 0$
Operating point	P_1=1 $P_2 = -\frac{1}{\sqrt{2}}$	-	-
Operating conditions	P_1=1 $P_2 = -\frac{1}{\sqrt{2}}$	$\frac{s_{C,up}}{C_{up}} = 1.43\%$ $\frac{s_{\overline{C,up}}}{\overline{C_{up}}} = 0.64\%$ $\frac{s_{C,down}}{C_{down}} = 1.38\%$ $\frac{s_{\overline{C,down}}}{\overline{C_{down}}} = 0.62\%$	-
Installation	P_1=1 $P_2 = -\frac{1}{\sqrt{2}}$	-	-
Combined uncertainties of types A and B		$\frac{s_{EF}}{EF} = 2.6\%$ $\frac{s_{\overline{EF}}}{\overline{EF}} = 1.1\%$	≈ 0
Combined uncertainty of filter efficiency		$\frac{u_{EF}}{EF} = 2.6\%$ $\frac{u_{\overline{EF}}}{\overline{EF}} = 1.1\%$	
Total uncertainty of filter efficiency (k=2)		$\frac{U_{EF}}{EF} = 5.1\%$ $\frac{U_{\overline{EF}}}{\overline{EF}} = 2.1\%$	

Appendix B

Alternative results in Chapter 7

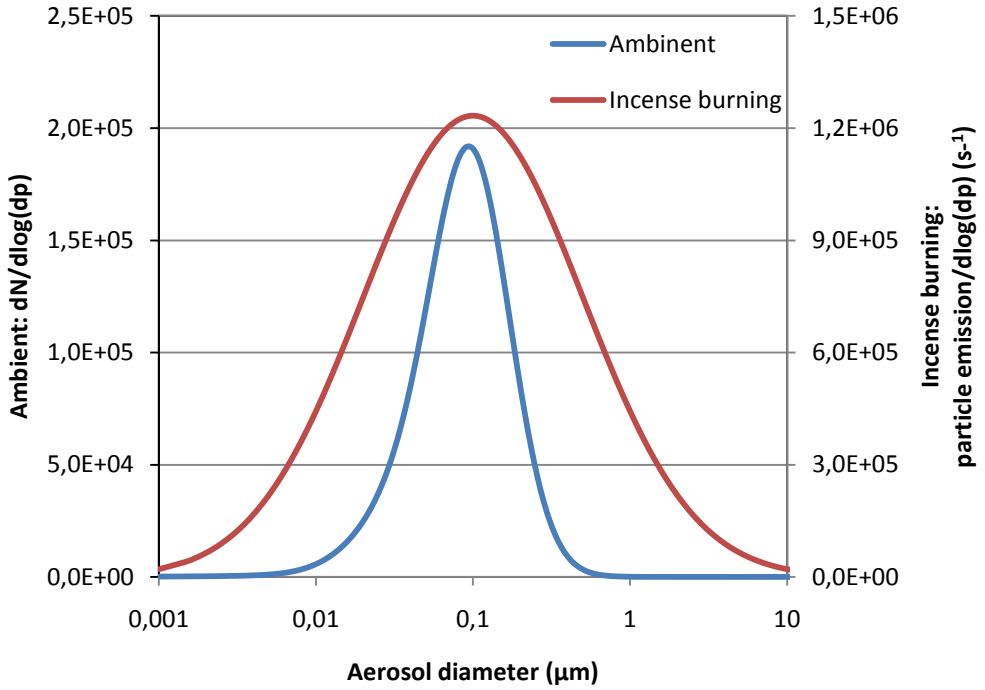

Figure A1 Adopted size-resolved number concentration of ambient particles[73] and particles emission from incense burning[51]. The size of peak concentration of ambient particles is removed from 0.013 µm to 0.1 µm. The incense is assumed to burn for 1 hour in a room with a volume of 30 m^3.

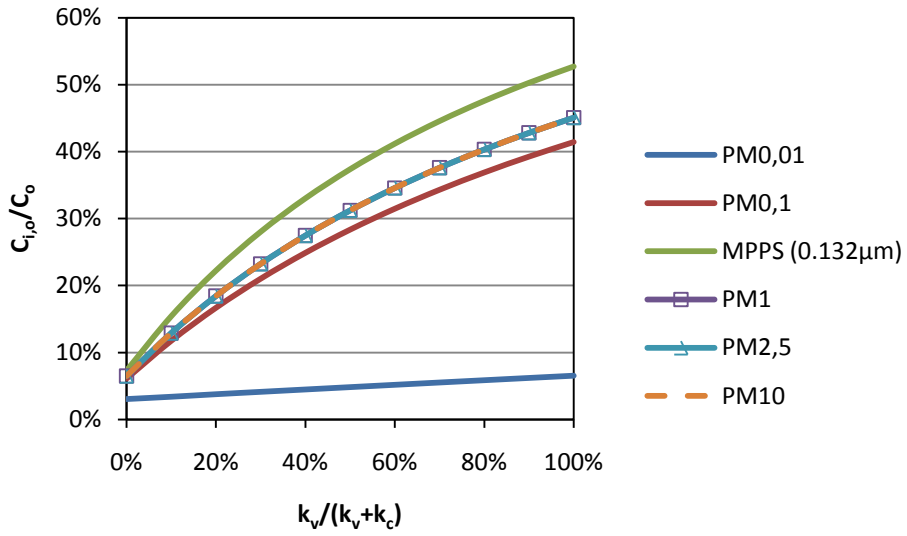

(a)

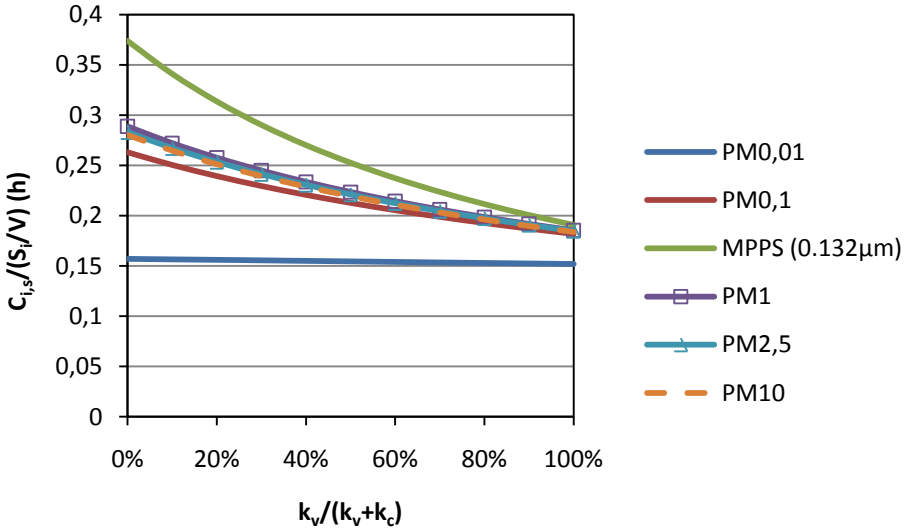

(b)

Figure A2 Integrated *Ci,o/Co, Ci,s/(Si/V)* in the size range of $PM_{0.01}$, $PM_{0.1}$, PM_1, $PM_{2.5}$, PM_{10} and MPPS (0.132µm) at varied outdoor air flow percentage with filter class F7. The supply air flow rate is 5 h-1. (a) Ci,o/Co; (b) Ci,s/(Si/V). The calculated particles size-distribution is in Figure A2.

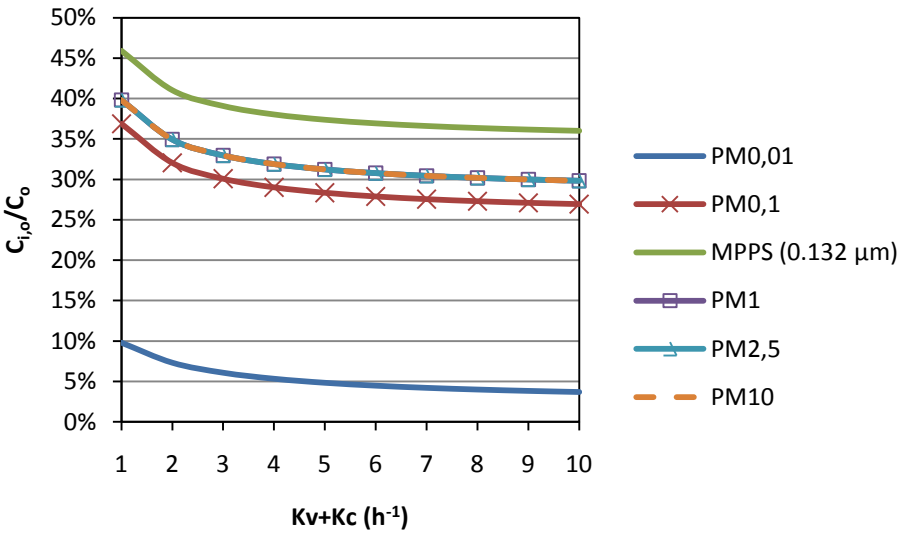

(a)

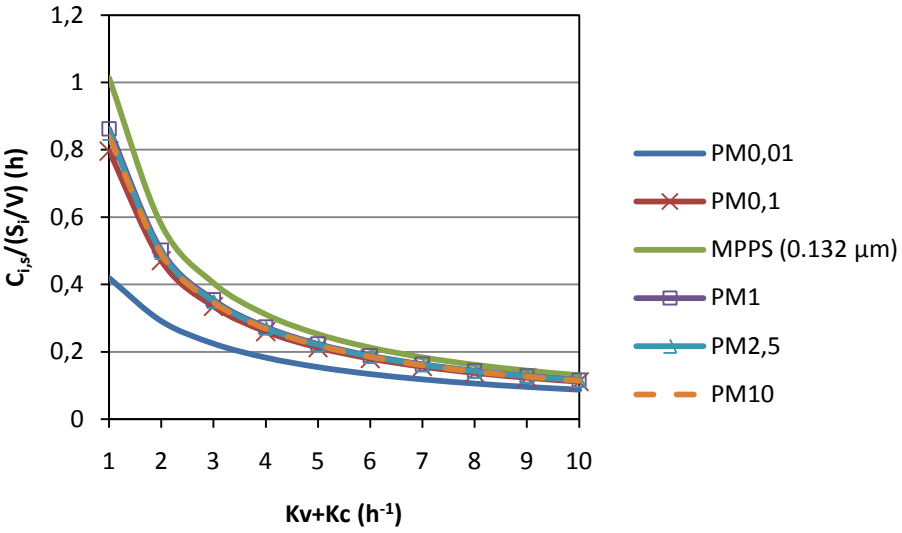

(b)

Figure A3 Integrated $C_{i,o}/C_o$, $C_{i,s}/(S_i/V)$ in the size range of $PM_{0.01}$, $PM_{0.1}$, PM_1, $PM_{2.5}$, PM_{10} and MPPS (0.132µm) at with different supply air exchange rates and with filter class F7. The outdoor air flow percentage is constant at 50%, i.e. $k_v/(k_v+k_c)=50\%$. (a) $C_{i,o}/C_o$; (b) $C_{i,s}/(S_i/V)$. The calculated particles size-distribution is in Figure A2.

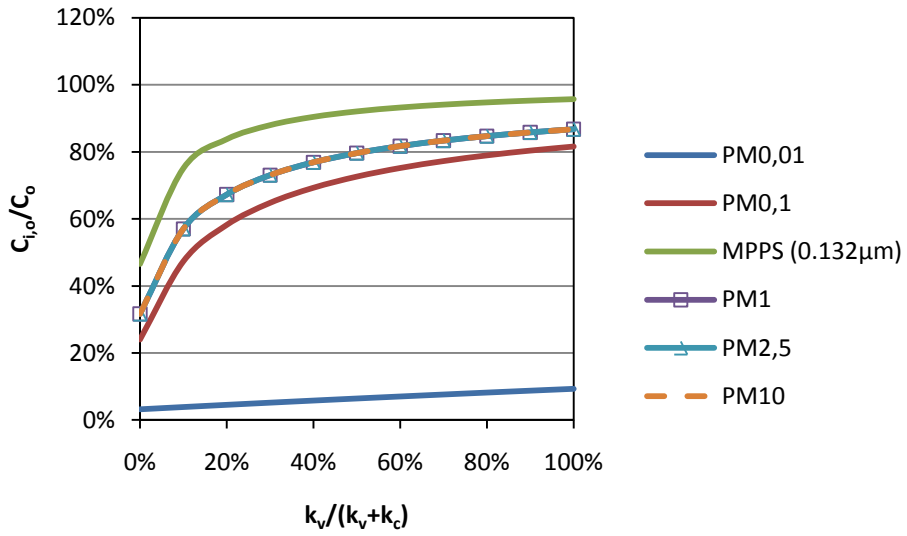

(a)

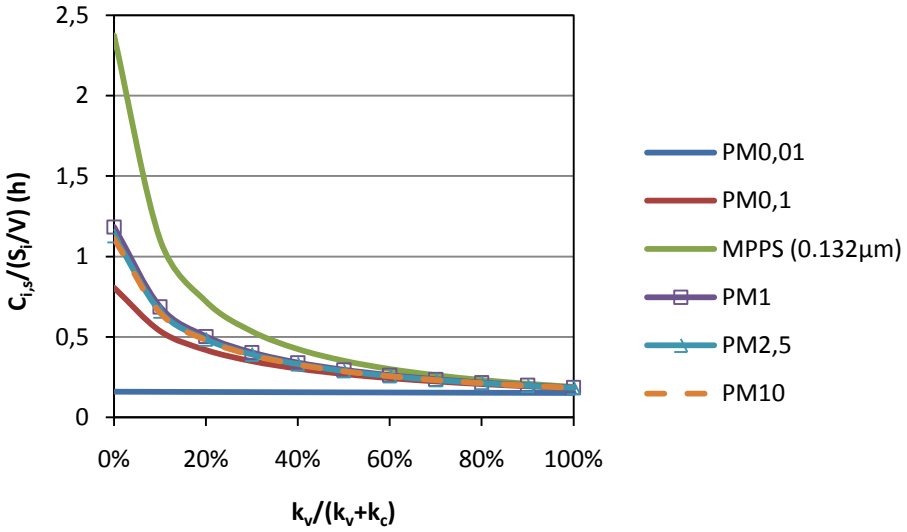

(b)

Figure A4 Integrated $C_{i,o}/C_o$, $C_{i,s}/(S_i/V)$ in the size range of $PM_{0.01}$, $PM_{0.1}$, PM_1, $PM_{2.5}$, PM_{10} and MPPS (0.132µm) at varied outdoor air flow percentage with filter class F5. The supply air flow rate is 5 h^{-1}. (a) $C_{i,o}/C_o$; (b) $C_{i,s}/(S_i/V)$. The calculated particles size-distribution is in Figure A2.

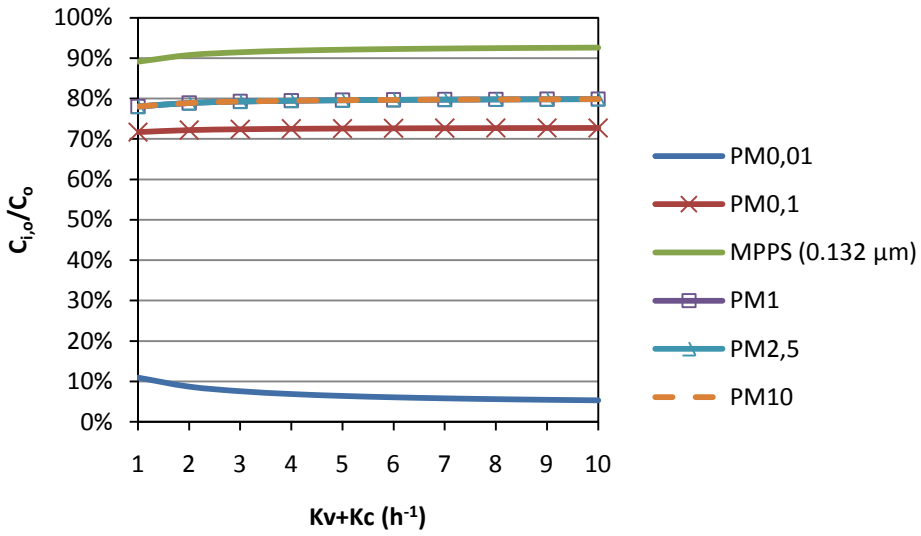

(a)

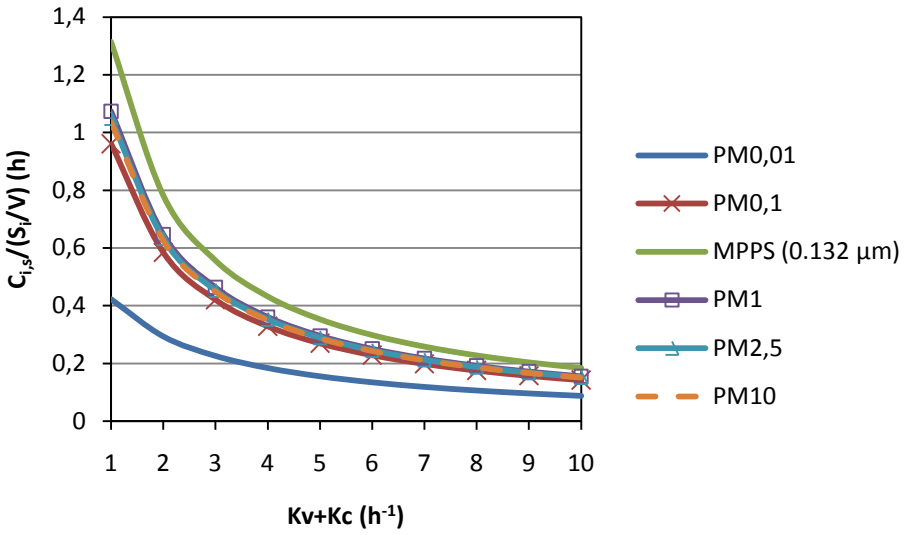

(b)

Figure A5 Integrated $C_{i,o}/C_o$, $C_{i,s}/(S_i/V)$ in the size range of $PM_{0.01}$, $PM_{0.1}$, PM_1, $PM_{2.5}$, PM_{10} and MPPS (0.132µm) at with different supply air exchange rates and with filter class F5. The outdoor air flow percentage is constant at 50%, i.e. $k_v/(k_v+k_c)=50\%$. (a) $C_{i,o}/C_o$; (b) $C_{i,s}/(S_i/V)$. The calculated particles size-distribution is in Figure A2.

Appendix C

Alternative results based on the short lifetime comparison for Figure 8.7

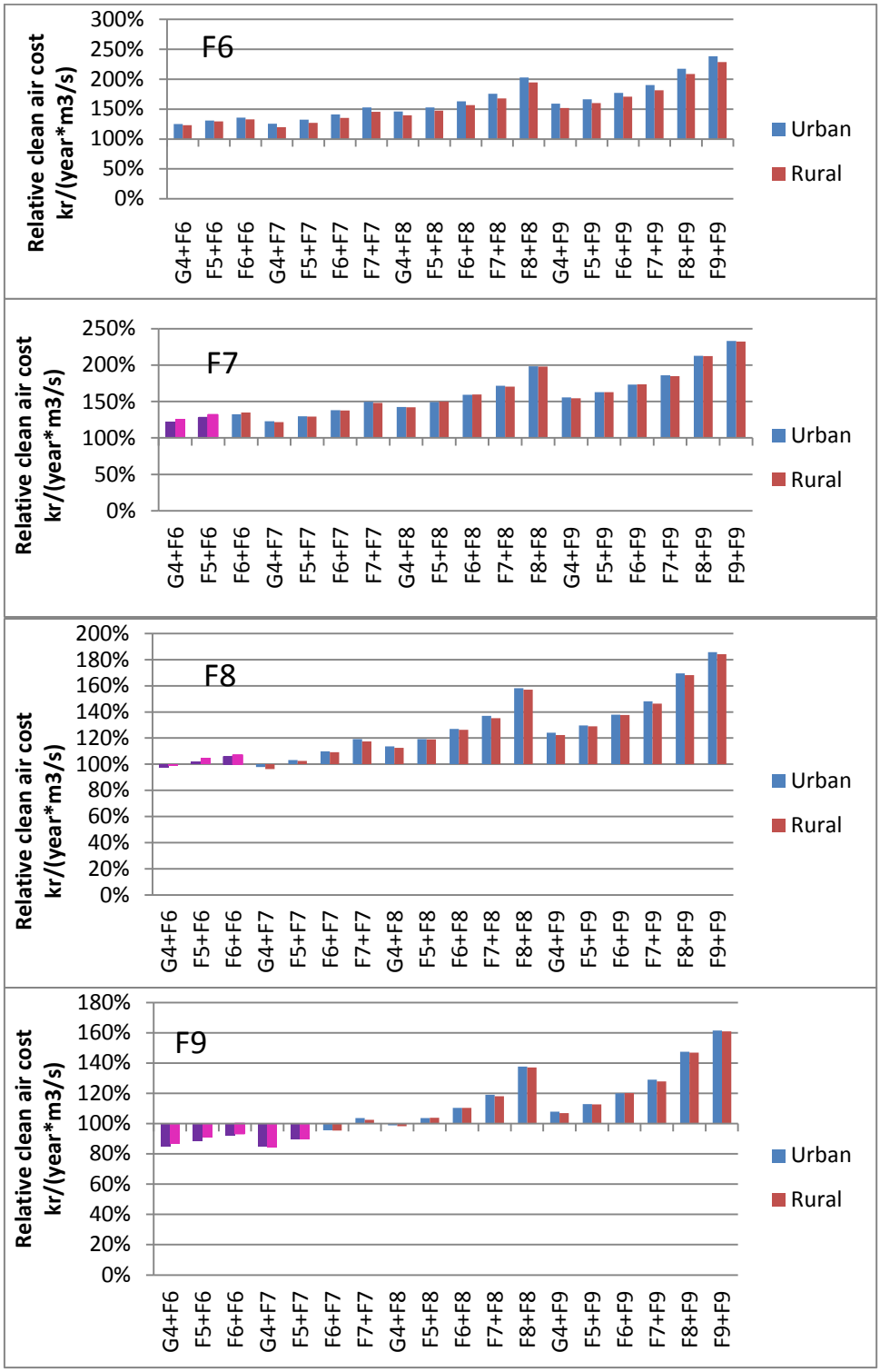

(a)

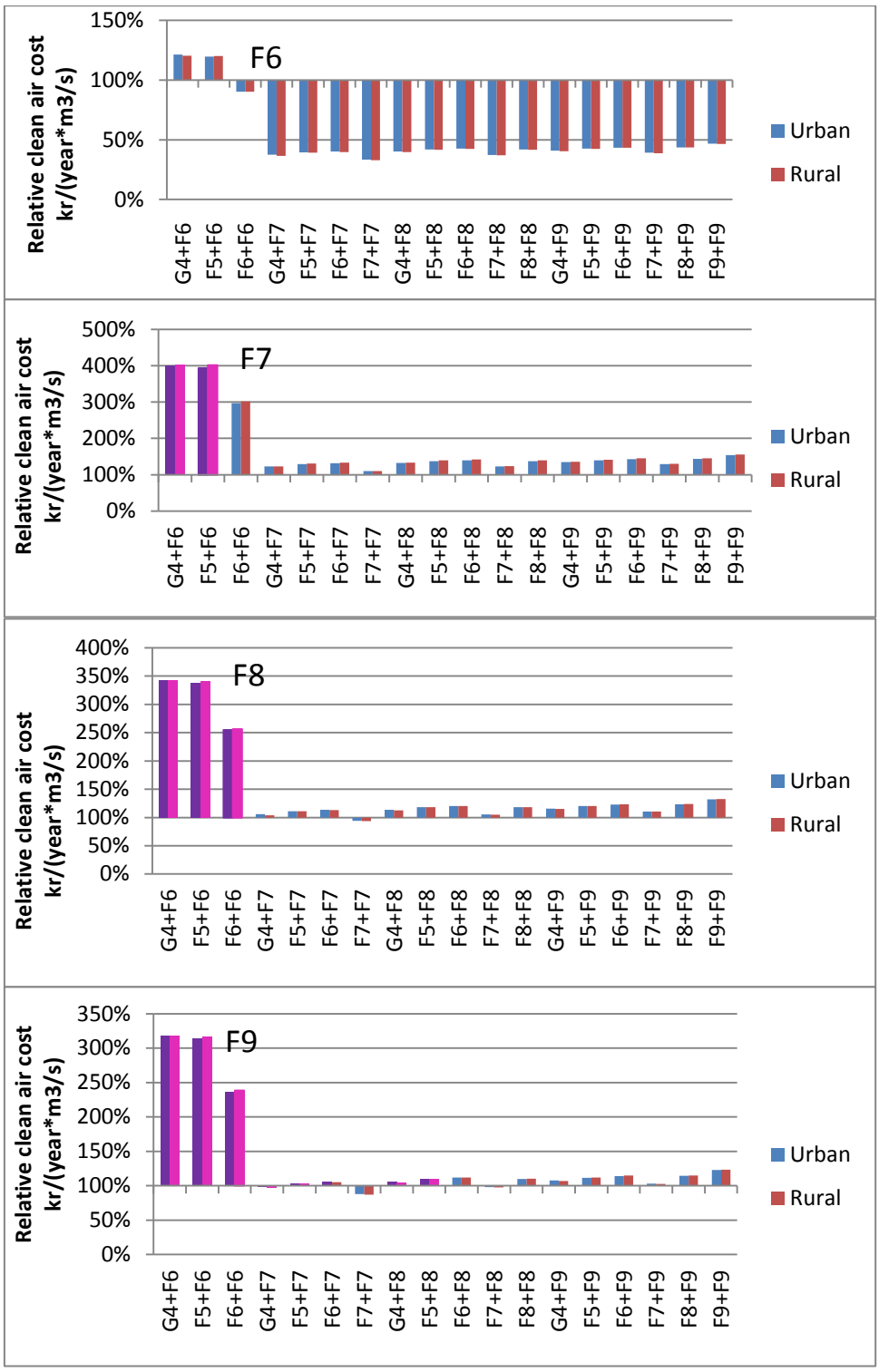

(b)

Figure A6 Relative clean air flow cost of combined filters compared to single filters. (a) Clean air flow for UFPs; (b) Clean air flow for MPPS-sized particle. The lifetimes of combined filters are 6 months for per-filter and 12 months for main filter. The lifetime of a single filter is 6 months.